Somatic GNA11/Q mutations- clues to cause and consequence of primary aldosteronism? And Feasibility study of RadioFrequency endoscopic ABlation, with ULtrasound guidance, as a non-surgical, Adrenal Sparing treatment for aldosterone-producing adenomas (FABULAS Study).

Giulia Argentesi

A thesis submitted in partial fulfilment of the requirements of the degree of Doctor of Philosophy

April 2023.

I, **Giulia Argentesi,** confirm that the research included within this thesis is my own work or that where it has been carried out in collaboration with, or supported by others, that this is duly acknowledged below, and my contribution indicated. Previously published material is also acknowledged below.

I attest that I have exercised reasonable care to ensure that the work is original and does not to the best of my knowledge break any UK law, infringe any third party's copyright or other Intellectual Property Right, or contain any confidential material.

I accept that the College has the right to use plagiarism detection software to check the electronic version of the thesis.

I confirm that this thesis has not been previously submitted for the award of a degree by this or any other university.

Signature: Date: 07th April 2023.

Collaborations:

Dr Junhua Zhou also performed transfection of H295R cells with GNA11 plasmid. Immunohistochemistry of double mutant tissue. Performed immunofluorescence of primary cells with double GNA11/ CTNNB1 mutation.

Dr Elena A.B. Azizan (Department of Medicine, University Kebangsaan, Malaysia) also performed transfection of H295R cells with GNA11 plasmid.

Dr Xilin Wu (William Harvey Research Institute, London) performed transfection of CADM-1 on H295R cells.

Dr Emily Goodchild (William Harvey Research Institute, London) performed H and E staining and CYP11B2 staining of pathology samples.

Dr Sam O'Toole (William Harvey Research Institute, London) performed immunofluorescence of primary cells with double GNA11/ CTNNB1 mutation.

Nadia Rahman and the Pathology team at QMUL (Wolfson Centre, London) performed immunohistochemistry of TMEM132E and CHRNA7.

Linda Hammond (Barts Cancer Institute, London) and Laura Perna (John Vane Institute, London) taught me how to use the Nanozoomer and Confocal Microscopes.

James Boot, Chaz Mein and Eva Wozniak (The Barts and the London Genome centre, Blizard Institute, London) performed RNA sequencing and quality control on H295R cells control and TMEM132E knockdown.

Professor Rajesh Thakker and his team at Oxford for the GNA11/Q plasmids.

Dr Alison Marker and team (Department of Pathology, Addenbrooke's Hospital, Cambridge) performed immunohistochemistry on FABULAS samples and FNA samples.

Mr Dan Gillet (Department of Endocrine molecular imaging, Addenbrooke's Hospital, Cambridge) provided pre- and post- ablation nuclear images.

The FABULAS research team at Barts Health, London, Addenbrooke's Hospital, Cambridge and UCLH, London organised patients, looked after patients, collected data, collected samples, and put data onto the online MACRO version 4 data collection site.

King's Clinical Trial Unit for the maintenance and upkeep of the MACRO version 4 database.

Dr Stephen Morant, University of Dundee, Scotland provided the original FABULAS statistical calculations.

Publications:

Publications:

1. Nature genetics: *Zhou et al. Somatic mutations of GNA11 and GNAQ in CTNNB1-mutant aldosterone-producing adenomas presenting in puberty, pregnancy or menopause. NatureGenetics volume 53, pages1360–1372 (2021).*
2. Nature medicine*: Wu et al. [11C]metomidate PET-CT versus adrenal vein sampling for diagnosing surgically curable primary aldosteronism: a prospective, within-patient trial. Nature Medicine | Volume 29 | January 2023 | 190–202.*

Oral presentations:

- RSM Endocrinology Clinical Cases, London March 2019 *Explosive onset of Primary Aldosteronism at puberty, caused by somatic mutation of CTNNB1*. Second Prize for best oral presentation.
- British Endocrine Society conference in Edinburgh November 2021: *Somatic mutations of GNA11 and GNAQ in CTNNB1-mutant aldosterone-producing adenomas presenting in puberty, pregnancy or menopause*. 1st Prize: best oral presentation in the Adrenal and Cardiovascular category.
- November 2021 presentation *Somatic mutations of GNA11 and GNAQ in CTNNB1-mutant aldosterone-producing adenomas presenting in puberty, pregnancy or menopause* to visiting ENDO society president, Professor Gary Hammer.

Poster Presentations:

- British Endocrine Society Conference in Harrogate November 2022: FABULAS study.

Thesis Abstract:

Primary aldosteronism (PA) is the potentially curable cause of high-risk hypertension in 5-10% of unselected patients, and in > 20% of those with resistant hypertension. Landmark Whole exome sequencing (WES) have paved the way to better understanding of this condition. The gold standard treatment for unilateral disease is adrenalectomy where the cure rate achieved varies between 30-60%.

The first part of this thesis investigates a molecule, TMEM132E, which was the most consistently upregulated gene in the aldosterone producing adenomas (APA) discovered to have the double somatic mutation of *CTNNB1*, in exon 3, and either *GNA11* or *GNAQ*, at residue p.Gln209. Transfection of the *CTNNB1*-mutant adrenocortical cell line, H295R, with wild-type or mutant GNA11, reproduced the increase in CYP11B2 (encoding aldosterone synthase) seen in all APAs, and TMEM132E was the only gene to be significantly upregulated, out of the nine which are uniquely upregulated in the double-mutant APAs. Because TMEM132E is a deafness gene, whose vital function may be to traffic cholinergic ionotropic receptors $\alpha 9/\alpha 10$, to the plasma membrane, I investigated whether the 30-40% homologous adrenocortical receptor, $\alpha 7$ – also upregulated in double-mutant APAs – enables cholinergic stimulation of aldosterone production. Treatment of H295R cells with Carbachol (an acetylcholine agonist) increased aldosterone secretion.

The second part of this thesis presents results from FABULAS: Feasibility study of Radio**F**requency endoscopic **AB**lation, with **UL**trasound guidance, as a non-surgical, **A**drenal **S**paring treatment for aldosterone producing adenomas. This was a phase 1 study to determine the safety and efficacy of endoscopic ultrasound guided radiofrequency ablation (RFA) as an alternative to adrenal surgery for left sided APAs. By design, surgery was contra-indicated in ~half of the 28 patients because of co-morbidities, or because the diagnosis of unilateral PA was ambiguous. The primary outcome was safety. None of the pre-specified serious adverse events occurred, namely perforation, haemorrhage, or infarction of major organs within the first 24-48 hours. 3 patients had severe events related to the procedure, which rapidly resolved. The secondary outcomes of efficacy – anticipated to be lower than in surgical patients because of the eligibility criteria – were the PASO (Primary Aldosterone Surgical Outcome) criteria of biochemical and clinical success 6-months post-procedure, and changes in CYP11B2 signal, measured by 11C-metomidate PET CT. 14/28 and 4/28 patients achieved complete biochemical or complete clinical success, respectively. There was significant reduction in ARR (aldosterone renin ratio), and defined daily dose of antihypertensive medications, but average blood pressure was unchanged.

These results show endoscopic RFA to be safe and potentially effective, enabling a head-to-head comparison with surgery that is now underway.

Acknowledgments:

Firstly, I would like to thank all the patients who contributed to these studies. Their consent for tissue collection and the time they have dedicated to attending appointments have been invaluable to my thesis.

I am deeply indebted to my sponsor the British Heart Foundation (BHF) for the sponsorship of my clinical research training fellowship (FS/19/50/34566) and for the sponsorship of the FABULAS study (PG/16/40/32137).

Thank you to my supervisor Professor Brown for enabling me to discover the wonderful world of primary aldosteronism, for all the invaluable ideas and support.

To my other supervisor, Professor Will Drake, thank you for all your support, clinical guidance and helping me become a better clinician.

I have been incredibly lucky to have some wonderful colleagues during the course of my thesis. Many thanks to Dr Emily Goodchild, Dr Xilin Wu, Dr Kate Laycock and Dr Yun-ni Lee for your friendship and support, I could not have done it without you. To Dr Elena Azizan who was only ever an email or text away: thank you for all your guidance and support. Thank you also to Dr Sam O'Toole, our Clinical lecturer, and to Dr Junhua Zhou for all her guidance and help at the start of my PhD journey.

I would like to also thank our Research Group at QMUL, Sn Daniela Benu and Sister Jackie Salsbury.

Many thanks also to the wider FABULAS research group, Dr James Macfarlane, Dr Russell Senanayake, August Palmer, Dr Heok Cheow and Professor Mark Gurnell in Cambridge and thank you to Professor Steve Pereira and Dr Alex Nay at University College London Hospital.

Thank you also to Dr Li Chan and Professor Leo Guasti who were always happy to chat through scientific ideas.

Finally, I would like to thank my husband Alexander Borthwick for all the encouragement, support, and kindness I have needed. He has held my hand every step of the way.

Also, to my wonderful family: my parents Dr Flavio Argentesi and Joan Argentesi - thank you for always believing in me and encouraging me- and to my best friend and sister Livia Harriman.

Table of Contents

List of Abbreviations:

ACC	Adrenal Cortical Carcinoma
ACE	Angiotensin Converting Enzyme
ACTH	Adrenocorticotrophic hormone
AE	Adverse Event
ALP	Alkaline Phosphatase
ALT	Alanine transaminase
Ang I	Angiotensin I
Ang II	Angiotensin II
APA	Aldosterone Producing Adenomas
APM	Aldosterone Producing Micronodules
ARC	Active Renin mass Concentration
ARR	Aldosterone Renin Ratio
AT-1/-2	Angiotensin type 1 and 2
ATP	Adenosine Triphosphate
AVS	Adrenal Vein Sampling
BAH	Bilateral Adrenal Hyperplasia
BHCG	Beta Human Chorionic Gonadotropin
BMI	Body Mass Index
CCT	Captopril Challenge Test
C-HA	C-terminal Human influenza hemagglutinin
CK	Creatinine Kinase
CRP	C-reactive protein
CT	Computed Tomography
CTNNB1	Catenin Beta-1
CYP11B1	11 ß -hydroxylase
CYP11B2	Aldosterone synthase
DDD.	Defined Daily Dose
DHEA	Dehydroepiandrosterone

DKK1	Dick Kopf Related protein 1
DRC	Direct Renin Concentration
DBP	Diastolic Blood Pressure
EDTA	Ethylenediaminetetraacetic acid
EUS	Endoscopic Ultrasound
EUS-RFA	Endoscopic ultrasound-guided radiofrequency ablation
EV	Empty vector
FAP	Fibroblast Activation Protein
FBS	Fetal bovine serum
FNA	Fine needle aspirate
FST	Fludrocortisone Suppression Test
FZ	Foetal Zone
GNA11/Q.	G protein subunit alpha 11/Q
GDP	Guanine Diphosphate
GFP	Green Fluorescent Protein
GNRH	Gonadotropin Releasing Hormone
GTP	Guanine Triphosphate
IF	Immunofluorescence
IHC	Immunohistochemistry
$IP_{3.}$	Inositol Triphosphate
K^+	Potassium
LH	Luteinising Hormone
LHCGR	Luteinising Hormone/Choriogonadotropin Receptor
mAChR	Muscarinic Acetylcholine Receptor
MR	Mineralocorticoid Receptor
MRA	Mineralocorticoid Receptor Antagonist
MRI	Magnetic Resonance Imaging
Na^+	Sodium
nAChR	Nicotinic Acetylcholine Receptor
NaCl	Sodium Chloride

NHS	National Health Service
PA	Primary Aldosteronism
PASO	Primary Aldosteronism Surgical Outcome
PBS	Phosphate Buffer Saline
PCR	Polymerase Chain Reaction
PET	Positron Emission Tomography
PNMT	Phenylethanolamine N-methyltransferase
PRA	Plasma Renin Activity
qPCR	Quantitative polymerase chain reaction
RAAS	Renin Angiotensin Aldosterone System
RFA	Radio Frequency Ablation
SAE	Serious Adverse Events
SBP	Systolic Blood Pressure
SF1	Steroidogenic Factor 1
SiRNA	Small interfering RNA
SIT	Saline Infusion Test
SLC35F1	Solute carrier family 35, member F1
StAR	Steroidogenic acute regulatory protein
SUV	Standardised Uptake Values
SUVmax	Maximum standard uptake value
TMEM132E	Transmembrane protein 132E
TMIE	Transmembrane inner ear protein
TOF	Time Of Flight
WCC	White Cell Count
WES	Whole exome sequencing
WGA	Wheat germ agglutinin
WHO	World Health Organisation
WT	Wild-type
ZF	Zona Fasciculata
ZG	Zona Glomerulosa

ZR	Zona Reticularis

Chapter 1:

Introduction

1.1 Epidemiology:

Primary aldosteronism (PA) is the potentially curable cause of high-risk hypertension in 5-10% of unselected patients, and in > 20% of those with resistant hypertension, but less than 1% is ever diagnosed [1]. Hypertension is one of the leading contributors to all causes of death and disability world-wide [2]. According to the World Health Organisation, (WHO) 1.38 billion adults worldwide suffer with hypertension, with two-thirds of hypertensive patients coming from low to medium economic countries. The prevalence of hypertension is increasing with ageing populations, the epidemiology shifting to the right with advancing age, and is also increasing secondary to poor high salt diets, obesity, and poor physical activity trends [3] [4]. It is one of the most common preventable risk factors for cardiovascular and cerebrovascular disease [5]. In England, 1 in 4 adults are affected by hypertension. Hypertension is diagnosed when blood pressure is persistently above 140/85 mmHg in people under 80 years of age, and above 150/90 mmHg in those over 80 years. It has been shown that decreasing blood pressure by only 10mmHg leads to a reduction of 13% in all-cause mortality, as well as a significant reduction in cardiovascular disease and stroke [6]. Hypertension costs the National Health Service (NHS) over £2.1 billion per year [6]. A reduction of only 5 mmHg would save the NHS £850 million over a 10-year period, emphasising the potential value of high-quality practice-changing research within this field.

1.2 Definition:

PA was previously referred to as Conn's syndrome, after the physician who first described it in 1955 [7]. Conn described a 34-year-old female with severe hypertension, hypokalaemia, and mild hypernatremia who was found to have significantly elevated levels of what was then termed electrocortin, subsequently called aldosterone. Aldosterone is a mineralocorticoid steroid hormone synthesized in the outer zona glomerulosa (ZG) layer of the adrenal cortex. PA is a condition characterised by renin-independent excess aldosterone production inappropriate to total body sodium (Na^+). The autonomous production is independent of its major regulators such as angiotensin II (Ang II), potassium (K^+), and (to a lesser extent) adrenocorticotrophic hormone (ACTH) concentration.

1.3 Clinical features:

The signs and symptoms of PA are either due to hypertension or the hypokalaemia that can develop. Hypertension, when left untreated, leads to symptoms such as headaches, visual disturbances, dizziness,

epistaxis, chest pain, and occasionally shortness of breath. Hypertension can also, over time, lead to damage to the cardiovascular, cerebrovascular, and renal systems. Organs dependent on fine vasculature, such as the retina, are also prone to damage if it goes untreated.

Symptoms of hypokalaemia can entail polyuria, muscle cramps and palpitations. Other symptoms that have been associated with PA are those of fatigue, anxiety, memory/ cognition problems, and depression. Stress and anxiety have been found to be greatly increased compared to patients with essential hypertension [8].

Prompt diagnosis of PA is crucial, as end-organ damage in PA is more severe than in age-matched patients with essential hypertension, resulting in 4-12 fold greater incidence of complications such as stroke and atrial fibrillation [9]. Furthermore, a systematic review and meta-analysis from the Lancet indicated that, following a median of 8.8 years from the diagnosis of hypertension, patients with PA compared to those with essential hypertension had not only a significant increased risk of stroke, atrial fibrillation, ischaemic heart disease, and heart failure but also an increased risk of metabolic syndrome and diabetes [10]. Although the mechanisms remain to be elucidated fully, it is widely accepted that high levels of aldosterone have a deleterious effect on cardiovascular tissues independent of high blood pressure. The main pathways of destruction appear to be pro-inflammatory; studies have pointed to increased correlation between a raised aldosterone level and markers of oxidative stress [11].

1.4 Pathogenesis:

1.4.1 The adrenal gland:

The adrenal glands sit bilaterally above either kidney. They were first described as “super renal” structures as early as 1563 by Bartolomeo Eustachi in his “Opuscola Anatomica” but it was not until much later that the cortex and medulla were characterised. In 1855, Thomas Addison, a physician at Guys and St Thomas Hospital, began to describe conditions associated with the “suprarenal capsule.” In 1866, Arnold - and then Gottschau in 1883 - illustrated that there was evidence of cortical zonation, and the three zones of the cortex were distinguished. The adrenal glands are essential to life, the so-called “powerhouse” that provides stress response hormones, the “fight or flight” response, blood pressure control, and immune function. Anatomically, they lie within the perirenal space and are enclosed within the superior renal fascia. They weigh around 5 grams and measure roughly 50mm x30mm x10mm in height, breadth, and width. Whilst the left adrenal is more crescentic

in shape, the right appears pyramidal [12]. The left adrenal lies anatomically between the abdominal aorta and spleen, and above the splenic artery and vein, whilst the right lies posterior to the inferior vena cave, just below the liver.

The adrenal cortex is highly vascularised, receiving a large amount of cardiac output [13]. Heavily supplied by the aorta, renal and inferior phrenic arteries, the vessels penetrate the ZG and form complex capillary networks to the rest of the cortex. These ensure cholesterol, growth factors, and trophic hormones are rapidly available at times of physiological challenge. Vascularisation occurs from the cortex to the medulla and the gland drains into a single vein, which then drains from the left gland into the renal vein, whilst the right drains directly into the vena cava.

1.4.2 Adrenal cortex:

The adrenal cortex has 3 layers known as zones, the zona glomerulosa (ZG), zona fasciculata (ZF) and zona reticularis (ZR). It is covered by a strong fibrous external capsule. Each zone secretes a different steroid hormone and is subject to a different independent regulatory control. The cells of the adrenal cortex arise from stem cells in the outer cortex/capsule and change their phenotype as they move centripetally through the zones, eventually apoptosing post the ZR [14].

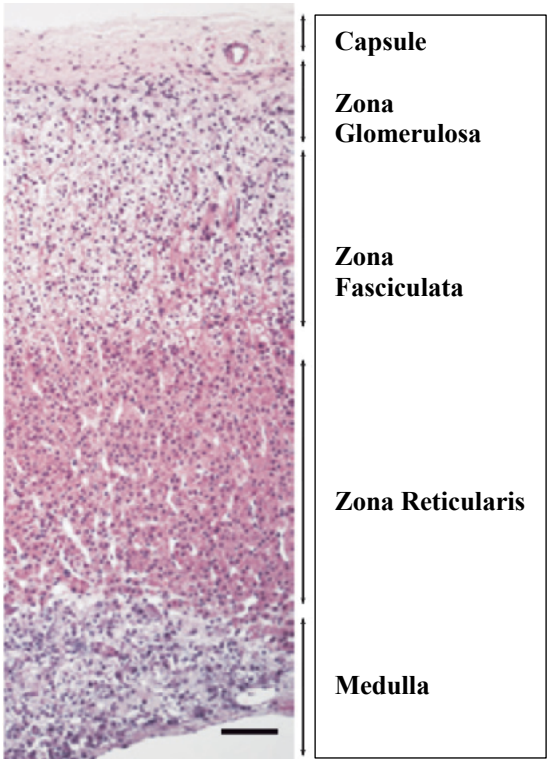

Figure 1 1: Haemolyin and Eosin stain of the adrenal gland, histologically illustrating the different zones [15].

1.4.3 Zona Glomerulosa:

The ZG is the outermost zone situated below the fibrous external capsule. The cells of the ZG are arranged in glomerulus (Latin for ball) or ovoid, sometimes described as rosette clusters, and are separated by trabeculae extending inwards from the fibrous capsule that encapsulates the adrenal gland. The trabeculae contain the capillary network that keeps the ZG well vascularised. The cells of the ZG are lipid poor, which distinguishes them from the more lipid rich cells of the second zone of the adrenal cortex, the zona fasciculata (ZF). The ZG makes up ~15% of the adrenal cortex and its rosette cell structures regularly combine ionic, hormonal, and paracrine signals. These lead to membrane depolarisation and catalyse the process to produce the mineralocorticoid hormone aldosterone. It took scientists over 20 years and international collaboration to finally isolate and discover aldosterone in 1954 [16]. The adrenal cortical zones are tightly regulated under the direct control of specialist enzymes to produce only their specific hormones. Aldosterone for example in mammals is made solely within the ZG.

1.4.4 The Renin angiotensin aldosterone system (RAAS):

Aldosterone, first isolated in 1954 [16], forms part of the complex haemodynamic regulating renin-angiotensin-aldosterone system (RAAS). The RAAS regulates longer term blood pressure, sodium-potassium balance (and as a result extracellular fluid volume status) and has often been a target therefore for antihypertensive therapies [17] (Figure 1 2). The proteolytic enzyme renin is released from the juxtaglomerular cells of the kidneys in response to sympathetic nerve stimulation by ß 1- adrenoreceptors. Pro-renin is moved into the acidic secretory granules within the juxtaglomerular cells and 43-amino acids are irreversibly cleaved off and renin is formed. Renin is controlled by four mechanisms: firstly, the macula densa located within the distal nephron of the kidney; this plaque contains chemoreceptors that are very sensitive to low intratubular sodium levels. The sodium tubular content is measured via the movement of sodium chloride (NaCl) through the sodium chloride-potassium (*NKCC2*) channel. Secondly, the juxtaglomerular cells contain stretch receptors that can sense afferent renal perfusion pressure and therefore are alerted to low intravascular volume. Orthostatic changes also lead to renin being released by the sympathetic nervous system, as it activates the ß 1- adrenoreceptors. Finally, renin is susceptible to negative feedback from local hormones, such as Ang II, atrial natriuretic peptide, and electrolytes such as Na^+ and K^+ [18-20].

Renin is the rate-limiting step within the RAAS and subsequently goes on to cleave angiotensinogen (produced in the liver) to angiotensin I (Ang I). Ang I is then further cleaved by angiotensin converting enzyme (ACE),

produced mainly within the lungs, to form the octapeptide Ang II. Ang II binds to the angiotensin type 1 and 2 (AT-1 and AT-2) receptors leading to the activation of aldosterone synthesis. Ang II concentration in the plasma in resting conditions is usually around 10-60 pM; this can rise to >100 pM in conditions such as salt or water depletion or haemorrhage [21].

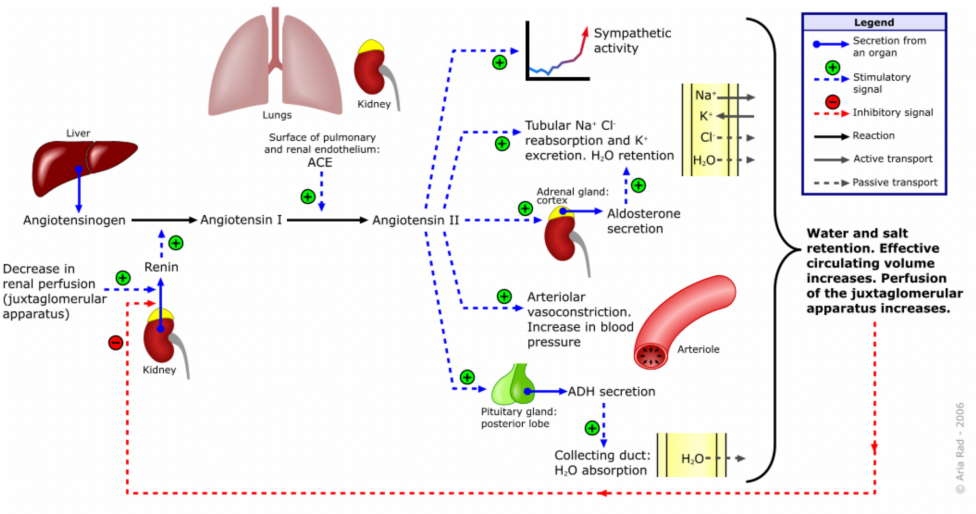

Figure 1 2: Illustrates the RAAS. Aria Rad-2006 Creative Commons Attribution-Share Alike 3.0 Unported license.

1.4.5 Aldosterone synthesis:

Aldosterone synthesis is activated by three main molecules, Ang II, K^+ and adrenocorticotrophic hormone (ACTH).

1.4.5.1 Ang II and K^+:

The negatively charged resting membrane of the ZG cells is tightly maintained by extra- and intracellular K^+ concentrations controlled by the function of the Na^+-K^+- ATPase pump. This works to maintain a higher concentration of Na^+ extracellularly and K^+ intracellularly. Ang II binding to the AT-1 receptor, and/or increased concentrations of extracellular K^+ leads to depolarisation of the membrane of the ZG cells. This depolarisation leads to an increase in cytosolic calcium. K^+ leads to mainly T and L- type voltage-gated calcium ion channels opening and an influx of calcium. Ang II binding to the AT-1 receptor leads to the hydrolysis of a phospholipid within the membrane called phosphatidylinositol 4,5- bisphosphate (PIP2). Hydrolysis occurs via phospholipase

C (PLC) to form diaglycerol DAG which remains in the membrane and Inositol triphosphate (IP_3). IP_3 passes through the cell binding to its receptor on the endoplasmic reticulum [10], activating the calcium/calmodulin-dependent protein kinases (CaMK), leading to calcium release from stores into the cytosol [20] [22].

It is the rise in Ca^{2+} which kickstarts the steroidogenic process for aldosterone production. Like most other adrenal steroid hormone- producing cells, the ZG utilises cholesterol as the primary precursor. Cholesterol is a structural component of cells with a unique 27 carbon structure. It has a central sterol ring made up of 4 hydrocarbon rings and a hydroxyl group. It also contains a hydrocarbon tail. Along with steroid hormones, it is utilised to produce vitamin D and bile acids. The liver is the most industrial centre for cholesterol production, but it can be produced within individual cells to a lesser extent [23]. The ZG cells either source cholesterol by uptake of lipoproteins via the low-density lipoprotein (LDL) receptor or via the high-density lipoprotein (HDL) receptor. Otherwise, they synthesize it de novo from cholesteryl esters or acetate stored in lipid droplets within the cell. The rise in calcium mobilises the cholesterol across the mitochondrial membrane to the inner mitochondrial membrane in order for the enzyme *CYP11A1*, a member of the cytochrome P450 family of enzymes, to cleave it. The cytochrome P450 is a super dynasty of enzymes; all are characterised by a heme component and an ability to accept electrons from NADPH. They also hydrolyse and oxidise using molecular oxygen. They work on the elimination of metabolites including drugs, as well as the breakdown and synthesis of hormones. During the first process cholesterol is cleaved to pregnenolone. This is a rate-limiting step and is regulated by the presence of the steroidogenic acute regulatory protein StAR. StAR is a protein essential for adrenal steroidogenesis. It is formed as a 285 amino acid preprotein within the cytoplasm. It is then imported into the mitochondria and processed into its final form through phosphorylation [24]. Pregnenolone then diffuses through to the ER where type 2 3β-hydroxysteroid dehydrogenase (HSD3B2) converts it to progesterone. CYP21 then hydroxylates progesterone to deoxycorticosterone, which progresses to the mitochondria where the three final steps of 11β- and 18-hydroxylation and 18-oxidation are performed. These are performed by a unique single enzyme known as aldosterone synthase (CYP11B2) [22, 25].

DAG, a product of Ang II's activity to the receptor, also indirectly increases StAR production by phospholipase D (PLD), as well as by PLC. It can activate protein kinase C enzyme, which phosphorylates serine/ threonine residues and leads to cAMP response element binding protein (CREB) and StAR activation [21].

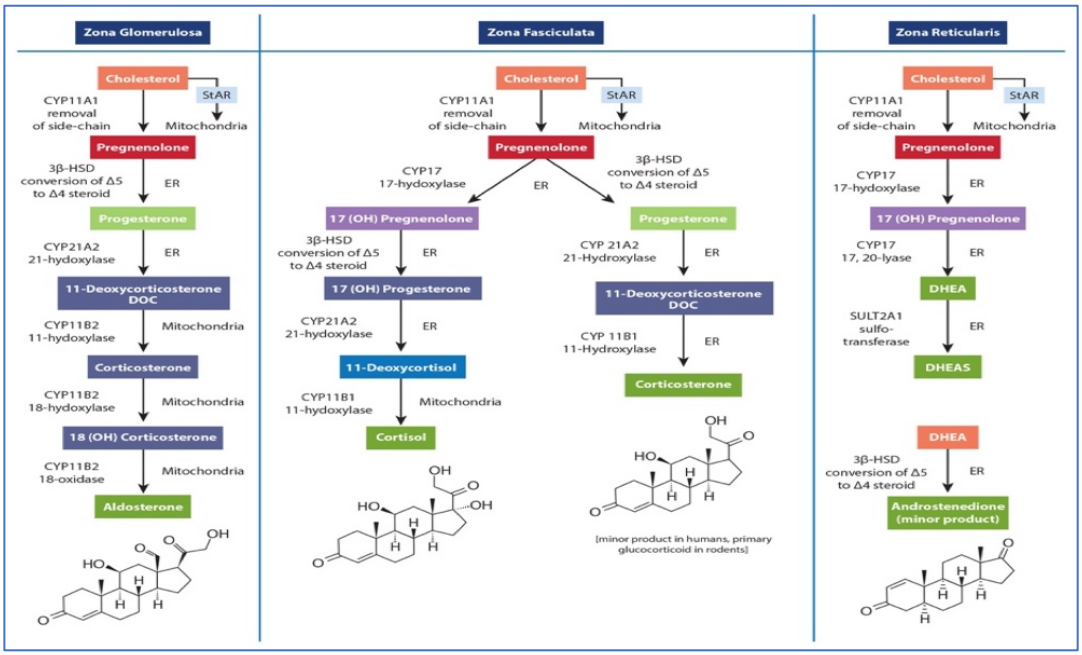

Figure 1 3: Shows the various pathways of adrenal steroid biosynthesis within the adrenal cortex zones. Cholesterol being the master steroid.

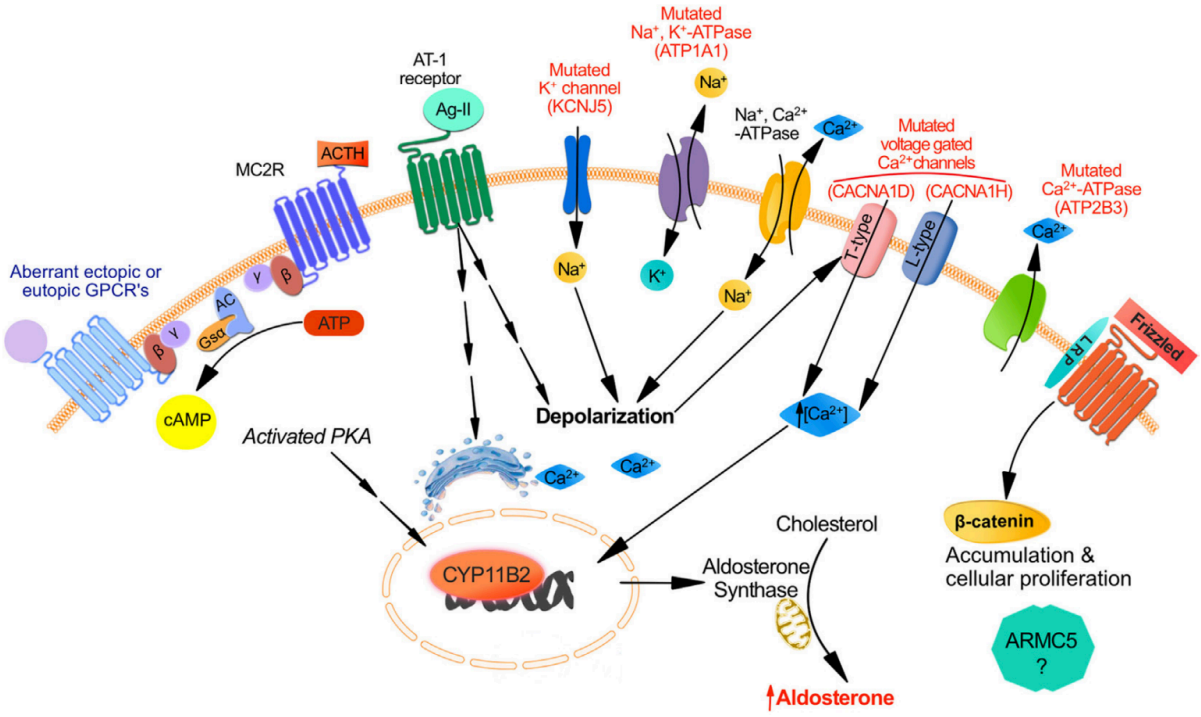

Figure 1 4: Illustrates the various receptors and intracellular signals involved in aldosterone production, and the points where somatic mutations (discussed below in section 1.11.3) take effect. Figure taken from *Ghorayeb et al* [20].

1.4.5.2 ACTH:

Ang II and K^+ however do not work alone if blood pressure and sodium drop significantly. ACTH is released from the anterior pituitary and works synergistically with Ang II to stimulate aldosterone production [26]. ACTH is a 39 amino acid peptide and belongs to the family of melanocortins. It is formed through tissue and site-specific proteolysis of the propepetide proopiomelanocortin (POMC) after it is cleaved by prohormone convertase enzymes. The hormones alpha to gamma- melanin stimulating hormone also form part of this family [27]. ACTH is produced by corticotropes in the anterior pituitary but has also been found in the adrenal medulla and skin. ACTH works via activation of the melanocortin 2 receptor MC2R, a G- protein coupled receptor, found not only within the ZG but also the ZF. The melanocortin receptors are a family of 5 receptors that span the membrane with 7 domains. MC2R is the smallest of the receptors. When ACTH binds to the receptor, it dissociates the Gsα-subunit, which activates the intracellular signalling of cAMP (cyclic adenosine monophosphate) from ATP. cAMP activity then leads to protein kinase A activation and, through the release of the functionary subunit, PRKACA leads to increased phosphorylation of StAR to form aldosterone [21]. Protein Kinase A has also been shown to directly increase the expression of *CYP11B2* [28].

Acute aldosterone synthesis within seconds to minutes is regulated by StAR, but long-term (hours to days) synthesis is regulated by the expression of CYP11B2. *Gomez-Sanchez et al* in 2014 developed a monoclonal antibody for CYP11B2, therefore helping to demarcate the adrenal cortex layers further [29].

Confining aldosterone production to its specific zone within the ZG is maintained by several factors. Firstly, CYP11B2 is solely expressed within the ZG. Secondly, there is an absence of the enzyme CYP17 seen in the other adrenal cortex layers. Lastly, the centripetal blood flow within the adrenal cortex helps to keep the synthesised hormones in their anatomical domains [22].

1.4.6 The Zona fasciculata:

The zona fasciculata (ZF), in contrast to the ZG, is lipid rich. Its cells lie within the second layer of the adrenal cortex. These cells secrete the glucocorticoid, cortisol. Cortisol is secreted under tight hypothalamic-pituitary-adrenal (HPA) control, under the influence of ACTH. It is an essential hormone party to circadian rhythm, as well as stress response. It also participates in glucose and protein homeostasis. The cells of the ZF have rounder nuclei and are more columnar in shape. Similarly, the final step of cortisol synthesis is executed by 11 ß - hydroxylase (CYP11B1) an enzyme almost identical in structure, bar 4 amino-acids, to CYP11B2.

1.4.7 The Zona Reticularis and Medulla:

The third and innermost zone of the adrenal cortex is zona reticularis ZR. This is as large as the ZG. It contains vacuolated cells, which secrete the adrenal androgens dehydroepiandrosterone (DHEA) and its sulphate (DHEAS). The cells are arranged in a net like pattern, hence its “reticular” name.
The inner part of the adrenal gland is the medulla, which consists of chromaffin cells grouped around blood vessels. The medulla secretes the catecholamines, adrenaline and noradrenaline, and small amounts of dopamine under sympathetic nervous system regulation. It arises from the neural crest in embryology, therefore differing from the adrenal cortex in origin.

1.5 Aldosterone function:

On its release, aldosterone binds to MRs predominantly within the cytosol of epithelial cells of the renal connecting tubule and collecting ducts of the kidney. It has also been shown to exert effects upon the colon and parotid glands. On binding to the receptors within the cytosol, the MR complex dimerises upon aldosterone’s activation, and heat shock protein 90 is dissociated. This allows the hormone receptor complex to migrate to the nucleus, where it inserts itself into a specific DNA sequence (steroid response elements, SRE). The process then begins whereby targeted genes are expressed to exert aldosterone’s function on epithelial cells. The ultimate goal is sodium reabsorption [30]. Early effects of aldosterone gene expression include signalling for proteins that lead to post translational changes to ion channels. Na^+/ K^+ ATPase functions as a transporter on the epithelial Na^+ channel (ENaC) within the epithelial cell membrane monolayer, to exchange Na^+ for K^+. As Na^+ is reabsorbed into the cell, water follows. Aldosterone has also shown to increase expression of the $Na^+/K^+/$ Cl- cotransporter, and the Na^+/H^+ exchanger (NHE3) to enable Na^+ movement. ENaC is supported by various

signalling proteins, which are seen to rise 15-30 minutes post aldosterone's arrival. These proteins are serum- and glucocorticoid regulated- kinase 1 (SgK) and Kirsten- Ras GTP- binding protein A (Kir-Ras A). SgK is thought to phosphorylate the ENaC, whilst Kir-Ras A is thought to maintain the patency of the ENaC to maximise its potential. The presence of aldosterone also increases the activity of the lipid kinase PI3K, although aldosterone is not directly responsible for its expression. PI3K seems to work synergistically, aiding aldosterone, insulin, and antidiuretic hormone to use the same pathway to act via the ENaC and Na^+/ K^+ ATPase [31, 32]. Lastly, corticosteroid hormone induced factor (CHIF) is only expressed within the basolateral membrane of the epithelial cells. It is highly expressed at times of low sodium concentration and provides a specific structural and functional support to the Na^+/ K^+ ATPase [33].

The MR has a high affinity for most steroids as well as aldosterone, including cortisol, progesterone, deoxycorticosterone, and corticosterone. Cortisol has a higher affinity for the MR and is present in the circulation at concentrations a log order greater than aldosterone. Its serum concentration is almost 1000-fold higher and plasma 100 times, due to 95% of it being protein bound [34]. Its illicit occupation of the MR is prevented by the efficient action of 11 β hydroxysteroid dehydrogenase 2 (11-BHSD2). This enzyme converts cortisol to cortisone, such that cortisol is unable to occupy the MR receptor. When cortisol is bound within the receptor, it acts as an aldosterone antagonist in that the same effect is not executed within the cell, but it does still have deleterious effects such as oxidative stress and tissue damage.

Genetic mutations of 11-beta HSD2 or consumption of large quantities of liquorice result in the deficient conversion of cortisol to cortisone and a clinical picture similar to PA (hypokalaemic hypertension with a suppressed renin) appears, although circulating aldosterone concentrations are low [35]. MRs are also found in vascular endothelium and in the heart. Their role at these locations is not fully understood, but it is thought they are involved in maintenance of cardiac electrophysiology and cardiomyocyte function [36].

1.6 Foetal adrenals:

The adrenal glands arise from two different embryological origins. The adrenal cortex originates from the intermediate mesoderm and the adrenal medulla from the neural crest cells. The adrenal glands and gonads (adrenogonadal primordium) have a close ontogenic partnership, originating as the coeloemic mesoderm adjacent to the urogenital ridge. At 4-5 weeks, steroidogenic factor 1 (SF1), a key regulator protein of gonadal and adrenal development, marks the adrenogonadal primordium [37]. SF1 studies in mice models and human foetal observations have indicated failure of the gonads and adrenals to develop, should SF1 be disrupted, making its disruption incompatible with life. Therefore, its importance cannot be stated enough [38] [39]. At 7-8 weeks, cells marked by SF1 migrate towards the intermediate mesoderm. The majority going on to form the gonadal primordium, whilst those expressing the most SF1 to form the adrenal primordium. By the 8th week, a structure resembling the cortex is ultrastructurally visible and shows signs of steroidogenic capability [40]. During this period, the adrenal starts to become encapsulated and expands rapidly. The cortex structure known as the foetal zone (FZ) begins to produce cortisol in response to ACTH by week 8. Studies have shown there is a fully functional hypothalamic -pituitary- adrenal axis at this stage, with cortisol produced in response to ACTH secretion and controlled by negative feedback mechanisms [41]. The foetal adrenal consists of an outer definitive zone, a transition zone and the FZ. The FZ develops a close working relationship with the placenta during foetal life and therefore the majority of the hormones it secretes are DHEA and its sulphate DHEAS, which is synthesised by the placenta to form oestrogen. This interplay develops as the placenta is unable to produce oestrogens de novo due to the lack of P450 cytochrome enzyme CYP17 [42]. The foetal zone produces more steroids in this period of life than at any other time, but interestingly the foetal adrenal produces no aldosterone. Whilst the adrenal primordium is developing neural crest cells, chromaffin cells begin to migrate into the forming adrenal gland and start to form the adrenal medulla. This will go on to secrete adrenaline and noradrenaline. In contrast, the gonads remain bipotential for longer and it is upon secretion of *SRY* and, subsequently, *SOX9* gene in the XY determined foetuses, that testicular development begins. Testicular development and the development of the male phenotype is largely dependent on steroidogenesis. Upregulated so called ‘adrenal’ genes in the foetal testes reflects this [43].

Due to their shared origin, it is no surprise that foetal adrenals and gonads share similar expression of certain genes and that disruption in these genes can lead to pathology in both organ systems [44].

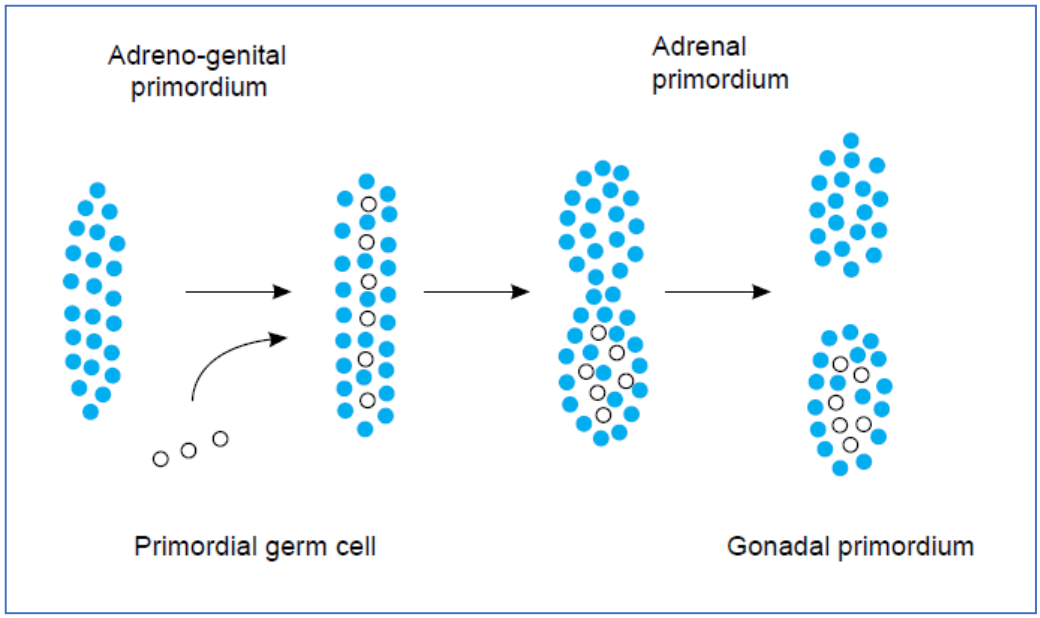

Figure 1 5: Diagram of the adrenal gonadal primordium formation, highlighting their shared origin [37].

1.7 Diagnosis:

Less than 1% of patients with PA are ever diagnosed. This is in part due to the significant diagnostic challenge the condition poses to clinicians. In addition, it has not been at the forefront of their differential list because it has become embedded in clinical thinking that PA is rare and invariably associated with spontaneous hypokalaemia; neither is correct. According to Endocrine Society guidelines, the diagnosis of PA should be considered in patients who meet the following clinical criteria: hypertension with hypokalaemia or diuretic-induced hypokalaemia, hypertension and an adrenal nodule, an uncontrolled blood pressure greater than > 140/90 mmHg on three antihypertensive medications, a controlled blood pressure of 140/90 mmHg on four antihypertensive medications, hypertension in association with sleep apnoea and lastly patients below the age of 40 with a diagnosis of hypertension or who have had a cerebrovascular event and a family history of PA [1]. Diagnosis is usually confirmed firstly via peripheral serum tests of renin, potassium, and aldosterone. It is important that a non-salt-restricted diet is adopted two weeks prior to testing, normokalaemia is achieved and all medications affecting the RAAS are stopped where possible (see Figure 1 7 below for medications and their interactions).

1.8 Investigations:

1.8.1 Renin:

Renin is usually measured as either plasma renin activity PRA or active renin mass concentration (ARC). The assay for PRA measures angiotensin I levels, in vitro, arising from angiotensinogen when incubated in plasma renin. This is a radioimmunological assay, whereby radioisotope antigens attach themselves to angiotensin I, and the renin activity associated is calculated. It is susceptible to false positives and negatives in conditions of low or high angiotensinogen. False positives arise in conditions such as liver disease and heart failure, and false negatives in high oestrogen states [45]. Measured in ng/ml/hr, the reference range for normal PRA is 0.6-4.3 ng/ml/hr and 0.5-3.5 when measured in nmol/l/hr. The ARC assay on the other hand is a chemiluminescent assay and was established to be a more stable form of renin measurement. Samples do not need to be taken on ice. It is independent of endogenous angiotensinogen levels and can be calibrated against an international reference standard. The assay arose from the development of a renin monoclonal antibody, and as angiotensinogen is not measured the assay is more reliable and reproducible. ARC is measured in ng/L. Reference range is from 7 ng/L –25 ng/L supine and from 12 ng/L - 43 ng/L erect.

In a study by *Unger et al* comparing 50 adrenal cortex lesions, 10 had confirmed PA (via imaging, confirmatory tests and ARR), 7 were cortisol secreting, 12 were phaeochromocytomas and 21 were non-functioning. These were compared to 10 hypertensive and 23 normotensive volunteers. This study indicated that both PRA and ARC assays were reliable to aid the diagnosis of PA and that there was a marginal difference between the two assays. However, ARC was recommended as preferable because of the advantages highlighted above [45]. These results were further confirmed by *Morganti et al* in a 12-centre study. Both assays were deemed reliable but ARC had the superior advantage of interlaboratory reproducibility [46].

1.8.2 Aldosterone:

Aldosterone can be measured either in blood serum or urine. In serum, it is measured as pmol/L (picomole per litre) or ng/dL. Normal reference ranges are: 100 - 450 pmol/L or 3-16 ng/dL supine, and 100-800 pmol/L or 7-30 ng/dL erect. It is best measured two hours after waking and when patients have been in a recumbent position for 5-15 minutes. Aldosterone is measured through a chemiluminescent immunoassay or radioimmunoassay. In a chemiluminescent assay, the true marker of the analytical reaction is a luminescent marker. In direct chemiluminescence assays, ruthenium esters and acridinium are used as luminophores, whilst in indirect assays these are dependent on enzymatic reactions. In these cases, alkaline phosphatase with adamantyl 1, 2-dioxetane aryl phosphate (AMPPD) substrate and horseradish peroxidase with luminol is used.

The chemical reaction within the assay leads to electrons moving from an excited state into a ground state and releasing energy, which is emitted as light with wavelength, λ = 300–800 nm [47]. Chemiluminescent immunoassays were revolutionary when first discovered. They hold a significant number of advantages: they are highly specific, quick to perform and are stable experiments with low consumption of reagents. The disadvantages are limited antigen detection and high cost to perform.

The other method of aldosterone measurement is through radioimmunological assay. Radioimmunoassays were first described in 1960 for the plasma measurement of the hormone insulin. Most plasma hormones are measured this way. Within these assays, a radiolabelled antigen competes with a known amount of so called "cold" antigens for antibodies and receptor sites. The radioactive isotope often used are ^{125}I or ^{131}I. As more of the "cold" antigens are introduced the radioactive antigens are displaced and can be measured. A secondary antibody is introduced to the antigen- antibody complex and precipitation is performed to determine bound from unbound antigens. This technique is extremely sensitive and specific. Whilst the machinery required is costly, the assay overall is inexpensive. The only drawback is that radioactive components are used.

One study in 168 patients showed that the overall correlation for aldosterone in a chemiluminescent assay and radioimmunoassay was highly significant ($R = 0.782$; $P < 0.001$). This has been confirmed in previous literature [48].

A fully suppressed renin of < 0.6 ng/ml/hr (normal reference range: 0.6 – 4.3) or +/- hypokalaemia, K^+ <3.5 mmol/l (normal reference range: 3.5-5) and an aldosterone level > 550pmol/l is considered diagnostic by society guidelines.

1.8.3: Aldosterone Renin Ratio:

A positive ARR is the most reliable screening test. This is a constant less likely to be susceptible to day-to-day fluctuations. It has grown in popularity over the last few years, as both renin and aldosterone measurements are considered, and this is more reliable than either factor alone. The ARR is calculated in ng/dL of aldosterone per ng/(ml/hr) of renin. It can also be given in pmol/L per µg/(l/hr), where aldosterone is in molar concentration. One can convert the former to the latter by multiplying by 27.6. An ARR >23.6 ng/dL per ng/ml/hr has a sensitivity of 96.8% and specificity of 94.1%, so any value below this ARR value is indicative of a low likelihood of PA [49, 50]. ARR is not only more sensitive for diagnosing PA but patients with elevated ARRs in the general hypertensive population have also been shown to have unfavourable renal and cardiac outcomes [51, 52].

	PRA (ng/ml/h)	PRA (pmol/l/min)	ARC (mU/L)	ARC (ng/L)
Aldosterone (pmol/l)	750 1000	60 80	91 122	144 192
Aldosterone (ng/L)	20 30 40	1.6 2.5 3.1	2.4 3.7 4.9	3.8 5.7 7.7

Figure 1 6: Table adapted from Endocrine society guidelines on thresholds for diagnostic ARR dependent on assays. Taken from *Funder et al* [1].

Another challenge is capturing so-called “clean” biochemistry. Commonly used agents work upon the RAAS system and therefore affect the interpretation. Factors affecting the ARR and leading to false positive or negatives are highlighted in the table below.

Cause	Effect on Renin (Mass)	Effect on Aldosterone	Effect on ARR (Mass)
Electrolytes:			
Hypokalaemia	Unchanged/Increased	Decreased	Decreased
Potassium Loading	Unchanged	Increased	Increased
Sodium Restriction	Increased	Increased	Decreased
Sodium Loading	Decreased	Decreased	Increased
Medications:			
ACE inhibitors	Increased	Decreased	Decreased
Angiotensin II type 1 receptor blockers	Increased	Decreased	Decreased
Potassium wasting diuretics	Increased	Unchanged/Increased	Decreased
Potassium sparing diuretics	Increased	Increased	Decreased
Calcium Blockers	Increased	Unchanged/Decreased	Decreased
Alpha Blockers	Decreased	Decreased	Increased
Beta Blockers	Decreased	Decreased	Increased
Other:			
Pregnancy	Increased	Increased	Decreased
Menstruating Women*	Decreased	Unchanged/Increased	Increased
Advancing Age	Decreased	Decreased	Increased
Renovascular Hypertension	Increased	Increased	Decreased
Malignant Hypertension	Increased	Increased	Decreased

Figure 1 7: Chart indicating the effect of various conditions on renin Mass, aldosterone, and ARR. * In premenopausal, ovulating women, plasma aldosterone levels measured are like those of men but rise briskly in the luteal phase of their menstrual cycle. Because women's renin levels are lower, the ARR is higher than in men for all phases of the cycle, but especially during the luteal phase.

In absence of hypokalaemia, further confirmatory tests are recommended to check for raised ARR in the context of normal salt to avoid the risk of false positive ARRs undergoing further invasive tests.

1.8.4 Confirmatory tests:

If there is no evidence of hypokalaemia, a suppressed renin, or a plasma aldosterone concentration below 20 ng/dl (550 pmol/l), then further confirmatory testing is advised. It is estimated that up to 50% of raised ARR's aldosterone levels when challenged with confirmatory tests will suppress normally [53]. The skill is in demonstrating an insuppressible aldosterone level in the context of a high salt diet.

The four confirmatory tests as recommended by society guidelines include fludrocortisone suppression test (FST), saline infusion test SIT, captopril challenge test (CCT) and oral sodium loading. There is no gold standard as to which test should be performed and this choice is up to local endocrinologist preferences and resources.

The fludrocortisone suppression test has been deemed by specialists as the most reliable of the PA confirmatory tests. However, it is time intensive, costly and requires hospital admission. The test comprises an inpatient stay where the patient is given 0.1mg of fludrocortisone, a pharmacological synthetic form of aldosterone, every 6 hours for 4 days. This is accompanied by salt loading 30 mmol three times per day, aiming for a urinary sodium excretion rate of at least 3 mmol/kg body weight. Urea and creatinine are checked daily, as well as potassium and blood pressure. Potassium is replaced, aiming for roughly a concentration of 4 mmol/l. On the fourth day, aldosterone is measured alongside cortisol, taken at 7 am and 10 am. An aldosterone level of >6 ng/dl (170 pmol/l) at 10 am with a suppressed renin confirms a diagnosis of PA. It is essential that the cortisol samples are reviewed and that the 10 am cortisol level is below the 7 am cortisol to ensure there is no ACTH effect upon aldosterone [1]. This is deemed one of the most sensitive tests and less invasive than other confirmatory tests, but it is difficult to perform on patients as outpatients.

The following two tests, the SIT and the CCT, are better known as they are readily performed in day case units. The SIT is comparable to FST [54]. Patients lie in the recumbent position for 4 hours and have 2 litres of 0.9% saline infused. For best practice, the patient is sat recumbent for 30 minutes to 1 hour prior to starting. This test is undertaken usually in the morning at around 9-10 am. Blood pressure and blood tests for plasma renin, plasma aldosterone, serum potassium, and cortisol are drawn at the start and after 4 hours. An aldosterone level of > 10 ng/dl (280 pmol/l) indicates PA is highly likely. Where the level is <5 ng/dl (140 pmol/l) PA is not the diagnosis. The difficulty arises when the aldosterone level is between 5-10 ng/dl (140-280 pmol/l). *Giacchetti et al* reviewed the SIT in 157 patients with a raised ARR, and found the sensitivity and specificity of the SIT to be almost 100% when the aldosterone was > 7ng/dl (190 pmol/l) in patients with a raised ARR above 40 [55]. Once again cortisol is reviewed for ACTH effect. SIT is contraindicated in patients with severe uncontrolled

hypertension, severe hypokalaemia, cardiac arrythmia, or patients in cardiac or renal failure. Therefore, other options must be reviewed.

A further confirmatory test option is the CCT. Patients are given 25-50mg of captopril orally and plasma renin, plasma aldosterone and cortisol are measured 1 hour post captopril and at 2 hours. The patient is kept in the recumbent position for this period of time. A diagnosis of PA is confirmed when the test fails to suppress aldosterone by >30% and renin remains suppressed. The CCT has been criticised by researchers for giving false negatives, leading to caution in interpretation [56, 57].

The oral sodium loading test is seldomly used within the UK and like SIT is contraindicated in several conditions. It involves patients increasing their sodium consumption to >200 nmol/l (~6g) per day for 3 days. Diagnosis is based on urinary aldosterone concentrations. Urine must be collected over 24 hours, leading to the unpopularity of this test. The advantage of 24-hour urinary aldosterone collection is that it is independent of circadian rhythms.

1.9 Lateralisation studies:

1.9.1 Adrenal Vein Sampling (AVS) and Computed Tomography (CT):

The next challenge is distinguishing unilateral from bilateral disease: identifying the unilateral aldosterone producing adenoma from the bilateral/unilateral hyperplasia. This is called subtyping. Tests can be multiple, time intensive and invasive. However, when lateralised correctly, >90% biochemical success is achieved in patients selected for adrenalectomy, which is the gold standard treatment for unilateral disease. These tests fail to predict who will be completely cured of hypertension but give patients the best chance.

With the development of less invasive radiological advances over the antiquated retrograde adrenal phlebotomy, it was considered whether higher quality imaging modalities, such as CT developing so called “finer cuts” and magnetic resonance imaging (MRI), may take the forefront of lateralisation. Unfortunately, MRI has held no advantage over designated CT adrenal scans due to its increased expense and poor spatial resolution. Although promising, the CT scan has also faced its own challenges [1]. Most APAs are smaller than 3 cm in diameter and microadenomas can be less than 1cm. This makes them difficult to visualise on CT, and they may therefore be wrongly interpreted as hyperplastic tissue. Adrenal incidentaloma, non-cancerous, non-functioning adenomas are extremely prevalent and increase with age (5% of all CT abdomens) [58]. The CT struggles to identify the endocrinologically hot nodule from the more commonly seen type that are “without function”. Multiple studies have attempted to compare AVS and CT, and overall lend superiority to AVS. One such study by *Young et al* took 203 patients with PA and compared CT with AVS. Based on CT findings, 21.7% would have not been referred for adrenalectomy and 24.7% would have undergone an inappropriate adrenalectomy by wrongly identifying an APA [59]. Another study by *Kempers et al* concluded that 37.8% of CT findings did not match those of AVS and subsequently would have led to 19.1% of patients not undergoing adrenalectomy and 14.6% undergoing an inappropriate one. 3.7% of patients would have undergone an adrenalectomy for the wrong side [60]. A prospective randomised control trial of 200 patients compared AVS with CT but found no benefit to subsequent treatment, with surgery or medication, or to intensity of antihypertensive medications or clinical benefit one year later [61].

1.9.2 Adrenal Vein Sampling (AVS):

AVS is the front runner and recommended [1] procedure for subtype diagnosis and has been used for four decades. Its availability to the patient population, however, is dependent on centre and the skill of the radiologist. Very few centres left in the United Kingdom offer it as a service. It should also be reserved for only those patients wishing to pursue a surgical treatment option, should that be the outcome.

Despite it being considered the "gold standard" there is no standardised protocol or interpretation of criteria. Therefore, there is no unified practice within the speciality. Due to it being costly and technically demanding, few centres are able to perform it to a high standard. Though practice differs, the various criteria do tend to have three similar components. Firstly, the selectivity index (SI), which the ratio of the cortisol of the adrenal vein to the IVC (periphery). This determines whether the catheter was correctly placed within the adrenal vein. Secondly, the lateralisation index (LI), which is calculated by dividing aldosterone by cortisol from each gland. It is upon comparing these results that we can determine which gland is suppressed and which is hypersecreting. The third criterion is whether the AVS is performed under ACTH stimulation or not. Within institutions, the lateralisation index cut off varies, but society guidelines recommend a value >4. This gives a 95% sensitivity and 100% specificity. Below a value of 3 is considered bilateral disease [59]. It is stipulated that a selectivity index between >2 in unstimulated and >5 stimulated is considered successful cannulation [62, 63].

Prior to an AVS, the patient undergoes a CT adrenal to rule out the extremely rare, but life threatening, adrenal cortical carcinoma (ACC). This is seen in less than 1-2 per million people, of which less than 2.5% secrete aldosterone. Its detection is nevertheless vital prior to proceeding with an APA diagnosis [64]. AVS by society guidelines is not recommended in patients under 35 years of age with a clear unilateral adenoma identifiable on CT, spontaneous hypokalaemia and aldosterone excess, making this group of patients exempt. Another group, are those with large adenomas, > 4cm, which are automatically removed surgically, due to the risk of ACC. Other patients must be once again "washed off" interfering medications for the appropriate time points per drugs, have had a free salt diet and be normokalaemic.

AVS is usually performed as a day case procedure in the morning following a minimum one-hour recumbent lie. The procedure occurs under local anaesthetic. The femoral artery is accessed percutaneously, and the catheter fed up into the inferior vena cava (IVC). The right adrenal vein is then cannulated roughly at the thoracic level of T11-T12. The right adrenal vein comes directly off the IVC, whilst the left adrenal vein unites with the inferior phrenic vein, forming a common trunk draining directly into the left renal vein (see figure 1 8). Depending on operator preference, some are able to cannulate both sides simultaneously, whilst in other cases

one vein is cannulated after the other. After both veins are cannulated (positioning is confirmed by contrast injection and X-ray), samples are taken for aldosterone and cortisol. The most common reason for an unsuccessful procedure is failure to cannulate the right adrenal vein. There is currently much debate as to whether accessory hepatic veins are present that lead to the technician's error and false cannulation. Researchers have indicated that, in 8-16% [65] [66] of cases, extra hepatic veins were present. There has also been evidence of further accessory adrenal veins present in some patients. Cannulation of the right vein as opposed to an accessory vein can occasionally be confirmed if discomfort arises when contrast is injected. Complications of AVS include vein rupture and haemorrhage, which can lead to abdominal discomfort.

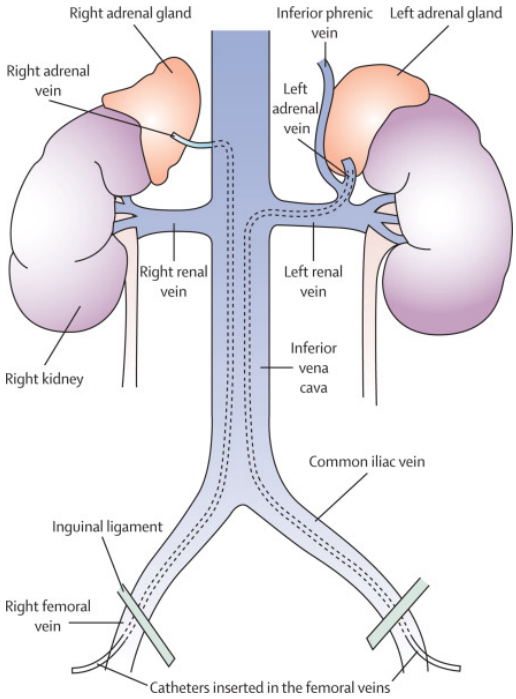

Figure 1 8: Highlights the underlying anatomy and catheter placements during AVS [67].

1.9.3 ACTH vs no ACTH stimulation:

There has been much debate for endocrinologists as to whether synthetic ACTH, so called cosyntropin, should be administered during AVS or not. This was first proposed in 1979 by *Weinberger et al* to overcome the pulsatile nature of aldosterone that may become heightened at times of stress [68]. Cosyntropin is either administered as a continuous infusion, given 30 minutes before and during the procedure at 50µg/h or as a bolus of 250µg.

Cosyntropin is used for the following reasons. It minimises stress fluctuations in aldosterone that can be induced during the procedure, particularly when each vein is cannulated independently. Studies have shown it increases the SI, the marker of successful cannulation of the adrenal vein. It increases the levels of cortisol and therefore the gradient between the adrenal vein and IVC is maximised. It is because of this that the consensus for SI cut off values is the following: for unstimulated AVS the SI index is lower at 3, sometimes even 2 whilst, for those stimulated, it is >5. The AVIS-2 study, a multi-centre review of 1625 AVS studies, indicated that the higher the SI cut off, the more unstimulated AVS failed to meet the cannulation criteria. It was, therefore, deemed to have "failed". Cosyntropin also maximises the secretion of aldosterone from the APA. However, this may also be the case from the contralateral side. The AVIS-2 study also illustrated stimulated AVS reduced lateralisation rates, therefore reducing the chance of identifying the dominant side [69]. Smaller studies however have suggested this can be mitigated by lowering the dose of ACTH given [70] [71]. Some institutions also calculate a contralateral suppression ratio alongside a lateralisation index, to help identify the pathological side. Contralateral suppression indicates lack of aldosterone production on the non-dominant side, the ratio is calculated as: ((Aldosterone)/(Cortisol))ContralateralAV/((Aldosterone)/(Cortisol))PV. Contralateral suppression, CLR≤1 [72].

It has been reported that 5-21% of all APAs also co-secrete cortisol [73-75]. This can sometimes pose a challenge with AVS, as the cortisol value is used to ensure successful catheterisation and correct dilutional value of aldosterone. The cortisol will become very high on the dominant side and suppressed on the other side, leading to a falsely low SI and LI on the culprit side. To avoid this, some clinicians have looked to measuring other hormones such as metanephrines [76] [77].

1.9.4 Nuclear medicine scans:

In recent years, there has been another contender who has come to the forefront to help the lateralisation challenge: the radio labelled ligand used in conjunction with positron emission tomography [78] with high resolution CT. Several isotopes have been developed to aid the imaging of APAs, and with the scope to take over AVS. Once such isotope is ^{11}C- metomidate, a potent inhibitor of the enzymes, CYP11B1 (11-betahydroxylase) and CYP11B2 (aldosterone synthase). First developed in Uppsala, Sweden patients with adrenal adenomas were scanned with ^{11}C- metomidate, a methyl analogue of etomidate. The study concluded that patients with known PA (confirmed on histology) had the highest standard uptake value (SUV) of isotope [79]. The standardised uptake value (SUV) is a value for quantifying the activity and uptake of tracer within a lesion. The higher the value, the more metabolic the lesion and the more tracer is seen within it. Further work on ^{11}C- metomidate was carried out in Cambridge by *Burton et al,* who compared ^{11}C- metomidate PET scans and AVS results in 40 patients with known unilateral disease, bilateral disease or incidentalomas. Their findings confirmed a previous study by *Jennings et al,* that administering the steroid, dexamethasone, regularly 3 days prior to the scan significantly decreased the uptake of tracer in the normal adrenal, therefore increasing the specificity of the tracer for CYP11B2 and decreasing the competitiveness for CYP11B1. This study also determined, through a ROC curve analysis, that the calculated SUV max ratio to determine unilateral disease was 1.25 [80].

Our group's NIHR-EME funded "MATCH" study sought to determine whether **M**etomidate PET-CT was superior to **A**drenal venous sampling in predicting ou**TC**ome from adrenalectomy in patients with primary **H**yperaldosteronism. This was the largest prospective trial, with 142 patients recruited. The principal finding was that ^{11}C- metomidate PET was equal to predicting outcome from surgery as AVS and therefore an alternative lateralisation option. It also found that a higher proportion of patients were diagnosed with unilateral disease than usual practice leading us to question how much unilateral disease is being missed. [81] ^{11}C-Metomidate unfortunately has some limitations. Firstly, the uptake in the liver is high which due to its proximity to the right adrenal. This may lead to PET measurements becoming unreliable. Secondly, ^{11}C also has a short half-life (20 minutes) therefore limiting it to PET centres that have inhouse cyclotrons. It is because of this that further isotopes have been explored, such as ^{18}F-CETO. This tracer has a higher specificity for aldosterone synthase activity than ^{11}C- Metomidate and has overall less uptake in the liver and a longer half-life, therefore making it a viable alternative. [82] Current in vivo trials are underway not only as part of our MATCH study, which had a 25-patient extension for ^{18}F-CETO scans, but also in the Cambridge trials unit (ClinicalTrials.gov

identifier NCT04529018). Data is still preliminary, but it is suggested that there was a small difference between the ability of CETO or Metomidate to pick up unilateral adenomas (P=0.344). In general, it must be said however, CETO was overall in concordance with Metomidate over high, medium and low probability of unilateral adenomas. The SUV max by time of flight (TOF) was much lower in CETO over the liver**. Please note, preliminary data is taken from a British Endocrine Society abstract 2022 of Dr Emily Goodchild**. **"Novel radiolabelled ligand, Para-chloro-2-[18F] fluoroethyletomidate (CETO), compared to [11C] metomidate-PET (MTO) for the lateralisation of primary aldosteronism (PA)."**

1.10 Management:

1.10.1 Lifestyle:

Lifestyle changes, particularly reduction in salt consumption (<2g NaCl per day), is thought to be beneficial in controlling potassium loss, as well as blood pressure [83].

1.10.2 Medical:

In 1957, *Kagawa et al* synthesised the first MR antagonist (MRA). The development of these therapeutic antagonists was on the back of animal studies with high aldosterone expression. Spironolactone, the first MR antagonist, is a steroid lactone. Its structure comprises 17-alpha-pregn-4-ene-21, with 17-carbolactone substituted with an alpha-acetyl sulfonyl group at position 7 and an oxo group at position 3. It has a strong anti-mineralocorticoid effect, competing with aldosterone. [84] In particular, it affects Na^+ transporting epithelial receptors on the renal tract. Sodium, instead of being reabsorbed in exchange for potassium, is released leading to potassium retention.

Although not formally licensed outside the setting of pre-operative preparation, the clinical reality is that spironolactone is first-line medical therapy for PA patients, and this has been the case for the last five decades for those patients unsuitable for a unilateral adrenalectomy. The dose ranges from 25-400mg per day. Its effect on potassium sparing is usually seen within 48 hours, but its effect on blood pressure may take several weeks.

Spironolactone is a progesterone derivative, and like progesterone binds to plasma proteins. It also binds to the progesterone receptor, albeit with less affinity. This may still lead to side effects, which may be dose-dependent, such as erectile failure and gynaecomastia in men and menstrual irregularity in pre-menopausal women. Therefore, some patients require eplerenone as an alternative. This has little or no anti-androgen activity and has a greater affinity for the MR receptor. However, some studies suggest it does not have the antihypertensive effect to the level of spironolactone [85]. It requires twice daily dosing due to a reduced half-life (4-6 hours) and is significantly more expensive.

MRA treatment is usually first line treatment for patients with bilateral primary aldosteronism and familial hyperaldosteronism. It is also used in the run up to patients awaiting surgery for their APA, or those that have declined to proceed with surgery.

Landmark MR antagonist trials of spironolactone and eplerenone have been shown to significantly improve morbidity and mortality in cardiac heart failure, for example, in the Randomized Aldactone Evaluation Study (RALES) trial for patients with severe heart failure and a left ventricular ejection fraction <35%. The trial had to

be stopped early due to the overwhelming benefit to patients in the spironolactone receiving arm of the trial. They had a 30% reduction in morbidity and 35% reduction in hospitalisation rate. The Eplerenone Post-Acute Myocardial Infarction Heart Failure Efficacy and Survival study (EPHESUS) trial was comparable to RALES, especially when eplerenone was administered to patients with similar ejection fraction as those in RALES [86]. Curiously, although those studies are compelling, the mechanisms by which these beneficial effects occur are not clear. Possibilities include anti-inflammatory, anti-oxidative, and anti-fibrotic effects [36].

Whilst spironolactone and eplerenone are the forerunners of treatment, there is a possibility that, through the process of blocking the MR, they lead to raised levels of renin and aldosterone. This not only reduce the effectiveness of treatment, but aldosterone may then be free to target other receptors leading to end organ damage.

Another current medical option for PA is amiloride, a potassium sparing diuretic. This helps to retain potassium and lower blood pressure and is favourable as it has no effect on the androgen receptors. However, it does not directly block aldosterone, therefore cannot counteract the endothelial dysfunction caused.

A further option, having made their way through clinical phase II trials, are aldosterone synthase inhibitors. The oral aldosterone synthase inhibitor LCI699 has shown some promising effects in reducing blood pressure and aldosterone levels in PA. However, a challenge has arisen due to the proximity in structure of CYP11B1. LCI699 is not fully selective for CYP11B2, leading to concerns of hypocortisolism within these patients, which seems to become more evident with increasing dose [87, 88].

The outcomes of the phase II trials however have been promising. Braxdrostat was given daily for 12 weeks at varying doses of 0.5mg, 1mg and 2mg. The patients on 2mg had a greater reduction in blood pressure. In this study of 248 patients, there were no episodes of hypocortisolism [89].

1.10.3 Surgery:

The gold standard treatment for unilateral disease is laparoscopic adrenalectomy. First described in 1992 by *Gagner et al* [90], laparoscopic adrenalectomy soon became the operation of choice for adrenal gland removal. The size of the gland lends itself well to this technique. The benefits of laparoscopic compared to open surgery are multiple. It is minimally invasive, leads to a shorter hospital admission, quicker recovery time with less dependency on analgesia and is cosmetically more pleasing. Due to the anatomy of the adrenal gland, multiple approaches have been approved, including lateral trans retroperitoneal, transthoracic, or lateral and posterior retroperitoneal [91]. Complications are rare in laparoscopic adrenalectomies. The morbidity of the procedure is

6.7-6.8%, whilst the mortality rate is <0.5% [92]. Complications may include infection, small bleeds and, rarely, pneumothorax from the trocars. The most common complication likely to lead to open conversion of the abdomen is a vascular injury; most notably, a liver injury or injury to the IVC due to their anatomical proximity to the right adrenal gland [93]. Unfortunately, laparoscopic adrenalectomy practice suffers the same shortfall as AVS. A study in the US suggested 90% of adrenalectomies were performed by surgeons who dedicated <25% of their workload to endocrine surgery, with 50% of adrenalectomies being performed by surgeons who performed 1-2 per year [94]. This leads us to suggest that fewer centres with more experienced surgeons may be the future of practice.

The reported success rate of adrenalectomy for unilateral disease has varied greatly across centres: between 20-72%. These studies represented success as patients being normotensive off all antihypertensive medications [95] [96] [97]. *Williams et al* held an international consensus on outlining a set of criteria that could determine what success post adrenalectomy for unilateral adrenalectomy would look like. This was called the PASO (Primary Aldosteronism Surgical Outcome) criteria [98]. This consensus comprised 31 international experts including 6 surgeons from 28 centres world-wide. Six outcomes were agreed upon: complete, partial and absent clinical success, and complete, partial and absent biochemical success. These were based on blood pressure, antihypertensive medication, potassium levels and renin and aldosterone. Data was reviewed at 6 and 12 months post-surgery. Of 699 patients within this study, complete biochemical success was seen in 95% of them, with complete clinical success in 37% and partial clinical success in 47%. Therefore, success rate did not differ too greatly to previous studies, which had ranged between 16-72%. What the PASO study did illustrate, which has led on to *Burrello et al's* work, is the need for a prediction score for those patients who would do well from surgery. Factors that lead to patients doing well from surgery are the following: female sex, younger patient, and patients with a lower BMI. These patients tend to have a more successful clinical outcome, along with fewer antihypertensive medications, shorter duration of PA, and no evidence of end organ damage such as LVH [99].

1.10.4 Adrenal sparing interventions/ Radiofrequency ablation (RFA):

As documented above, the gold standard treatment for unilateral PA is surgery, but this entails the complete removal of the adrenal gland for a benign condition. Intrabdominal surgery is not risk free and can be a financial cost to healthcare institutions. It is with this in mind that more adrenal cortex sparing options have been explored. In recent years the development of thermal ablation techniques of adrenal lesions has included cryoablation, microwave ablation and radio frequency ablation (RFA). RFA has been increasingly utilised in primary and secondary malignancies, such as pancreatic, liver, lung, oesophagus, kidney and bone. Radiofrequency is an electromagnetic wave frequency from approximately 10^4 to 3 x10^{12} Hertz (Hz), between infrared and audio waves. RFA uses energy harnessed from radio broadcasting waves for the destruction of biological tissues. The frequency used is usually within the range of a medium wave for radio broadcasting (300-3000 KHz), the most optimal being around 500 KHz. This is sufficient to cause molecular frictional heating, but still low enough to give controlled energy to a defined place [100]. This wavelength is deemed safe when used correctly, as it does not lead to over radiation and triggering of neuromuscular junctions. The probe is also insulated leading to heat reaching the desired place.

Almost all studies to date involving RFA of adrenal lesions were performed percutaneously under CT or ultrasound guidance, and in patients with ACC, adrenal metastases, and patients with PA. Most studies have also been single centre studies, small and retrospective. Several studies have performed percutaneous RFA on APA with promising results. For example, *Liu et al* performed RFA on 24 lesions. In 23 patients, PA was cured biochemically with normal ARRs documented at 6 months [101]. *Szejnfeld et al* performed 9 RF ablations on patients with confirmed APA, 8 of whom had a significant reduction (p=0.008) in aldosterone and (p=0.001) in blood pressure [102]. *Yang et al* compared 7 APA who underwent RFA with 18 similar sized APA who underwent laparoscopic adrenalectomy. They reported 100% success rate in the RFA group compared to 94.4% in the adrenalectomy group [103]. However, these three studies did not strictly use the PASO criteria to measure successful outcome [98]. Studies that did incorporate PASO criteria to measure successful outcome included *Bouhanick et al,* who performed a prospective study on 30 RFA patients. In these patients successful clinical and biochemical success was achieved in 47% of patients [104]. *Cano-Valderrama et al* performed a retrospective study comparing 24 adrenalectomies to 10 RFA procedures. 29.2% of the adrenalectomy group had complete cure compared to 0% in the RFA group. 50% of the adrenalectomy group achieved partial cure compared to 70% of the RFA group [105].

RFA has sparked interest to specialists in the field as an alternative option to surgery for PA. Firstly, it spares the remaining cortex and adrenal gland, which is appealing in an otherwise benign condition. It is also associated with a shorter hospital admission, less anaesthetic and could be more available to patients with comorbidities, where surgery is not an option. It is also thought to be less costly, saving public run health systems money in the long run. *Costa et al* put the difference in cost of RFA to be 2-3 times lower than surgery [106]. The risks of RFA include haemorrhage, perforation of major organs, infarction, pneumothorax and pain. Hypertensive crisis during the procedure has also been reported. Hypertensive crisis is considered when the blood pressure intraoperatively rises to above 180/120 mmHg. Most often, the cause is catecholamine surge following irritation of the medulla. Multiple studies have reported hypertensive episodes during RFA to the adrenal gland [107-110]. The general consensus has been that one should alpha and beta blockade with antihypertensive medications, as one does prior to a phaeochromocytoma excision. The risk is thought to be mitigated by appropriate alpha and beta blockade of the patient prior to the procedure. One PA RFA study did not alpha and beta blockade prior to RFA and 8 out of the 12 patients (67%) had a hypertensive crisis. All resolved afterwards [111]. In other studies where alpha and beta blockade was used, the risk was lower.
Endoscopic RFA under ultrasound guidance is a well-practised therapeutic option for patients with pancreatic malignancy or benign cysts, however it has never been utilised before for the adrenal gland. The left adrenal gland sits anatomically next to the stomach, so it was with this in mind that our group proceeded to design a multicentre phase 1 study. This study was to determine the safety and efficacy of endoscopic ultrasound-guided ablation as a nonsurgical, adrenal-sparing treatment for aldosterone-producing adenomas, the **FABULAS study:** Feasibility study of Radio**F**requency endoscopic **AB**lation, with **UL**trasound guidance, as a non-surgical, **A**drenal **S**paring treatment for aldosterone producing adenomas (**FABULAS**).
The primary outcome of this study was to test that EUS-RFA of APA of the adrenal gland was a safe method. Secondary outcomes were to evaluate the efficacy of EUS ablation using biochemical and radiological measurements. This study is discussed in greater detail in the fourth chapter of this thesis.

1.11 Aetiology:

The most common form of PA is bilateral adrenal hyperplasia, which accounts for about 60% of PA. The second most common cause is the solitary unilateral sporadic APA, unilateral adrenal hyperplasia, or bilateral solitary APAs. Rarer causes include familial primary aldosteronism and aldosterone secreting ACCs.

1.11.1 Bilateral hyperaldosteronism:

Bilateral hyperaldosteronism is the most common cause of PA. It thought to be caused by bilateral adrenal hyperplasia or by bilateral APAs [112]. BAH usually arises sporadically. It has been difficult to perform cellular or genetic work on their adrenals, as these patients are often treated on pharmacotherapy and do not undergo surgery. It is believed the ZG hyperplasia is more Ang II and ACTH responsive leading to excess aldosterone. Another potential culprit within BAH could be the so-called aldosterone producing micronodules (APM) [35] or cell clusters as they were once called. These were first described by *Nishimoto et al,* when 1-3 mm autonomous APMs were found in > 30% of seemingly normal adrenals [113]. These discrete nodules were undetectable on H&E staining but appear on IHC particularly in the presence of the specific anti-sera CYP11B2 [29] [114]. APMs are nests of cells that lie underneath the adrenal capsule and often protrude into cortisol secreting areas of the cortex. They are also found adjacent to APAs in an environment which is usually suppressed and void of Ang II stimulation, next to the APA, suggesting they are autonomously driven.
What we have come to understand about APMs is the following. Firstly, that their prevalence increases with age and, secondly, that 25% of APMs found in 'normal' adrenals have the same mutations such as *CACNA1D* and *ATP1A1* like ZG- like APAs [114, 115]. This rises to 60% of the APMs which underlie 15/16 cases of bilateral 'hyperplasia' [116]. It has never been clear how the transition from ZG cells to APA arises and Nishimoto has gone further and described potential APM to APA transitional nodules driven by somatic mutations [113].

1.11.2 Familial Hyperaldosteronism:

In patients who have confirmed PA before the age of 20, and in patients with a strong family history of PA or stroke below the age of 40, genetic testing for familial hyperaldosteronism type I (FH-I) is recommended. FH-I is also known as glucocorticoid-remediable aldosteronism (GRA). It is characterised by a severe presentation of PA with significant hypertension, hypokalaemia, suppressed renin and raised aldosterone. Rarely patients can present with normal BP. It is autosomal dominant in inheritance and 1% of the PA population are affected. It leads to a chimeric gene for CYP11B1 and CYP11B2 leading to significant cross over and ectopic expression of aldosterone mediated by ACTH within the ZF. The hallmark of the condition is a build-up of the hybrid

steroids, 18-hydroxycortisol and 18-oxocortisol. A simple PCR of the *CYP11B1/CYP11B2* mutation can now be performed for testing. Treatment is often dexamethasone to suppress ACTH [117].

Familial hyperaldosteronism type II (FH-II) is also autosomal dominant, however, it is non glucocorticoid remediable with no response to dexamethasone. It is also difficult to distinguish its presentation from sporadic causes of PA. In families with FH-II it is important to look for a germline mutation of the voltage gated chloride channel CLCN2 [118].

Type 3 presents in early childhood with such a fulminant form of PA that bilateral adrenalectomy is usually required as it is so treatment resistant. The mutation is germline within the *KCNJ5* gene, which codes for the Kir 3.4 potassium channel. Mutations lead to continuous influx of sodium, as the channel loses its ion selectivity. The cell depolarizes leads to activation of the calcium signalling pathway described above [119].

Type 4 is very rare and presents as an autosomal dominant mutation of *CACNA1H* gene, which codes for a subunit of the L-voltage calcium channel.

1.11.3 Sporadic PA:

Landmark whole exome sequencing (WES) of APAs revealed ion-channel/transporter genes with recurring somatic mutations e.g. *KCNJ5, CACNA1D/H, ATP1A1* and *ATP2B3*. These mutations have paved the way for better understanding of adrenocortical pathology within PA and have supported the usual concept that divides PA into unilateral, curable APAs, and bilateral hyperplasia. [120], [121], [122], [123].

KCNJ5 gain of function mutations were the first to be discovered and account for around ~70% of mutations in European and Japanese populations [116]. The *KCNJ5* gene as described above codes for the Kir 3.4 potassium ion channel. The mutations most commonly seen are p.G151R which occurs within the ion channel and p.L168R, located near the selectivity of the ion channel. The ion channel is no longer able to maintain the strict Na^+, K^+ balance leading to a continuous influx of sodium into the cell. Depolarisation of the cell membrane and intracellular calcium activation leads to aldosterone production. These APA are larger, more solitary APAs and paradoxically resemble the normal adrenocortical ZF rather than the ZG cells, which are the physiological site of aldosterone production. They are more commonly seen in women and younger patients. *KCNJ5* mutant APAs often co-secrete cortisol in keeping with their cellular make up, albeit not at levels to cause clinical Cushing's syndrome, but often enough to fail an overnight dexamethasone suppression screening test.

Patients who harbour KCNJ5 mutations have much better outcomes with surgery and are more likely to be cured through surgical intervention [78, 124, 125].

APAs which resemble ZG cells have denser staining on immunohistochemistry (IHC) for CYP11B2 than the *KCNJ5*-mutant APAs. [123]. ZG-like APAs are often seen in men and are multiple and typically smaller than the *KCNJ5*-mutant tumours. They usually harbour somatic mutations for *CACNA1D/H* and *ATP1A1* and *ATP2B3*; these each account for <10% of all mutations. The *CACNA1D* gene encodes for Cav 3.2 and *CACNA1H* gene encodes for Cav 1.3. Gain of function mutations in this region affect conserved sites within the functional components of the L- and T- voltage gated channels. This leads to continual activation of these channels and a steady stream of calcium influx into the cells, and therefore aldosterone synthesis. These driver mutations have been more readily described in Afro Caribbean patients [126].

ATP1A1 and *ATP2B3* mutations account for 7% of all APAs. *ATP1A1* codes for the alpha subunit in the Na^+/K+-ATPase. Disruption of this leads to Na^+ influx and intracellular calcium signalling. *ATP2B3* codes for the plasma membrane calcium-transporting ATPase 3 and helps to maintain calcium homeostasis. Mutations lead to increased intracellular calcium concentration [122].

Other mutations have been uncovered that do not impact ion channels and have been of great interest for my work, as I discuss later in this thesis.

1.11 14: Aldosterone in pregnancy:

Aldosterone usually rises in pregnancy. By 8 weeks it has already increased by 4-fold and continues to increase to 10-fold by term [127]. The increase in aldosterone is brought on by an increase in renin, which is catalysed by increased angiotensinogen produced by the liver under the influence of oestrogen. The increased renin leads to increased angiotensin II levels, which acts on the ZG. This creates an environment of salt and fluid retention essential to maintain the growing placenta [128, 129].

PA in pregnancy is still relatively rare with only 80 cases documented in the literature. There is speculation it could affect up to 0.6-0.8% of pregnant women [129, 130]. In the first trimester particularly, the increasing progesterone levels could compete and mitigate the effect of aldosterone. Therefore, women do not present very obviously with PA in pregnancy and their blood pressure may even improve [131]. Another possibility is that with increasing vascular expansion in pregnancy, the maternal vessels become resistant to Ang II [132].

Diagnosis in pregnancy can be particularly tricky and, if the ARR does not meet the threshold, waiting until the postpartum period is recommended. There are no guidelines to guide the physician but, if the ARR is positive, medical therapy is recommended. AVS should be avoided along with CT, but an MRI can be performed to determine if it is unilateral or bilateral disease.

Pharmacotherapy is the treatment of choice in pregnancy. First line would be α-methyldopa, beta blockers, labetalol, and calcium antagonists, such as nifedipine. MR antagonists have no safety data for pregnancy and are not used. If the hypertension and hypokalaemia become unmanageable, adrenalectomy can be performed within the second trimester [129].

1.12: GNA11/GNAQ double mutations:

In 2015, the lab reported 3 patients who presented with explosive onset of PA, 2 during pregnancy and 1 in early menopause [121]. The index case was found on WES of 10 ZG-like APAs, being the sole APA without an ion-channel mutation. Inclusion of this APA in a microarray led to recognition of LHCGR, the receptor for LH and 'pregnancy hormone' (beta-HCG) as the most upregulated gene, by 750-fold, compared to other APAs. Targeted sequencing of Catenin Beta 1 (*CTNNB1)* identified the other 2 APAs. All 3 had somatic mutations of a ser/thr residue of exon 3. The 3 patients' APAs had similar increases in expression of LHCGR, GNRHR and GATA4. GATA4, a family member of the zinc finger transcription factors, is often seen in human foetal adrenals, but has usually disappeared by the time the adrenal reaches adulthood [133].

This prompted the identification of further patients with *CTNNB1* mutation. In total over the span of several years, we have found 10 patients. 9/10 were female patients, most presenting at pregnancy and one at menopause. The single male patient presented with the onset of augmented LH secretion at puberty. These patients came to be known as our British/Irish cohort [134]. The discovery of the pubertal male through WES led us to the discovery of a further mutation within his APA of the G-protein *GNA11,* at the position of Q209. When the British/Irish cohort was then rereviewed, they all contained a *CTNNB1* mutation in exon 3 which varied between S45F and P, G34E and R, T41A and S33C. They also all had an exon 3 G protein subunit alpha 11 (*GNA11)* p.Gln209 his or pro mutation, or its closely homologous *GNAQ*. This has not previously been described before in APAs. All 10 patients post definitive treatment of surgery have performed well; they remain normotensive 2-12 years after adrenalectomy, including a 52-year-old woman with an average BP 190/100 mmHg on 5 antihypertensive medications prior to surgery. We attributed the explosive onset of hypertension to activation by LH/HCG during times of elevated secretion, puberty, pregnancy and menopause. We attribute the noticeable high cure rate (n=10) to the short exposure to aldosterone excess, secondary to the short lived explosivity of its onset.

Through collaboration with groups in Paris and Sweden we were able to find further double mutant patients. In total our British/ Irish cohort consisted of 10 patients. The French cohort consisted of 5 patients who had a double mutation and the Swedish cohort contained one. The French and the Swedish cohort comprised all women, but it was difficult to determine those who had presented at time of pregnancy.

The following table is the complete clinical and biochemical outcomes of the 10 British/Irish cohort.

Patient ID	Gender	Age at surgery	Onset presentation	Tumor genotype		Measurements before adrenalectomy					Measurements after adrenalectomy				
				CTNNB1	*GNA11* *GNAQ*	SBP *mmHg*	DBP *mmHg*	Plasma renin *mU/liter*	Aldosterone *pmol/liter*	Serum potassium *mmol/liter*	SBP *mmHg*	DBP *mmHg*	Plasma renin *mU/liter*	Aldosterone *pmol/liter*	Serum potassium *mmol/liter*
1	Male	12	Puberty	S45F	Q209P	180	120	<2	1,358	2.7	110	75	7	74	4.2
2	Female	35	Pregnancy	S45P	Q209P	155	85	<2	559	2.6	123	76	16	283	4.0
3	Female	20	Pregnancy	T41A	Q209H	215	120	<2	1,330	2.5	121	68	N/A	N/A	N/A
4	Female	34	Pregnancy	S33C	Q209H	190	100	<2	2,885	2.0	111	69	31	250	4.1
5	Female	26	Pregnancy	S45F	Q209H	140	86	<2	2,590	2.0	120	70	N/A	N/A	N/A
6	Female	52	Menopause	G34R	Q209P	190	100	<2	672	3.1	118	79	9.0	158	4.1
7	Female	39	Pregnancy	S45F	Q209H	160	101	<2	2,382	2.5	120	83	16.1	124	4.7
8	Female	41		S45F	Q209P	160	90	<2	480	3.2	101	65	91	236	4.5
9	Female	23	Pregnancy	G34E	Q209H	167	114	<2	2000	3.3	121	85	N/A	N/A	N/A
10	Female	26	Pregnancy	G34R	Q209L	170	110	<2	603	4.1	123	78	14	408	4.7

Table 1.1: Comprehensive list of all the patients within the British/Irish cohort. *GNA11* mutations highlighted in purple and *GNAQ* in pink. Blood pressure measurements pre and post adrenalectomy, as well as biochemistry [134].

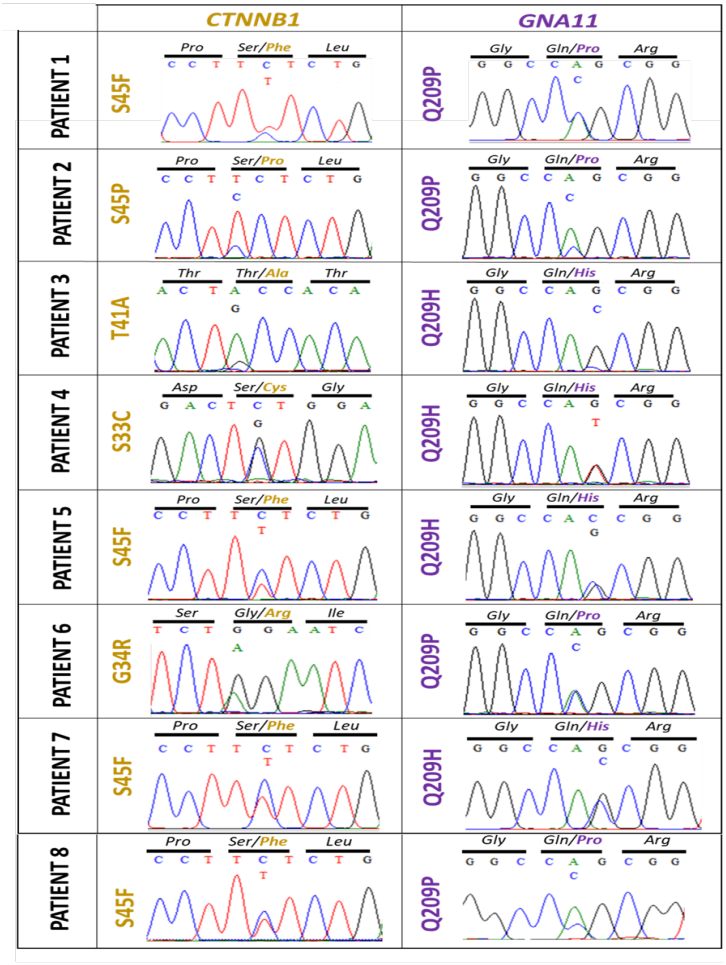

Figure 1 9: Sanger Sequencing of *GNA11* double mutant patients 1-8 within the British/Irish cohort. The left column illustrates the *CTNNB1* mutations; S45F, S45P, S33C, T41A and G34R. The *GNA11* mutations varied between Q209H and P.

1.13 *CTNNB1*:

The β-catenin / Wnt pathway is essential for adrenal development and maintenance and cell differentiation within the adrenal cortex, particularly within the ZG [135]. The Wnt signalling pathways are a collection of pathways that not only hold an important role in embryogenesis, ensuring the formation of the embryonic axes, but also hold crucial roles. These roles extend from embryogenesis to adulthood, in cell fate, cell differentiation, proliferation and migration. Wnt stimulates β-catenin accumulation within the cytoplasm of the cell, and β-catenin activates the T-cell factor/lymphoid enhancer factor (TCF/LEF) family, which is a family of multifunctional proteins that have specific gene targets to upregulate within the nucleus [136]. The following tumour suppressor complexes - glycogen synthase kinase 3 (GSK3), casein kinase 1 α (CK1α), axin, adenomatous polyposis coli (APC), protein phosphatase 2A (PP2A) - target β-catenin by forming complexes that phosphorylate it, therefore tagging it for ubiquitination, which leads it to be digested by the proteasome [137]. Wnt signalling inhibits this phosphorylation process. Inability of β-catenin to be phosphorylated and degraded leads to upregulation of the canonical pathways, which leads to problems such as tumour formations in cancer and diabetes. One of the most well-known mutations in Wnt is within the APC gene; this leads to bowel cancer.

B-catenin /Wnt signalling pathway mutations have been more commonly observed in adrenal cortical carcinomas (ACCs) rather than APAs. Around 40% of ACCs harbour *CTNNB1* mutations, whilst only ~5% of APAs do [138]. 20-30% of which comprise of *CTNNB1* mutations in exon 3 [139]. Published transcriptomes for ACC make no mention of *GNA11/Q* mutations [140] [139]. *CTNNB1* mutations mainly involve serine/threonine residues in the GSK3 binding domain in exon 3, like in our cohort of patients with the double mutation. In this study, *CTNNB1* mutations were found exclusively alone [138], however *CTNNB1* mutations have been described along with the mutation *CACNA1D* in other studies [126].

1.14 *GNA11/ GNAQ* mutations:

The *GNA11/GNAQ* genes encode for guanine nucleotide binding proteins, which make up part of the G-protein coupled receptor structure. G-protein coupled receptors are one of the largest families of transmembrane signalling receptors found in eukaryotic cells. They receive messages extracellularly and modulate/ transduce them into intracellular signals, which are then amplified. G-protein receptors are heterotrimeric, consisting of an extracellular N-terminus, an intracellular C-terminus and a 7-domain transmembrane component. A ligand with an affinity for the receptor binds to it, instigating a change within the transmembrane domains, which interact with a small number of G proteins to initiate intracellular signalling cascades. G-proteins are usually 3 units grouped together: alpha, beta and gamma. Activation arises when the G- alpha subunit is bound by GTP, and intracellular signalling occurs through the MAP kinase pathway. For example, G-protein couples aldosterone's main physiological stimulus, Ang II, to its intracellular signal, inositol triphosphate (IP3).

GNA11 was first identified in 1989 and encodes one of the alpha subunits (alpha 11). Its paralogue is *GNAQ*. *GNA11* has been found as a somatic mutation in 46% of primary uveal melanomas at the position of Q209 and R183 in GNA11 and *GNAQ*. It has also been recognised in blue naevi and conditions of vascular overgrowth (Sturge Weber syndrome). In some dermatological conditions, the underlying genetics form mosaicism, with the mutations having been found in different sites [141] [142]. *GNA11* mutations have also been identified in familial hypocalciuric hypercalcaemia type 2 and autosomal dominant hypocalcaemia type 2 [143]. Artificially introduced mutations at Q209 of *GNAQ/11* were shown in 1992 to cause continuous activation of GTPase, a decade ahead of their discovery in tumours and congenital lesions.

The Q209 position of *GNA11* is exactly analogous to the Q227 position in GNAS. This is seen in McCune Albright syndrome, a condition caused by a post zygotic somatic mutation, leading to a monoclonal population of mutated cells within various affected tissues, so-called mosaicism. A constellation of features such as precocious puberty, café au lait skin lesions and polyostotic fibrous dysplasia (POFD) are its defining features. The clinical spectrum is determined by the distribution of mutant cells. The mutation leads to continuous activation of the alpha subunit of the G protein coupled receptor, leading to multiple endocrinopathies such as acromegaly via growth hormone excess and hypercortisolism of the adrenal tissues. In our double mutant cohort, GTP is not broken down to GDP; therefore, there is likely no “reset” mechanism leading to continuous downstream signalling and activation of CYP11B2 and aldosterone synthesis.

What is difficult to determine is the relationship between our two mutations and how they arise. Does one precede the other? Or do they act as co-driving mutations? Driver mutations bestow growth advantages on the

cells carrying them. They are specifically selected in the growth of the tumour or cancer to enable its tumorigenic process. Conversely, passenger mutations do not contribute to tumour growth and spread, but are ancestors within the cancer cells and are continued in the cell line [144]. *CTNNB1* mutations found in ACCs are often found to have driver mutations in genes such as *TP53, MED12* [140]. *GNA11* has not been seen before as a co-driver mutation with *CTNNB1*.

A relevant question is whether one mutation arises before the other. There is growing evidence to suggest upregulation of one driver mutation may lead to activation of the second mutation as a so-called "second hit".

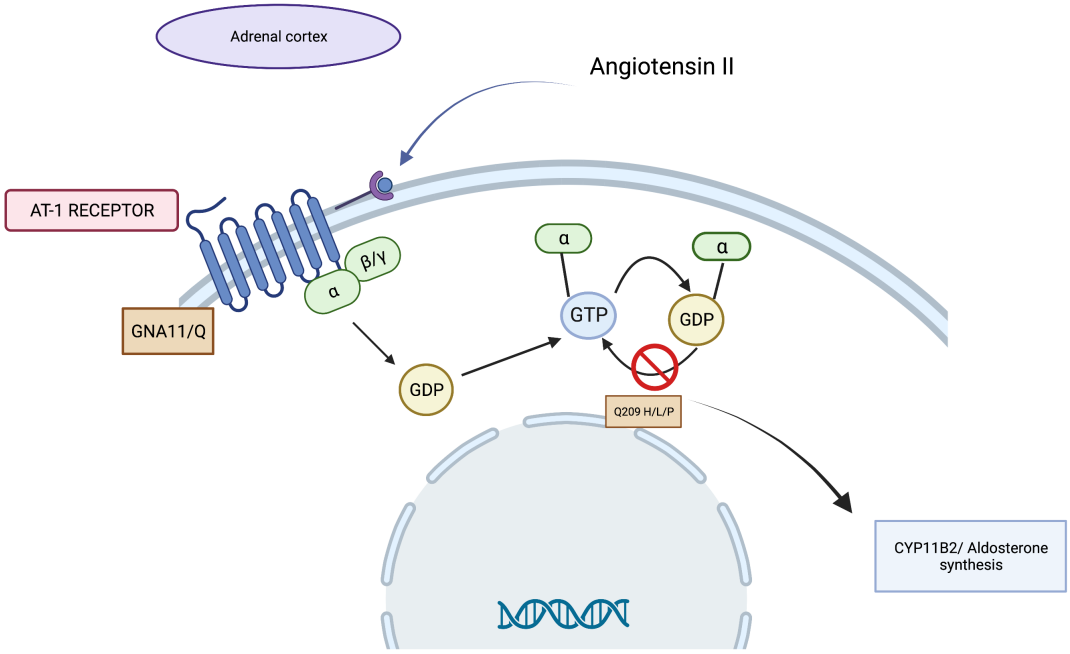

Figure 1 10: Schema illustrating the *GNA11/Q Q209H/L/P* mutation effect upon the G-protein coupled receptor, AT-1. CYP11B2 expression and aldosterone synthesis is continuous, as the mechanism fails to be reset at the GTP-GDP level. (Designed on Biorender).

1.15 Upregulated genes in double mutants APAs:

Microarray studies of ZG- like APAs versus double mutant APAs led to an interesting observation in our group. The double mutant APAs expressed a unique group of "hallmark" genes, not seen in other APAs. The most striking was *LHCGR* and the second most significant gene of interest was *TMEM132E.* The other upregulated genes comprised of *DKK1, SLC35F1, RDH12, MPP3, FAP* and *C90R54.* (Figure 1 11).

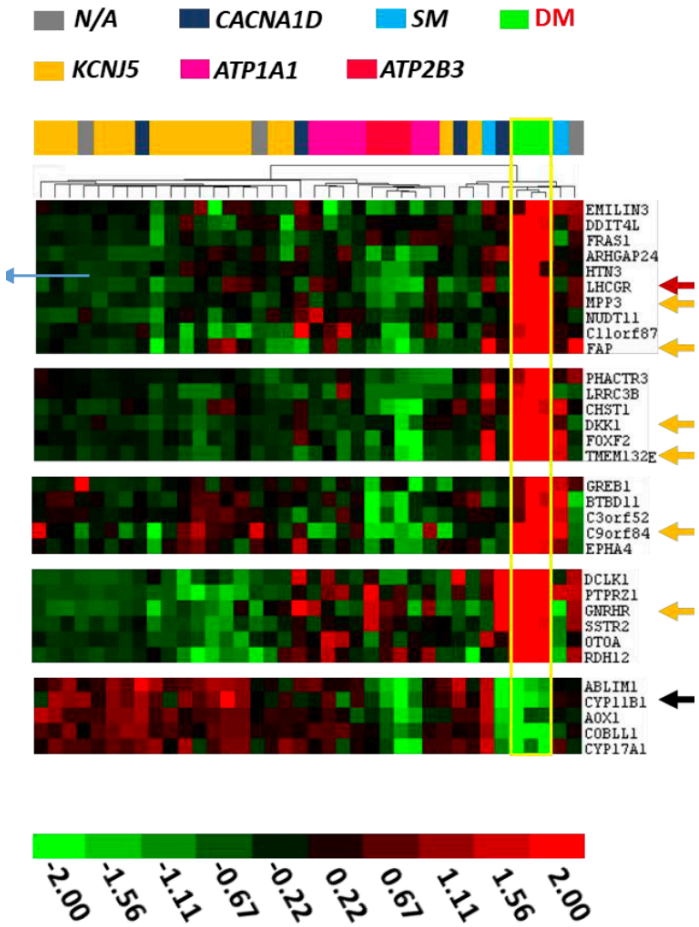

Figure 1 11: A **highlighted** section of a heat map of APA from at least one of 3 transcriptome studies [145] [146]. Each column represents the APAs expression profile. The unsupervised cluster analysis of samples, indicated by the bracketing above the heat map, separated the expression profiles of GNA11/Q and CTNNB1 double mutant APAs (boxed green with yellow border) from those APA harbouring single mutations (CTNNB1(SM), KCNJ5, CACNA1D and ATP1). Red indicates high expression and green colours indicate low expression levels, relative to the mean. The genes highlighted with yellow arrows are unique to double mutants compared to single gene mutations. CYP11B1 is illustrated with a black arrow due to its down regulation [134].

This heat map was kindly generated by Dr Claudia Cabrera, Queen Mary's University of London.

1.15.1 LHCGR/GNRHR:

The gonadotrophins luteinising hormone (LH), follicle stimulating hormone (FSH) and human chorionic gonadotrophin hormone (HCG) are a group of glycoproteins, involved in puberty and reproduction. They are all three heterodimeric structures, around 40 kDa, and are structurally very alike. Consisting of two peptide chains they contain a similar alpha chain, but it is their beta chain which differs and gives them affinity and selectivity for their receptors. HCG and LH's beta chain differs by 24 amino acids. The hypothalamic-pituitary-gonadal axis, whilst briefly active in the early neonatal period, remains quiescent through childhood until the onset of puberty. The hypothalamus secretes gonadotrophin releasing hormone, which stimulates gonadotrophic cells via gonadotrophin releasing hormone receptors (GNRHR) of the anterior pituitary, to secrete LH and FSH. Particularly, at times of physiological demand such as puberty, ovulation in females and testosterone production in males. Raised gonadotrophins are seen in menopause due to the loss of the negative feedback regulation from the gonads, via oestradiol, to the anterior pituitary. HCG on the other hand is secreted from syncytiotrophoblasts of the placenta during pregnancy.

LH and HCG share a common receptor, the luteinising hormone/ choriogonadotropin receptor (LHCGR), a receptor usually expressed on the gonads, such as the ovaries and testes. A G-protein coupled receptor, part of the rhodopsin/β2- adrenergic receptor subfamily, it has two known intracellular activation pathways: cAMP (cyclic adenosine monophosphate) and inositol phosphate leading to a downstream increase in calcium ion levels [147]. Although both hormones bind to this receptor, HCG binds with a higher affinity [148]. It is known that there are LHCGRs present in the adrenal gland, and could be involved in steroidogenesis, in particular, DHEAS production. Immunohistochemistry studies have shown that *LHCGR* expression is found more in the ZR but it is also present within the ZF [149]. In our group's most recent work, expression of LHCGR was also found on immunohistochemistry of the medulla of the adrenal gland. However, its role there is not yet fully understood. Given the presence of LHCGR receptors within the adrenal cortex, it is therefore possible that, at times of elevated LH/HCG, LHCGR expression may increase and lead to pathology.

The first work adopted in the 1970s-1980s illustrated that incubating adrenocortical carcinoma cells in LH/HCG led to an increase in cAMP and steroidogenesis [150, 151]. Multiple mice and various animal models have illustrated that, following gonadectomy, *LHCGR* expression increases within the adrenal cortex. Tumour

formation or adrenal hyperplasia can ensue [152, 153]. One study in particular looked at domestic ferrets who had undergone gonadectomies. They found higher expression of *LHCGR* in their adrenals, as well as adrenal hyperplasia and growth. In ferrets with hyperadrenocorticism, GNRH stimulation tests led to an increase in androstenedione production, compared to healthy ferrets [154, 155]. There has also been a case report of an APA in a ferret after it was spayed [156]. In the foetal adrenal, there has been documented expression of LH/HCG receptors in multiple non-gonadal organs, including the adrenal gland. It is difficult to determine their role; they may be contributing to foetal growth through their receptors, or may be involved in autocrine functions [157]. Prior to our British/Irish cohort, a case report emerged in 2011 of a patient presenting with PA in pregnancy, whose aldosterone levels pre-adrenalectomy increased significantly following a GNRH stimulation test. 100μg intra venously was administered. This was significantly increased compared to controls. Upon adrenalectomy, their APA stained strongly for LHCGR, suggesting this was likely a double mutant [158]. In humans, other hormone secreting adrenal neoplasias have been described, such as LH-dependent cortisol secreting adenomas [159]. They have presented in pregnancy, and one case in menopause [160]. LH- dependent androgen secreting tumours of the adrenal cortex have also been documented [161]. Our group has described LH-dependent aldosterone secreting adenomas [121]. Recently, there has also been a phaeochromocytoma (adrenaline secreting tumour of the medulla) presenting within the first trimester rise of HCG [162]. *LHCGR* expression was one of the most unique features of the double mutant cohort. *LHCGR* was significantly upregulated ($P<0.001$), especially when it was compared with control APAs who harboured sole CTNNB1 mutations, and other control APAs harbouring other somatic mutations, such as, KCNJ5. Only one double mutant patient had low levels of *LHCGR* [134].

1.15.2 Transmembrane protein 132E (*TMEM132E*):

TMEM132E belongs to a large family of transmembrane proteins. Transmembrane proteins are integral membrane proteins that span across cell membranes in their own unique orientation. They traverse the lipid bilayer and act as gateways that lead to transportation of substances across the membrane. They come in alpha helical or beta barrel formation, with most in eukaryotic cells being alpha helical. There are 5 main genes within the TMEM132 family: A, B, C, D and E. Considered neuronal cell adhesion molecules, studies have shown that the *TMEM132* architecture is ancient in cellular ancestry, preceding metazoans, comprising continued repeated adherin domain-containing proteins whose main role are thought to be connecting extracellular matrix and the actin cytoskeleton with neighbouring cells [163] [164]. They have amino (N) terminals or carboxy (C) terminals that either reside within the intracellular cytoplasmic environment or outside within the extracellular, luminal environment. Transmembrane proteins have been determined to have multiple roles, including receptor and signal transduction pathways, the movement of molecules and ions and protein targeting and trafficking to the membrane. The transmembrane 132 family accomplish most of their work and activity within neuronal cells and structures such as the brain and peripheral and central nervous system. Their pathology also comprises of malignancies not only within the nervous system such as gliomas but also in renal and pancreatic cancer.

Found on chromosome 17q12, *TMEM132E* is in the DFNB99 locus, and contains 10 exons. It is highly expressed within the inner ear, particularly in cochlear hair cells, but also other organ tissues such as brain, kidney, colon, stomach, lung, liver, testes and spleen [165]. It is poorly described or understood but is thought to play a role in neuronal function and cochlear development within the ear [165, 166]. *TMEM132E* has also been described in conditions such as hearing loss (autosomal deafness), narcolepsy and panic disorders but has yet to be described in the adrenal gland [165]. An important paralogue to it is *TMEM132C.*

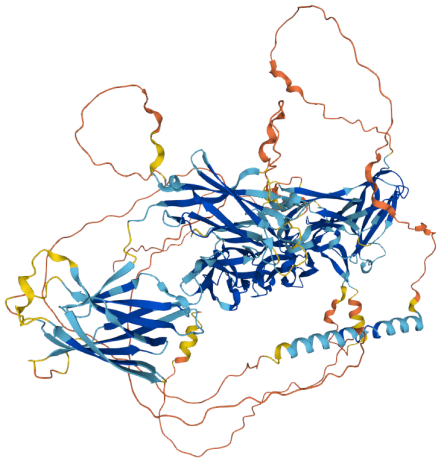

Figure 1 12: the proposed structure of TMEM132E.

Although TMEM132E has not previously described in the adrenal gland, increasing evidence has pointed to a potential commonality between inner ear genes and common ZG gene. One such gene is *CACNA1D*. Loss of the receptor CA_v 1.3 (*CACNA1D*), a somatic mutation of APAs, has led to congenital deafness [167, 168]. In CA_v 1.3 knock out mice, deafness was profound with a distinct disruption in inner hair cells [169]. It must be stressed however, within the mice this is a loss of function mutation, whilst *CACNA1D* mutations in APAs are gain of function.

1.15.3 Nicotinic Acetylcholine receptors and TMEM132E:

In recent years novel proteins and molecules have been uncovered that appear to be essential for nicotinic acetylcholine receptor function. Acetylcholine (AChRs) receptors, identified almost 100 years ago, are neurotransmitter receptors that are ligand-activated. There are two classes of AChRs, the metabotropic muscarinic receptors and the ionotropic nicotinic receptors.

Nicotinic AChRs are a large family of neurotransmitter gated ion channels. Pentameric in shape, they are formed from nine α (α2 to α10) and three β (β2 to β4) subunits, the ring that is formed surrounds the ion channel pore. They are usually heteropentametric with various combinations of a mixture of α subunits or α and β. However, the ancient α7 is able to form a functional homopentameter, the simplest lay out for a ligand gated ion channel [170]. The assembly of the nAChR is a precise and closely regulated affair, the subunits undergo post translational modifications prior to their linkage. One common so called “chaperone” of this process is the protein, calnexin [171].

nAChRs function as Na^+, K^+ and Ca^{2+} ion channels. Their role in steroidogenesis is likely through the calcium influx pathway. Muscarinic AChRs, on the other hand, work through muscarine. Nicotinic and muscarinic AChRs have been well described in the adrenal medulla as they play an active role in catecholamine release, however, they have not been described within the adrenal cortex. Evidence does seem to suggest that glucocorticoid stimulation from the cortex is needed in order to activate PNMT, phenylethanolamine N-methyltransferase, the catalyst enzyme involved in the synthesis of adrenaline from noradrenaline, from the medulla which works through nAChRs particularly α7 [172].

The nACh receptors are overall expressed in central and peripheral nervous system and mediate physiological effects of ACh as well as addictive properties for example of nicotine. They are also key in the communication

between the nervous system and skeletal muscle. Specialised focal pockets of nAChRs have also been found in other areas such as – of most interest to us - the cochlear hair cells, but also in lymphocytes and adipocytes. They are therefore naturally implicated in multiple neurological and psychiatric pathologies and have also therefore become an experimental therapeutic target.

Endogenously nAChRs are stimulated by acetylcholine. Acetylcholine in nervous tissue is either released in the usual manner by vesicles into the synaptic cleft or it can also be released in a paracrine manner by swellings in neuronal axons. Acetylcholine then binds to the nAChR and opens the ion channel. When the process is done, acetylcholine releases itself and is cleaved back into acetyl co-enzyme A and choline by acetylcholinesterase, an enzyme who lies in the wings of the synaptic cleft ready to perform. Cholinergic agonists that directly affect the nAChR and mAChR are choline esters such as methacholine, carbachol, acetylcholine and bethanechol and also alkaloids such as pilocarpine, muscarine and cevimeline.

Carbachol, also called carbamylcholine, is a parasympathomimetic that mimics the effect of acetylcholine on both nAChR and mAChR. Clinically, it has been used within ophthalmology to reduce intraocular pressure via contraction of the iris and the ciliary muscle. Resistant to acetylcholinesterase, its effects can last up to 24 hours. Previous studies in rodents and bovine adrenal cortex have illustrated the presence and potential role of mAChRs in steroidogenesis. These studies illustrated that choline agonists such as carbachol, a steady cholinergic agonist, increased intracellular calcium activity and therefore steroid production most likely through the M3 acetylcholine receptors [173].

A further study by *Malaiyandi et al* treated HAC-15 (a cell line derived from H295R cells) with carbachol and found a significant increase in M3 acetylcholine receptor expression and a rise in aldosterone synthesis, although not as great as cells stimulated with Ang II. An increase in intracellular calcium was observed [174].

It is becoming increasingly clear that these so-called accessory functions seem to act at different steps of the assembly and the formation of the nicotinic acetylcholine receptor and are quite essential to it. Of these molecules, some appear to have basic auxiliary chaperoning roles whilst, for example, transmembrane inner ear (TMIE) protein not only works upon nAChRs within inner ear hair cell membranes but also to mechanosensitive channels involved in sound wave conduction and cochlear function.

The relationship between TMEM132E and acetylcholine receptors initially was explored by *Gu et al* whilst researching the assembly of the α9α10 nicotinic acetylcholine receptors (nAChRs) within the olivocochlear synapse of auditory hair cells. *Gu et al* found that α9α10 nicotinic acetylcholine receptor function was enhanced robustly by the presence of TMEM132E and TMIE. TMEM132E worked as an

auxiliary subunit to enable α9α10 to function. This not only led to higher expression of the α9α10 nicotinic acetylcholine receptors on the cell membrane visualised on immunofluorescence but led to higher calcium evoked signalling on functional work. This leads us to think that TMEM132E has a neurotransmitter accessory function to the acetylcholine receptor [175]. This is in keeping with TMIE knockout mice that are deaf and have abnormal α9α10 receptor function [175].

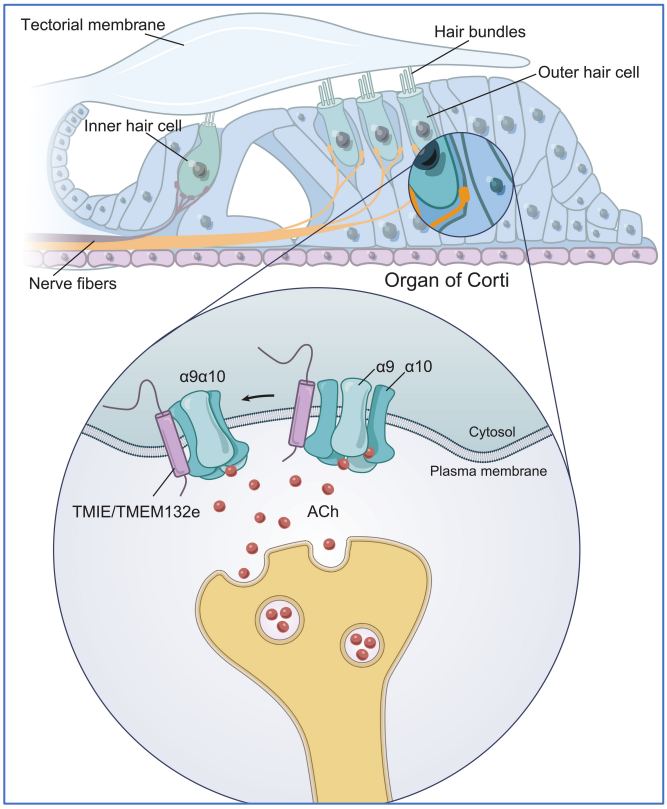

Figure 1 13: This figure illustrates the auxiliary subunits of TMEM132E/TMIE enabling the function of the α9α10 subunit within the cell membrane of the inner hair cell within the inner ear [176].

1.15.4: *CHRNA7*:

It is therefore intriguing to consider whether *TMEM132E* may be playing a role alongside acetylcholine receptors in aldosterone synthesis. With this in mind, we went back to review data from our double mutant APAs, and it was determined that the nAChR that was highly expressed within these APAs was the α 7 neuronal nicotinic receptor coded by the gene *CHRNA7*, which lies on chromosome 15q14. This was almost 200-fold higher in one of our double mutant APAs compared to APAs with other somatic mutations. α7 subunits form a highly calcium permeable homopentameter nAChR, highly expressed in the brain and

undergoes rapid desensitisation. They usually undertake modulatory functions at the pre and post synapses within nerve cells, [177] as well as chemical transmissions. α7 receptors are highly permeable to calcium and therefore this is their pathway of activation. Malfunction of α7 nAChRs leads to schizophrenia and psychiatric dysfunctions, including Alzheimer's disease [178]. In the lung they have a high affinity for nicotine which can lead to tumorigenesis and lung cancer formation [179]. In recent years, α7 has become of increased interest as it is the closest ancestor gene that evolved millennia ago. Research on α7 receptors could lead to a better understanding of nAChRs and their potential role as therapeutic targets.

In the quest to find nAChRs and their accessory proteins, *Gu et al* noted that calcium influx greatly increased in CHRNA7 overexpressed HEK cells when treated with a novel positive allosteric modulator, (5-chloro-2,4-dimethoxyphenyl)-3-(5-methyl-isoxazol-3-yl)-urea (PNU-120596) [180] and acetylcholine, in the presence of a clone taken from a library of 3,880 clones of cDNA of transmembrane and accessory proteins [171]. Derived from TMEM35 this 167 amino acid originating in the endoplasmic reticulum was called nAChR regulator (NACHO). This protein has previously been described in the zona glomerulosa of rat adrenals, where its expression was significantly increased in salt deplete conditions which favoured aldosterone synthesis [181]. This study by Gu et al also illustrated that, not only did NACHO lead to maturation, folding and increased membranous expression of α7 nAChRs, but that NACHO seems to be client specific for alpha- nicotinic receptors α7, α4β2 and α6β2β3 [171]. NACHO does not modulate the receptor directly but requires N-glycosylation and calnexin chaperone activity [182]. Another key component to CHRNA7 assembly is the Ric-3 protein, also known as resistance to inhibitors of cholinesterase 3. Ric-3 works via another pathway to shuttle α7 receptors to the membrane. It has also been found to be working in α7 receptors where NACHO is not present, especially for example in non-neuronal cells such as skin cells or endothelial cells [176].

TMEM132E and CHRNA7 have not been described together before; however, malfunctions in both genes have been described in patients with schizophrenia [183].

1.15.5 Solute carrier family 35, member F1 (*SLC35F1*):

SCL35F1 is a protein that has not been well described. It is known to arise from a family of sugar transporters involved in trafficking substances to the membrane. It is highly expressed within neurological tissue such as the brain. Disruption to it has been associated with the condition, Retts.

1.15.6 Dick Kopf related protein 1 (*DKK1*):

DKK1 is a secreted glycoprotein and is an antagonist of the Wnt signalling pathway. It promotes internalisation of LRP5/6 for degradation by forming a ternary complex with the transmembrane KREMEN reducing β catenin levels. It has been shown in animal studies to be extremely important in the control of embryogenesis and prevents the overexpression of cell fate so preserving structures from malformations [184]. In human diseases, it has been described in Alzheimer's and is highly expressed in osteolytic lesions in melanoma. It has not been described in the adrenal gland before.

1.15.7 Fibroblast activation protein (*FAP*):

Fibroblast activation protein belongs to the S9 proteases family. Other members of this regulatory protein family include dipeptidyl peptidase 4 (DPP4), DPP8, DPP9 and prolyl endopeptidase. These enzymes are involved in cleaving the post proline bond usually resistant to degradation. FAP has been found to have increased expression in embryogenesis, tumorigenesis and inflammatory processes such a liver fibrosis [185]. FAP has been observed to be highly regulated in stromal tumours and therefore is used as a biomarker and potential therapeutic target [186]. DPP4 is its relative and only cleaves dipeptidyl peptidase but it has been found in gut hormones and neuropeptides and has been used as an effective therapeutic target in diabetes. FAP has not been previously described in the adrenal gland but further exploration is required to evaluate it as a potential biomarker in double mutants.

1.15.8 Down regulation of CYP11B1:

Our double mutant APAs also had downregulation of CYP11B1. This is in keeping with their more ZG like appearance. APAs that have more ZF type features were noted to have higher expression of CYP11B1 [145]. There was a significant downregulation of CYP11B1(P=0.0001) compared to sole CTNNB1 mutation APA and P=0.0003 compared to other APAs harbouring other somatic mutations [134].

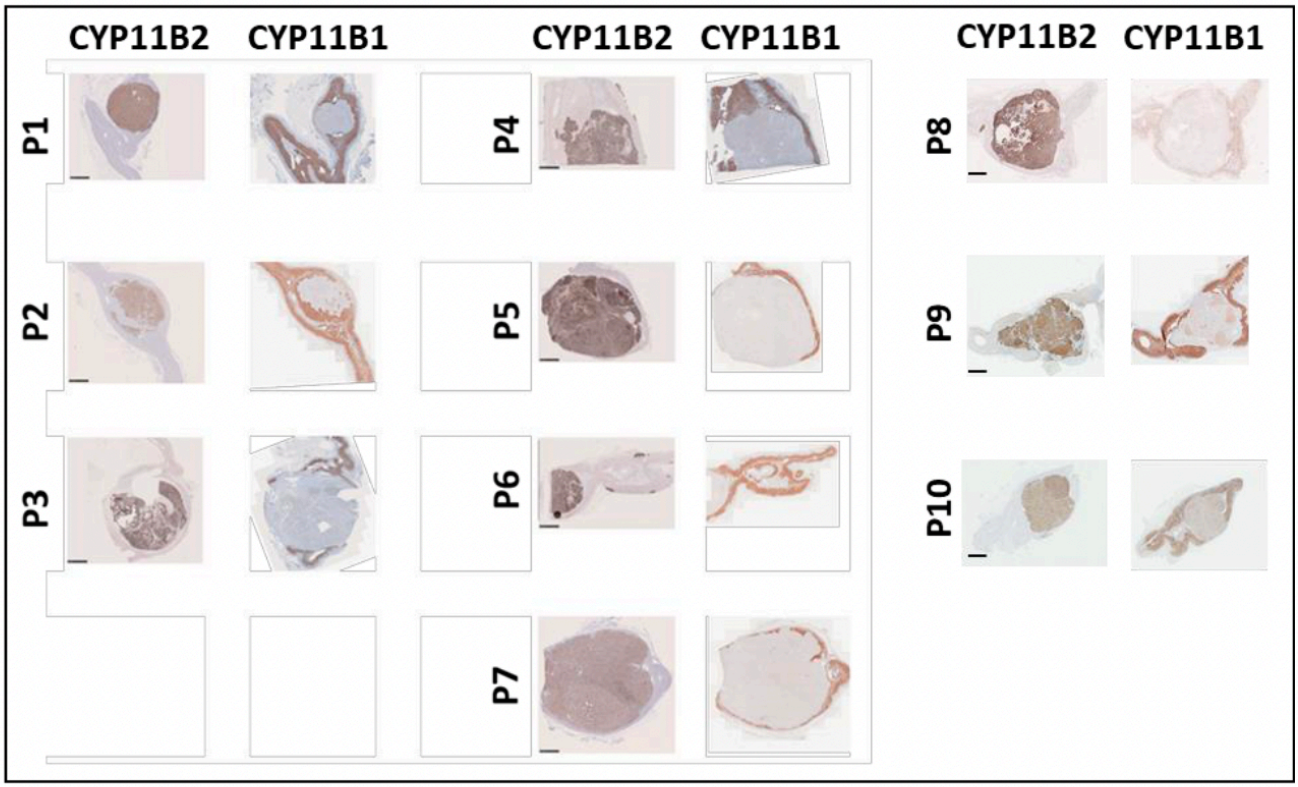

Figure 1 14: Immunohistochemistry of the 10 double mutant APA of the British/Irish cohort stained for CYP11B2 and CYP11B1. The protein expression of the APA pathology is representative of the mRNA expression with a higher CYP11B2 to CYP11B1 ratio. Anti-CYP11B2 #ab168388 (1:200; Abcam, UK) and anti-CYP11B1 #MABS502, clone 80-7 (1:100; Sigma- Aldrich, USA). Scale bar, 2.5 mm. **IHC and figure of IHC courtesy of Dr Junhua Zhou and Dr Wanfeng (Addenbrookes, Cambridge) [134]**

Aim of thesis:

The basis of modern evidence-based medicine is developed upon the close relationship between the scientific bench and the medical practitioner. The overall aim of this thesis was to broaden our understanding of a unique form of PA that presents in pregnancy, puberty, and menopause, this work was continued on from work published in Nature genetics by Zhou et al [134]. The second part of this thesis was dedicated to the **FABULAS study:** Feasibility study of Radio**F**requency endoscopic **AB**lation, with **UL**trasound guidance, as a non-surgical, **A**drenal **S**paring treatment for aldosterone producing adenomas (**FABULAS**).

A study to determine whether a safe and viable adrenal cortical sparing therapy is on the horizon. This thesis will be split into two parts with a laboratory chapter and a clinical chapter.

Chapter 2:

Material and Methods

Laboratory:

2. 1. Cell Culture:

All experiments were conducted in the William Harvey Research Institute at Charterhouse Square at Queen Mary University London unless stated otherwise. Cells were cultured in incubators at 37 degrees Celsius and 5% CO2 and the media was changed every 24-72 hours. Cells were grown in Falcon™ flasks 75 cm^2 or 150cm^2 with vented caps (BD, 75 cm^2 :353136, 150cm^2: 355001).

2.1.1 NCI-H295R:

The immortal NCI-H295R cell line was the main cell line used for most of the transfection studies. A pluripotent immortal cell line arising from the adrenocortical cancer (ACC) of a 48-year-old Afro-Caribbean female established by A.F Gazdar in 1980. Under the right conditions, this cell line can represent the adrenal cortex and secrete mineralocorticoids, glucocorticoids, and androgens. H295R are also able to express all the following enzymes CYP11B2, CYP11B1, CYP11A, CYP17, CYP21, HSD3B2, 3β-hydroxysteroid, and sulfotransferase [187] [188]. H295R cells also contain a stable S45P *CTNNB1* mutation and are wild type for *GNA11/GNAQ*, *TMEM132E* and *CHRNA7,* therefore, making them a viable cell model for our experiments. H295R cells were cultured in "complete" growth medium consisting of supplemented Dulbecco Modified Eagle Medium/Nutrient F-12 Ham (Sigma-Aldrich D6421). Complete medium was supplemented with 10% foetal bovine serum (Sigma-Aldrich F9665), 5% antibiotic: penicillin-streptomycin-Gentamicin (Sigma-Aldrich G1146), and 1% Insulin-transferrin-selenium (Gibco I3146). H295R cell lines passages ranged from 14-27. The lab team had originally purchased this cell line from ECACC and some passages were gifted from Professor Guasti's research group.

2.1.2 Primary Adrenal cells:

Adrenal adenoma and cortex cells were harvested fresh and directly from the surgical operating theatre at St Bartholomew's hospital, The Royal Free Hospital or sometimes private institutions such as Great Portland Street Hospital. Prior to surgery written consent was obtained from the patient. On collection slices of adrenal were put directly into complete media falcons and carried back to the laboratory on ice.

The capsule and medulla were carefully removed, and cortex and adenoma cells were mashed separately and cut very finely with a sterile scalpel (Swann Morton 0508) to release cells. The pureed tissue was then added to collagenase type IV from Clostridium histolyticum (Sigma C9697) and left to agitate in the 37 degrees Celsius water bath for 2 hours with 30 minutely vortexes. After centrifugation, the cells were washed with Dulbecco's Phosphate Buffered Saline (PBS) (Sigma D8537) and resuspended in complete media. The first cell's supernatant was resuspended in complete media into flasks. Cells were left to settle for 72 hours then media changed. Cells were either used for experiments or frozen within 2 weeks of having obtained them. If adenoma cells were used, we endeavoured to find the underlying somatic genetic mutation.

2.1.3 OVCAR and HEK-293 cells:

OVCAR-3 cells are an immortal cell line derived from epithelial cells collected from a patient with malignant ascites following high- grade serous ovarian adenocarcinoma. Epithelial ovarian cancers account for 90% of all ovarian cancers diagnosed [189]. OVCAR 3 cells were grown in Gibco Roswell Park Memorial Institute (RPMI) 1640 Medium (21875034) with 20% FBS.

OVCAR-4 cells an alternative ovarian immortal cell line were also reviewed, these cells are also derived from a patient with high-grade serous adenocarcinoma of the ovary. OVCAR-4 cells were fed with the same complete medium described above for H295R cells. These cells were gifted by Dr Helen Hocking.

HEK (Human Embryonic Kidney) 293 cells were also tried later in my thesis for CHRNA7 work. An immortal cell line derived from embryonic kidney cells of a likely miscarried female foetus in 1973. They grow easily and are very amenable to transduction.

2.2 Cell passage:

Cells were passaged when they reached about 80% confluency. Cells were washed in pre-warmed PBS twice and then trypsinised with pre-warmed Trypsin-EDTA (Ethylenediaminetetraacetic acid) solution (Sigma T4299), trypsin was applied for 3 minutes at 37 degrees and then neutralised with complete media. Cells and media were moved into a 15 or 50ml falcon tube and centrifuged at 800-1000 rpm for 3 minutes. The supernatant was subsequently removed, and the cell pellet resuspended in media and either cells were counted with a haemocytometer and plated into well plates or resuspended into flasks. As cells are passaged, they

become older becoming more are at risk and susceptible to infections, can lose their morphology and lose their steroidogenesis potential, therefore, younger passages were favoured.

2.3 Cryopreservation and thawing:

When required cells were frozen down and placed into short term storage in our -80ºC freezer or longer-term storage in liquid nitrogen -196ºC provided by Cryotech. Freezing media was made with 10% Dimethyl sulfoxide (DMSO), 20% FBS and 70% Complete media. Cells were washed x2 in prewarmed PBS and tryspsinised with trypsin for 3 minutes at 37ºC and then neutralised with complete media. Cells and media were moved into a 15 or 50ml falcon tube and centrifuged at 800 -1000 rpm for 3 minutes. The supernatant was removed, and the cell pellet resuspended in freezing media. The cell solution was then aliquoted into cryogenic storage vials and fitted within a Corning Cool Cell (15552771), this apparatus when placed in -80ºC cools the cells -1ºC per minute. DMSO is a cellular cryoprotectant as it aids to freeze the cells. When cells are required for experiments, cells are thawed in the 37ºC water bath and resuspended in complete media.

2.4 Cell culture pharmacotherapy:

All cell lines were starved in nil media, Dulbecco Modified Eagle Medium/Nutrient F-12 Ham (Sigma-Aldrich D6421) for a minimum of 6 hours before treatment with the following medications all treatments were given for 24-48 hours.

Treatment:	Producer / Catalogue number	Concentration/ Action.
Angiotensin II	Sigma/ Catalogue: A9525	$10x^{-8}$, MCR receptor agonist
Endothelin I	Sigma/ Catalogue: E7764	$10x^{-8}$, MCR receptor agonist
Carbachol-Carbamoylcholine chloride	Biotechne/ Catalogue- 2810.	Various concentrations 0.5 mM-20mM, Non selective cholinergic agonist.
Luteinising Hormone (LH)	Biotechne/ Catalogue- 8899-LH	Various concentrations: $1x10^{-7}$ to $1x10^{-9}$.
Beta Human chorionic gonadotrophin hormone (BHCG)	Biotechne/Catalogue- 7727-CG	Various concentrations: $1x10^{-7}$ to $1x10^{-9}$

Table 2 1: Pharmacological treatments used in cell culture experiments.

2.5 Gene therapy:

2.5.1 GNA11 plasmid:

H295R cells were transfected with pBI-CMV2 vector (Figure 2 1), containing a green fluorescent protein (GFP) probe. *GNA11* empty vector (EV), wild-type WT and mutant Q209L plasmids were kindly gifted by Professor R.V. Thakker from the University of Oxford. Site directed mutagenesis using NEB Q5® Site-Directed Mutagenesis Kit (NEB, E0554) was performed by our lab to obtain Q209H and Q209P plasmids. Sequencing was then performed with primers DOCUMENTED below.

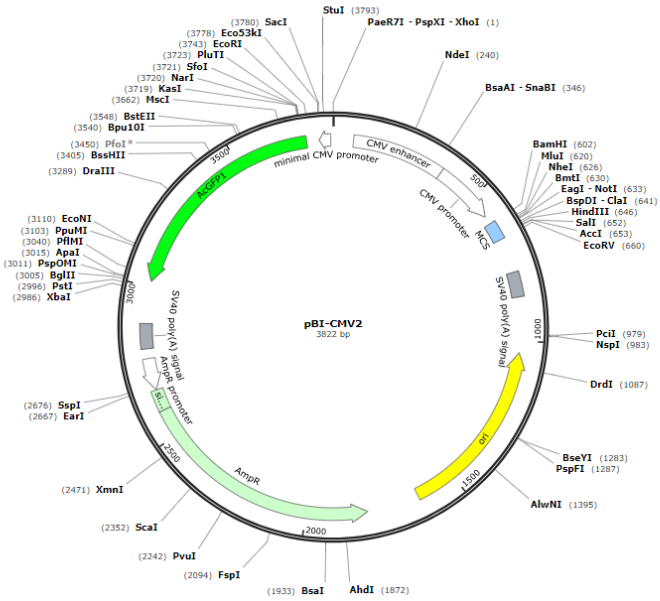

Figure 2 1: Outline of the pBI-CMV2 plasmid used as the base of our plasmid work. The structure highlights the GFP tag and the plasmid's ampicillin resistance.

2.5.2 GNAQ plasmid:

Our GNAQ plasmid was also a gift from Professor R.V Thakker from the University of Oxford and contained a GFP probe, GNAQ EV, WT, and mutant Q209H were kindly gifted. Site-directed mutagenesis using NEB Q5® Site-Directed Mutagenesis Kit (NEB, E0554) was performed by our lab to obtain Q209L and Q209P plasmids. Sequencing was then performed.

2.5.3 TMEM132E and CHRNA7 plasmid:

TMEM132E plasmid was purchased from Sino biological, pCMV3-TMEM132E cDNA ORF clone, C-HA tag (HG27874-CY), and control plasmid, pCMV3 Negative control vector (CV013).

Nicotinic acetylcholine receptor alpha 7 (CHRNA7) with a turbo GFP tag, was purchased from Origene (CAT#: RG221382), and a control plasmid: pCMV6-AC-GFP Mammalian Expression Vector also from Origene (CAT #: PS100010).

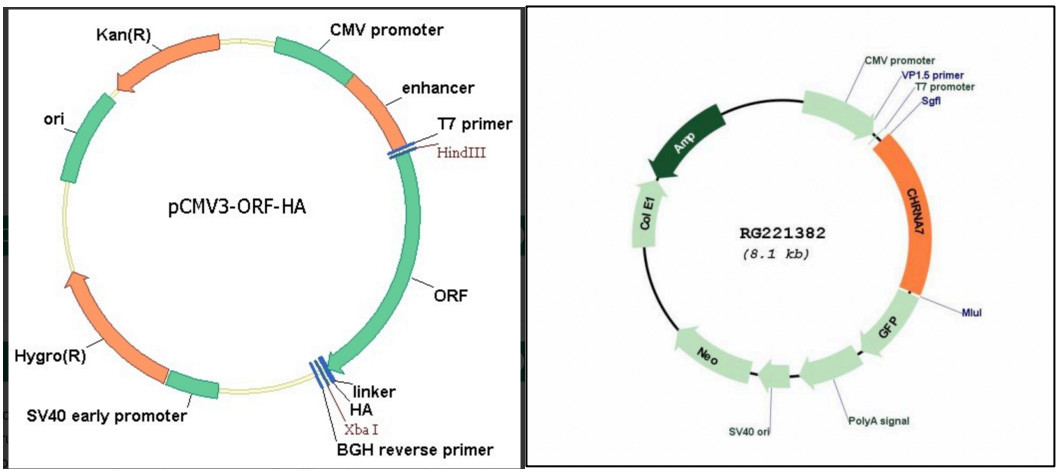

Figure 2 2 : pCMV3-TMEM132E cDNA ORF clone, C-HA tag taken from Sino biological website on the left, this plasmid contained a C-HA tag and was Kanamycin resistant. The figure on the right is taken from the Origene website illustrates the skeleton of the CHRNA7 plasmid, it contained a Turbo GFP tag and was Ampicillin resistant.

2.5.4 Plasmid Transformation:

Plasmid transformation was performed with the NEB Q5® Site-Directed Mutagenesis Kit. The first step is exponential amplification where 25 µl of reaction mixture is made from 12.5 µl Hot start NEB master mix, 1.25µl of forward and reverse primer for your gene of interest, 1µl of plasmid DNA and 9 µl of RNase free water. This is then set in the thermocycler for initial denaturation at 98°C for 30 seconds then 25 x cycles: 98°C for 10 seconds, 50°C for 10 seconds, 72°C for 20-30 seconds/kb, and a final hold of 72°C for 2 minutes then cooled to 4°C.

Heat shock transformation is similar to that described below but prior to this 1µl of the above PCR mixture is added to 1µl of 10x KLD enzyme mix which contains three enzymes: kinase, ligase and DpnI, and 5µl of 2x KLD reaction buffer, and 3µl of RNase free nuclear water.

2.5.5 Plasmid boosting:

The first step of plasmid boosting was performed via heat shock transformation of New England Biolabs (NEB) 10 beta competent E.coli (High efficiency) (C3019H). Heat shock transformation allows foreign DNA to enter the E.coli cell. This process is facilitated by the calcium chloride within the mixture that counteracts the bacterial membrane and plasmid DNA repulsing each other. The sudden increase in heat creates pores in the plasma membrane which allows the plasmid DNA to enter. E.coli were thawed on ice for 10 minutes and 1-5 µl of up to 100 ng of plasmid DNA was mixed to the tube and carefully flicked 4-5 times to mix cells. The cells were then placed on ice for 30 minutes before being heat shocked for 30 seconds at 42 degrees and then placed back on ice for 5 minutes. 950 µL of stable outgrowth media was added to the mixture and the vials are left to shake at 250rpm at 37^0C for 1 hour.

Selection culture plates were prepared and poured following autoclave of Sigma Lennox LB broth with agar (L7025). Gibco™ Ampicillin, sodium salt, irradiated (Thermofischer 11-593-027) or Gibco Kanamycin sulphate (15160054) was added depending upon the resistance of the plasmid vector. Once formed they were heated and 50-100 µl of cell solution was spread on the plate and incubated overnight at 37ºC.

2.5.5.1 Midi boosting:

The following day one colony is picked and emersed into 5ml of pre-warmed LB Lennox broth (Sigma, L7275) with antibiotics within a valve breathing tube. This is boosted at 250 rpm overnight in 37ºC.

2.5.5.2 Maxi boosting:

250 µl of the previous step is then put into 250mls of antibiotic broth and further agitated at 250 rpm overnight in 37ºC.

The plasmid DNA was then harvested using anion-exchange chromatography technology whereby an anion-exchange resin with specific pore size and charge captures the product of interest as it flows through the column, in this case DNA. We used the PureLink™ HiPure Plasmid DNA Purification Kit (Thermofischer, K210006). The overnight LB broth with E.coli was spun at 4000 xg for 10 minutes, the cells then formed a pellet at the bottom of the tube and the supernatant was discarded. The pellet was then resuspended in 10 mL in

Resuspension Buffer (R3) with RNase A and then mixed gently with 10 mL of Lysis Buffer (L7) until the mixture was thoroughly homogenous and left to incubate for 5 minutes at room temperature. 10mL of precipitation Buffer (N3) was then added and the tube was mixed by inverting the tube until it is thoroughly mixed through. Whilst this process is ongoing the column whereby the DNA is captured into to be eluted is equilibrated with 30 mL Equilibration buffer (EQ1). Following precipitation, the cell lysate is loaded onto the equilibrated column and allowed to flow through, the DNA is captured onto the column. The negatively changed phosphates on the backbone of DNA interact with the positive ions of the resin. The DNA is then washed with 60mLWash Buffer (W8) proteins, carbohydrates, RNA, and other impurities are washed away as it drains through the column by gravity. The next stage was DNA elution under high salt conditions as 15 ml of Elution Buffer (E4) is loaded into the column and the flow through is captured into a sterile falcon tube. The last step is alcohol precipitation to desalt and concentrate the DNA, this is performed by adding 10.5 mL Isopropanol to the elute and then mixed. The solution is then centrifuged at >12,000 x g for 30 minutes at 4ºC, the supernatant carefully removed and resuspended in 5mL of 70% ethanol and re-centrifuged for 5 minutes, the supernatant is carefully removed, and the pellet left to air dry and then resuspended in RNase free water. The concentration is then checked on the nanodrop aiming for a concentration of 1000ng/µl.

2.5.6 Transfection: overexpression of gene experiments:

Transfection of cell lines has been a powerful method and advancement in biotechnology which has allowed us to study protein and gene expressions better. Electroporation is the process that I used in my functional experiments, thanks to commercial apparatuses it is readily reproducible and safe. A hight voltage electrical field is applied to the cell leading to a temporary breakdown of the cell membrane making it more porous and allowing DNA into the cell and ultimately the cell nucleus, critical features of this process is the maximum voltage of the shock applied and the pulse. The pores then naturally reseal themselves. Once parameters have been determined it is a useful method for transfecting lots of cells in one experiment. One of the main drawbacks of electroporation is high cell death this is exacerbated by the heat produced in electroporation, some methods advise electroporating on ice, zero degrees, to counter this. Another cause of cell death could be change in the pH of the cells medium which can be remedied with buffers [190]. All plasmids for overexpression were transfected with electroporation using the Neon™ Transfection System. The Neon™ device is an electroporation chamber with parts including, a gold-plated electrode Neon™ pipette tip that is loaded with harvested cells and plasmid or SiRNA, a Neon™ tube containing electrolyte buffer (E2) and an electrode near

the bottom, and a pipette station that holds the tube and the pipette inserted within it. The system delivers a high electric impulse to the biological sample. The electric field lies between the electrode on the gold tip and the electrode on the tube. The gap between the electrodes is maximised but the surface area is small leading to a stable electric field, with minimal Ph change and heat generation.

Cells were washed in pre-warmed PBS then trypsinised off their flask with pre-warmed Trypsin-EDTA solution, the trypsin was left on the cells for 3 minutes at 37 degrees and was then neutralised and resuspended with media into a 50ml flacon tube. This was then subsequently centrifuged at 800 rpm at room temperature for 3 minutes and then resuspended in PBS and re-centrifuged, the PBS was then aspirated. Finally, the pellet of cells was resuspended in R-buffer, resuspension buffer that is specific to the Neon transfection process. The 100 µL Kit (Invitrogen™MPK10096) was used, 100 µL of a mixture of cells, buffer, and DNA to a concentration of 5-15 µg was taken up and electroporated with the following parameters which have been laid out in the guidance for H295R cells: 1 pulse, 400mv and for 20 seconds.

After electroporation, cells were delivered into a in 6-well culture plate for 24h into pre warmed complete media without antibiotics. The following day media was changed to complete media at 48 hours they were then trypsinised and each well seeded into 3 wells of a 24-well plates in culture medium. Each different plasmid variation into 3 wells. At 72-96 hours the cells were harvested for either RNA for mRNA gene expression, protein extraction, and supernatant media was collected for aldosterone measurement (please see below for methods).

Transfection success and rate was determined by visualising the GFP under EVOS microscope as well as qPCR for the gene of interest.

2.6 SiRNA:

Dharmacon ON-TARGET plus Human Smartpool for TMEM132E (L-023299-02-0005) was purchased for knockdown experiments and ON-TARGETplus Non-targeting Control Pool (D-001810-10-05) for control. SiRNA is a form of RNA interference, a technology developed to lead to knockdown or silencing of a gene by double-stranded RNA that targets complimentary mRNA and causes its degradation [191]. SiRNA was delivered into the cell once again via the electroporation method of electroporation. The SiRNA strand was: 5'->3' GAGUCUCGAGGGUCCAUGAtt and antisense: 3'->5' UCAUGGACCCUCGAGACUCtt. Targeted SiRNA was ultimately used aside from Smartpool.

2.6.1 Transfection: Knockdown experiments:

Cells were washed in PBS then trypsinised off their flask with Trypsin-EDTA solution (Sigma T4299), the trypsin was then neutralised and resuspended with media into a 50ml flacon tube. This was then subsequently centrifuged at 800 rpm at room temperature for 3 minutes and then resuspended in PBS and re-centrifuged, the PBS was then aspirated. Finally, the pellet of cells was resuspended in R-buffer, resuspension buffer. The 100 µL Kit (Invitrogen™MPK10096) was used, 100 µL of a mixture of cells, buffer, and SiRNA to a concentration of 200nm was taken up and electroporated with the following parameters: 1 pulse, 400mv, and for 20 seconds. The cells were then delivered into wells of a 24 well culture plate into antibiotic free media. At 24 and 48 hours the media was changed and at 72 hours the cells were harvested for RNA and protein and media collected for aldosterone measurement.

2.7 RNA extraction:

RNA was extracted using the spin column kit PureLink™ RNA Mini Kit (Invitrogen, 12183018A). Lysis buffer was mixed with 2- Mercaptoethanol to make 1% Mercaptoethanol, 200 µl of buffer mixture was added to each well of 24 well plate and cells were scraped and collected into 1.5 ml RNase free Eppendorf tubes. 1.5 volume of 100% ethanol is added to the cell lysate and vortexed. 700 µl of the sample was loaded into the spin cartridge and the sample centrifuged at 12,000g for 30 seconds, the flow-through discarded this step was repeated twice to ensure that RNA binds to the column. The process of RNA washing was then performed with 350µl of washbuffer I added to the column recentrifuged at 12,000g for 30 seconds and the flow through discarded. 80µl of DNase treatment, Purelink™ DNase (Invitrogen 12185010) was then added to the spin cartridge membrane and was left to incubate at 15 minutes at room temperature. Then a further 350µl of washbuffer I was added to the spin cartridge and centrifuged again at 12,000g for 30 seconds, the flow through discarded. RNA is further washed by washbuffer II which is applied twice to the spin cartridge and centrifuged through, the flow through discarded. The spin cartridge is then spun at 12,000g for 1 minute at room temperature. For the elution process 30µl of RNase-free water is applied to the centre of the spin cartridge and left to incubate for 1 minute and then further centrifuged the flow through now containing RNA. This was then quantified by nanodrop in ng/µl.

2.8 Reverse transcription:

High-Capacity RNA-to-cDNA kit (Fisher Scientific, 4387406) was used to obtain cDNA. Reactions were made up to 20µl samples. 10 µl of 2x RT buffer mix, 1µl of 20x RT enzyme mix, and the remaining 9µl was made up with RNA to the amount of 20ng and the mix brought up to 20µl by RNase free water.

The solution was then run in the thermocycler for 60 minutes at 37 ºC, 5 minutes at 95 ºC and then cooled to 4 ºC.

2.9 mRNA expression studies:

mRNA expression of our genes of interest was performed by Quantitative Polymerase Chain Reaction (RT-qPCR), a readily available commercial TaqMan gene expression probes were purchased. (Please see Table 2 2).

The qPCR solution was made up to 20 µl per sample. 10µl of TaqMan advanced fast master mix (Thermofischer, 4444557) was mixed with 4µl of RNase free water, 1 µl of gene expression probe, and 5µl of the cDNA of interest. The samples were aliquoted in duplicates.

The RT-qPCR analysis was done on a C1000 Touch Thermal Cycler machine (Bio-Rad, USA), the programme was the following: Results were analysed using the $2^{-\Delta\Delta CT}$ method using the housekeeping *18S* rRNA (Life Technologies, USA) for normalisation. Controls with nuclease-free water were used as well as transfected cells with empty vector/ control were used as control to assess fold change. The following thermocycling conditions were used: 2 minutes at 50º C, 10-minute hold at 95º C, 1 second denature at 97º C, 20 second anneal/extend at 60º C (40X PCR cycle).

Gene	Assay ID	Amplicon Length	Properties
LHCGR	Hs00896336_m1	105	Probe spans exons
CYP11B1	Hs01596404_m1	137	Probe spans exons
CYP11B2	Hs01597732_m1	137	Probe spans exons
DKK1	Hs00183740_m1	68	Probe spans exons
FAP	Hs00990791_m1	64	Probe spans exons
RDH12	Hs00288401_m1	61	Probe spans exons
C90RF84	Hs00330277_m1	124	Probe spans exons
GNRHR	Hs00171248_m1	109	Probe spans exons
GNA11	Hs01588833_m1	140	Probe spans exons
GNAQ	Hs00387073_M1	78	Probe spans exons
TMEM132E	Hs01368963_m1	68	Probe spans exons
CTNNB1	Hs00355045_m1	86	Probe spans exons
18S	Hs99999901_s1	187	Primer and probe within same exon
CHRNA7	Hs01063372_m1	101	Probe spans exons

Table 2 2: Table illustrating all the Taqman assay probes used for qPCR work.

2.10 Aldosterone assay:

For measurement of aldosterone in cell culture media the Cisbio Aldosterone assay kit (64ALDPEH) was used. Media was collected at significant time points pertinent to individual experiments. 10µl of each sample was put into three wells, triplicates, within a 384 well plate (BioScience #784075). The Cisbio kit utilises Homogeneous Time- Resolved Fluorescence (HTRF) mechanisms, aldosterone is detected via a competitive assay. Europium cryptate labels an anti-aldosterone antibody whilst a XL665 dye labels aldosterone. When they dyes are near each other the excitation of the Europium cryptate leads to a Fluorescence Resonance Energy Transfer (FRET) to the XL665 which acts as an acceptor and fluoresces at the wavelength 665 nm. The aldosterone competes with this transfer and prevents the FRET from occurring, this specific signal is inversely correlated to the aldosterone concentration. For each well of sample or standard 5µl Europium cryptate and 5µl of XL665 was added that had come from stock solution and diluted to 1:50 in detection buffer. This led to 20µl of assay in each well, the negative control wells did not have XL665 but a further 5µl of detection buffer 3.

The standard curve of solutions were diluted in the following way to achieve their aldosterone working solutions:

STANDARD	SERIAL DILUTIONS	ALDOSTERONE WORKING SOLUTION (ng/mL)
Standard Stock solution	Thawed stock solution	100,000
Intermediate standard solution #A	10 µL Standard stock solution + 990 µL Diluent	1,000
Standard 9	40µL Intermediate Standard Solution #A + 210 µL Diluent	160
Standard 8	50 µL standard 9 + 100 µL Diluent	53.3
Standard 7	50 µL standard 8 + 100 µL Diluent	17.7
Standard 6	50 µL standard 7 + 100 µL Diluent	5.9
Standard 5	50 µL standard 6 + 100 µL Diluent	2
Standard 4	50 µL standard 5 + 100 µL Diluent	0.65
Standard 3	50 µL standard 4 + 100 µL Diluent	0.22
Standard 2	50 µL standard 3 + 100 µL Diluent	0.07
Standard 1	50 µL standard 2 + 100 µL Diluent	0.02
Standard 0	100 µL Diluent	0

Table 2 3: Taken from Cisbio website: https://uk.cisbio.eu/media/asset/c/i/cisbio_dd_pi_64aldpeg-64aldpeh.pdf.

The plate was left to incubate in the dark at room temperature for one hour and then read in our FLUOstar Omega plate reader (BMG Labtech, UK) at 665 nm and 625 nm. The software within the plate reader was then able to calculate the ng/ml quantity of aldosterone by calculating the % delta F which reflects the signal of the sample to the background signal, the negative control is the internal assay control.

2.11 Protein extraction:

Protein extraction from cells was performed for proteomic applications such as western blots and for correcting aldosterone concentrations. The lysis buffer we used to solubilize proteins was Radioimmunoprecipitation assay buffer (RIPA, Pierce 89900), this buffer was utilised as it is preferable for nuclear, or membrane bound proteins. RIPA was mixed 50:1 with protease inhibitor cocktail (Promega, G6521). Protease inhibitor was used to reduce the process of protein destruction, proteolysis, during cell lysis as proteases are released and can destroy the very proteins one is attempting to extract and yield. To limit further denaturation and dephosphorylation extraction was performed on 4 ºC and all equipment was kept as cold as possible. During the first step, the cell plates were kept on ice and washed with ice cold PBS two times. 200µl of lysis buffer was applied to each well in a 24 well plate and the cells were scraped and transferred to a pre-cooled Eppendorf tube. The samples were then agitated for 10 minutes at 4 ºC to help with extraction and solubility of the proteins. The samples were then centrifuged for 20 minutes at 12,000 rpm at 4 ºC, the samples were then put on ice and the supernatant aspirated into a fresh tube. Aliquots were then created to be used when required.

2.12 Protein quantification:

We used the colorimetric Bicinchonic acid (BCA) protein assay (Pierce, 23225), for protein assessment. The colorimetric technique measures using a spectrophotometer the concentration of coloured compounds within a solution. The first step of this assay is known as the Biuret reaction and leads to the detection of peptide bonds this produces a light blue chelated complex when amino acid residues bind with cupric ions in an alkaline environment. In the second step of the assay the BCA detects the cuprous cation (Cu^{1+}) which is produced following reduction of Cu^{2+} to Cu^{1+} and a deep purple colour reaction occurs. Two BCA molecules chelate with one Cu^{1+} and this leads to a linear absorbance at 562 nm with increasing protein concentrations. The reaction has particular affinity for four amino acid residues: cysteine, cystine, tyrosine, and tryptophan.

A 1 ml sample of albumin standard 2mg/ml was diluted to the following concentrations:

Dilution Scheme for Standard Test Tube Protocol and Microplate Procedure (Working Range = 20–2,000 µg/mL)			
Vial	**Volume of Diluent (µL)**	**Volume and Source of BSA (µL)**	**Final BSA Concentration (µg/mL)**
A	0	300 of Stock	2000
B	125	375 of Stock	1500
C	325	325 of Stock	1000
D	175	175 of vial B dilution	750
E	325	325 of vial C dilution	500
F	325	325 of vial E dilution	250
G	325	325 of vial F dilution	125
H	400	100 of vial G dilution	25
I	400	0	0 = Blank

Table 2 4: taken from Pierce ™ BCA Protein Assay Kit User Guide.

25µl of each sample and standard curve was pipetted into each well, each a duplicate, into the microplate required for the assay and for it to read in the microplate reader, FLUOstar Omega plate reader. Each sample a duplicate and working reagent (WR) was added at a ratio of 1:8. WR is made by mixing 50 parts of BCA reagent A with 1 part reagent B, 200 µl of WR is added to each well. The microplate was then mixed, and the assay is left to incubate for 30 minutes in 37 ^{o}C. The microplate was then read in the microplate reader at a wavelength of 562 nm. The working range of the assay = 20–2000 µg/mL.

2.13 Western blot:

2.13.1 Protein preparation:

Proteins samples were prepared for loading into gels. Antibodies used in western blot often recognise a small portion the so called “epitope” of the protein, often in order for this epitope to be accessed the 3D structure of the protein needs to be unfolded. Denaturing is often performed by adding an anionic detergent sodium dodecyl sulfate (SDS). 1.4 grams of SDS works for every 1 gram of protein, roughly 1 molecule of SDS per 2 amino acids. SDS works as a surfactant by negatively charging the proteins as they attach to its anions, therefore conferring a uniformly negative charge to the entire polypeptide. This allows the protein to migrate based on its molecular weight through the gel as opposed to whether it is positively or negatively charged.

The SDS solution we used was Laemelli buffer 2-5x, Laemelli buffer consists of 4% SDS, 20% glycerol, 10% 2- mercaptoethanol, 0.004% of bromophenol blue, and 0.125 M Tris HCl to bring it to a pH of 6.8. The glycerol adds to the density of the sample to help load into the well of the gel and allows for even loading. The bromophenol blue enables the sample to be visualised as it migrates and the 2- mercaptoethanol reduces disulphide bridges allowing the proteins to separate.

The sample and buffer were added either in a 1:1 ratio or 4:1 ratio. The mixture was then boiled between 70-100^{o} C for 5 minutes. Better results were achieved for TMEM132E when the temperature was lowered around to 70-75^{o}C or ofte not boiled at all. Samples were made up to 25-30 µl for each well with 10-30 µg of protein.

2.13.2 Western blot:

4–20% Mini-PROTEAN® TGX™ Precast Protein Gels (BioRad, 4561093) with 10 wells were loaded with 30 µl samples. The first well always comprised the protein standard ladder, Colour Pre-stained Protein Standard, Broad Range (10-250 kDa) (NEB, P7719S). The gel was then run-in running buffer (TGS, Tris-Glycine/SDS) at 140 volts for 30 minutes. The gel was then transferred onto a PVDF, polyvinylidene difluoride membrane, this membrane enables a high binding capacity for proteins. A wet transfer was performed cold, the buffer tank kept within ice. Transfer buffer which runs at a pH of 8.3 and consists of 25mM Tris base, 190 mM glycine, and 20% methanol was used and transfer occurred over 2 hours at 80-100 volts. The membrane was then blocked in 5% bovine serum albumin mixed with TBST (Tris- buffer saline with tween) for 1 hour.

2. 13.3 Antibodies:

After the blocking stage the membrane was put into the primary antibody (please see table 2 5 for list of antibodies) and incubated overnight at 4°C. The following morning the membrane was washed 3 x for 5 minutes in TBST. The secondary antibody was then applied at room temperature for 1 hour. The membrane was then incubated for 5 minutes in the enhanced chemiluminescent substrate, ECL, and read on the Bio-Rad machine. ECL substrates bind to the horseradish peroxidase conjugates on the secondary antibodies allowing the protein bands to be read.

Antibody	Producer/ Catalogue number	Use/ concentration
TMEM132E Polyclonal antibody. Rabbit IgG.	Thermofischer Scientific- PA5-85900	WB: 1:500
Ha Tag monoclonal antibody Mouse.	Thermofischer Scientific- 26183	WB: 1:200
Nicotinic Acetylcholine Receptor alpha 7/CHRNA7 Antibody. Rat	Santa Cruz- sc-58607	WB:1:200
Anti-GAPDH antibody, Mouse monoclonal	Sigma Aldrich-G8795	WB: 1:25,000

Table 2 5: Antibodies used for western blot.

2. 14 Polymerase chain reaction:

Primers used for *CTNNB1*, *GNA11*, *GNAQ*, and *GNAS* amplification in gDNA and cDNA samples are shown in Table 2. PCR in 20 µl reactions using AmpliTaq Gold™ Fast PCR Master Mix (Thermo Fisher, USA). Sanger sequencing of PCR products was performed using LIGHTRUN Tube sequencing service from Eurofins (Germany).

Gene:	Exon	5' to 3'	3' to 5'
GNA11	4 and 5	TACCTGACCGACGTTGACC	TCACGTTCTCAAAGCAGTGG
GNAQ	4 and 5	GTAGCTGACCCTGCCTACC	AGAATAACCGAGGAGTTCTGGA
GNAS	7 and 8	CAAGCAGGCTGACTATGTGC	GCGGTTGGTCTGGTTGTC
CTNNB1	3	1. TGATGGAGTTGGACATGGCC 2. GCTGATTTGATGGAGTTGGACA	1. CGAGTCATTGCATACTGTCCA 2. GTACCCTCTGAGCTCGAGTC

Table 2 6: Primers used for sanger sequencing of cDNA samples.

2.15 Immunofluorescence (IFC) of cells:

H295R cells were transfected onto 8mm sterilised glass cover slips in each well of a 24 well plate. On day 3 the media was removed, and cells covered in wheat germ agglutinin (WGA). A widely used lectin that binds to *N*-acetylglucosaminyl residues and *N*- acetylneuraminic acid (sialic acid) on cell membranes, therefore helping to elicit the cellular architecture. I used conjugate antibody WGA with Alexa 647. The WGA was warmed in Hank's balanced salt solution (HBSS) at a concentration of 5%. This was applied in 37º C incubator for 15 minutes. Cells were then fixed with paraformaldehyde solution (PFA) 4% warmed and applied to cells for 15 minutes. The formaldehyde is made up in solution with phosphate buffer solution. Fixation is important when assessing cellular structure as it aims to capture the cell in a "state of life" and tries to maintain the physical and biochemical aspects of the cell enabling antibodies to label integral cellular structures. PFA acts as a glue forming covalent cross link bonds between the cell membranes and leading to fixation of cytosolic proteins, this process stops cellular decay and degradation, giving the cell a rigid structure and making it better to visualise. The cells were then washed two times with PBS and Triton X-100 at a concentration of 0.1% was applied for 10 minutes. Triton solution is made up once again with PBS and the detergent is used to permeabilise the cell membrane this enables antibodies that would normally be too large or ionic to pass through the membrane, therefore antibodies are allowed to pass and target specific organelles. The cells were then washed with PBS two further times to ensure over permeabilization does not occur.

The next step in the procedure was to apply the dye Sudan Black, for 20 minutes. Sudan Black is made up with 70% ethanol, as an azo dye it optimises conditions by reducing the background autofluorescence we used it to a concentration of 0.1%.

The cells were then further washed in PBS. Block was then applied for one hour and then primary antibodies applied overnight at 4ºC.

On day 2 the cells were washed in PBS 3x and secondary antibodies were applied for 1 hour and then washed 3x again in PBS. DAPI was used for nuclear staining at a concentration of 1:1000 and cells were then washed. Glass cover slips were then extracted and mounted onto glass slides with mounting agent and sealed with nail varnish.

The glass slides were allowed to dry and then were visualised on the Zeiss LSM 880 with Airyscan laser confocal microscope, with of 20x 40x, and 63x.

Antibody	Producer Catalogue Number	Concentration
TMEM132E Polyclonal antibody. Rabbit IgG	ThermoFischer Scientific- PA5-85900	IF: 1:500
Goat anti- Rabbit IgG (H+L), Alexa Fluor 568	Thermofischer Scientific- A-11036	IF: 1:100
Nicotinic acetylcholine Receptor alpha 7/CHRNA7 antibody. Alexa Fluor 488.	Santa Cruz- sc-58607 AF488	IF: 1:200
Nicotinic acetylcholine Receptor alpha 7/CHRNA7 antibody	Santa Cruz- sc-58607	IF: 1: 50
Rabbit anti-Rat IgG (H+L). Alexa Fluor 488	Thermofischer Scientific A-21210	IF: 1:100

Table 2 7: Table of antibodies and fluoro tagged secondaries used in IFC work.

Clinical Methods:

2.16 Identification of subjects:

All subjects were identified at our approved research NHS trusts. All patients were confirmed to have PA by raised aldosterone/renin ratio, positive confirmatory tests, and lateralisation studies (CT/PET CT, MRI and AVS) according to our institutional protocol and in accordance with the Endocrine Society guidelines. All patients gave written informed consent for genetic and clinical investigation according to local ethics committee guideline, Cambridgeshire Research Ethics Committee for Addenbrooke's Hospital, University of Cambridge or the Cambridge East Research Ethics Committee for St Bartholomew's Hospital, Queen Mary University of London.

Full clinical methods for the FABULAS study are outlined in Chapter 4.

2.17 Statistical analyses:

For cell work, sample sizes were calculated using preliminary data and G*power software. 3 wells of cells was equal to N=1 for transfection. All statistical analyses were performed using GraphPad Prism v9 Software. Data was analysed using unpaired T-TEST if data followed a normal distribution as determined by Shapiro Wilk test. If the data did not follow a normal distribution, nonparametric tests such as Mann- Whitney U test were performed. Mean values have been given in charts with standard error of the mean bars. A P-value less than 0.05 was considered significant.

Chapter 3:

Somatic GNA11/GNAQ mutations- clues to cause and consequence of Primary Aldosteronism?

Abstract:

Primary aldosteronism (PA) is a common cause of hypertension. We recently discovered a unique recurrent somatic mutation, in aldosterone-producing adenomas (APAs), of the G-protein coupled receptor, *GNA11/Q*, at the residue, Q209, required for GTPase activity. *GNA11/Q* mediates the aldosterone response to renin-angiotensin stimulation. We found Q209P or Q209H mutations in 10/10 APAs, in which somatic mutations of *CTNNB1* were previously shown to cause LH/HCG-triggered PA, at times of high LH/HCG. 9 of these APAs also demonstrated a ~100-fold increase of *LHCGR* expression, which was replicated by transfection of adrenocortical cells by mutant *CTNNB1* [121]. Microarray indicated other genes expressed > 20-fold more by the double-mutant APAs compared to other somatic mutations, including the neuronal cell adhesion molecule, transmembrane 132E (*TMEM132E*). This protein has not been previously described in the adrenal gland. My theory is that a rise in *TMEM132E* (a deafness genes) stimulates aldosterone by enabling or trafficking of the nicotinic acetylcholine receptor (*CHRNA7*), as previously described within the inner ear with *CHRNA9/10* [175]. I also theorise that cholinergic stimulation through the drug carbachol could also lead to a rise in aldosterone synthesis.

Our immortal NCI-H295R adrenal cell line already harbours a *CTNNB1* S45P mutation. H295R were further transfected with *GNA11* Q209 H, L, P and *GNAQ* Q209H mutations, as well as wild type and empty vector. mRNA expression for *CYP11B2* was increased in cells transfected with *GNA11* Q209L (P= <0.001) and *GNAQ* Q209H (P=<0.05), relative to empty vector. Aldosterone synthesis was significantly upregulated in both, relative to empty vector (P=<0.0001). *TMEM132E* mRNA expression was upregulated to vector, particularly in cells transfected with *GNA11* Q209L (P=<0.05). H295R cells were then in further experiments transfected with a *TMEM132E* overexpression plasmid (P=<0.0001). Aldosterone synthesis increased relative to vector (P=<0.05). H295R cells treated with carbachol (a cholinergic agonist) at 15mM-20mM had a modest rise in *TMEM132E, CYP11B2,* and aldosterone synthesis (P= <0.05, P=<0.0001), compared to untreated cells. When cells were transfected with *TMEM132E* overexpression plasmid and treated with carbachol 15mM, a modest rise in *CYP11B2* was seen (P=<0.05). However, aldosterone synthesis was not significant compared to untreated vector. Another set of experiments were conducted, where H295R cells underwent knockdown of *TMEM132E* with SiRNA (P=<0.001). *CYP11B2* mRNA expression reduction was not significant, but aldosterone synthesis was (P=<0.001), compared to scrambled (control).

Aims and Objectives:

The aim of this chapter was to further investigate the genotype and pathophysiology of the double mutant APAs, that harbour *CTNNB1* and *GNA11/Q* mutations. These mutations are rarer in APA genotypes than ion channel mutations and therefore, can allude to other mechanisms that enable tumour formation and aldosterone secretion. This double mutation leads to a florid form of PA, with high levels of serum aldosterone at times of high LH/HCG secretion, such as pregnancy, puberty, and the menopause. Most of these tumours also expressed a high level of LHCGR, the composite receptor for LH/HCG, a receptor not commonly seen within adrenocortex pathology. The aim of this piece of work was to explore the functional analysis of these gene mutations, in our adrenal cortical cell line. Of interest, was the especially highly secreted trans membranous neuronal cell adhesion molecule TMEM132E, not previously described in the adrenal before.

The hypothesis entailed that when the double mutation occurs in combination a higher secretion of aldosterone would be appreciated. LHCGR clearly holds a pivotal role in pathophysiology of these APAs. I further hypothesised that *TMEM132E* overexpression would lead to increased aldosterone production. Its mechanisms are wholly unknown, however, relevant literature suggests, like in the inner ear, it likely traffics or works as an accessory function/ chaperone to the nicotinic acetylcholine receptor to the cell membrane (as shown for *CHRNA9/10*) [175]. *CHRNA7* the gene coding for the α7 nAChRs was highly upregulated in our double mutant APA. Could therefore TMEM132E be facilitating α7 function, via assembly or trafficking to the cell membrane. Further consideration is whether cholinergic stimulation of α7 receptors, which endogenously would be acetylcholine, but experimentally would be via the drug Carbachol, a cholinergic agonist, would increase aldosterone expression. Lastly, I wished to establish the relationship between TMEM132E and *CHRNA7* (α7 receptors). To appreciate their location and functions within the cell and whether they work in conjunction to increase aldosterone production.

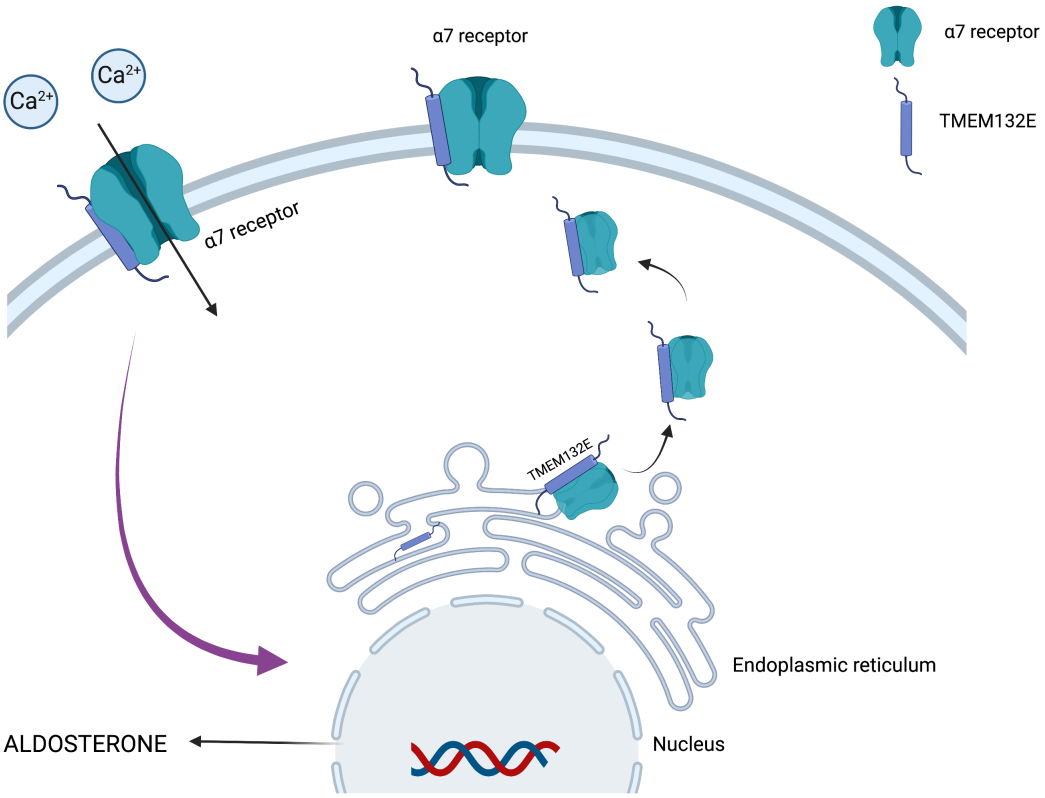

Figure 3 1: Schema illustrating the hypothesis of TMEM132E facilitating the assembly/ trafficking the α7 receptor to the membrane. α7 receptors acting as ion channels allowing the influx of calcium and kickstarting the process of aldosterone synthesis. (Designed on Biorender).

The first objective was to further evaluate the double mutation in *invitro* experiments. To further explore the role of the LHCGR as well as other upregulated genes expressed within the double mutant APAs.

The second objective was to overexpress *TMEM132E* and knockdown *TMEM132E* in H295R cell lines. With the scope to review aldosterone synthesis compared to vector-controlled cells and un-transfected cells, referred to as wild type H295R cells.

The third objective was to determine whether Carbachol has modest stimulatory effect on aldosterone production; in treated, or vector-transfected cells (empty vector) and ultimately wild-type cells.

The fourth objective was to transfect *TMEM132E* and to evaluate whether substantially carbachol-stimulated H29R5 cells increased aldosterone production further, relative both to TMEM-transfected, non-carbachol-stimulated cells *and* to TMEM132E un-transfected, carbachol-stimulated cells. In Silencing of *TMEM132E,* we set out to see if aldosterone production was reduced, with a greater fold-reduction of carbachol-stimulated, than basal aldosterone production.

The fifth objective was to determine whether *TMEM132E* and *CHRNA7* co-transfection in H295R cells could enable us to better visualise through confocal work the proteins within the cell.

The double mutant work data was included in work published in the following publication in Nature genetics:

Nature genetics: *Zhou et al. Somatic mutations of GNA11 and GNAQ in CTNNB1-mutant aldosterone-producing adenomas presenting in puberty, pregnancy or menopause. NatureGenetics volume 53, pages1360–1372 (2021).*

3.1 Case reports:

Within our NIHR-EME funded MATCH study two further patients were discovered who completed the ten patients in the British/Irish cohort of *CTNNB1/GNA11/Q* mutations. Each one, once again presenting with explosive onset of PA. One at time of puberty and the other during the first trimester of pregnancy. Both harboured a *GNAQ,* a paralogue of *GNA11,* mutation which were novel to our cohort. Invaluable data was obtained from these two patients and their tissue.

3.1.1 Patient A: Patient A or determined patient: 9 within our British/Irish cohort, was a 23-year-old Caucasian female, who was found to be incidentally hypertensive age 9. This came about when she measured her blood pressure on her grandfather's blood pressure machine. She was investigated under the care of the paediatricians and no cause for her hypertension was found. She was discharged from their care and advised to monitor her blood pressure. During her first pregnancy she presented with PA within the first trimester. She was treated with Amiloride, which is deemed safe within pregnancy. On screening renin was <0.2 nmol/hr and aldosterone: 973 pmol/l

A CT scan of her adrenals indicated a bulky left adrenal and on further scanning with the molecular medicine ^{11}C- metomidate PET scan indicated a high probability of a left sided secreting adrenal adenoma (please see figure 3 2). An AVS under ACTH stimulation showed a lateralization value of 139.5:1 to the left adrenal and she underwent a left adrenalectomy. She has achieved complete clinical and biochemical success off all medications. She has had subsequent pregnancies with no concerns.

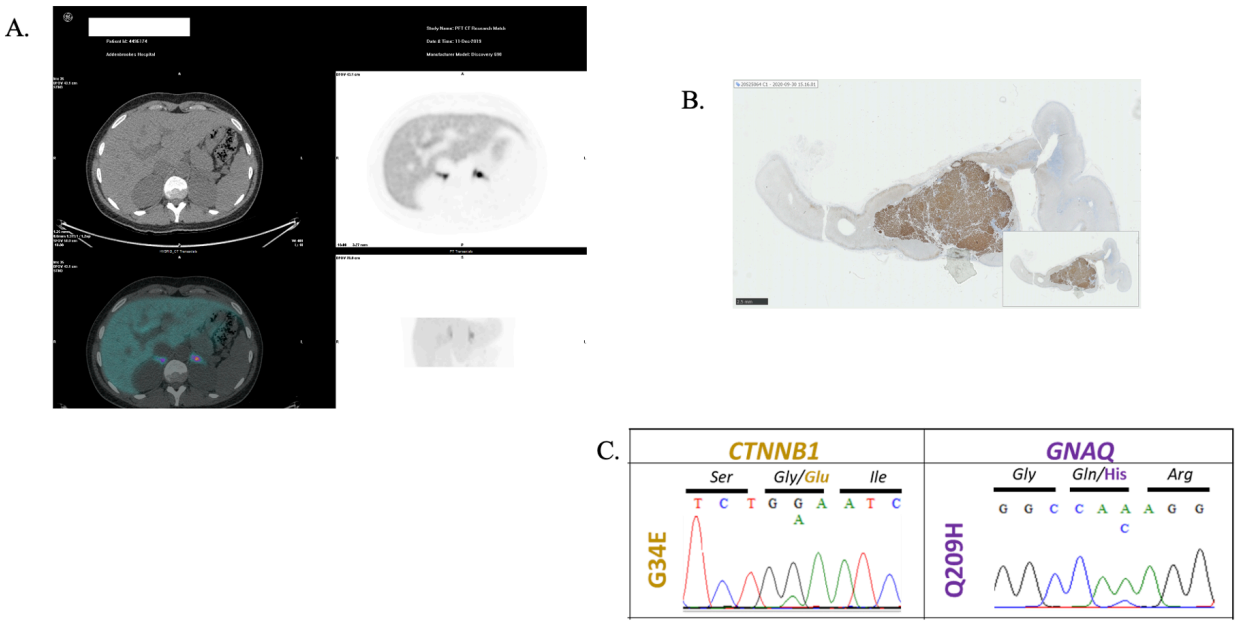

Figure 3 2: a. illustrating the coronal and axial ^{11}C metomidate PET CT scan overlay of Patient A/9. The very metomidate avid nodule in black and white, on the images in the right is the APA. The nodule is also appreciated in colour on the left sided image. This illustrates the focal point of the aldosterone producing cells that take up the isotope b. Immunohistochemistry of CYP11B2 expression within Patient A/9's tumour. It stains densely within the tumour with very little in the surrounding normal adrenal tissue particularly to note the ZG. c. RNA was extracted from fresh tumour and normal tissue collected within RNA later. The RNA was then converted to cDNA for sequencing and for qPCR to appreciate the expression of the unique genes upregulated within double mutant APAs. Sanger sequencing of patient A/9's APA showed a *CTNNB1* mutation of G34E in exon 3. Glycine changed to a Glutamine shown above in the figure. Patient A's APA also showed a mutation of *Q209H GNAQ* mutation Exon 3, Glutamine changed to a Histidine.

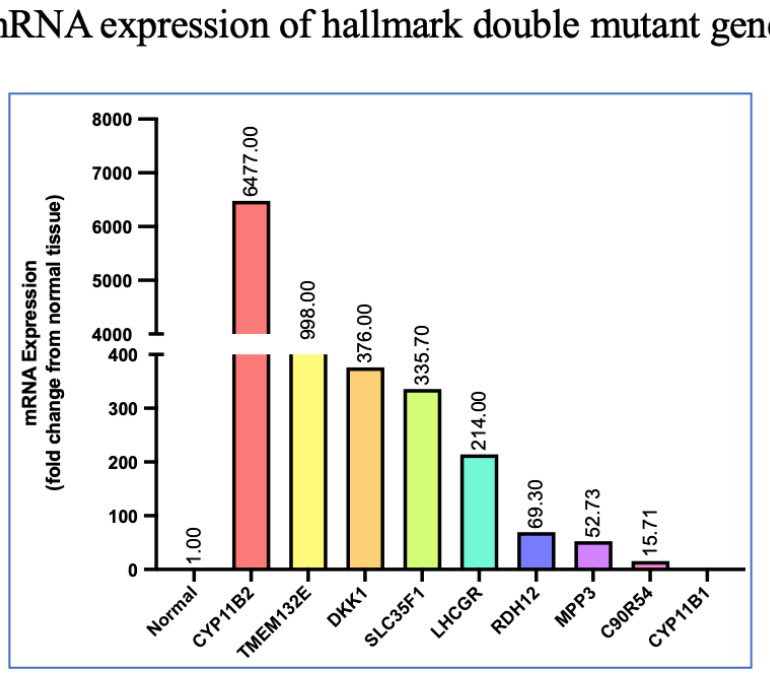

Figure 3 3: indicating the mRNA expression of known upregulated genes described in patients with the double mutation of *CTNNB1* and *GNA11/Q.* Demonstrated in the APA of patient A/9. Fold change was relative to normal adjacent adrenal tissue. One can appreciate there was a sizeable upregulation of *CYP11B2, TMEM132E, DKK1*, *SLC35F1, RDH12, MPP3* and *C90R54. CYP11B1* was fully suppressed.

3.1.2 Patient B: Patient B also known as patient 10 within our cohort, was a healthy 23-year-old. Unfortunately, at the age of 19 she had a miscarriage, but subsequently went on to have a further pregnancy. Within this pregnancy she was diagnosed with hypertension. She was formally diagnosed with PA several years later and referred to the MATCH study. She lateralised to the left and underwent a left sided adrenalectomy. Despite a small episode of hypertension, likely gestational in her last pregnancy following adrenalectomy she is cured and off all medications.

Patient B's tumour differed to our other double mutant APAs; in that it had a very low expression of *LHCGR.*

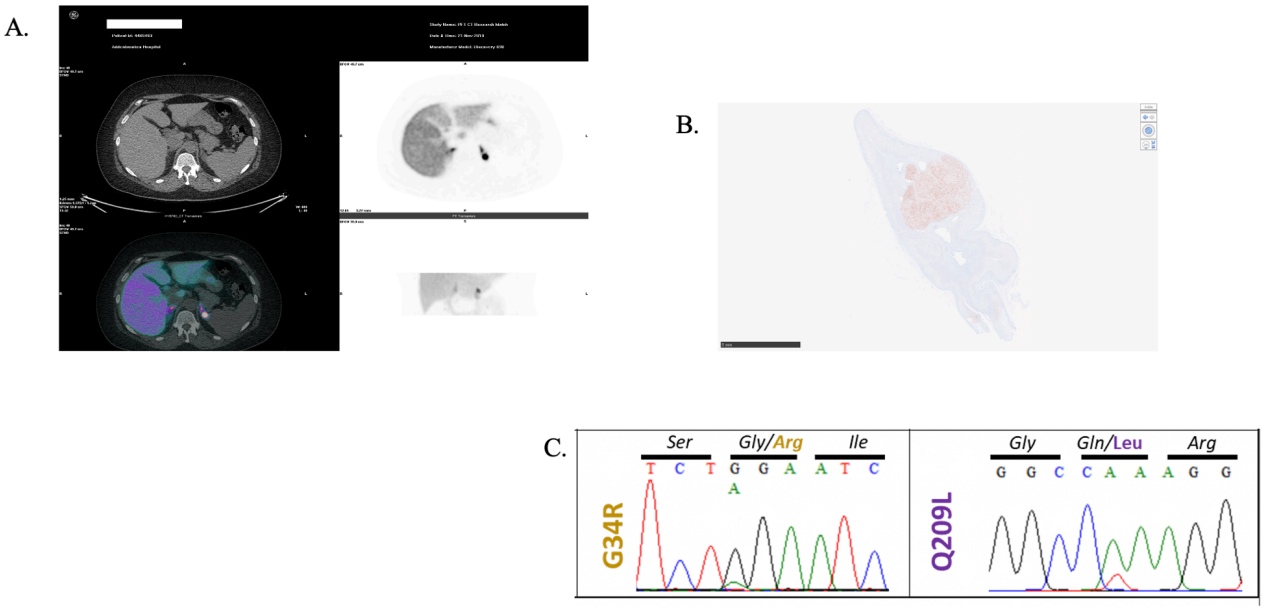

Figure 3 4: a. illustrating the coronal and axial ^{11}C metomidate PET CT scan overlay of Patient B/10. The very metomidate avid nodule is appreciable on the lateral images in black and white. This shines bright yellow on the left sided images in colour. This illustrates the focal point of the aldosterone producing cells that take up the isotope b. Immunohistochemistry of CYP11B2 expression within Patient B/10's tumour. It stains strongly within the tumour with very little in the surrounding normal adrenal tissue particularly to note the ZG. C. RNA was extracted from fresh tumour and normal tissue collected within RNA later. Sanger sequencing of patient B/10's APA showed a *CTNNB1* mutation of G34R in exon 3. Glycine changed to Arginine. Patient B/10's APA also showed a mutation of *Q209L GNAQ* mutation Exon 3, Glutamine changed to a Leucine.

3.2.1 *GNA11* and *GNAQ* mutations in *CTNNB1* harbouring H295R cells lead to increased expression of CYP11B2 and aldosterone:

We hypothesised that the unique double mutation of *CTNNB1* and *GNA11* and its paralog *GNAQ* lead to an increase in *CYP11B2* mRNA expression. Therefore, increasing aldosterone synthesis, as occurred in the APA tumours. The immortal NCI-H295R cell line already harbour an S45P *CTNNB1* mutation and therefore *GNA11* Q209 H, L and P mutation containing plasmids were transfected into the cells as well as *GNAQ* Q209H. H295R cell passages varied between 18-24. All plasmid constructs held a GFP tag. mRNA, protein, and culture media were all harvested at 72 hours. For mRNA expression measurement of fold change in each case was calculated relative to empty vector (control) or wild type.

1. **Assessment of transfection rates:**

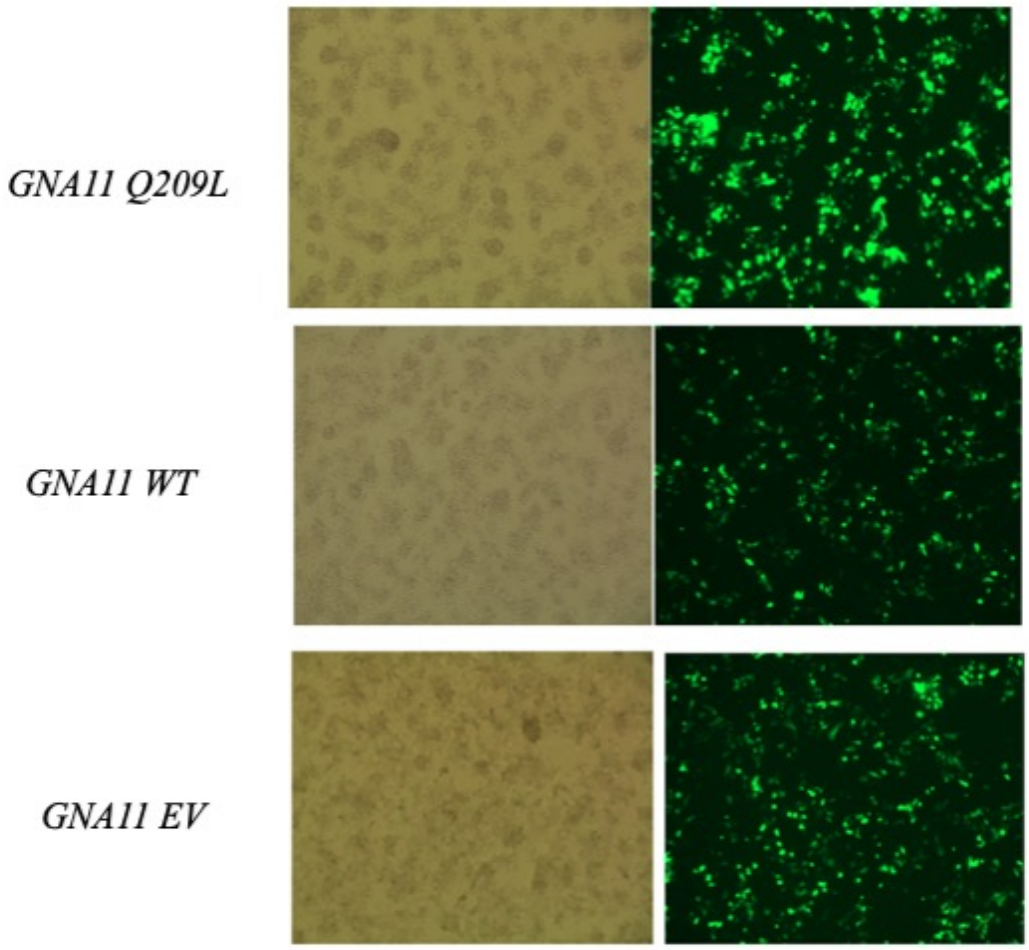

Figure 3 5: Microscope image of H295R cells P22, 24 hours post transfection with *GNA11* Q209L plasmid x10 magnification. a) = brightfield, b) = GFP. The plasmids contained a GFP tag and therefore transfection rate was estimated to be around 60-70%. Transfected cells could be easily visualised.

2. Transfection rates *GNA11* and *GNAQ* expression:

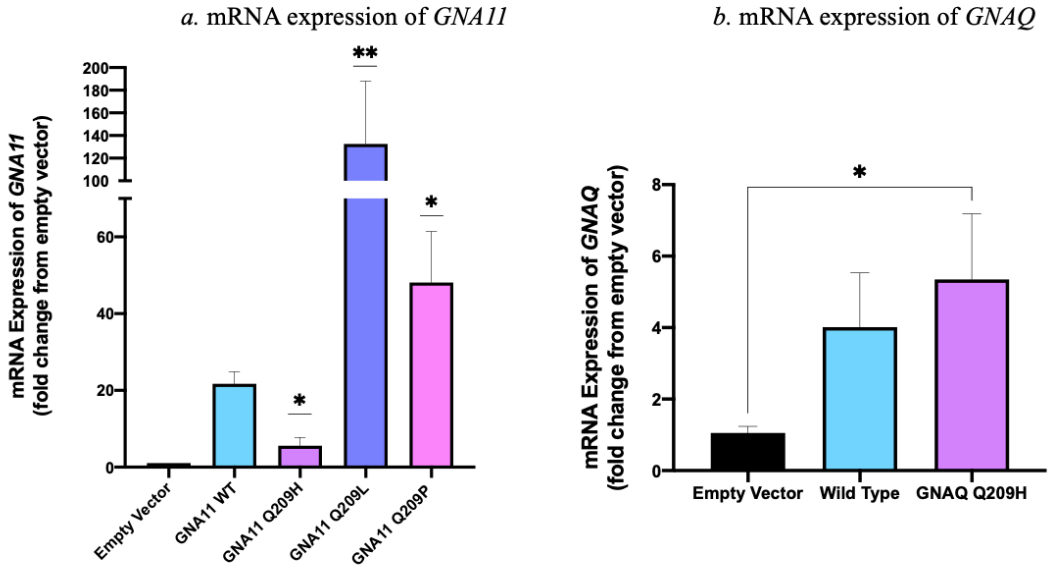

Figure 3 6: To enable us to better quantify transfection rate of each plasmid. The mRNA expression of *GNA11* and *GNAQ* in transfected cells was measured relative to vector and wild type. The above figure a. illustrates the mRNA expression of *GNA11* in the three different mutation subtypes and b. *GNAQ* mRNA expression. This indicated that when mRNA expression was compared to vector, a good transfection rate was achieved. *P=<0.05, **P= <0.001, those with no star noted no significance (Mann Whitney test). The most striking being Q209L. (N=4-10)

3. *CYP11B2* and Aldosterone secretion:

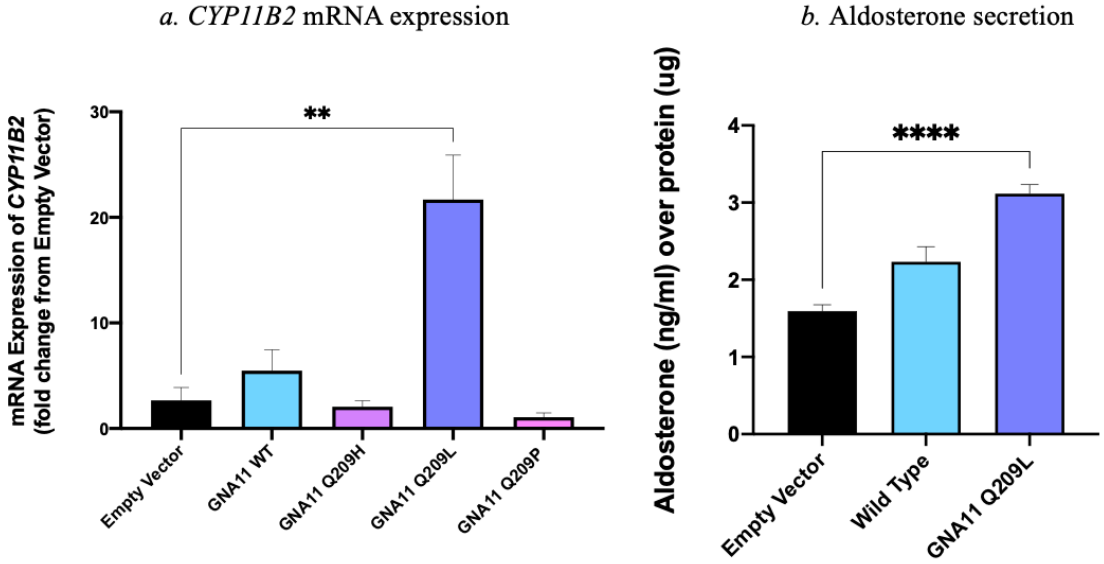

Figure 3 7: a. Demonstrates the upregulation to a statistical significance in mRNA expression of *CYP11B2,* in H295R cells transfected with *GNA11* gene types Q209H, L, and P relative to vector. Gene expression was over 20-fold (**P=<0.001 Mann Whitney test) greater, than vector for Q209L. Q209H and P were not significant. (N=6-10). b. Demonstrates an increase in aldosterone secretion corrected for protein, in cells transfected with *GNA11* Q209L (****P= <0.0001, Mann Whitney test). (N =4-5).

a. *CYP11B2* mRNA expression:

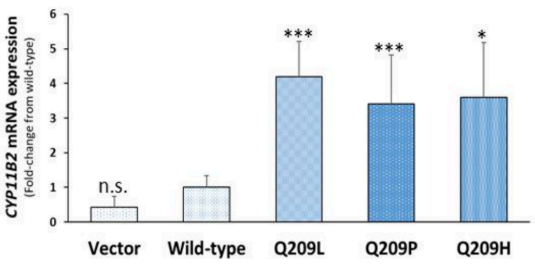

b. Aldosterone secretion:

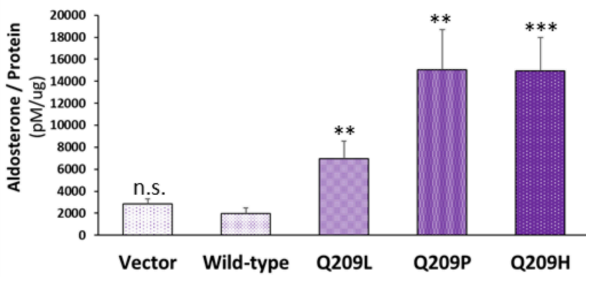

Figure 3 8: a. Demonstrates accumulative data from figure 3 7 and further data (N=12-26). Illustrating once again increased *CYP11B2* expression in H295R cells transfected with *GNA11* Q209H, L, P. b**.** Indicates aldosterone secretion corrected for protein in cells transfected with *GNA11* Q209H, L, P. (N=40). n.s., not significant; *P<0.05,**P<0.005,***P<0.0005 compared to wild-type. (two-sided Student's t-test).

Further data, figure and statistics courtesy of Dr Elena Azizan and Dr Junhua Zhou.

4. **H295R cells, passages: 19-23, transfected with *GNAQ* EV, WT and mutant Q209H. Fold change was measured relative to empty vector (control).**

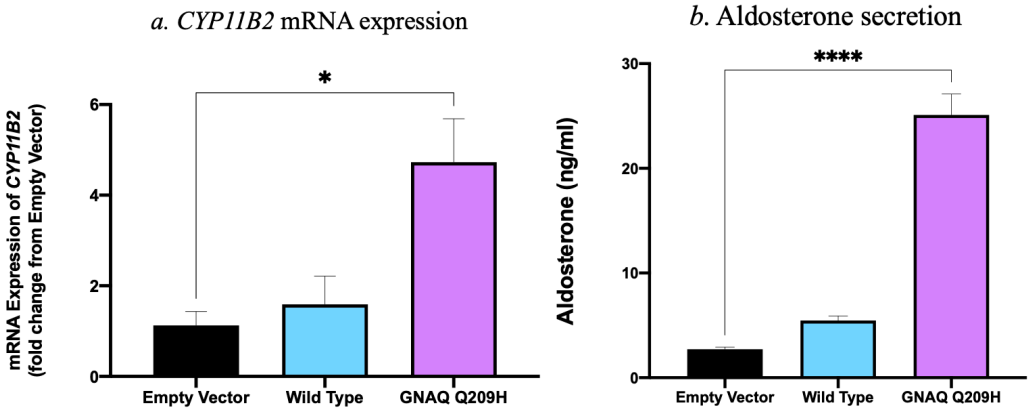

Figure 3 9: a. Illustrates increased *CYP11B2* mRNA expression in H295R cells, fold change in expression relative to empty vector. *P= <0.05 (Mann Whitney test). b. Increased aldosterone secretion in H295R cells transfected with *GNAQ* Q209H. ****P= <0.0001. (Unpaired T-Test). (N=6).

As hypothesised transfections leading to cells harbouring double mutation increase *CYP11B2* expression and aldosterone secretion. The double mutation likely works in conjunction, as although there was a modest effect with wild type cells, that just contain *CTNNB1* mutation, it is most marked when there is the double mutation present. The rise in aldosterone is fitting with the *CYP11B2* expression, the drive seemingly coming from biosynthesis of the aldosterone molecule. The double mutation working in conjunction was also proven by Dr Elena Azizan. Dr Azizan illustrated that in H295R cells transfected with *GNA11* Q209H and P when *CTNNB1* was knockdown by *CTNNB1* SiRNA or indeed when the Beta catenin inhibitor ICG-001, a treatment that actively blocks beta catenin transcription, was applied to cells for 24 hours, aldosterone was reduced significantly in; vector, wild type and cells with GNA11 Q209H and P (P=<0.0005) [134] . Interestingly it did not blunt aldosterone production entirely. This strongly points in favour of a “double effort” from both mutations leading to increased aldosterone synthesis.

3.1.3 GNA11 and *GNAQ* mutations in *CTNNB1* harbouring H295R cells lead to a reduced expression of CYP11B1.

An interesting phenomenon was noted in double mutant APAs. The APAs had little to no expression of *CYP11B1*. This was not only alluded to in RNA sequencing but was well demarcated on IHC. Whilst this is what would be expected in an area of high *CYP11B2* expression, we do not always appreciate this in APAs. As mentioned previously some APAs also co-secrete cortisol and therefore have protein staining for *CYP11B1* and mRNA expression.

1. **Functional *CYP11B1* expression.**

Once again as in the above experiments, H295R cells were transfected with this time *GNA11* Q209H and P plasmids and mRNA was measured for *CYP11B1.*

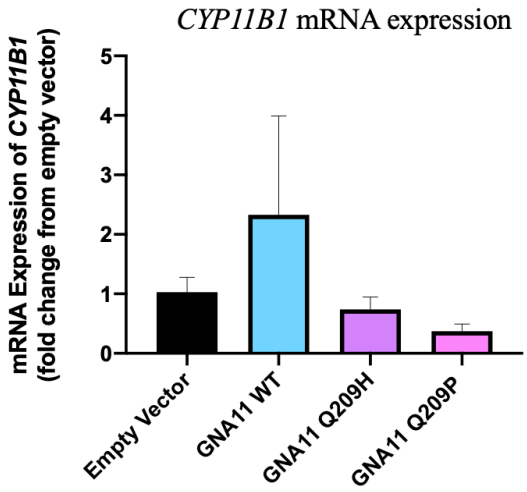

Figure 3 10*:* Demonstrates downregulation of mRNA expression of *CYP11B1* with no statistical significance (Mann Whitney test) relative to vector and wild type. Q209L was not performed on this occasion. (N=2-4).

This trend was in keeping with the double mutant APAs, who were all found to have reduced *CYP11B1* expression compared to those APAs that harboured sole *CTNNB1* mutations and other somatic mutations. Whilst the APAs that co-secrete cortisol and therefore *CYP11B1* lend themselves to a more "Zona fasciculata" cell type of APA. We can thoroughly appreciate the double mutants sit nicely within the more "Zona Glomerulosa" type category.

3.1.4 GNA11 and *GNAQ* mutations in *CTNNB1* harbouring H295R cells lead to an increased expression of *TMEM132E, DKK1, FAP* and *GNRHR.*

The most upregulated gene in the double mutant APAs was *LHCGR*, this was the initial heralding signal that drew our attention to the microarray [145]. However, this was not consistent in all the double mutant cohorts especially when there was a weaker association with pregnancy. Therefore, the question was raised of other genes that may be uniquely upregulated in these tumours. Unsupervised hierarchical clustering was performed on two of the British double mutant patients and of a Swedish patient whose data was readily within the public domain [146]. This led to the discovery of several "hallmark" genes that were greatly upregulated compared to other APAs. One of the most interesting genes was *TMEM132E* the neuronal transmembrane protein as documented in the introduction above (1.15.2). We theorised that transfection into H295R cells of *GNA11* and *GNAQ* would lead to an increase in mRNA expression of *TMEM132E*. H295R do express small quantities of their own *TMEM132E,* (it is difficult to quantify endogenous amounts) so we looked for an appreciable rise. Other genes that were upregulated also included *DKK1, FAP, GNRHR, SLC35F1,* and *C9ORF84*.

1. **TMEM132E expression within H295R cells transfected with *GNA11* Q209H, L, P, and *GNAQ* Q209H.**

TMEM132E mRNA expression

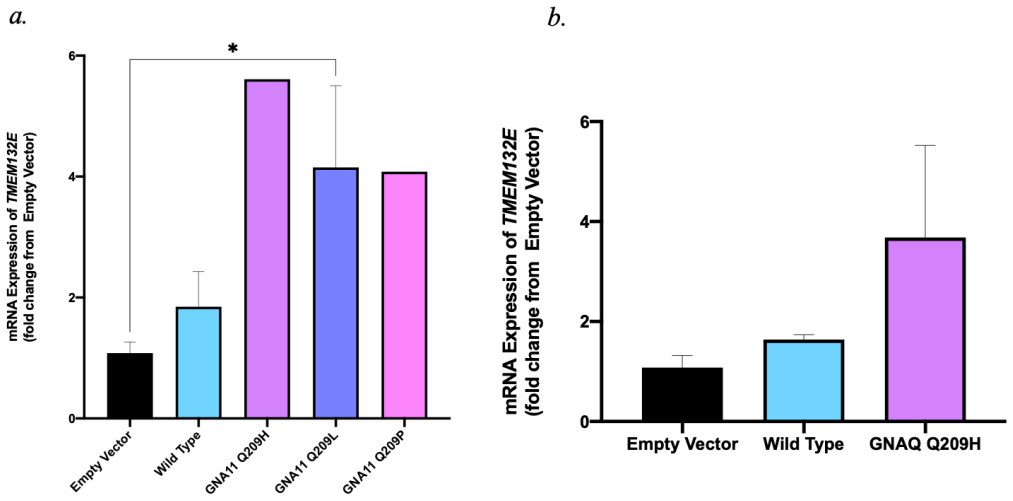

Figure 3 11: a. Demonstrates upregulation in the mRNA expression of *TMEM132E* in gene type Q209L with *GNA11* transfection. Gene expression was over 4-fold (*P=<0.05 Unpaired TTEST) greater than empty vector. (N=1-11). The other conditions held no significance. b. demonstrates mRNA expression of *TMEM132E* in *GNAQ* Q209H transfected cells but to no significance.

1. **FKK1, FAP and GNRHR expression**.

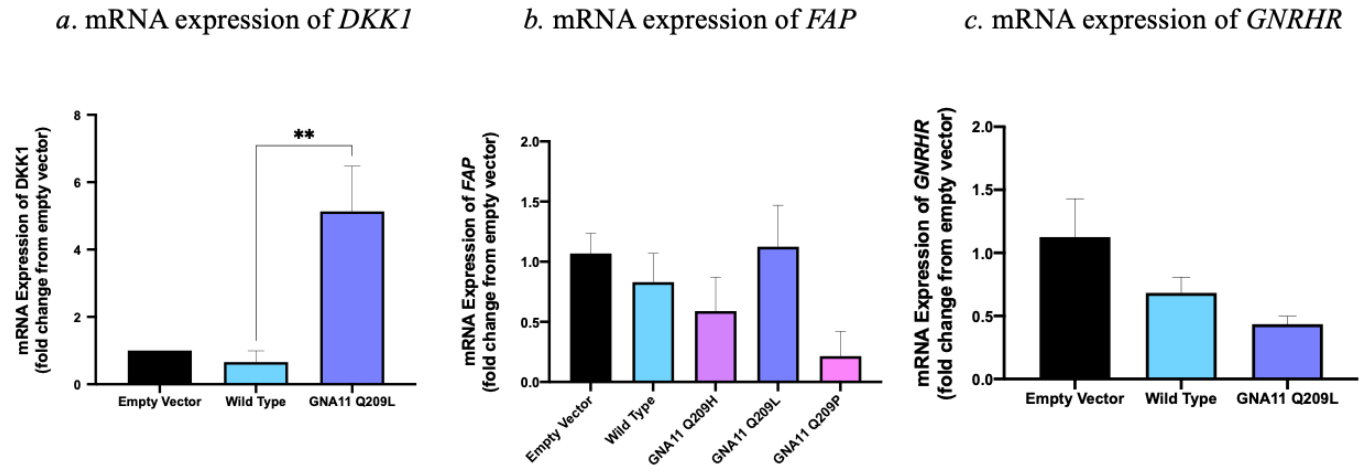

Figure 3 12: a. Demonstrates the upregulation in mRNA expression of *DKK1* in gene type Q209L. Gene expression was over 5-fold (**P=<0.001 Mann Whitney test) greater than wild type. Q209H and P were not performed on this occasion. (N=2-11). b and c demonstrate the mRNA expression but not to a statistical significance of both *FAP* and *GNRHR* in gene types Q209H, L and P relative to vector or wild type. (N=2-11).

2. **Further gene expressions.**

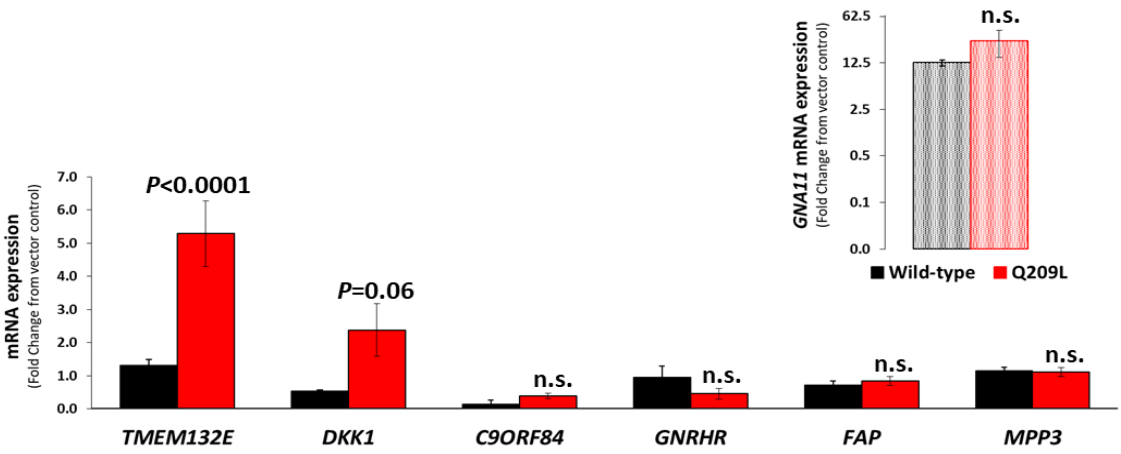

Figure 3 13: Gene expression profile of *GNA11* wild-type and Q209L transfected H295R cells by qPCR (n=3-20). There was a statistically significant interaction between the effects of genotype on gene expression (P=0.0012; two-way ANOVA) n.s., not significant. **Further data, figure and statistics courtesy of Dr Elena Azizan and Dr Junhua Zhou** [134].

Multiple genes are unique to the double mutant APA cohort. RNA sequencing, mRNA gene expression of double mutant APA, and also functional experiments relative to control have all indicated a significant rise in *TMEM132E* as well as *LHCGR*. I, therefore, felt *TMEM13E* was a particular gene of interest and wanted to fully investigate it and look at is role.

3.1.5 Double mutant patients have high expression of *LHCGR.*

One of the most distinctive and fascinating features of the double mutant APAs was the significantly increased expression for the LHCG receptor. This is attributed to the elevated levels of the hormones LH/FSH and Beta HCG in circulation at times of presentation. The LHCG receptor is a well-known G-coupled protein receptor and therefore we theorised its presence acts as a signalling receptor leading to downstream activation of aldosterone synthesis. Questions, therefore, arose of its presence within double mutant APAs and whether it was a subsequence cause of *CTNNB1* mutation or *GNA11/Q* mutations alone, or whether both had to be present together for LHCGR to be activated. *LHCGR* was significantly upregulated ($P<0.001$) especially when it was compared with control APAs who harboured sole CTNNB1 mutations and other control APAs harbouring other somatic mutation such as KCNJ5. Only one double mutant patient had low levels of *LHCGR* [134].

1. **IHC of LHCGR expression in a double mutant APA:**

A crucial experiment was to confirm on a protein level, that LHCGR was present within the double mutant APAs, compared to controls. Difficulties arose when using LHCGR antibodies, the one previously used in the NEJM paper from 2015 [121] had gone out of production. Various different antibodies were explored ultimately deciding upon the anti-LHCGR no. NLS1436 (1:200; Novus Biological).

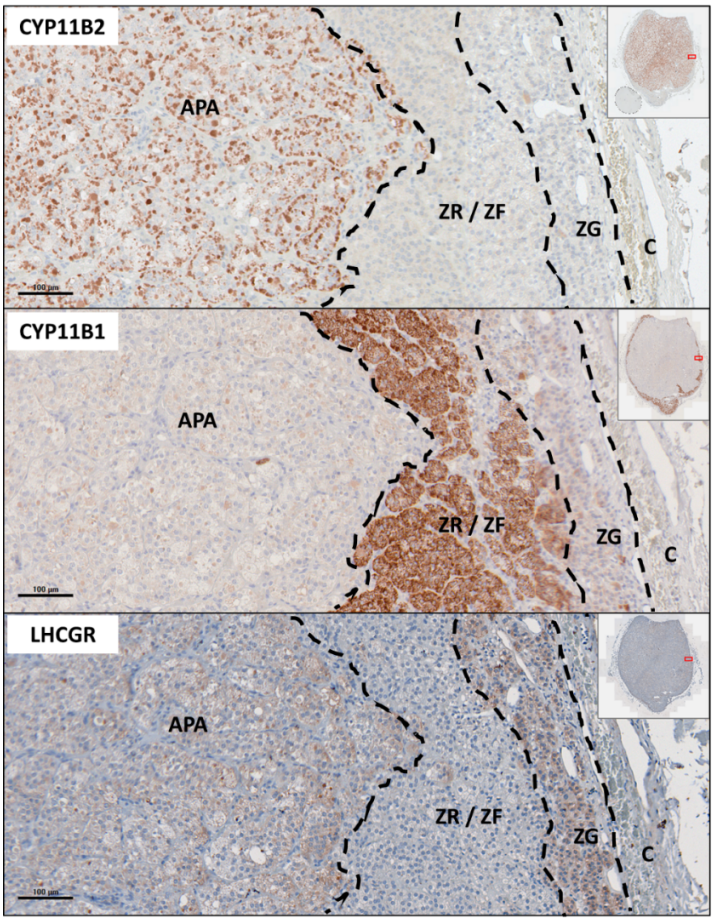

Figure 3 14: The above figure illustrates the expression zones of various proteins on IHC of a double mutant APA. Patient 7 (presented in pregnancy) of our British cohort. In the top figure on the left is CYP11B2 staining (anti-CYP11B2 antibody was gifted from Celso Gomez Sanchez) within the APA but little to none within the ZG. There IS dense staining of CYP11B1(anti-CYP11B1 antibody also gifted from Celso Gomez Sanchez) within the ZR and ZF but none within the surrounding layers. LHCGR was not only found to be within the APA but also within the ZG and medulla.

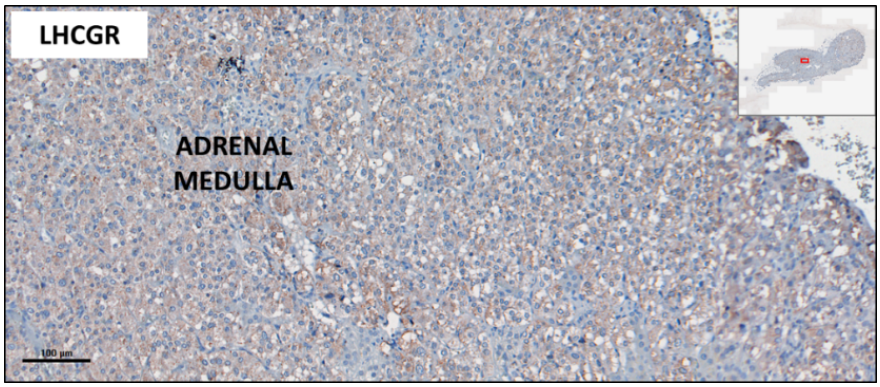

Figure 3 15: This slide indicating Medulla in one of our control patients who did not harbour a double mutation. One can appreciate the staining within the medullary region.

IHC performed by our team along with the Pathology department at Queen Mary University of London.

The presence of LHCGR within the medulla was somewhat novel to us. The medulla does not come from the same cell lineage as the adrenal cortex and gonads. I was put to task to further evaluate the presence of LHCGR within the medulla. Medulla and ZF as control were extracted from four control patients from the MATCH study and double mutant patient A/9. To ensure medulla was correctly extracted, the marker Phenylethanolamine N-methyltransferase (PNMT) was used. PNMT is highly abundant in the adrenal medulla where it methylates noradrenaline to adrenaline thus making it a reliable marker. As patient B/10 had little to no LHCGR production from her APA this was used as a negative control. Patient A/9's highly expressive tumour for LHCGR was used as a positive control. A further MATCH patient's APA was used as negative control for PNMT. This had been determined by RNA sequencing of MATCH APAs. Medulla is often well demarcated due to its distinctive colour, slices of fresh frozen adrenal were cut relatively thick >1mm on the cryostat on to RNAse free slides, tissue was then scraped into Eppendorf's on ice, and tissue was homogenised by hand. RNA was then subsequently extracted, and qPCR performed.

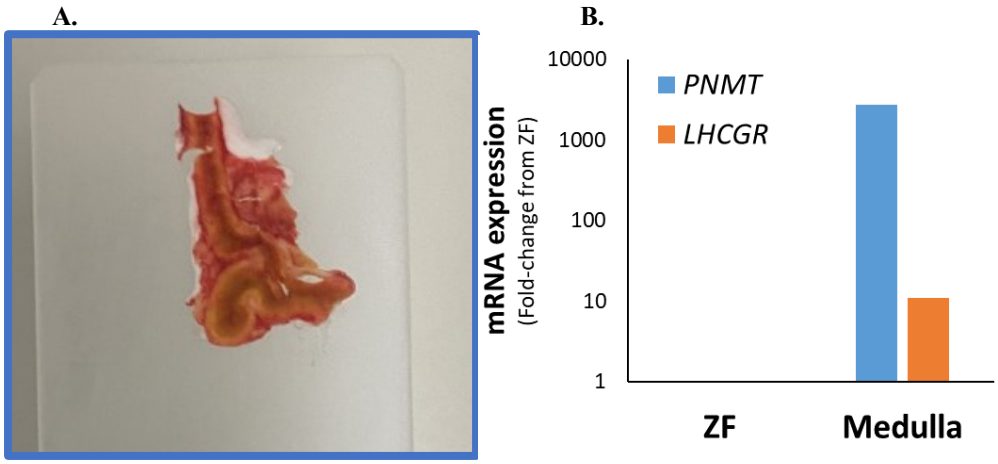

Figure 3 16: A. Shows a fresh slice of adrenal, with the well demarcated darker brown of the medulla and the more golden colour of the cortex surrounding it. B. Indicates mRNA expression of PNMT in blue and LHCGR

in orange indicating there is an elevated level of expression of LHCGR in the medulla and this is in keeping with the IHC. (N=5)

This, therefore, strengthened our case that within medullary tissue, there is also evidence of LHCGR expression. The antibody was therefore correctly binding to protein and its presence in double mutant APAs could not be disputed.

3.1 6 H295R cells do not express *LHCGR*.

As our immortal adrenal cell line, H295R was a staple for functional studies, it was a challenge when we realised, they do not express LHCGR. There may be various reasons for this, the most likely being they have become so far removed down the passages from their original tumour and cell origins making it hard to express certain proteins and hormones.

One of my studies involved several conditions to see if the mRNA expression of LHCGR in H295R cells would increase. I incubated the cells for 6, 24, and 48 hours in beta HCG or luteinising hormone. Our aim was to see if we mimicked the environment "in vivo" of the double mutants, this may "switch on" LHCGR receptors within the cells. Cells were treated with Luteinising hormone at concentrations of 1 x10^7(L7), 1x 10^8(L8) and 1 x10^9 (L9) and Beta HCG at 1 x10^7(H7), 1x 10^8(H8) and 1 x10^9 (H9).

A.

Name	Sample	18S	LHCGR
6.L7	S01	9.02	0.00
6.L7	S01	8.83	0.00
6.L8	S02	8.45	0.00
6.L8	S02	8.47	38.83
6.L9	S03	9.59	39.45
6.L9	S03	9.24	37.45
6.H7	S04	16.07	0.00
6.H7	S04	15.94	0.00
6.H8	S05	11.87	0.00
6.H8	S05	11.45	0.00
6.H9	S06	9.21	0.00
6.H9	S06	11.09	0.00

B.

Name	Sample	18S	LHCGR
24.L7	S07	8.85	0.00
24.L7	S07	8.73	0.00
24 L8	S08	9.38	39.00
24 L8	S08	9.48	0.00
24 L9	S09	8.78	0.00
24 L9	S09	8.78	0.00
24.H7	S11	8.25	39.04
24.H7	S11	8.16	0.00
24.H8	S12	9.39	0.00
24.H8	S12	9.39	0.00
24 H9	S13	8.50	38.98
24 H9	S13	8.66	39.65

C.

Name	Sample	18S	LHCGR
48 L7	S01	10.81	0.00
48 L7	S01	10.89	39.54
48 L8	S02	8.81	0.00
48 L8	S02	9.42	0.00
48 L9	S03	8.83	0.00
48 L9	S03	8.26	0.00
48 H7	S04	9.82	0.00
48 H7	S04	8.42	0.00
48 H8	S05	9.76	38.77
48 H8	S05	9.35	0.00
48 H9	S06	9.70	38.61
48 H9	S06	9.41	0.00

Figure 3 17:A. Indicates the qPCR results of both *18s* (the housekeeper gene) and *LHCGR* of H295R cells after 6 hours of treatment, with various concentrations of LH and BHCG. B. Indicate the results at 24 hours and C. 48 hours.

Most results for *LHCGR* read as 0.00 or likely interference at 38-39 cycles. When I reviewed these results individually with their graphs, they were not in fact true readings. It was concluded that we would have to find other cells to do functional *LHCGR* work on. We had discussions on OVCAR ovarian cell lines but when we tested them, they did not seem to express much *LHCGR.* Ultimately, the closest cells would be primary adrenal

cells. Primary adrenal cells harvested from APAs collected at surgery are carefully cultured; however, they often yield very few cells and the cells do not undergo division. Transfection of these cells can be trickier as during electroporation there may be a high death rate which can render the few cells even scarcer. Another factor to consider is these cells are also cultured with other adrenal cells: ZF, ZR, Medulla, and fibroblasts that have been collected inadvertently within the mix.

Primary adrenal adenoma cells were subsequently transfected with empty vector, *CTNNB1* Δ45 mutation alone (plasmid held no tag), *GNA11* 209P mutation alone (GFP tag), and *CTNNB1* and *GNA11* combined.

3.2 TMEM132E:

3.2.1 TMEM132E is highly expressed in double mutant patients compared to other APA somatic mutations.

TMEM132E as documented in the introduction is a gene and protein highly upregulated in our double mutant patients. Identified initially on RNA sequencing, as the second most upregulated gene in our double mutant APAs. It has not been readily described in the adrenal gland before but rather in neuronal cell structures. It is fairly unique to APAs, not having previously been noted in other somatic mutations of APAs and not previously described within the adrenal gland. TMEM132E is readily expressed within hair cells of the inner ear and as described in the introduction there are genes of the inner ear that are also found to be present within the adrenal cortex, which leads us to question their role there.

TMEM132E was upregulated 25-100-fold in double mutant APAs (P=0.0025) compared to APAs harbouring sole *CTNNB1* mutations and APAs with sole *KCNJ5* mutations [134].

The closest we have seen it to aldosterone producing pathology is within studies conducted on the somatic mutations in Cell adhesion Molecule 1 (CADM-1). CADM-1 is a transmembrane cell adhesion molecule involved in cell-to-cell communication. Our lab uncovered two patients with somatic mutations of CADM-1, one at the position of Gly379Asp (V379D) and the second VAL380Asp (G380D) both presenting with PA. *TMEM132E* was found to be upregulated in H295R cell transfected with both the mutations of V379D and G380D and particularly in those stimulated with Angiotensin II. (Figure 3 20)

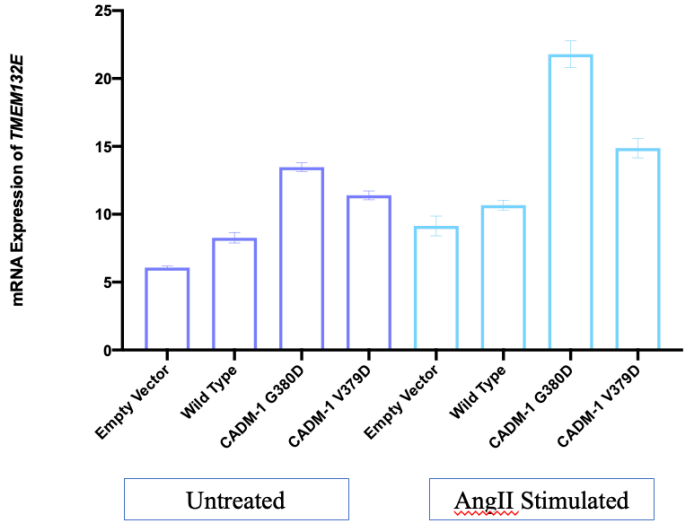

Figure 3 18: Graph indicating the mRNA expression of *TMEM132E* in H295R cells, transfected with empty vector, wild type, the CADM-1 mutation G380D and CADM-1 mutation in V379D. Taken at 72 hours. The violet bars represent untreated cells, whilst the blue cells indicate those treated with Angiotensin II 1 $x10^{-7}$ concentration. There is an almost 20-fold upregulation in *TMEM132E* in cells transfected with CADM-1 G380D mutation and stimulated with Angiotensin II.

Raw RNA sequencing data taken from studies performed by Dr Xilin Wu.

3.2.2 *TMEM132E* overexpression in H295R cells leads to increased mRNA expression of *CYP11B2* and aldosterone synthesis.

I hypothesised that *TMEM132E* upregulation may be associated with increased expression of aldosterone synthesis. The double mutant APA patients all had extremely high levels of serum peripheral aldosterone and a well-documented PA phenotype. One potential pathway to increase aldosterone synthesis was via LHCG receptors as documented above however one of our patients (patient B/10) tumour did not have high expression of *LHCGR* but stood out remarkably for her high *TMEM132E* value. As mentioned above H295R cells do not express *LHCGR,* yet in functional studies were still able upon transfection with *GNA11/Q* to elicit significantly elevated autonomous *CYP11B2* expression and aldosterone. This leads us to wonder if TMEM132E as it is so abundantly present may be playing a role in the synthesis of aldosterone.

Our immortal cell line H295R was transfected with a *TMEM132E* plasmid construct and a plasmid control "empty vector" construct for comparison. The plasmid construct for *TMEM132E* contained a C-HA tag. Experiments were also compared to wild-type H295R cells these are labelled as **"WT H295R cells"**. *TMEM132E* is endogenous to H295R cells but in small amounts. H295R passages ranged from 19-23.

1. **TMEM132E transfection.**

a.

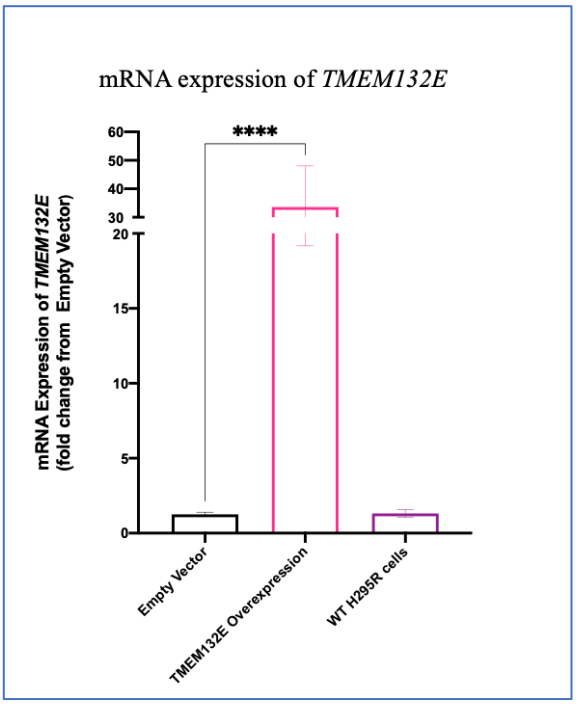

b.

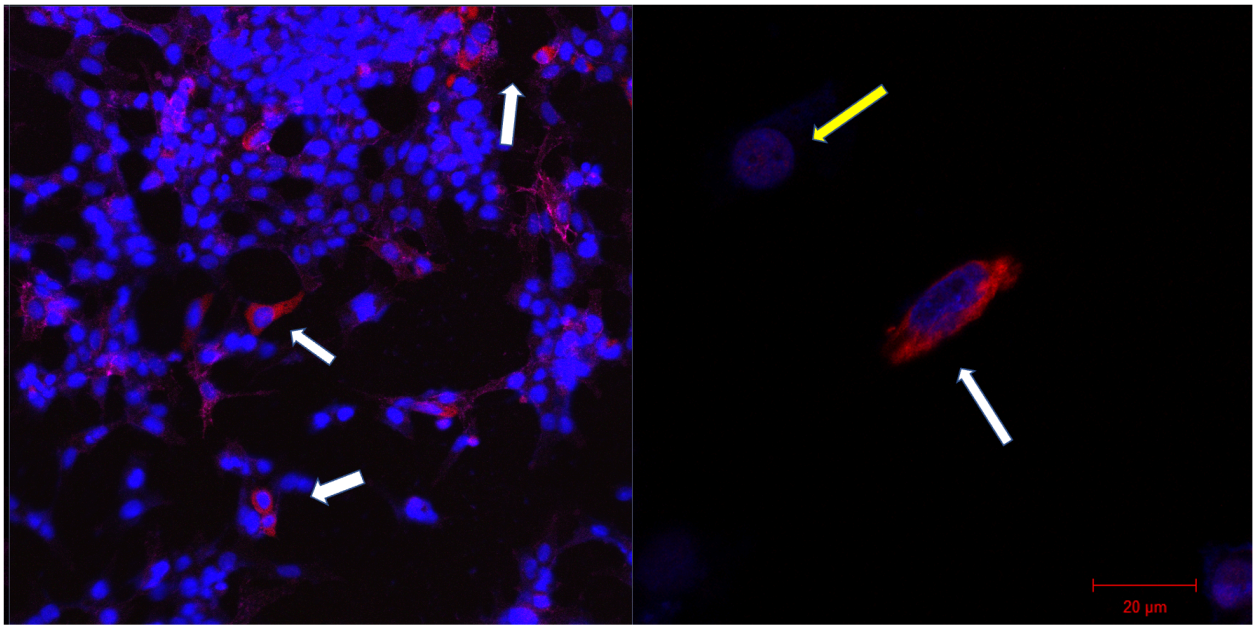
20 µm

c.

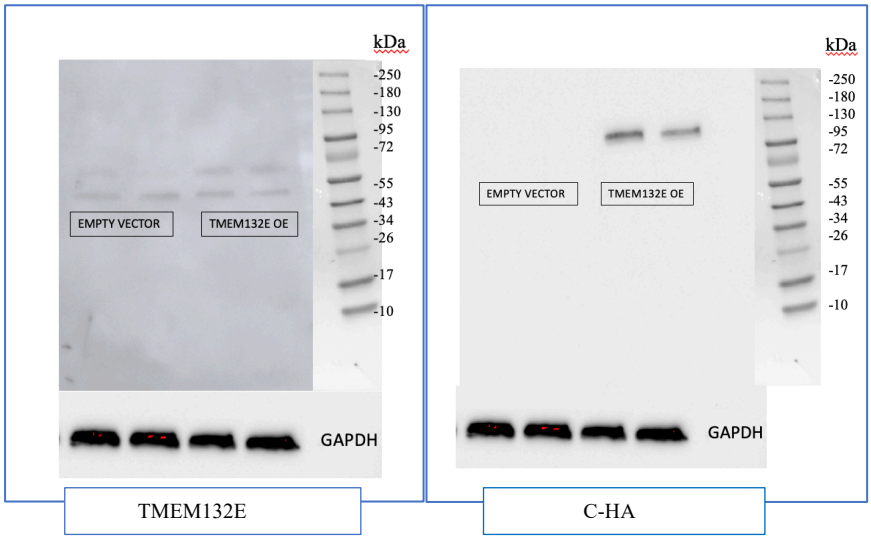
kDa
-250
-180
-130
-95
-72
-55
-43
-34
-26
-17
-10
EMPTY VECTOR
TMEM132E OE
GAPDH
TMEM132E
kDa
-250
-180
-130
-95
-72
-55
-43
-34
-26
-17
-10
EMPTY VECTOR
TMEM132E OE
GAPDH
C-HA

Figure 3 19: a. This figure demonstrates the upregulated mRNA expression of *TMEM132E* in H295R cells transfected with *TMEM132E* plasmid. Fold change is calculated from empty vector. ****P= <0.0001 (Mann Whitney test). (N=12-17). This graph highlights a good transfection rate of H295R cells.

b. Two confocal images both illustrating H295R cells transfected with *TMEM132E* plasmid construct x20, x63. *TMEM132E* has been tagged with an Alexa fluor 588 tag, in red. DAPI has been used to stain the nuclei blue and Wheat germ agglutinin Alexa fluor 647 for cell membrane (magenta). The image on the left indicates multiple transfected cells highlighted by white arrows. The image on the right illustrates one transfected cell (white arrow) and one non transfected cell (yellow arrow) next to each other, within the same focus. This enabled me to confirm that in transfected cells, the increase in mRNA expression was being translated into cellular protein.

c. Illustrates two immunoblots. The blot on the left, the protein, has been stained for antibodies for TMEM132E at a concentration of 1:500. The size of TMEM132E is calculated around 116 kDa, however, for TMEM132E over expression one can appreciate two bands in each lane. The top two bands are at the positioning of TMEM132E at 67 kDa, the lower bands may represent non-specific binding due to SDS or that the protein exists in multiple isoforms. 67kDa is in keeping with the Thermofischer TMEM132E Antibody (PA5-141158) we used however not with the size of TMEM132E.

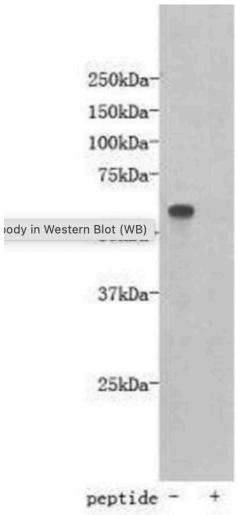

Figure 3 20: Antibody testing data and image from Thermofischer of the antibody TMEM132E found at 67kDa.

The TMEM132E antibody was a particularly difficult antibody to use for western blot, I had to try multiple parameters; including using the antibody in 5% BSA, varying concentrations of the antibody 1: 250-1000. Multiple bands was often a feature. We did wonder if the band we were seeing at 67 kDa may have been cleaved TMEM132E and therefore smaller. Another theory is could this antibody not be specific and be staining for an immunoglobulin (Ig) protein domain of a similar structured protein.

The second blot on the right on the other hand is stained for the C-HA tag within the plasmid construct. This becomes attached to the final TMEM132E protein, here you can appreciate it is in the overexpression cells but not empty vector control. The molecular weight is roughly around 116 kDA which is the correct weight of the TMEM132E protein. GAPDH was used as control and was always found at 37 kDa on the blot.

2. ***A. CYP11B2* expression and Aldosterone synthesis.**

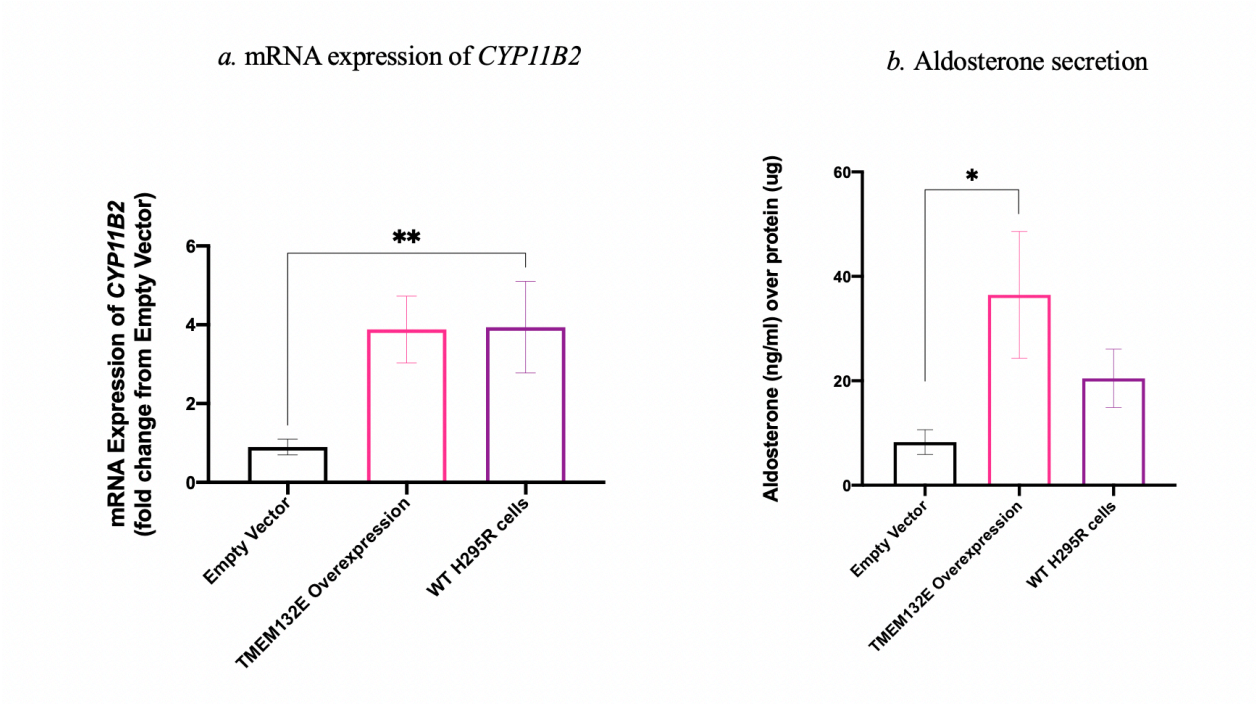

Figure 3 21: a. Illustrates mRNA expression of *CYP11B2* fold change relative to Empty Vector. *TMEM132E* overexpression (pink) and WT H295R cells (purple) increased by 4-fold. *TMEM132E* overexpression= ns, WT H295R cells, **P=<0.01 (Unpaired TTEST). Aldosterone corrected for protein *TMEM132E* overexpression *P=<0.05, WT H295R cells= ns. (Unpaired TTEST). (N=11-16). These graphs appreciate a rise in *CYP11B2* in overexpressed H295R cells with TMEM132E and a significant increase in aldosterone secretion. This, therefore, strengthens the hypothesis that increased *TMEM132E* expression leads to a rise in aldosterone production.

B. Different concentrations of *TMEM132E* overexpression:

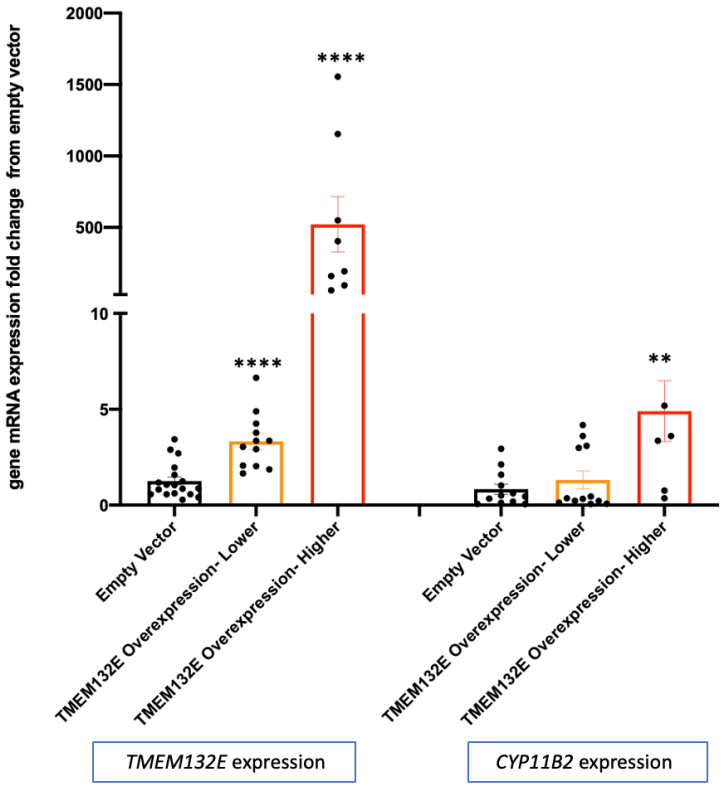

Figure 3 22: mRNA expression on the left side of the graph indicates the gene *TMEM132E* and on the right *CYP11B2* expression. Fold change was always calculated relative to empty vector. The yellow bars represent experiments where H295R cells were transfected with 5 µg of *TMEM132E* plasmid DNA per well, within a 24 well plate. The red bars represent experiments where cells were transfected with 15 µg of *TMEM132E* plasmid DNA per well, within a 24 well plate. The *TMEM132E* expression at the lower concentration had a fold change of 3-4 ****P=<0.0001 (Mann Whitney test) whilst at the higher concentration the fold change was 500-fold ****P=<0.0001 (Mann Whitney test). *CYP11B2* expression at the lower concentration of *TMEM132E* plasmid was non-significant but at the higher concentration **P=<0.01(Mann Whitney test) it was almost double indicating that increasing concentrations of *TMEM132E* expressed within the cells led to increased *CYP11B2* expression. ((N=4-18).

3.2.3 Carbachol treatment of H295R cells leads to increased expression of *TMEM132E* and aldosterone.

A large component of my study and hypothesis was the concept that TMEM132E acts as an accessory protein to nicotinic acetylcholine receptors (nAChRs). Please see Figure 3 1. We speculate TMEM132E could work as a membrane trafficker, shuttling nAChRs to the membrane or it may also play a role in the assembly and function of nAChRs. A nicotinic receptor subunit which was found through RNA sequencing to be upregulated in our double mutant APA cohort was α7 coded by the gene *CHRNA7*. When we looked through the nAChRs expressed within H295R cells, we found *CHRNA7* to be present. It was for this reason we decided to study this nAChR in the context of TMEM132E. The literature had previously pointed to the receptor α9/α10 working in conjunction with TMEM132E. It must be said however that α7 and α9/α10 are 30-40% homologous.

In order to stimulate nAChRs within H295R cells, a relatively easy to come by pharmacological agent we found was carbachol. Carbachol is a well-recognised pharmacological cholinomimetic drug, an acetylcholine receptor agonist. Often used as a drug in ophthalmology, it works via two functions. It indirectly stimulates acetylcholine receptors by inhibiting acetylcholinesterase, as well as directly stimulating the motor end plate. It comes readily available for cell culture work and is effective within 8-24 hours. Previous studies have used concentrations as little as 1mM to 12.5 mM [174, 192].

1. **Treatment of wild-type H295R cells with carbachol at varying concentrations:**

Firstly, I wanted to observe the effect of carbachol alone on wild-type H295R cells and the effect this may have on *TMEM132E* expression and subsequently *CYP11B2* expression and aldosterone synthesis.

I made up a titration curve of carbachol to varying concentrations with cell nil media. Cells were starved for a minimum of 6 hours before carbachol treatment was applied. Carbachol treated media was applied for 24 hours before mRNA, protein and media was collected.

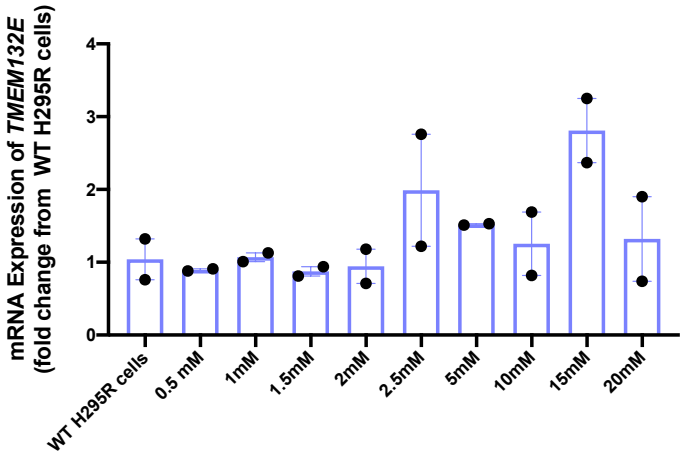

Figure 3 23: mRNA expression of *TMEM132E* in cells treated with varying concentrations of carbachol (0.5mM to 20 mM). Fold change was compared to wild type (WT) H295R cells, these were **untreated cells**. At above 2.5 mM there was an increase in *TMEM132E* expression that reached a peak around 15mM, however this was not raised to any statistical significance. (N=2)

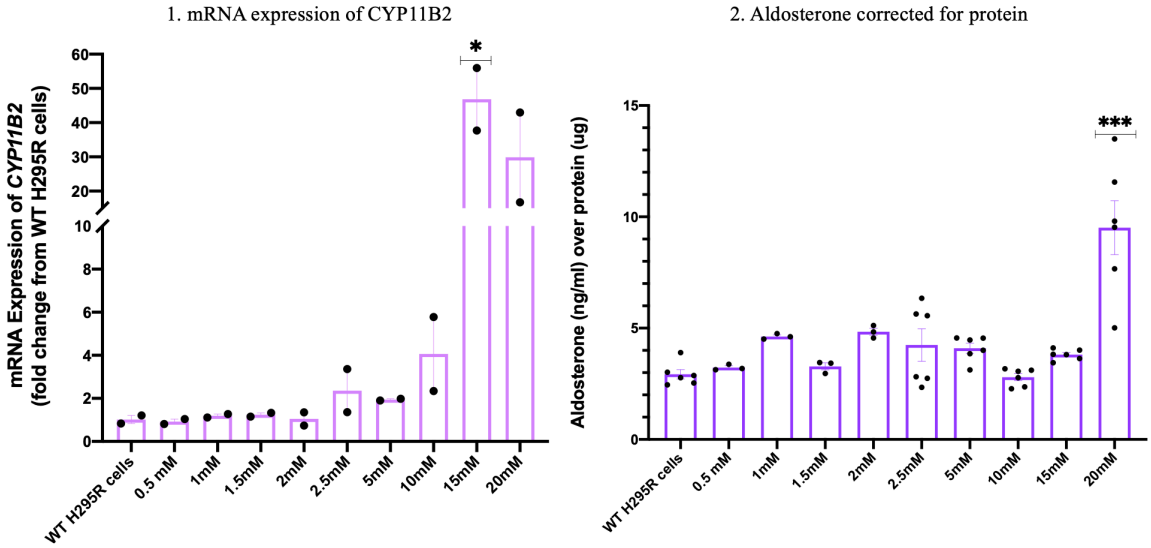

Figure 3 24:1. mRNA expression of *CYP11B2* in cells treated with carbachol at varying concentrations 0.5-20mM, fold change was measured against WT H295R cells/ untreated cells. At 15mM *P=<0.05. 2. The second graph indicates Aldosterone corrected for protein, at 20mM ***P=<0.0001 (unpaired TTEST). (N=2-6).

This seemed to suggest that when the concentration of Carbachol reached a threshold of 15-20mM, is when there was a significant rise in *CYP11B2* expression and Aldosterone synthesis.

3.2.4 *TMEM132E* overexpression in H295R cells treated with carbachol leads to increased aldosterone synthesis.

The next step was to treat cells that had been transfected with *TMEM132E* plasmid for overexpression and compare them to empty vector transfected cells or WT H295R cells. This time I picked three concentrations and treated to 2mM, 5mM and 15 mM of carbachol. I also compared carbachol treatment at 15mM with cells stimulated with Angiotensin II. Cells were also treated with combined carbachol 15mM and Angiotensin II, to see if they worked synergistically to increase *TMEM132E, CYP11B2* and ultimately Aldosterone.

1. ***TMEM132E* overexpression studies treated with varying concentrations of carbachol.**

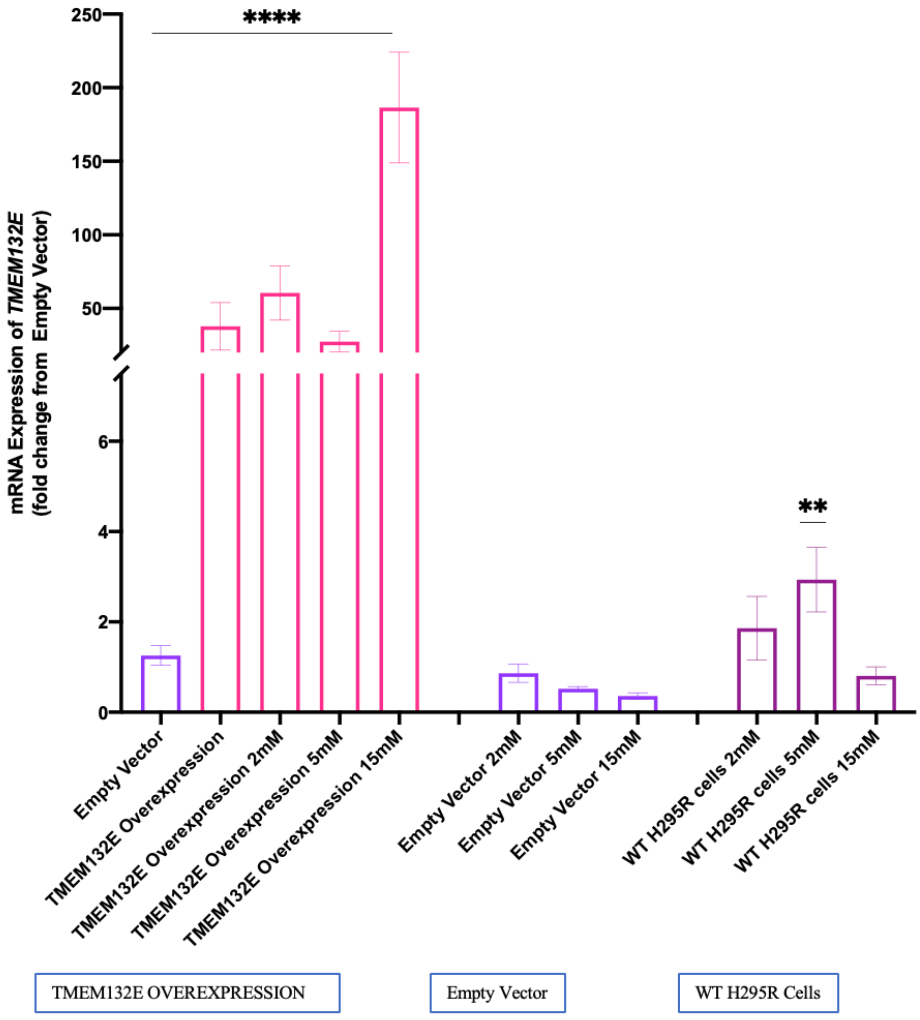

Figure 3 25: mRNA expression of *TMEM132E* in cells transfected with *TMEM132E* overexpression plasmid (pink), empty vector (violet) and WT H295R (purple). All were treated with varying concentrations of carbachol 2, 5 and 15 mM. Fold change was relative to untreated empty vector. *TMEM132E* overexpression compared to empty vector and *TMEM132E* overexpression treated with 15mM, **** P=<0.0001 (Unpaired TTEST). WT H295R cells 5mM **P= <0.01 (Unpaired TTEST). (N=4-7)

2. ***CYP11B2* and Aldosterone synthesis for *TMEM132E* overexpression studies treated with carbachol**.

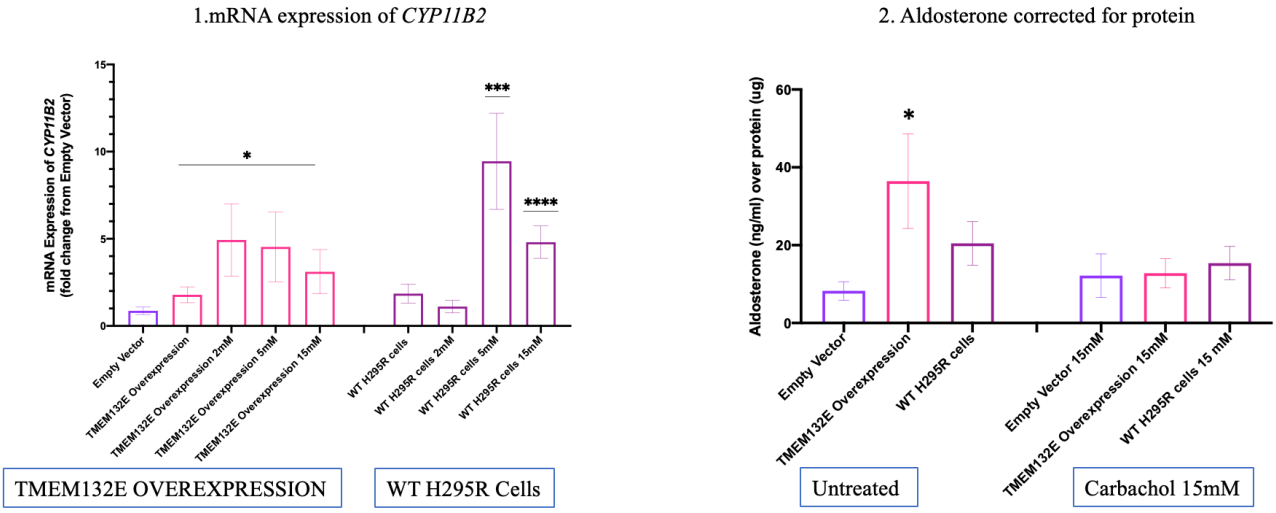

Figure 3 26: 1. mRNA expression of *CYP11B2* in cells treated with varying concentrations of carbachol: 2, 5 and 15mM. On the left of the graph in pink is *TMEM132E* overexpression, fold change compared to untreated empty vector (purple). *P=<0.05 (Mann Whitney test). On the right are WT H295R cells ***P=<0.001, ****P=<0.0001 (Unpaired TTEST). (N=4-7).

2. Is a graph showing aldosterone corrected for protein. The left side of the graph indicates untreated empty vector, *TMEM132E* overexpression (pink) and WT H295R cells (purple) and on the right cells treated with 15mM of carbachol. *TMEM132E* overexpression *P=<0.05 (Unpaired TTEST). (N=4-7)

These results were potentially very interesting, as it seems that carbachol in particular leads to increased expression of *CYP11B2* in both un-transfected H295R cells and those with *TMEM132E* overexpression.

3. *TMEM132E* overexpression studies treated with Angiotensin II.

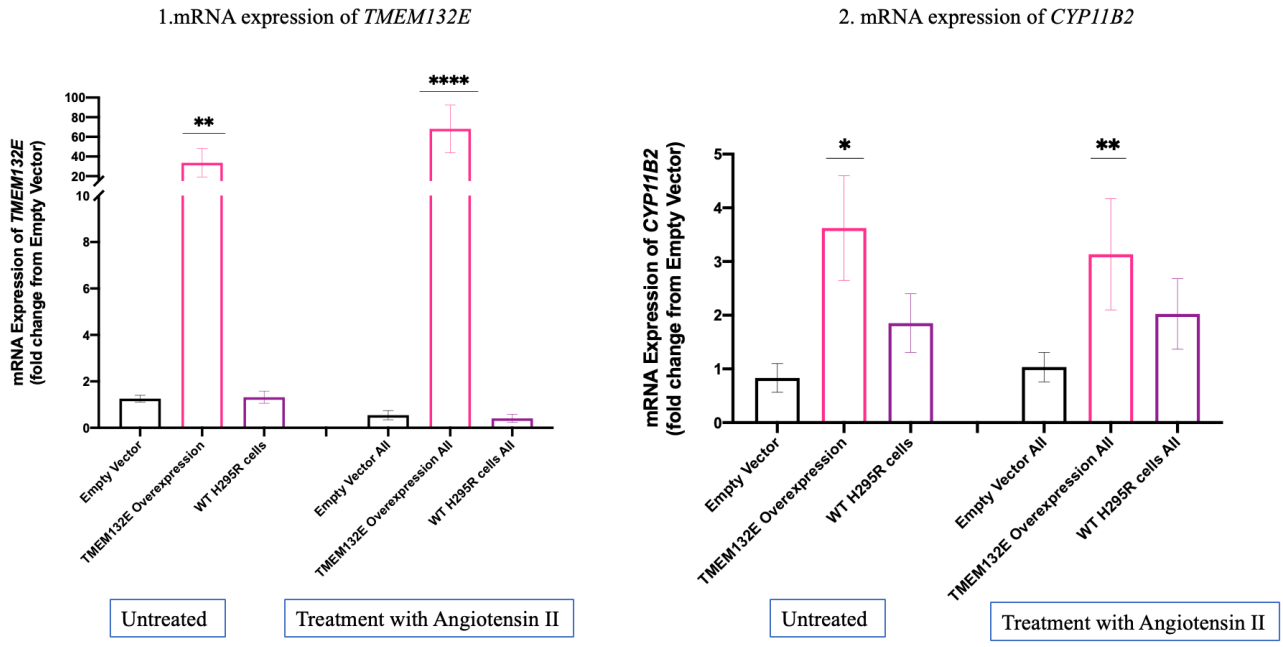

Figure 3 27: 1. mRNA expression of *TMEM132E* of empty vector (black), *TMEM132E* overexpression (pink) and WT H295R cells (purple) **untreated** and treated with Angiotensin II at a concentration of 1 x10^{-7}. Fold change was relative to untreated empty vector. **P=<0.01, ****p=<0.0001 (Mann Whitney test), rest deemed non-significant. (N=4-7)

4. *TMEM132E* overexpression studies treated with carbachol 15mM and Angiotensin II:

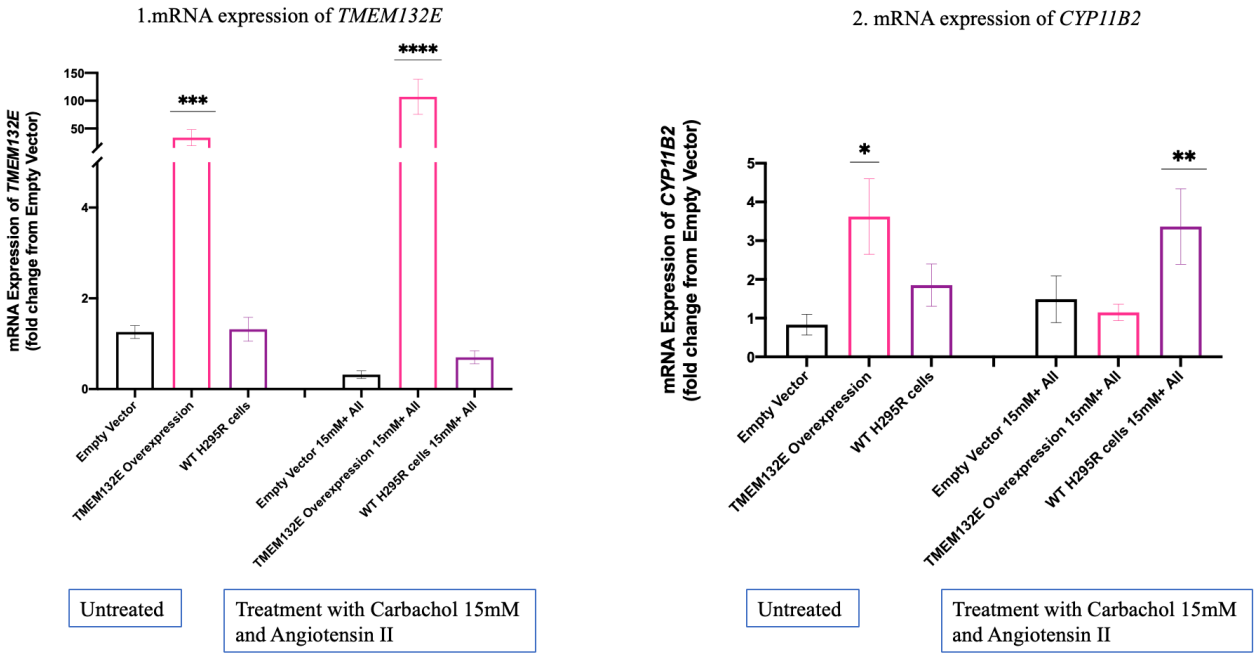

Figure 3 28: 1. mRNA expression of *TMEM132E* in untreated empty vector, *TMEM132E* overexpression and WT H295R cells and those conditions treated with Carbachol 15mM and Angiotensin II. Fold change was relative to untreated empty vector. *TMEM132E* overexpression and *TMEM132E* overexpression treated with carbachol and Angiotensin II. ***P=<0.001, ****P=<0.0001, rest non-significant. (Mann Whitney test).

2. mRNA expression of *CYP11B2* in untreated empty vector, *TMEM132E* overexpression and WT H295R cells and treated cells with Carbachol 15mM and Angiotensin II. Fold change was relative to untreated empty vector. *TMEM132E* overexpression untreated was significantly increased *P=<0.05 and WT H295R cells treated with carbachol 15mM and Angiotensin II **P=<0.01 (Unpaired TTEST).

Overall H295R cells that were transfected with *TMEM132E* overexpression plasmid had significant upregulation in *TMEM132E* expression, as we would predict and expect with sufficient transfection. *TMEM132E* overexpression was increased further with carbachol treatment. If indeed TMEM132E works in a partnership with nAChRs, then it would fit that stimulation of acetylcholine receptors through carbachol appears to stimulate *TMEM132E* expression.

3.2.6 *TMEM132E* knockdown in H295R cells lead to decrease in aldosterone synthesis.

Another objective in this study was to review the knockdown of *TMEM132E* expression with silencing RNA (SiRNA) and compared it to scrambled control and once again WT H295R cells. We hypothesised that knocking out the *TMEM132E* gene would lead to a reduction in *CYP11B2* expression and therefore aldosterone synthesis. SiRNA and scrambled control were introduced with electroporation. mRNA, protein, and cell media were collected at 72 hours. Initially I had some difficulty with transfection as I used the Dharmacon Smartpool for TMEM132E knockdown, this comprises of 4 SiRNAs within one formulation that is distributed into the cells. Unfortunately, the Smartpools can have undesired off target affects. I purchased the 4 individual components that make up a smart pool and found that component number 2 was much more efficient.

1. **mRNA expression of *TMEM132E*:**

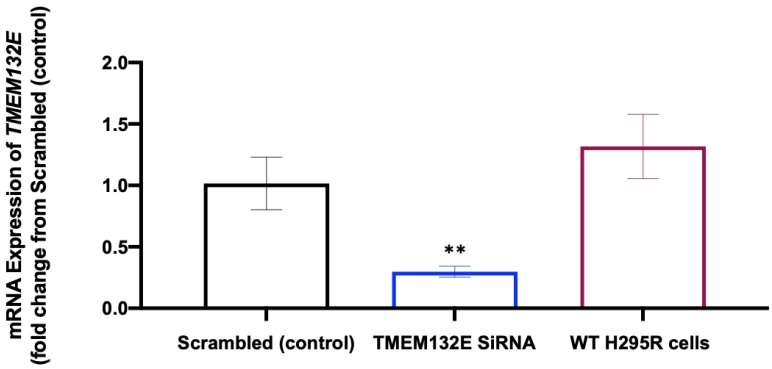

Figure 3 29: mRNA expression of *TMEM132E* in scrambled (control, black), *TMEM132E* SiRNA and WT H295R cells. Fold change is compared relative to scrambled. A significant knockdown of *TMEM132E* was achieved with product 2. **P=<0.001 (Unpaired TTEST) compared to vector. (N=10-15).

2. Knockdown of *TMEM132E*:

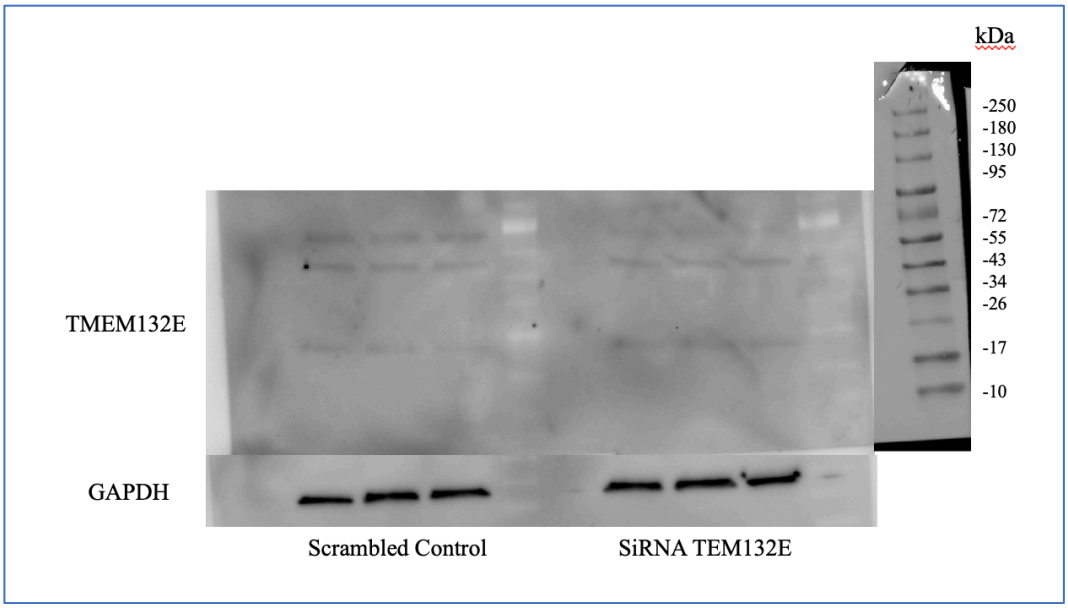

Figure 3 30: Immunoblot comparing protein stained for TMEM132E. The left indicates Scrambled control and the right SiRNA. TMEM132E is once again at 67kDa (discussed in figure 3 19). There is reduction of the bands in the SiRNA bands. The bottom layer of bands represents the housekeeper GAPDH at 37kDa.

3. mRNA expression of *CYP11B2* and aldosterone synthesis:

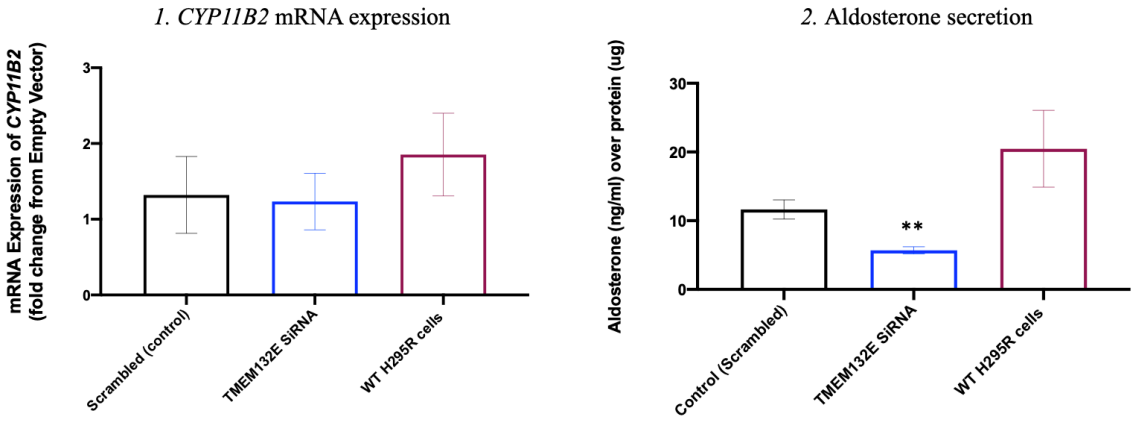

Figure 3 31: 1. mRNA expression of *CYP11B2* for scrambled (control) (black), *TMEM132E* SiRNA (blue) and WT H295R cells (plum). Fold change calculated relative to scrambled (control). There was no statistical

significance. N=10-15. 2. Aldosterone corrected for protein expression within the same cells indicated a reduction in aldosterone secretion within *TMEM132E* SiRNA. **P=<0.001 (Mann-Whitney test). (N=10-15)

3.2.7 *TMEM132E* Knockdown in H295R cells treated with carbachol does not lead to increased aldosterone synthesis:

1. **TMEM132E expression in *TMEM132E* Knockdown cells treated with carbachol and Angiotensin II:**

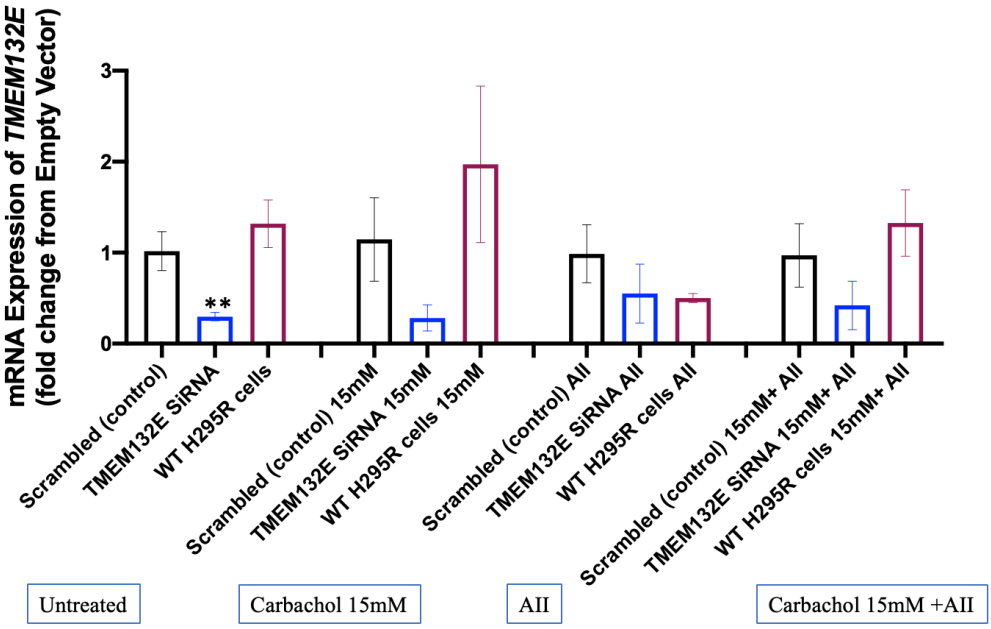

Figure 3 32: mRNA expression of *TMEM132E* fold change from untreated scrambled (control) in *TMEM132E* SiRNA and WT H295R cells. H295R cells were either untreated, or treated with; Carbachol 15mM, Angiotensin II or Carbachol 15mM and Angiotensin II together. **P=<0.001 (Unpaired TTEST). The rest were of no significance. (N=4-15).

2. **Aldosterone secretion in *TMEM132E* Knockdown cells treated with carbachol and Angiotensin II:**

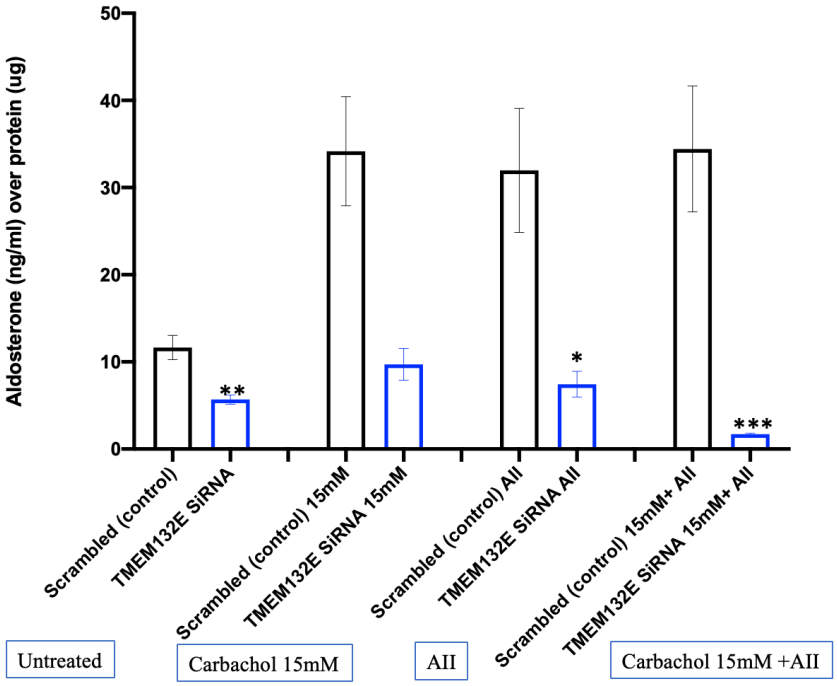

Figure 3 33: Aldosterone corrected for protein in scrambled (control) and *TMEM132E* SiRNA. H295R cells were either untreated, or treated with; carbachol 15mM, Angiotensin II or carbachol 15mM and Angiotensin II together. Compared to untreated scrambled (control), *p=<0.05, **p=<0.001, ***P=<0.0005 (Mann Whitney test). The rest was of no significance. (N=6).

In H295R cells overexpression of *TMEM132E* leads to increased *CYP11B2* and increased aldosterone synthesis. When WT H295R cells and cells with *TMEM132E* overexpression are treated with carbachol 15mM, Angiotensin II and carbachol 15mM and Angiotensin together. There is a rise in *TMEM132E* expression and appreciable rises in *CYP11B2* and aldosterone synthesis. Consequently, when *TMEM132E* is knocked down there is a reduction in *CYP11B2* and aldosterone synthesis. When treated with stimulants of nAChRs the aldosterone synthesis and also *TMEM132E* does not rise, therefore elucidating to the fact that in order for this to happen TMEM132E needs to be present to a certain amount.

3.2.8 RNA sequencing of *TMEM132E* knockdown leads to knockdown of heat shock proteins and other accessory proteins:

Samples of scrambled (control) cells and *TMEM132E* SiRNA were sent for RNA sequencing at the Genome Centre, Blizard institute. Partek software was utilised, data was filtered for contaminants, and counts normalised. Fold change below 0 was selected, to visualise what was down regulated. Anything with a P value <0.01 was considered significant.

The most significantly downregulated genes after *TMEM132E* were the genes coding for heat shock proteins 90 B1 and B2P (*HSP90B1* and *HSP90B2P*) Heat shock proteins are chaperone proteins. As their name suggests they usually arise after the cell has undergone thermic shock. HSP90B1 and HSP90B2P proteins are chaperone proteins mainly within the endoplasmic reticulum (ER) who are crucial to protein homeostasis and balance. Their role has previously been described as enabling assembly and function of proteins within the ER [193]. HSP90B1 genes have been involved in immunological response such as chaperoning Toll Like Receptors and Integrins, they are upregulated in tumour processes and have been associated calcium homeostasis [157, 194-197]. Heat shock protein 90 is also crucial in translocating the mineralocorticoid receptor to the nucleus so aldosterone can exert its effects.

The other genes listed in the figure are related to either protein coding or protein assembly. They are also chaperones or traffickers at either ER level, within the golgi apparatus or membrane. For example, *ARF3* is involved in vesicular trafficking and *PTGES3* is a chaperone protein for steroid receptors.

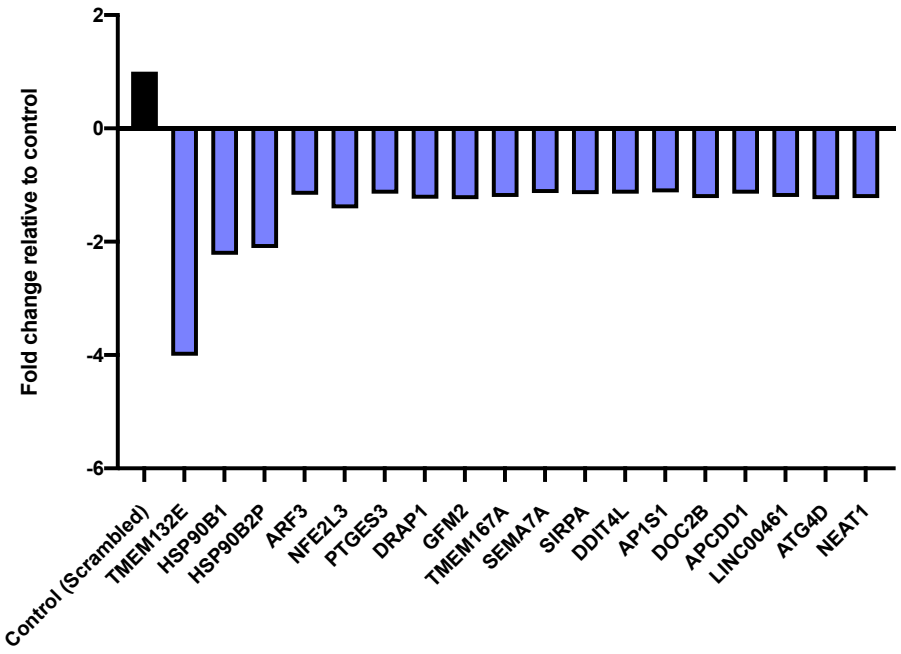

Figure 3 34: Figure illustrating the top downregulated genes in H295R cells with *TMEM132E* knocked down. The most significant were, *HSP90B1* P= 0.00002461 and *TMEM132E* P=0.00001. All other genes in this figure were knocked down to a significance of P=<0.0001.

This data was very interesting, it suggests strongly that *HSP90B1* is strongly disinhibited by the knock down of *TMEM132E*. HSP90B1 is a protein which enables the assembly and function of other proteins. Could it, therefore, be assisting TMEM132E to traffic α7 receptors to the membrane.

3.3 CHRNA7:

3.3.1 Double mutants have increased expression of *CHRNA7*.

On review of our double mutant APA's RNA sequencing, *CHRNA7* of all the nAChRs was the most upregulated. It is also 30-40% structurally homologous to the α9/ α10 receptor, therefore, this became the nAChR we looked into. An α7 subunit homopentamer structure, its role is likely to form an ion channel through which calcium influx is facilitated and downstream aldosterone signalling is triggered.

I hypothesised if CHRNA7 and TMEM132E are in a working relationship, when one is overexpressed, the other protein must also be upregulated. I also wanted to know whether overexpression of these genes individually or together leads to an increase in CYP11B2 and aldosterone synthesis. The final part of this project was to visualise within our H295R cell line the location of CHRNA7/ α7 receptors and TMEM132E within the cell. I hypothesised that we would most likely visualise the proteins together either in the cell membrane or within the cytosol enroute to the cell membrane.

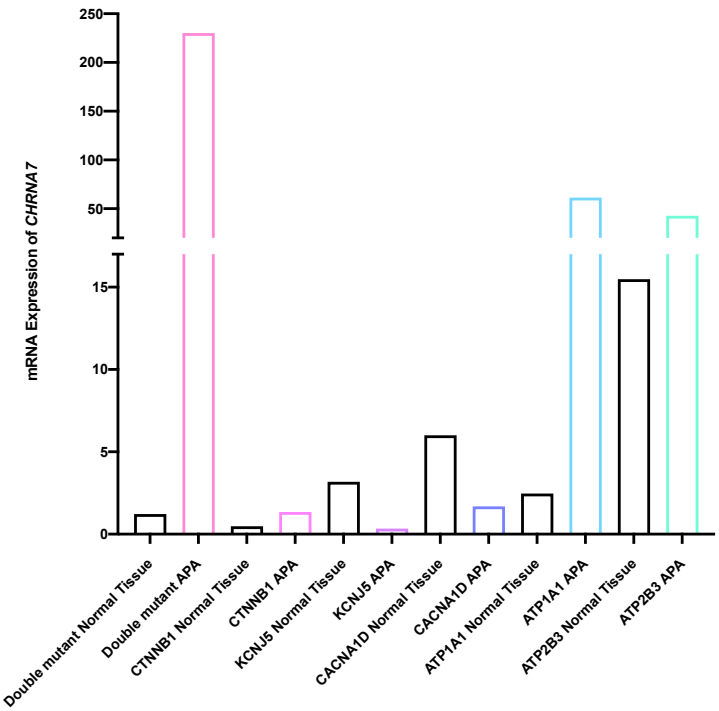

Figure 3 35: Graph illustrating mRNA expression of *CHRNA7* in pooled samples of APAs and their adjacent normal tissue, taken from RNA sequencing data. The APAs consisted of a double mutant APA, *CTNNB1* APA,

KCNJ5 APA, *CACNA1D* APA, *ATP1A1* APA and *ATP2B3* APA. The highest expressing tumour was one of our double mutant APAs, *GNAQ/CTNNB1*, with over a 200-fold increase. The next highest with an expression over 50-fold were the APAs with ATPase mutations.

The above graph indicates strongly that the α7 nAChR is likely involved in the function of these APAs as it is so highly expressed. There is a strong possibility it may be working in conjunction with TMEM132E. It was based upon this data that I decided to pursue CHRNA7 and its role within these double mutant APAs.

3.3.2 Staining of double mutant APAs indicate increased expression of CHRNA7 and TMEM132E:

One method to determine the expression of CHRNA7 and TMEM132E was to perform IHC on tissue from both double mutant APA and control APAs. We wanted to see if this better clarified if TMEM132E and CHRNA7 showed a similar distribution of expression. CHRNA7 (Santa Cruz- sc-58607) antibody was used at 1:100 and TMEM132E (ThermoFischer Scientific- PA5-85900) at 1:100 concentration. Comparison was also made with CYP11B2 expression.

Immunohistochemistry performed in collaboration with the pathology department at QMUL. H and E staining of double mutant and control and CYP11B2 of double mutant performed by Dr Emily Goodchild.

1. ***GNAQ/ CTNNB1* Patient:**

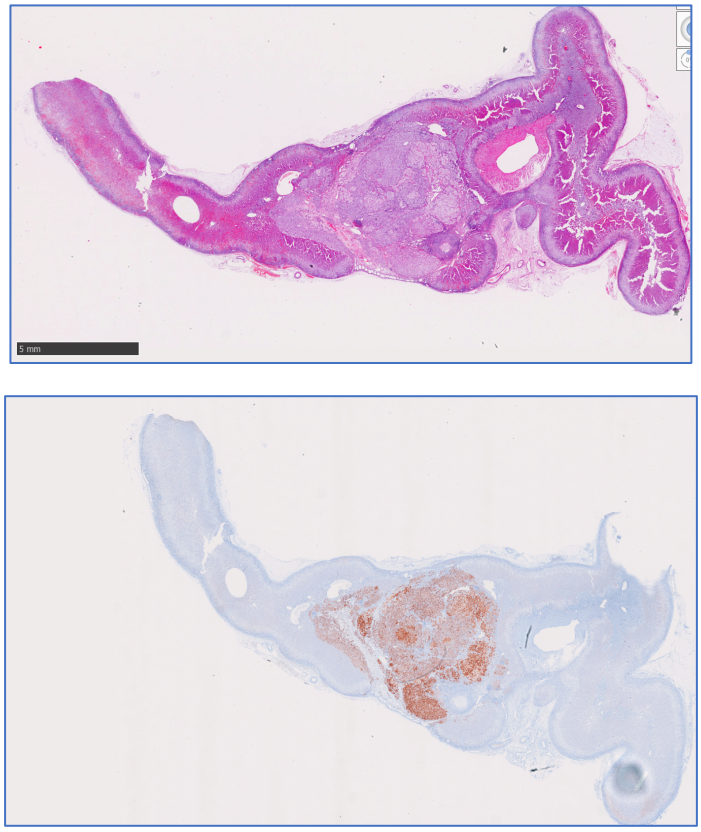

Figure 3 36: Above panel indicates H and E staining of adrenal A/9. The lower panel indicates CYP11B2 staining of the adenoma within the adrenal of A/9.

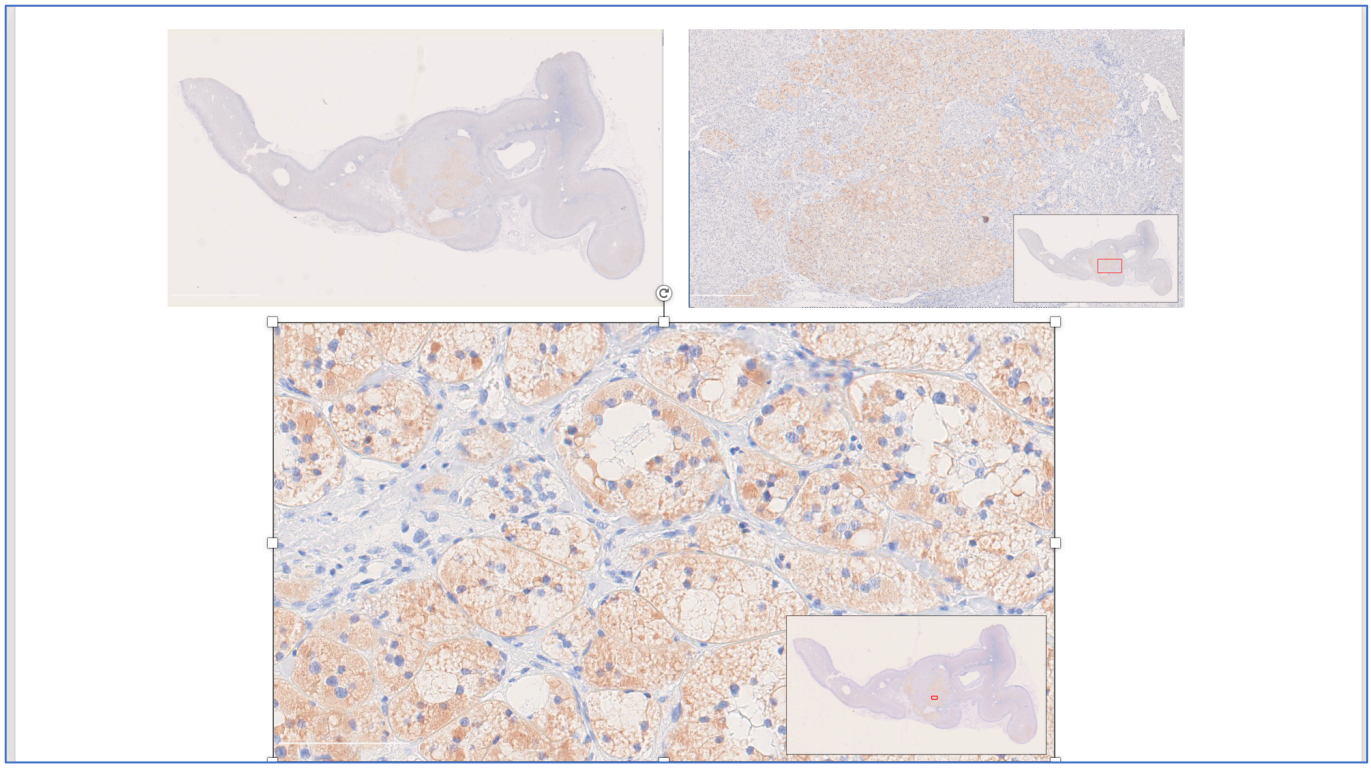

Figure 3 37: Histology figures at x1.25, x20, and x40 magnification of TMEM132E staining of the APA of A/9. One can appreciate compared to CYP11B2, the staining within the adenoma is patchy. At x40 the staining appears both membranous and cytosolic.

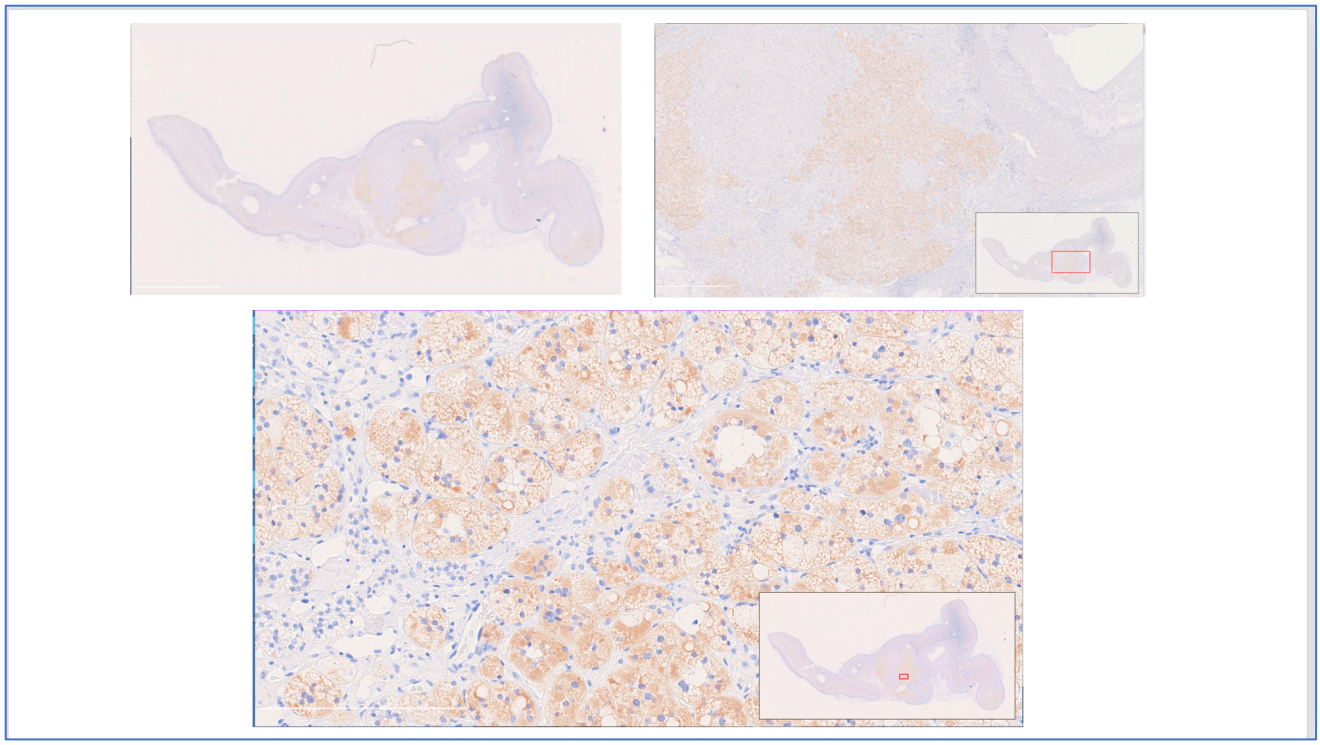

Figure 3 38: Histology figures at x1.25, x20, and x40 magnification of CHRNA7 staining of the APA of A/9. Once again one can appreciate, compared to CYP11B2, the staining within the adenoma is patchy and it follows a similar distribution to TMEM132E staining. At x40 the staining appears both membranous and cytosolic.

2. **Control Patient:**

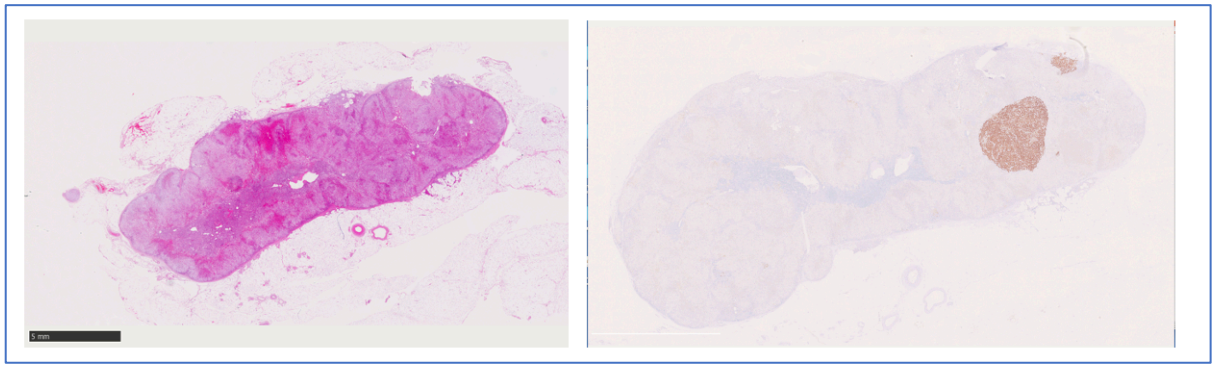

Figure 3 39: H and E and CYP11B2 staining of control patient taken from our NIHR funded MATCH study. Please note the APM stained with CYP11B2 in the top right corner of the adrenal gland as well as the APA.

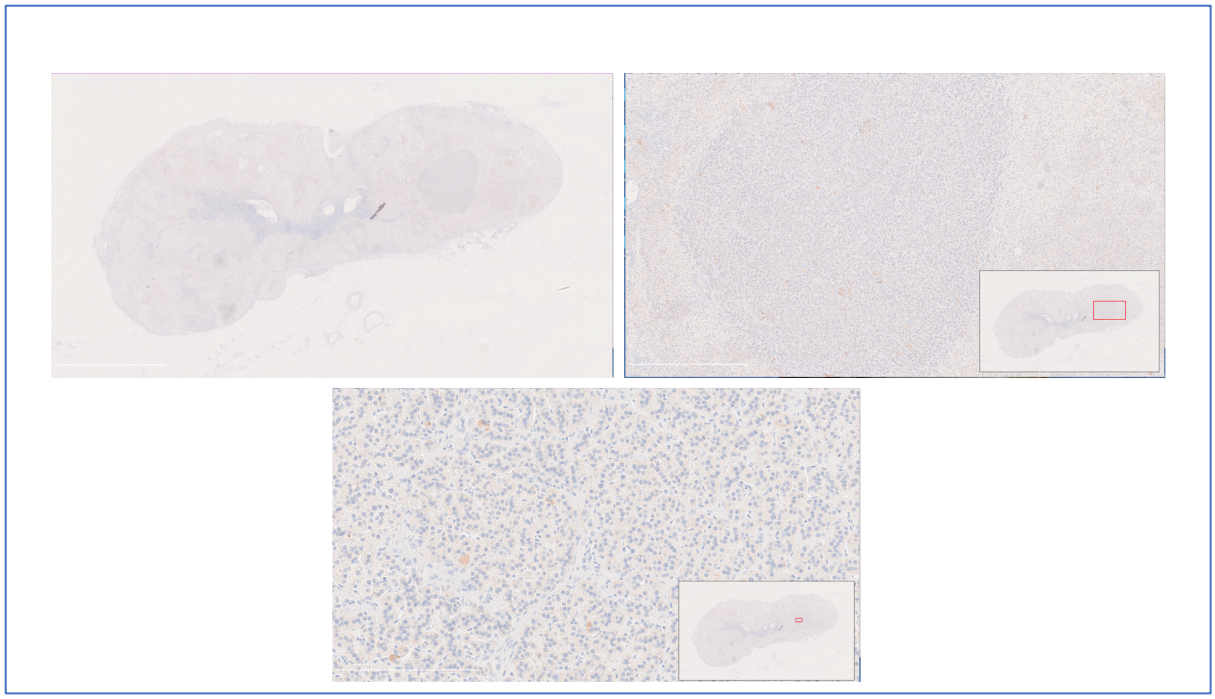

Figure 3 40: Histology figures at x1.25, x20, and x40 magnification of TMEM132E staining of the APA. There is no appreciable staining in the APA or the background adrenal.

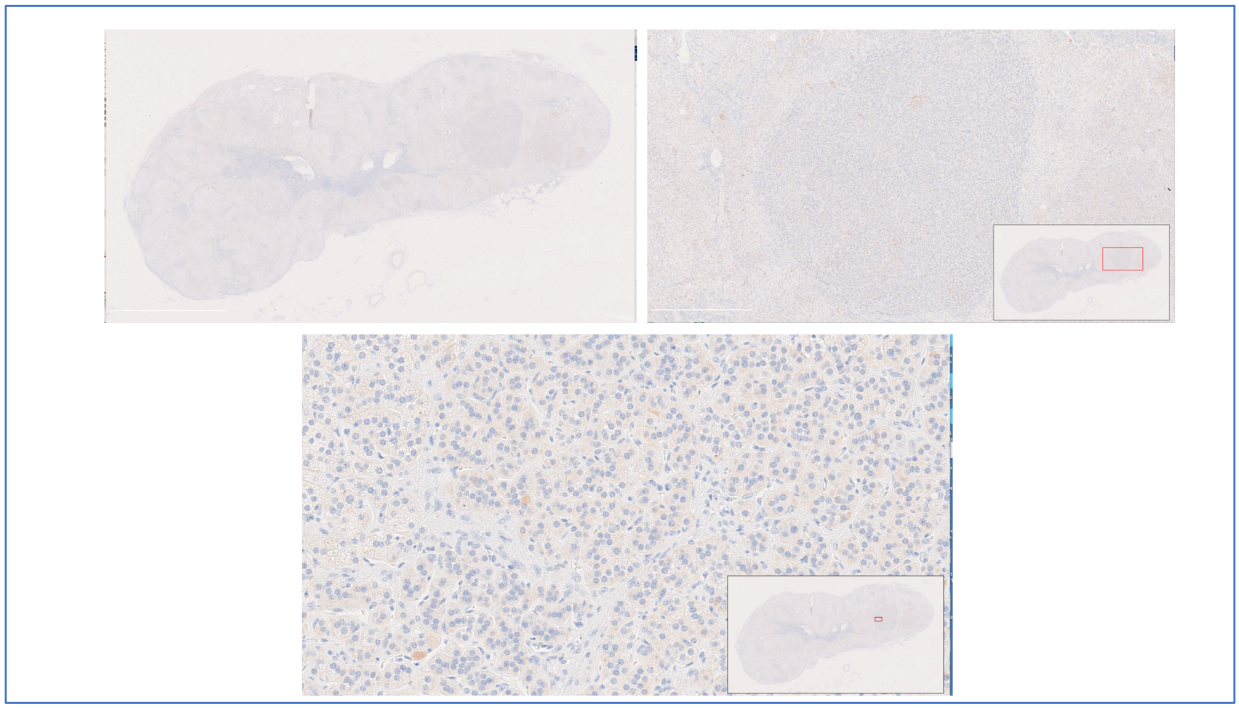

Figure 3 41: Histology figures at x1.25, x20, and x40 magnification of CHRNA7 staining of the APA. There is no appreciable staining in the APA or the background adrenal.

3.3.3 *TMEM132E* overexpression in H295R cells leads to increased expression of *CHRNA7.*

I hypothesized that if you increased the expression of the potential accessory protein, in this case TMEM132E, there must also be a rise in CHRNA7 in H295R cells transfected with *TMEM132E* overexpression plasmid when compared to control. RNA collected at 72 hours post transfection.

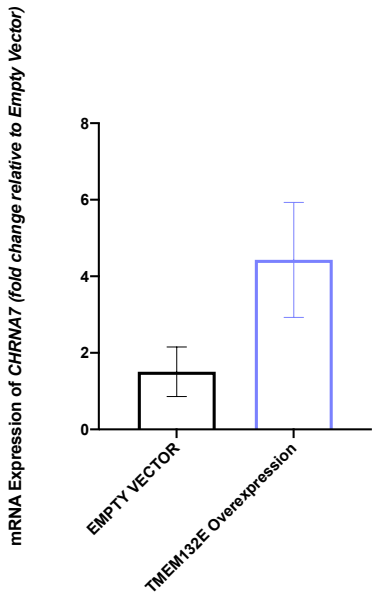

Figure 3 42: Graph illustrating mRNA expression of *CHRNA7* in cells transfected with overexpression plasmid relative to empty vector. CHRNA7 was 4-fold higher in the TMEM132E overexpression cells, but not statistically significant. (N=4).

3.3.4 *GNAQ* mutations in *CTNNB1* harbouring H295R cells lead to increased expression of *CHRNA7.*

In the RNA sequencing of our double mutant APA, *CHRNA7* was over 200-fold upregulated. Passages varied between 18-24. All plasmid constructs held a GFP tag. mRNA was harvested at 72 hours. For mRNA expression measurement of fold change was calculated relative to empty vector (control).

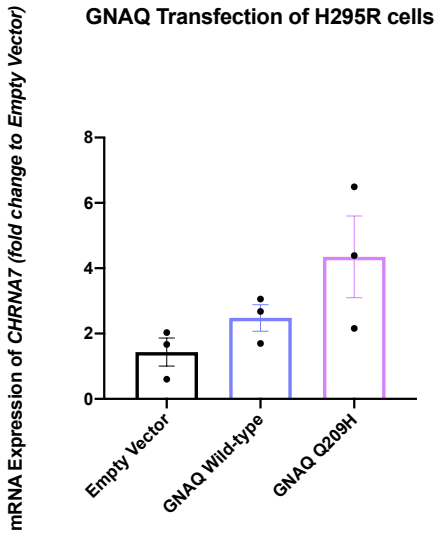

Figure 3 43: Illustrating mRNA expression of *CHRNA7* in H295R cells transfected with empty vector, *GNAQ* WT plasmid and *GNAQ Q209H. GNAQ 209H* showed a 4-fold increase relative to empty vector in *CHRNA7* expression but this was not statistically significant. (N=4).

3.3.5 *CHRNA7* overexpression leads to increased expression of *TMEM132E, CYP11B2* and Aldosterone synthesis.

H295R cells were transfected with a *CHRNA7* overexpression plasmid and an empty vector control plasmid. The nicotinic acetylcholine receptor alpha 7 (*CHRNA7*) plasmid, containing a turbo GFP tag, was purchased from Origene (CAT#: RG221382). A control plasmid: pCMV6-AC-GFP Mammalian Expression Vector also from Origene (CAT #: PS100010) was also purchased. Cells were transfected on day 0 and culture media, RNA and protein were collected on day 3 at 72 hours. H295R cell passages varied between 19-23.

There was some difficulty with the *CHRNA7* overexpression plasmid, I could not see the turbo GFP tag within transfected cells, although mRNA expression indicated transfection had occurred (Figure 3 43). Within the empty vector cells that had also undergone transfection at the exact same time, the GFP was visualised within transfected cells.

This could have been for several reasons. Firstly, the GFP tag could have been lost during plasmid boosting. However, I sequenced the plasmid and the GFP tag was indeed still attached. The tag could have had an effect on the function of the protein, the tag was a turbo GFP tag, and this can be very bulky and therefore, may have slowed the proteins progress. The GFP tag was also attached to the C-terminal end of the protein, this may have affected the function of the protein. The tag could have been cleaved off, this is a possibility, but would be difficult to determine without having performed a protein analysis such as a western blot. I did attempt multiple westerns images but struggled to get a clean film, there was often background interference on the blot.

Another important factor to consider was the linker protein, which links the protein and the tag together, however in this case it was ATG which is a recommended protein linker for tags. Without the visualisation of this tag this set of experiments became very tricky.

I subsequently moved on and tried to use superimposed antibodies for CHRNA7, a Nicotinic Acetylcholine Receptor alpha 7/CHRNA7 Antibody. (Santa Cruz, catalogue sc-58607) and its conjugate form Alexa Fluor 488. Sadly, once again I was unable to visualise CHRNA7 in either transfected or untransfected cells.

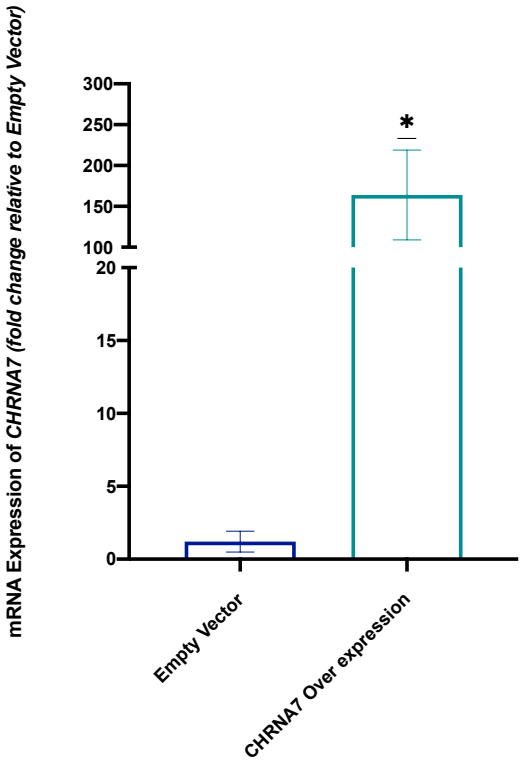

Figure 3 44: Illustrating mRNA expression of *CHRNA7* in cells transfected with the CHRNA7 overexpression plasmid. *CHRNA7* was upregulated 150-fold relative to empty vector control. *P=<0.05 (Unpaired TTEST). This illustrates a good transfection rate was achieved with this plasmid. (N= 6)

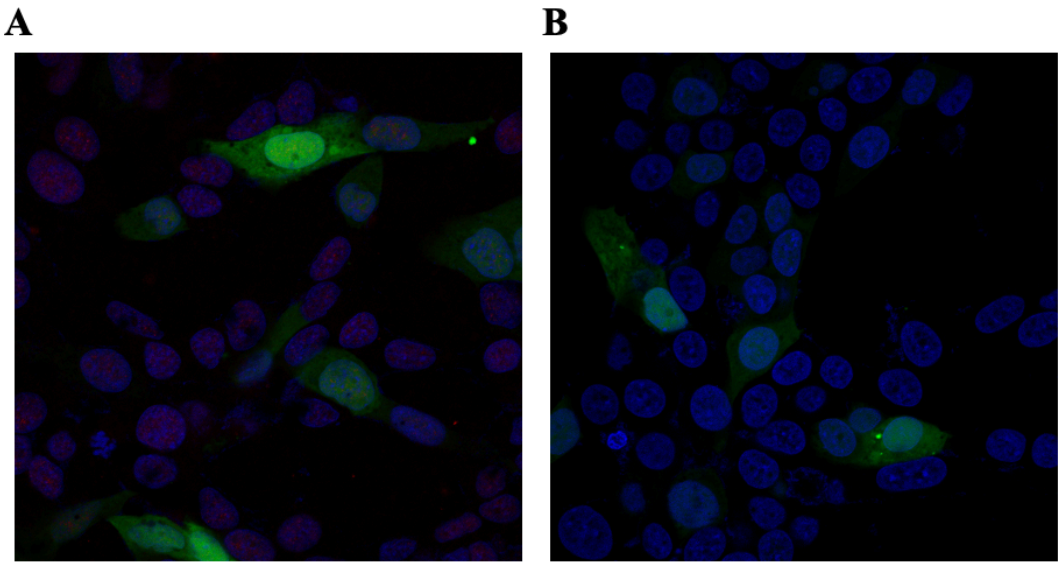

Figure 3 45: Confocal image of H295R cells showing turbo GFP expression in cells transfected with empty vector. DAPI blue was used for cell nuclei. Image taken at 72 hours. The tag easily visualised in the control cells.

1. ***TMEM132E* expression:**

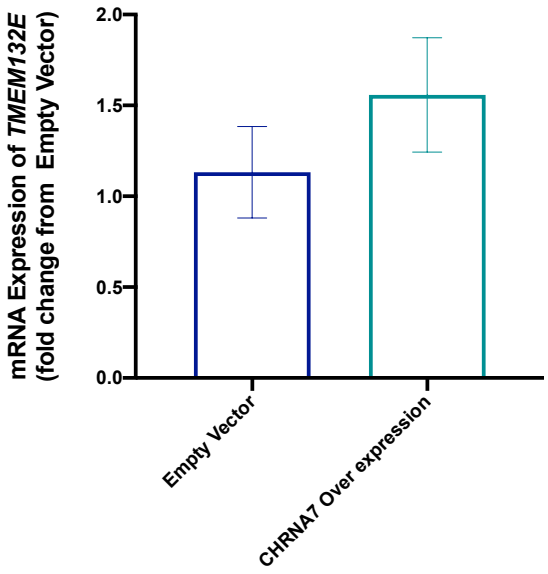

Figure 3 46: mRNA expression of *TMEM132E* in H295R cells transfected with *CHRNA7* overexpression plasmid and control empty vector. No significant increase was noted, although a rise was appreciated. (N=4).

2. CYP11B2 and Aldosterone synthesis:

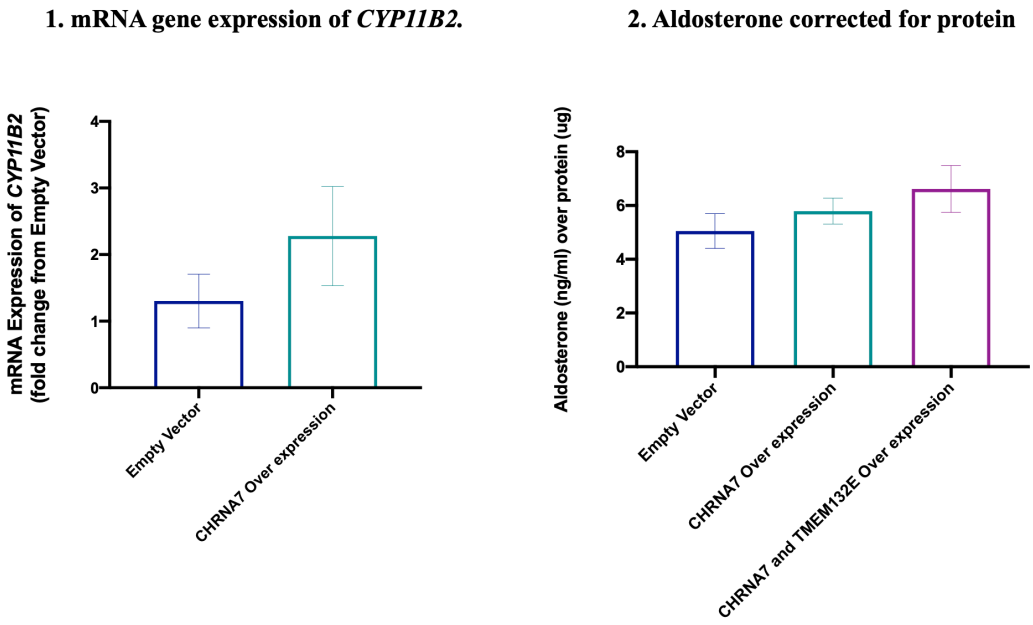

Figure 3 47: 1. mRNA expression of *CYP11B2* was twofold higher relative to empty vector but to no statistical significance. **2.** Aldosterone corrected for protein in cells transfected with empty vector, *CHRNA7* overexpression and *CHRNA7* and *TMEM132E* co-transfection. Appreciable rises from empty vector but to no statistical significance. (N=4).

3.3.6 Co-transfection leads to *TMEM132E* expression within the cell membrane.

One theory was to see if *TMEM132E* transfection enabled *CHRNA7* expression and function. I decided to co-transfect *TMEM132E* and *CHRNA7* into cells. The results were interesting, *TMEM132E* certainly had less cytosolic and nuclear expression and more membranous expression.

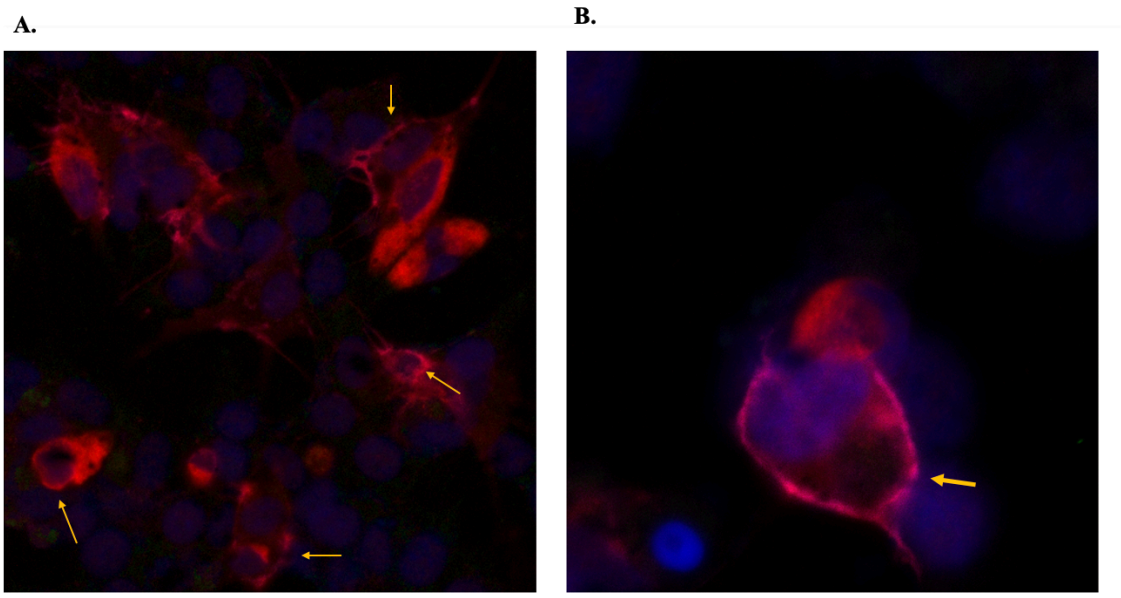

Figure 3 48: **A.** Confocal image x20 of multiple H295R cells co-transfected with *TMEM132E* and *CHRNA7*. TMEM132E is in red, nuclei in DAPI blue and WGA in magenta. The yellow arrows point to membranous TMEM132E staining. **B.** Confocal image x60 of one enlarged H295R cell with the yellow arrow pointing to TMEM132E membranous staining.

3.4 Discussion:

In 2015, an initial discovery was made, when three patients presented with PA in unusual circumstances at times of changing reproductive physiology, namely pregnancy and menopause [121]. All three on WES were initially found to have a canonical Wnt pathway mutation of *CTNNB1*. This mutation had been previously described in adrenocortex pathology, especially within ACCs (40%) as well as APAs (~5%). 20-30% of ACCs harbour the same mutation as APAs [198]. However, the story never seemed quite complete. *CTNNB1* mutations leading to APA formation have been well documented [138]. One study also indicated that older female patients with APAs harbouring *CTNNB1* were more likely to present with a short duration of hypertension, but most remarkably they were more likely to be left with residual hypertension following adrenalectomy compared to patients with other somatic mutations, such as KCNJ5 [199]. This outcome was at odds with the three patients who were completely cured post adrenalectomy, including the menopausal patient on multiple antihypertensive agents. Another inconsistency was that other centres had come forward in response to the 2015 NEJM paper [121] reporting that they too had patients with APAs containing *CTNNB1* mutations, but none had presented at times of high LH/HCG surge. It was only upon the presentation of the pubertal male [134] that the G-protein *GNA11/Q* mutation was uncovered at the position of Q209, through WES. This mutation made this cohort unique. The G11/Q mutation leads to continuous aldosterone synthesis via intracellular signalling and downstream pathways of IP3. Although these patients belong to a subset of patients with non-ion channel mutations that account for <5% of patients with PA, they posed some fascinating geneo-pathophysiological questions.

The majority of APAs harbour a gain of function mutation that results in dysregulated expression of CYP11B2. In our recent MATCH study [81], complete clinical success was strongly associated with APAs containing the first mutation to be described, which affected the potassium channel, KCNJ5. Most current knowledge about APA comes postoperatively and therefore too late for clinical decision-making. In KCNJ5 patients the level of 18-OH cortisol (a hybrid steroid generated by cells that express enzymes for both cortisol and aldosterone synthesis) is much higher than with APAs harbouring other somatic mutations therefore potentially serving as metabolic marker that could be translated into routine clinical use and guide the patient's journey. Understanding the mechanisms by which other mutations cause PA has the potential (as with KCNJ5) to lead to the discovery of biomarkers that provide clinically useful information for patient selection for surgery. Although the number of patients presenting with double mutation is small, the mechanisms, biomarkers and potential therapeutic targets are important in order to be able to streamline treatment. In this cohort, the gain of

function mutations seems to work together co-driving to present with exceeding high aldosterone levels in a short amount of time, producing an acute phenotype. This phenotype differs from other somatic mutations of PA, they can present more indolently and the timeline to diagnosis can be long and laborious.

The first hypothesis was: did the mutations need to occur together in order to increase *CYP11B2* and aldosterone synthesis? The transfection experiments of our H295R cells that already harbour a *CTNNB1* S45P mutation, and were further transfected with *GNA11* Q209H, L, P, and *GNAQ* Q209H, showed that *CYP11B2* mRNA expression and aldosterone were significantly upregulated compared to empty vector and wild-type. The wild type harboured the lone *CTNNB1* mutation although there was a modest rise in aldosterone with individual gene presentations it was the mutations together that led to the most significant aldosterone rise. This was also the case with *GNAQ, GNA11's* paralogue. Further work performed by Dr Azizan, in which *CTNNB1* was knocked down, also confirmed that the mutations need to arise within the cells together for a cumulative effect [134]. The relationship of the two mutations is unusual. Driver and passenger mutations have been readily studied in oncology for therapeutic targets but are rare in benign conditions and have not often been described in APAs. In oncology, driver mutations are deemed to be mutations that offer a survival/ fitness advantage to the somatic cells within their environment, whilst the role of the passenger mutation has long been debated. The debate has circulated around whether the passenger mutations could be latent drivers, "mini drivers", neutral participants or maybe even deleterious to malignancies, slowing their progress and therefore their ability to metastasize- a so-called "tug of war" effect [200-202]. There is also the "two hit" hypothesis, where the driver mutation does not offer any survival advantage, but the two mutations together have a significant cumulative effect. The passenger mutation often arises due to the genomic fragility of the malignancy as it rapidly divides or secondary to DNA damage incurred by chemo- and immunotherapies. It is hard to see the similarities within our double mutant APAs, although the double hit hypothesis is plausible. ACCs do harbour *CTNNB1* mutations but their passenger/ codriver mutations differ and are usually *TP53, MEN1* and *MED12* [140]. Does the differing *GNA11/Q* codriver enable it to maintain benign characteristics?

As mentioned, double mutations in PA are rare. *Nanba et al* did uncover *CACNA1D (p.G403R)* and *CTNNB1 (p.G34R)* mutations that were alongside one another in an APA but CACNA1D appears to be the main driver in these APAs that are so rarely found [126].

Work performed on *GNAQ* indicated that in conditions such as Sturge- Weber, a benign condition of vascular overgrowth, *GNAQ R183Q* mutations are often benign whilst that same mutation in uveal melanoma along with *GNAQ 209L* can be fairly malignant. One potential explanation could be that the *GNAQ* mutation in Sturge-

Weber arises due to somatic mosaicism and hence is post zygotically limited to a distinct population of cells and therefore they may require specific tissues to produce malignancy [203]. Moscaisim of *GNA11/Q* was also illustrated in the dermatological conditions, Phakomatosis Pigmentovascularis and Extensive Dermal Melanocytosis [141]. This prompted Dr Zhou to look into potential mosaicism within our double mutant APAs and indeed in the surrounding ZG to the APA. Incredibly, she did indeed find solitary homozygous and heterozygous somatic mutations of *GNA11*[134].

As a group we have hypothesised that *GNA11/Q* mutations may arise early, leading to a second *CTNNB1* hit, the *CTNNB1*mutation leading to cell proliferation and tumour formation. Studies have shown that, for example, in the melanogenesis pathway upstream, signalling from mitogen-activated protein kinase MAPK leads to β catenin pathway mutations that in turn leads to further spread and penetration of the naevus, resulting in malignant melanoma characteristics [204]. A further study in uveal melanomas speculated that, whilst driving tumorigenesis, the *GNA11/Q* mutations were unlikely to be sufficient for full tumour transformation, and another co-driving mutation was required [205].

LHCGR expression was proven to be one of the essential biochemical and histopathological phenotypes of the double mutant APAs [134]. Activation of the LHCG receptor leads to this G-protein receptor becoming activated, an increase in calcium and downstream signalling and *CYP11B2*/ aldosterone expression. the LHCGR, a well-known G-protein receptor, is clearly affected by the G-protein GNA11/Q mutation leading to continual cAMP activation and downstream signalling. It is well-documented that this receptor is involved in pathological states with increased steroidogenesis within the adrenal gland and even in functional studies. When H295R cells were transfected with a LH -receptor, they increased their *CYP11B2* expression and aldosterone synthesis [127]. It is usually expressed in low levels within the adrenal gland, however in this subset of APAs it is highly expressed. The adrenal and the gonads come from the same primordial cell line, which may suggest that the presence of these mutations drives the adrenal cells back into their primordial state and they begin to express more gonadal type features. This also fits with the work performed by *Teo et al,* who observed in the original three patients the presence of GATA4, a remnant signal of the foetal adrenal which has often vanished by adulthood [121].

One issue arose in our work when we realised that our cell line H295R does not express LHCGR. H295R cells arise originally from an ACC with cells of origin likely from the ZR. Although they have a wide steroidome capability, they are likely very far removed from the original primordial adrenal/ gonadal cells [206]. However

some groups have had success in H295R LHCGR expression [207]. In order to improve chances of LHCGR expression I treated H295R cells in high concentrations of HCG/LH. However, this had little to no effect. One explanation may be that cell lines start to lose certain functions with the passages of time. One option may have been to treat H295R cells with both mutations in HCG/LH to see if this could bring on LHCG receptor expression. For further work looking at LHCGR it therefore became necessary to use primary adrenal cells.

Dr Zhou and Dr O'Toole illustrated (Figure 3 42 below) through immunofluorescence work on primary adrenal cells that LHCGR too (along with other upregulated genes) was subject to the "double hit" phenomenon of both mutations. Both mutations seem to be a requirement to reach the high levels of expression of LHCGR within the adenomas. As they beautifully illustrated in one cell, it takes both mutations to be present to see the marked increase in red fluorescence, the marker chosen for LHCGR (Figure 3.5 7,) and therefore increase in mRNA expression.

LHCGR expression in the medulla through IHC work was quite unexpected. The adrenal medulla arises from neural crest cells and therefore a different primogenital cell line. Work I performed on extraction of medulla and ZF showed higher expression of LHCGR within the medulla, along with increased expression of PNMT. Work by *Lopez et al,* initiated by a patient presenting with phaeochromocytoma in pregnancy, illustrated *LHCGR* expression in phaeochromocytomas and paragangliomas but particularly those with high expression of PNMT, fitting with our findings [162]. I could not find any data to explain why the two may be related, suggesting further work is required.

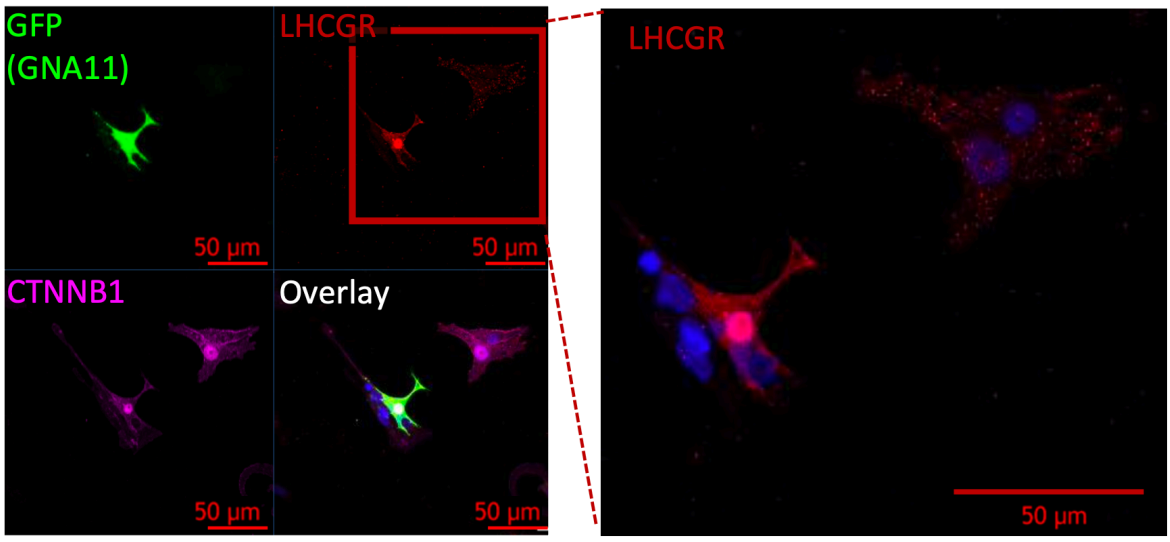

Figure 3 49: illustrates cells transfected with *GNA11 Q209P* (GFP tagged), *CTNNB1 Δ45* (untagged), and LHCGR. As illustrated in the blown-up picture LHCGR corrected fluorescence staining greatly increased in cells that had both *CTNNB1 Δ45* and *GNA11 Q209P* mutation compared to the un-transfected cell next to it. P=<0.05 (One way ANOVA). **Images courtesy of Dr Junhua Zhou and Dr Sam O'Toole.**

It is feasible that the LH/HCG receptors do not hold all the answers for the upregulation in aldosterone synthesis. I therefore hypothesised that for aldosterone upregulation a responsible protein may be TMEM132E, which is the second most upregulated in double mutant APAs but particularly in the patient who had low LHCGR expression in their APA. It is important to note that this patient presented on the day of her adrenalectomy on the first day of her period, which is a time in the menstrual cycle where circulating LH levels are lower by around 1.68–15 IU/L, compared to mid-cycle where they are at their highest, 21.9–56.6 IU/L. TMEM132E was also remarkably present in transfected H295R cells when LHCGR was not.

The overriding theory of the role that TMEM132E plays is that it acts as an accessory or chaperone protein to nicotinic acetylcholine receptors, more specifically α7 expressed within the double mutant APAs. Once α7 is assembled to the membrane, the membrane is permeable to calcium, leading to an influx and kickstarting of the steroidogenic pathway.

The presence of TMEM132E – and CHRNA7 - is unusual in adrenal pathology. My functional studies did elicit that TMEM132E does indeed have a role. The TMEM132E overexpression studies pointed to a modest, almost 3-fold, rise in *CYP11B2* expression but a significant increase in aldosterone production. TMEM132E knocked down/ silencing, caused a slight decrease in *CYP11B2* but a significant decrease in aldosterone synthesis. In the TMEM132E overexpression studies the *CYP11B2* rise was not significant. It may be at 72 hours the *CYP11B2* enzyme is already on the decline, having missed the enzyme at its highest. When I separated the data and illustrated low vs high *TMEM132E* expression, there was a significant increase in *CYP11B2* within the higher TMEM132E transfection cohort. This could be down to more CYP11B2 in circulation, or to a threshold having to be met in order for TMEM132E to increase the calcium evoked potentials and lead to downstream CYP11B2 mobilisation [175].

Carbachol, the choline receptor agonist, has previously been used in studies exploring steroidogenesis, [173, 174] but there has been firm belief this action is mitigated through the M_3 muscarinic receptors [208, 209]. We know however that carbachol has affinity for both nicotinic and muscarinic acetylcholine receptors and therefore it is perfectly possible that it targets nicotinic acetylcholine receptors.

Treatment of H295R cells with carbachol led to increased *TMEM132E, CYP11B2* expression and aldosterone synthesis, most likely through increasing calcium concentrations and activation of the StAR pathway. [208] The rise in TMEM132E could be explained by its accessory function capacity. As more nicotinic acetylcholine receptors are targeted by carbachol, the receptor requires an increase in its accessory protein in order to function. This was also observed in cells where TMEM132E overexpression had occurred and was in abundance.

The interplay between TMEM132E and carbachol was demonstrated in the TMEM132E knockdown data. Despite treatment with carbachol, aldosterone did not increase in cells where TMEM132E had been knocked down. There was however a significant increase in aldosterone secretion to carbachol and Ang II in scrambled (control) cells.

In my H295R experiments, neither carbachol nor Ang II seemed superior in stimulating aldosterone production, although literature points to Ang II being superior through sustained increase of calcium whilst carbachol seems to lead to calcium oscillation [174]. There was also discussion about whether to replicate physiology with the use of acetylcholine. Acetylcholine could have been used to treat cells but extensive literature points to it having the same efficacy in cell experiments as carbachol [173, 174, 176].

CHRNA7 overexpression was difficult to achieve within H295R cells. As documented above, visualisation of the tGFP tag was difficult to appreciate. Further, despite various antibody stains on transfected cells, it was difficult to see CHRNA7/α7 within the cells. Reports have indicated that issues have arisen with CHRNA7's α7 receptors as they do not fully function or oligomerize in all cell lines but only neuronal cell lines where they are native. [171, 210-212] Some studies have used HEK cells, with some success. I also tried HEK cells to little to no avail. Function and assembly may therefore be dependent on the presence of the chaperone/accessory protein such as NACHO or Ric-3 [175, 176, 210]. One of the genes that were knocked down with *TMEM132E* in Figure 3 34, such heat shock 90 may be crucial. These genes all have a chaperone/ trafficking or protein assembly function. I co-transfected *TMEM132E* and *CHRNA7*/ α7 together in the hope that doing so would enable assembly, but it remained difficult to discern the receptor on confocal imagery. It is possible that the α7 receptor was stuck within the ER process or at some other stage of protein function. An answer for the difficulty in visualising α7 receptors on confocal work may have been antibody related. Another consideration was the transfection method. During electroporation, a high voltage electrical field is applied to the cell leading to a temporary breakdown of the cell membrane, increasing its porosity, and allowing DNA into the cell and ultimately the cell nucleus. Critical features of this process are the maximum voltage of the shock applied and

the pulse. The pores then naturally reseal themselves. This may ultimately damage the structure wherein the α7 lies, so I also tried lipofectamine as a transfection method. In membrane fusion and lipofection protocols, neutral and cationic lipid carriers take up the DNA or product and pass it through the cell membrane releasing it into the cytoplasm. This process is slightly less toxic to the membrane. However, this too seemed to make no difference. My initial confocal work images in H295R cells overexpressed with TMEM132E indicate TMEM132E expression in the cytosol, nucleus, and membrane. This is in accordance with tissue atlas reference systems such as The Human Protein Atlas. When I co-transfected TMEM132E with CHRNA7 there was a convincing increase of expression of TMEM132E within the cell membrane and this is consistent with the relevant literature [175]. This likely suggests TMEM132E is moving to the membrane in order to facilitate something, maybe CHRNA7.

The IHC work in section 3.3.2 also illustrated TMEM132E and CHRNA7/ α7 expression. In the double mutant APA shown expression of TMEM132E and CHRNA7/ α7 is within the same distribution. A different overall distribution to CYP11B2, strongly indicating a close relationship between the two proteins.

In conclusion I have shown that we have a unique cohort of non-ion channel APAs presenting with rare co-driver mutations of *GNA11/Q* and *CTNNB1*. Their florid presentation of PA is likely down to multiple pathways for increased aldosterone synthesis. The *G11/Q* disruption to G-protein receptors, such as LHCGR, and increased TMEM132E expression. TMEM132E is likely a potential accessory/chaperone protein to the nAChR α7 expressed by *CHRNA7.* These patients do extremely well post adrenalectomy with 100% cure rate therefore a peripheral serum biomarker such as TMEM132E would help facilitate care. The possibility of also having a nAChR as a therapeutic target would be invaluable.

3.5 Future work:

As a team and through individual work we have illustrated that the co-drivers *GNA11/Q* and *CTNNB1* are reliant on each other to express the unique features and genes of these APAs.

In our H295R cells and in one patient the pathway of aldosterone synthesis through upregulated LHCGR was not present. I explored the potential accessory/chaperone protein TMEM132E. To further robust my data that TMEM132E is indeed an essential aldosterone secretion pathway protein one experiment I would like to perform is silencing of TMEM132E within H295R cells holding both *CTNNB1* and *GNA11/Q* mutations. It would be fascinating to see the effect upon aldosterone that is so highly upregulated when H295R cells have both mutations.

One interesting question I was unable to explore was why are nAChRs seen within these APAs. Muscarinic acetylcholine, but not nicotinic, receptors have been described within the adrenal cortex before. nAChRs have readily been described within the adrenal medulla. Interestingly, CHRNA7 is present in H295R cells that derive from a ZR type ACC. One project could be to perform serial staining in adrenal glands and APAs to see, firstly, if there is any staining and secondly, the pattern and distribution of CHRNA7.

An aspect of the project that, with further time, may have yielded additional results is the confocal work. Localising α7 receptors with TMEM132E within the cytosol or within the cell membrane would have enabled me to illustrate a true partnership. I would also have liked to have performed more co-transfection work of CHRNA7 and TMEM132E. One option would have been to conduct the experiment in a neuronal cell line, where reports have illustrated good assembly and function of α7 receptors [171, 176]. Another option would have been to explore whether there was still a further component missing, such as heat shock protein 90, that also required co-transfection.

Finally, for the true translational benefit for these patients, there is a TMEM132E ELISA kit (Lifescience market Catalog No.:ELI-18753h). This kit can measure serum TMEM132E levels. We have access to patients during the work up of their diagnosis in outpatients and clinical trials. Samples could either be taken peripherally or at time of AVS to determine whether the patient was a double mutant and would therefore benefit from adrenalectomy.

Chapter 4:

Feasibility study of RadioFrequency endoscopic ABlation, with ULtrasound guidance, as a non-surgical, Adrenal Sparing treatment for aldosterone-producing adenomas (FABULAS).

Abstract:

Outcomes post total adrenalectomy, the standard treatment for unilateral APAs, are variable. Between 30-60% are cured of hypertension [63]. Prediction of outcome is unreliable, and some patients are reluctant to have abdominal surgery to remove a whole adrenal gland.

EUS- guided RFA is an alternative treatment to surgery for pancreatic malignancies but has rarely been attempted for adrenal lesions. Given the proximity of the left adrenal gland to the stomach, we conducted a multicentre pilot study of EUS-RFA for left-sided APAs, to determine the safety and efficacy of this adrenal sparing treatment.

28 patients were recruited with confirmed unilateral (or dominantly asymmetrical) left sided aldosterone-secreting nodules confirmed by one or both of standard AVS or molecular imaging (^{11}C-Metomidate or ^{18}F-CETO PET scan) with SUV max lateralisation ratios > 1.25 [80]. Patients had an average age of 56 years and either comorbidities dictating surgical caution or had declined surgery (personal preference). 35 ablations were performed across three centres in 28 patients (21 male and 7 female) with 7 patients having a repeat procedure following careful consideration from a multi-disciplinary panel. All patients underwent alpha and beta blockade two weeks prior to procedure, and all procedures were performed with an anaesthetist present, with 31 undergoing general anaesthesia and 4 deep sedation only. A 5-10 mm 19G Starmed^{TM} probe was introduced transgastrically by EUS into functioning adrenal nodules that ranged in size from 9-36 mm. An electrode/ grounding pad was placed on all patients and energy generated at 10 watts to perform ablation. FNA samples were taken at time of ablation for immunocytochemistry to confirm (retrospectively) that CYP11B2 positive cells were the target and for further genotyping and RNA sequencing. Follow-up nuclear medicine imaging was used to assess completion of ablation. The primary outcome was safety of the procedure, which was achieved: expected serious adverse events such as perforation, haemorrhage and infarction of major organs did not occur within the first 24-48 hours (assessed by clinical examination, inflammatory markers (WCC and CRP), blood count and contrast CT abdomen). All serious adverse events, 9 in total, were accurately reported and reviewed and scored in severity by an independent safety committee. 3 were graded severe in level and thought to be procedure related. All severe SAEs resolved with no prolonged morbidity.

The secondary outcomes included the analyses of complete, partial or absent clinical and biochemical outcomes as determined by PASO criteria recorded at 1, 3 and 6 months post-procedure. After 6 months post first ablation or 3 months post second ablation, complete clinical success was achieved in 14.3% of patients. Partial clinical

success was documented in a further 14.3% and the rest were absent of clinical success. 50% achieved complete biochemical success, with 10.5% achieving partial biochemical success.

Renin was significantly de-suppressed (P=<0.0001) and a significant reduction in ARR (P=0.0019) 6 months post ablation was seen. There was no change in blood pressures either clinical or home over the 6 months post ablation but there was a significant reduction in the Defined Daily Dose (DDD) of medications (P=0.0008) and number of antihypertensives taken by patients (P=0.0008).

In conclusion, EUS-RFA is a safe alternative to complete adrenalectomy for left-sided aldosterone-producing nodules and has some modest outcomes on PASO criteria. EUS-RFA is less invasive and requires less time in hospital. This procedure could, in selective patients, be considered a cost benefit to health care providers compared to laparoscopic adrenalectomy.

Aims and Hypothesis:

This study was a multicentre phase 1 study to determine predominantly the safety and efficacy of endoscopic ultrasound guided radiofrequency ablation as an alternative to adrenal surgery as a form of treatment for left sided APAs.

Primary outcome: The primary objective of the study was to test the hypothesis that EUS-RFA of left sided APAs is safe. The primary outcome measure was patient safety – specifically, whether perforation, haemorrhage or infarction of major organs occurred, assessed at 24-48 hours post procedure by a combination of clinical assessment, measurement of markers of inflammation (full blood count (FBC), routine chemistry, creatinine kinase (CK), amylase, C-reactive protein (CRP), urinalysis) and abdominal imaging (contrast- CT abdomen).

Safety was also assessed by the accurate reporting of adverse events and their evaluation by an independent safety committee.

Secondary Outcome Measures: The secondary outcome was to measure efficacy. As judged by the clinical and biochemical criteria of the increasingly used international PASO criteria. Planned exploratory analyses included molecular imaging before and after the procedure to assess the completeness of ablation; and IHC of fine needle biopsies of the targeted lesion to determine, retrospectively, whether the lesion stained positive for CYP11B2.

Secondary outcomes were measured by the collection of the following data:

- Plasma electrolytes, U&Es.
- ARR at 3 and 6 months.
- Comparison of PET CT pre-ablation and 3 months post ablation for radiological disappearance, size of adenoma and SUV measurements.
- Patients who did not have a baseline PET at baseline did not have a 3–6-month PET CT scan post intervention.
- The reduction or cessation of supplementary potassium medication; and
- Home BP (measured 3 readings twice a day for 4 days preceding clinic visit).
- The reduction or cessation of antihypertensive medications.

4.1 Methods:

4.1.1 Study Outline:

A phase 1 study conducted over multiple centres. The centres taking part were University College London Hospital (UCLH), Barts Health and Cambridge University Hospital (CUH) Addenbrookes Hospital. To determine the safety and efficacy of EUS- RFA of left sided APAs in 30 patients. The trial was to take place over 3 years.

4.1.2 Inclusion criteria:

The inclusion criteria into this study comprised of basic inclusion criteria and then patients were recruited into three inclusion subset groups.

Basic inclusion criteria consisted of:

- Patients had to be aged 18 and above.
- A diagnosis of PA was made according to Endocrine Society guidelines [1].
- A positive ARR with positive radiological imaging such as CT or MRI.

The three inclusion groups consisted of the following:

1. **Group 1:**
    - **a.** Left-sided APA proven on either AVS or PET CT.
    - **b.** Patients wishing to take fewer drugs for their hypertension.
    - **c.** Patients meeting Endocrine Society criteria for considering curative treatment of unilateral disease, but who are often not referred for surgery because the benefit: risk is considered too low.
    - **d.** Patients aged ≥60 whose BP is at or near target (BP140/90 for most patient groups, BP 130/80 if co-morbidities listed in Hypertension guidelines) on treatment with tolerated antihypertensive medication.
    - **e.** Patients with identified macroadenomas (APAs >= 1 cm in diameter), who have at least 1 cm of peri-adrenal fat on axial and coronal projections.
2. **Group 2:**
    - **a.** Patients aged 18 years and above with diagnosis of PA and either: (i) a definite unilateral left APA, but the patient does not want surgery; or (ii) probable but not unequivocal evidence of a unilateral left adrenal APA.

3. **Group 3:**
    a. Patients over 18 years of age meeting criteria for surgery, but consent to undergo endoscopic ablation instead.

Exclusion criteria:

1. Inability to give informed consent.
2. Any patients continuing beta blockers/direct renin blockers.
3. Pregnant women or those unable or unwilling to take secure contraceptive precautions.
4. Any illness, condition or drug regimen considered a contraindication by the Principal Investigator/Clinical Investigator.

Inclusion and exclusion criteria taken from FABULAS study protocol IRAS ID 222446 Version 5/07/02202.

4.1.3 Study design:

A multicentre feasibility study of EUS-guided RFA of APAs of the left adrenal gland. 30 patients with pre-diagnosed left-sided APA were recruited sequentially to undergo RFA followed by safety and efficacy clinic visits as per schedule. Once the first two patients of group one had been performed at UCLH, events were reviewed by the safe committee. Further recruitment began at CUH and Barts Health, when the safety committee deemed ablations to be safe, following the first four. This was not only to maximise safety, but also increased availability and recruitment into the study. It also gave some early insight into whether the procedure could be rolled out over multiple centres.

The following assessments were completed. Initial radiological investigations were performed where possible within 3 months of treatment as part of routine assessment of disease activity.

A summary of all other investigations and assessments is provided below and summarised in the schedule of events table.

Month -3 to day 0 (before treatment on Day 1):

- Primary aldosterone Endocrine Guidelines used to identify patients **(Screening Visit):**
- Informed consent taken.
- Medical history obtained.

- Symptom and adverse events monitored.
- Physical examination performed by doctor.
- Recording of demographic data.
- Concomitant medications documented.
- Review of current supplementary potassium intake.
- Three clinic blood pressure recorded and heart rate measurements.
- Patients were provided with blood pressure monitor and BP diary with instructions for use.
- 12 lead electrocardiogram (ECG) performed.
- FBC, electrolytes, bicarbonate, urea, creatinine, renin, aldosterone, CRP, CK, liver function tests (LFTs), amylase or equivalent, and HCG for childbearing females taken.
- Copy of reports of other prior investigations (e.g. radiology PET CT/Adrenal vein sampling results, biochemical analyses)
- Urinalysis.
- 5mls of serum and 5mls plasma taken for storage.

Day 0 (treatment day/Baseline visit):

- Symptom and adverse event monitoring
- Review inclusion/exclusion criteria to confirm eligibility.
- Three clinic blood pressure and heart rate recordings before ablation.
- Further systolic, diastolic and heart rate measurements during procedure capturing the highest 3 measurements.
- Record home blood pressure and heart rates (4 days of recordings prior to clinic visit, 3 readings in morning and 3 in evening).
- Physical examination
- Review concomitant medication and supplementary potassium intake.
- FBC, electrolytes, bicarbonate, urea, creatinine, renin, aldosterone, CRP, LFTs, amylase or equivalent, and HCG for childbearing females taken.
- Plasma metanephrines and normetanephrines collection before and during ablation
- 5mls of serum and plasma for storage for future tests in development, predicting likelihood of cure of hypertension.

- EUS-FNA of left aldosterone producing adenoma (APA)

Day 1 (after treatment on Day 0):

- Any adverse events monitored.
- Physical examination performed by doctor.
- FBC, electrolytes, bicarbonate, urea, creatinine, renin, aldosterone, CRP, LFTs, CK and amylase or equivalent taken.
- Urinalysis
- Three clinic Blood pressures and heart rates recorded.
- Concomitant medication and potassium supplement intake review.
- CT scan of abdomen.
- 5mls of serum and plasma for storage

Day 2 (after treatment on Day 0):

- As above if not performed on day 1.

Month 1 (Post ablation of APA (s)):

- Adverse events noted.
- Physical examination performed by doctor.
- Concomitant medication and potassium supplement intake check.
- Weight documented.
- Three clinic blood pressure and heart rates recorded.
- Documentation of the home blood pressure and heart rate recordings taken prior to clinic visit (3 readings in morning and 3 in evening for 4 consecutive days).
- FBC, electrolytes, bicarbonate, urea, creatinine, renin, aldosterone, CRP, LFTs, amylase or equivalent taken.
- Urinalysis

Month 3 (post ablation of APA(s)):

- Adverse events noted.
- Concomitant medication and potassium supplement intake check.
- Weight documented.
- Three clinic blood pressure and heart rates recorded.

- Documentation of the home blood pressure and heart rate recordings taken prior to clinic visit (3 readings in morning and 3 in evening for 4 consecutive days).
- FBC, electrolytes, bicarbonate, urea, creatinine, renin, aldosterone, CRP, LFTs, amylase taken.
- Urinalysis
- PET CT scan NB: Patients not having baseline ^{11}C Metomidate PET CT did not have repeat scan at 3 months.
- Repeat RFA ablation considered if PET CT is not negative for patients having baseline ^{11}C Metomidate or ^{18}F CETO PET CT scan.

Month 6 (post ablation of APA(s)):

- Adverse events documented.
- Concomitant medication and potassium supplement intake check.
- Weight documented.
- Three clinic blood pressure and heart rates recorded.
- Documentation of the home blood pressure and heart rate recordings taken prior to clinic visit (3 readings in morning and 3 in evening for 4 consecutive days).
- FBC, electrolytes, bicarbonate, urea, creatinine, renin, aldosterone, CRP, CK LFTs, amylase or equivalent taken.
- Urinalysis
- 5mls of serum and plasma taken for storage.
- 12 lead ECG performed.

4.1.4 Timetable of study

Time Point	Screen	Baseline Ablation Week 0	Post ablation 24hr	Post ablation 48hr	Post ablation1month post-surgery	Post ablation 3month	Post Ablation 6month
Informed consent	X X						
Medical history	X						
Clinical examination	X				X		
Concomitant medications	X	X			X	X	X
Potassium supplement intake review	X	X			X	X	X
Weight	X				X	X	X
Ethnicity	X						
Inclusion/exclusion criteria check	X	X					
***Clinic BP & heart rate**	X	X	X		X	X	X
Home BP & heart rate		X			X	X	X
12 lead ECG	X						X
Blood tests – electrolytes with bicarbonate, urea, creatinine, CK	X	X	X		X	X	X
Plasma metanephrine		X					
Blood tests – plasma renin and Aldosterone	x	X			X	X	X
CRP, LFTs, FBC, Amylase		X	X		X	X	X
24-hour urinary electrolytes sodium/potassium	X						X
Urinalysis	X		X		X	X	X
HCG testing for CBP	X	X					
AE reporting		X	X		X	X	X
PET CT Scan (*,)**	X					X	
CT Scan				x			
Diagnostic FNA		x					
Stored serum, EDTA	X	x		x			x

Table 1: Study schema and schedule of events taken from FABULAS study protocol IRAS ID 222446 Version 5/07/022021.

*3 highest and lowest systolic and diastolic measurements recorded with heart rate during ablation procedure.

** Patients who did not have a baseline PET CT scan as per secondary outcome, did not require 3 month repeat scan.

4.1.5 FABULAS schematic Diagram:

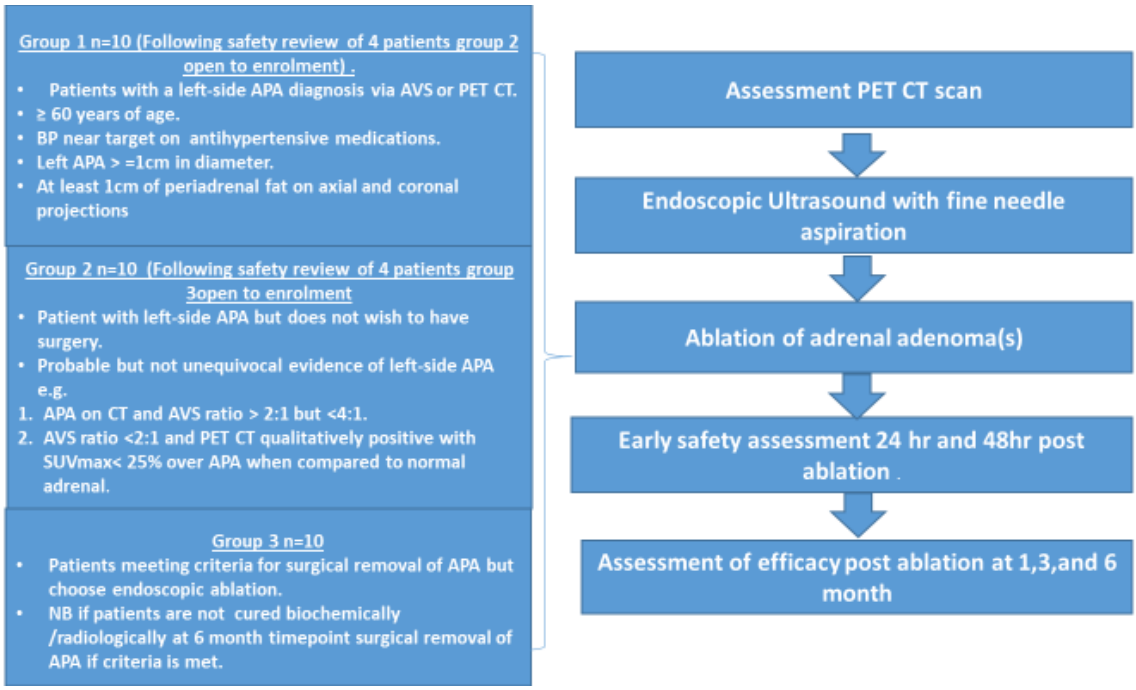

Figure 4 1: Schematic diagram of the FABULAS study taken from FABULAS study protocol IRAS ID 222446 Version 5/07/022021.

4.1.6 Pre-work up of patient and protocol of procedure:

Pre-procedure:

Once patients were determined to be included in the study and had consented, all patients gave written informed consent for genetic and clinical investigation. Consent was obtained according to local ethics committee guidelines: Cambridgeshire Research Ethics Committee for Addenbrooke's Hospital, University of Cambridge, or the Cambridge East Research Ethics Committee for Barts Health NHS Trust.

Once a date for the procedure was confirmed, patients were initially referred for an anaesthetic pre-assessment. Here the patients and their comorbidities were reviewed, with particular attention to their cardiovascular risk and morbidity. Where there were concerns about cardiac function, particularly left ventricular function, or valvular disease, an up-to-date transthoracic echocardiogram was performed. Other comorbidities, such as diabetes and renal impairment, were also carefully reviewed prior to procedure, particularly in patients who had been previously determined too high risk for surgery.

Patients were also commenced on two weeks of alpha and beta blockade. Patients were usually prescribed doxazosin titrated up to 8mg twice a day and bisoprolol titrated up to 5mg twice a day. Where doxazosin or bisoprolol were not tolerated, alpha and beta blockade was achieved with labetalol, a combined alpha and beta-adrenoceptor blocker, the dose of which was increased to 400mg twice a day. During the titration of medications, the patients tended to continue their current medications with careful blood pressure and heart rate monitoring.

One to two days prior to their procedure, the patient would have a full set of blood tests including electrolytes (U&Es, magnesium) and clotting to ensure there was no electrolyte abnormality. Most patients on anticoagulants were on direct oral anticoagulants (DOACs) and they were advised to stop these 24-hour pre-procedure. During the COVID pandemic, COVID PCR swab was taken the day prior to the procedure as per hospital protocol.

Intra- procedure:

Patients attended hospital on the day of the procedure having fasted for 12 hours. All theatre staff complied with WHO safety checklist. All procedures at UCLH and CUH were performed under general anaesthetic due to anaesthetist preference. An arterial line was inserted to allow the anaesthetist to have close monitoring of the patient's blood pressures in case of rapid haemodynamic changes, as well as easy access to obtain serum

samples. At Barts Health all procedure were performed under deep propofol sedation with no arterial line insertion.

With induction of general anaesthesia often patients would become hypotensive due to the alpha and beta blockade on board, as well as routine anaesthetic agents, leading the anaesthetist to give gentle vasopressors or sympathomimetics such as e.g Ephedrine if required. For higher risk patients, we ensured a defibrillator was in the endoscopy room (this is not a routine piece of equipment for endoscopy), in case arrhythmias occurred, and in the unlikely, event cardioversion was required. The anaesthetist would also ensure drugs were prepared for administration such as phentolamine (a non-selective alpha adrenergic receptor antagonist) or labetalol in case of a hypertensive crisis. During arterial or venous line insertions, serum samples were taken as per protocol.

The patient once anaesthetised, was then placed in a left lateral or supine position according to the preference of the endoscopist. A linear-array EUS endoscope (*Olympus, Keymed UK Ltd.; Pentax, Hitachi Medical Systems UK Ltd.*) was then passed into the stomach and from there the left adrenal gland was visualised using EUS.

The EUS-RFA (*Habib^{TM} or STARmed*) probes were the most commonly used. The probe is a 19-gauge monopolar needle electrode with a non-insulated 5mm/10-mm tip that delivers radio frequency current that is generated by alternating current system (*RITA 1500, RITA 1500X, ERBE VIO200D/300D or STARmed*).

The needle is gently introduced under radiological visualisation. Once the probe was introduced, a fine needle aspiration was taken of normal tissue and 2 samples were taken of the APA. One normal and one tumour samples were put into RNA later and one tumour into formalin. The biopsy was to ensure retrospectively that CYP11B2 expressing cells were targeted, as well as tissue to perform RNA sequencing of gene expression.

The tip of the RFA catheter was then positioned within the rim of the APA under sonographic guidance, occasionally a doppler was used to ensure the correct place. An electrode/ grounding pad was placed on all patients, and current delivered through the tip of the electrode into the APA, the catheter controlled by the endoscopist.

Bursts of RF up to 25 seconds were delivered at 10-30 Watts, when hyperechoic bubbles were observed (please see Figure 4 2) the energy was stopped, and a cooling period of 60 seconds was observed. The area of induced tissue necrosis could be estimated by the acoustic scattering of the gas bubbles. This process was repeated up to 10 times maximum depending on the size of the APA.

A repeat metanephrine and normetanephrine sample was taken post ablation to check for irritation of the medulla and a catecholamine rise.

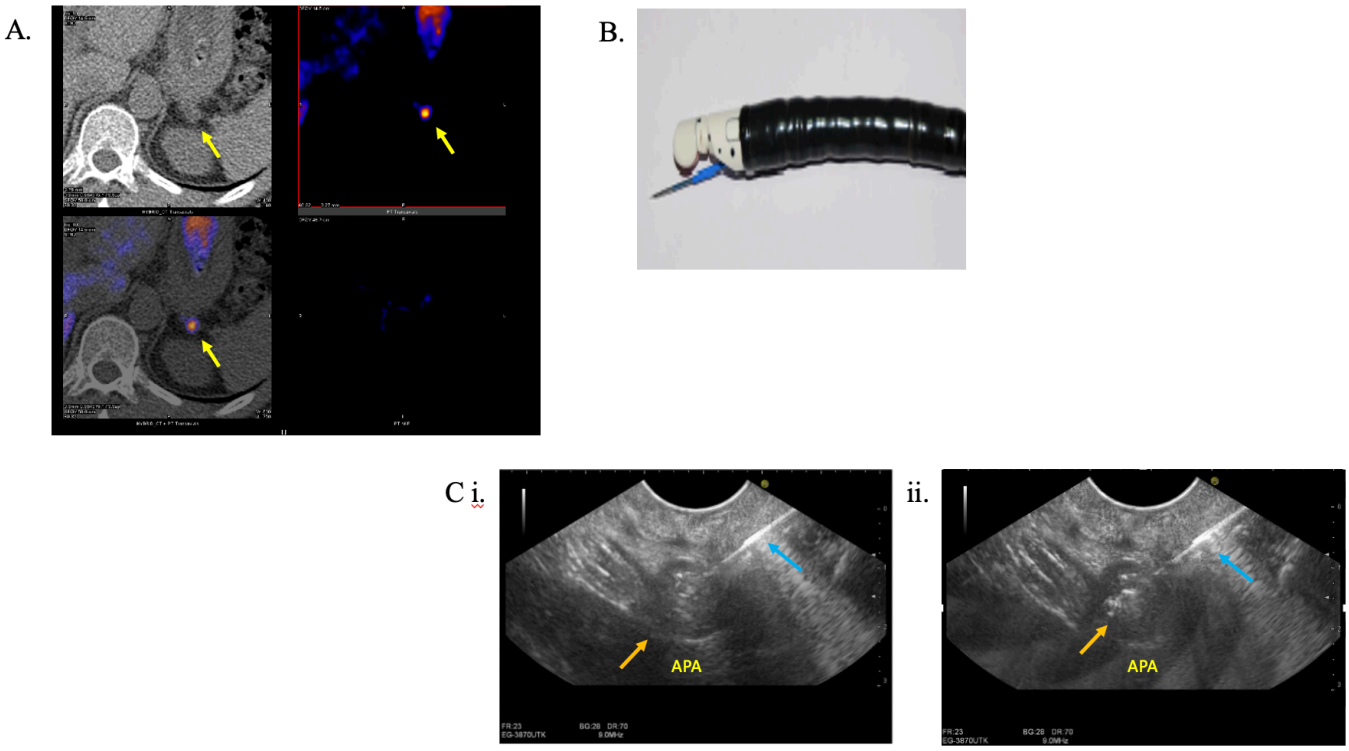

Figure 4 2: A. illustrates a cross sectional image from a CT PET of a left sided adrenal adenoma, which is lit up by the isotope ^{11}C- Metomidate, taken up by the aldosterone secreting cells. B. The EUS-RFS probe with the blue needle that goes through the stomach wall into the left sided APA. C. i. The view from the endoscopic probe, the APA is labelled as the circular structure, the orange arrow also indicating the APA and the needle guided into the APA is labelled with a blue arrow. This image is prior to RFA. ii. The second picture illustrates the same APA as i. following RFA, the orange arrow indicating the hyperechoic bubbles within the APA.

Images courtesy of Professor Stephen Pereira (UCLH).

Post procedure:

Once the procedure was complete, the patient was extubated and taken to the recovery area. Lower risk patients had their arterial line removed and they were moved to the gastroenterology ward after a period of 30-60 minutes in recovery. High risk patients were taken to high dependency units with continued invasive monitoring. All patients remained in hospital 24-48 hours for monitoring. At 24 hours every patient had a contrast abdominal CT to rule out any procedure related complications, such as perforation, haemorrhage, or infection. Careful examination of the patient was performed along with blood tests and blood pressures and heart rates. Often simple analgesia was all that was required to settle any discomfort. In some cases where possible antihypertensive medications were stopped. If the patient was well, they were then discharged home.

4.1.7 Follow up:

As described above patients were closely followed by their home teams at 1, 3, and 6 months. At these appointments home and clinic blood pressures were recorded, clinical examination was performed, blood serum analysis taken, and medications reviewed. Medication documentation was important in order to be able to work out the Defined Daily Dose (DDD) at the end of the study. The DDD is a technical unit of measurement devised by the WHO to avoid international confusion of drug consumptions, due to variability in cost and doses etc. The DDD is the assumed average maintenance dose per day for a drug that is used for its main indication. The WHO has determined the DDD for all medicines with an Anatomical Therapeutic Chemical Code (ATC).

At 3 months, where possible, a repeat PET CT scan was performed and reviewed along with biochemical data at a monthly multidisciplinary team (MDT) meeting. It is here with careful consideration that second ablations were considered for certain patients. These included patients who had overall performed well with one ablation, reduction in APA on nuclear medicine scan, improvement in blood pressures and biochemistry and who it was strongly felt would benefit from a further procedure.

4.1.8 Adverse events:

The primary outcome of this study was safety and therefore any adverse event was meticulously documented and discussed via an elected independent safety committee. These events were classified as follows.

An adverse event indicates any untoward or unintended response in a subject to whom a medical intervention or product has been administered. This includes any events which are not necessarily caused by or related to that process.

An adverse reaction is an untoward or unintended response in a subject to a medicinal product under investigation, related to any dose of the product administered.

An unexpected adverse reaction indicates a reaction that is not in keeping either in:

(a) in the marketing authorization or characteristics of that product,

(b) in the investigator's brochure of the investigational medicinal product, relating to that trial.

Events which do not require reporting to the Sponsor and Regulatory agencies:

The following events do not require reporting to the Sponsor, but must be recorded in the relevant section(s) of the MACRO database (CRF) and medical notes:

- expected adverse events,
- disease related deaths,
- hospitalisation for elective treatment.

Events which need to be reported as adverse events (AE):

- Any pre-existing medical condition that worsens following the intervention,
- Any adverse event emerging from treatment, a condition that arises following the treatment that was not there before, or any event that's worsened or prolonged secondary to the treatment,
- Laboratory abnormalities.

With adverse events documentation will require the investigator to make an assessment. Along with good clinical judgment and practice the following should be considered, firstly, is there a timing between the procedure and the event which can be used to link causality, and if so, should the study device be withdrawn, secondly is their reappearance or worsening of the event during treatment, could there be influence from a pre-existing disease, concomitant disease, or concurrent medication.

Events which need to be reported as Serious Adverse Events:

A Serious Adverse Event is officially defined as any untoward medical occurrence that results in:

- Death
- A life-threatening event
- Inpatient hospitalisation or prolongation of hospitalisation

- Severe or permanent disability
- Cancer (other than cancers diagnosed prior to enrolment in studies involving patients with cancer)
- Congenital anomaly
- Any grade 4 toxicity

Suspected Serious Adverse Reactions (SSARs):

SSARs are adverse reactions or events one may relate to the research procedure. With regards to EUS RFA procedures for left sided PA, the following SSARs were drawn up:

1. Related to anaesthetic agents used intra procedure such as midazolam:
    a. Drowsiness and confusion
    b. Anterograde amnesia
    c. Nausea and/or vomiting
    d. Respiratory depression
    e. Hypotension
    f. Pain at injection site
2. Related to EUS RFA:
    a. Abdominal pain
    b. Nausea and vomiting
3. Related to tissue damage or necrosis:
    a. Fever
    b. Anorexia, nausea, vomiting
    c. Abdominal pain
    d. Pancreatitis
    e. Bleeding
    f. Duodenal perforation
    g. Biliary tract damage/ obstruction.

Reporting of events:

All AEs and SAEs that occurred during the trial were recorded in hospital records, on the online data collection platform (MACRO) and the sponsors SAE log in according with the studies protocol. All SAEs were reported to the sponsor following completion of the form by the chief investigator of the study.

No SUSARs occurred during the trial but were they to have occurred the sponsor would have been notified immediately (or at least within one working day) according to the sponsor's written SOP. The sponsor would have notified the main REC of all SUSARs. SUSARs that could have been fatal or life-threatening would have been notified to the REC within 7 days after the sponsor had learned of them. Other SUSARs would have been reported to the REC within 15 days after the sponsor had learned of them.

Safety Committee:

An independent safety committee was selected to review initially the first two patients, then the second two patients and subsequently any adverse or serious adverse events. At the end of the study an extended safety meeting was held where ALL unexpected events, AEs and SAEs were discussed and scored. The below scoring system was drawn up and applied.

The safety committee comprised of three highly experienced individuals, a hepatobiliary surgeon, with experience of RFA, a very experienced endocrinologist with great knowledge of PA, and a radiologist specialising in the adrenal gland. No PI was present for any of the safety meetings.

Safety committee scoring system:

Level of significant event:

1. **Low:** Asymptomatic or mild symptoms, minimal or no clinical intervention indicated.
2. **Medium:** symptomatic, minimal invasive intervention indicated e.g intravenous fluids.
3. **High:** Severe to life threatening medically significant event. Requiring urgent intervention, hospitalisation, or prolongation of hospitalisation.

Likelihood of significant event being associated with intervention:

1. **Low:** no association.
2. **Medium:** minimum to moderate association.
3. **High:** as a direct consequence of.

4.1.9 Statistics:

Sample size calculation pre study:

As laid out within the study protocol It was determined a sample size of 30 patients would be recruited. The original statistical analyses were performed by Dr Stephen Morant, University of Dundee (statistician). Although the study was not exactly a phase 1 study of a novel drug therapy, the aim was to allow the Safety Committee to abort the study if any patient suffered harm, this was to permit escalating thresholds of safety that had to be met before progressing to patients where age or availability of surgery reduced acceptable levels of risk; and by the study-end therefore to permit high overall confidence of safety (and knowledge of hazards), and reasonable estimate of efficacy so that a comparative efficacy study could be designed. Dr Stephen Morant laid out the following probability, there will be a 90% probability of at least one serious complication occurring. In the first 6 patients if the risk per patient is >one in three ($(1-p)^6=0.1$). In the 10 patients recruited in each stage if the risk per patient is >one in five ($(1-p)^{10}=0.1$). In the 30 patients recruited overall there will be a 95% probability of least one serious complication occurring if risk per patient is >one in ten ($(1-p)^{30}=0.05$), and 80% probability of at least one serious complication occurring if risk per patient is >one in twenty ($(1- p)^{30}=0.2$). The study was not powered for efficacy. The graph below illustrates the predicted cure rate (%) to the observed number of cures. The 95% confidence intervals for all the possible cure rates that may be observed among 30 patients is illustrated in blue shadowing.

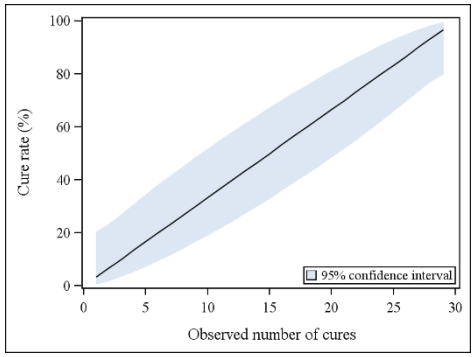

Figure 4 3: Graph of predicted cure rate (%) to observed number of cures. Taken from FABULAS study protocol IRAS ID 222446 Version 5/07/022021.

Post study statistics:

All statistics were performed by myself in this thesis. All statistical analyses were performed using GraphPad Prism v9 Software. Data normality distribution was assessed using Shapiro Wilk testing, where it was normally

distributed paired T-Test was performed where not normally distributed a non-parametric test such as Wilcoxon signed rank test was performed. A P-value less than 0.05 was considered significant. Most safety data was reported descriptively.

4.2 Results:

4.2.1 Patient demographics and enrolment:

The following results are all obtained from a data snapshot performed on the 24th of February 2023 on the MACRO software. At this point within the study, a total of 34 patients had been enrolled. 29 patients at Barts Health and 5 patients at Cambridge University Hospital (CUH). 6 patients withdrew due to either personal reasons (difficulty making appointments) or opting for surgery instead and one patient sadly passed away from an unrelated malignancy (hepatocellular carcinoma).

Of the 28 patients remaining, 4 underwent their procedure and all follow up care at CUH and underwent one RFA each at CUH. Of the remaining 24 patients, 7 patients underwent 2 ablations. The 24 patients underwent all their follow up care at Barts Health but of the 31 RFA procedures, 24 occurred at University College London Hospital (UCLH), 3 occurred at CUH, and 4 at Barts Health. Ablations for Barts patients occurred across multiple units, in part due to endoscopist skill and availability, but also the study was significantly delayed secondary to the COVID- pandemic. Some units had less bed pressures than others, therefore opportunities for RFA at multiple sites were seized. In total, the study took 4 years to complete.

All patients had been diagnosed with PA as part of routine clinical care, and all were demonstrated by lateralisation investigations (clinical AVS or molecular imaging) to have definite (the majority) or probable left-sided aldosterone excess. For lateralisation, 27 patients underwent a Metomidate ^{11}C PET CT scan or ^{18}F CETO PET CT scan and 1 patient lateralised via conventional AVS.

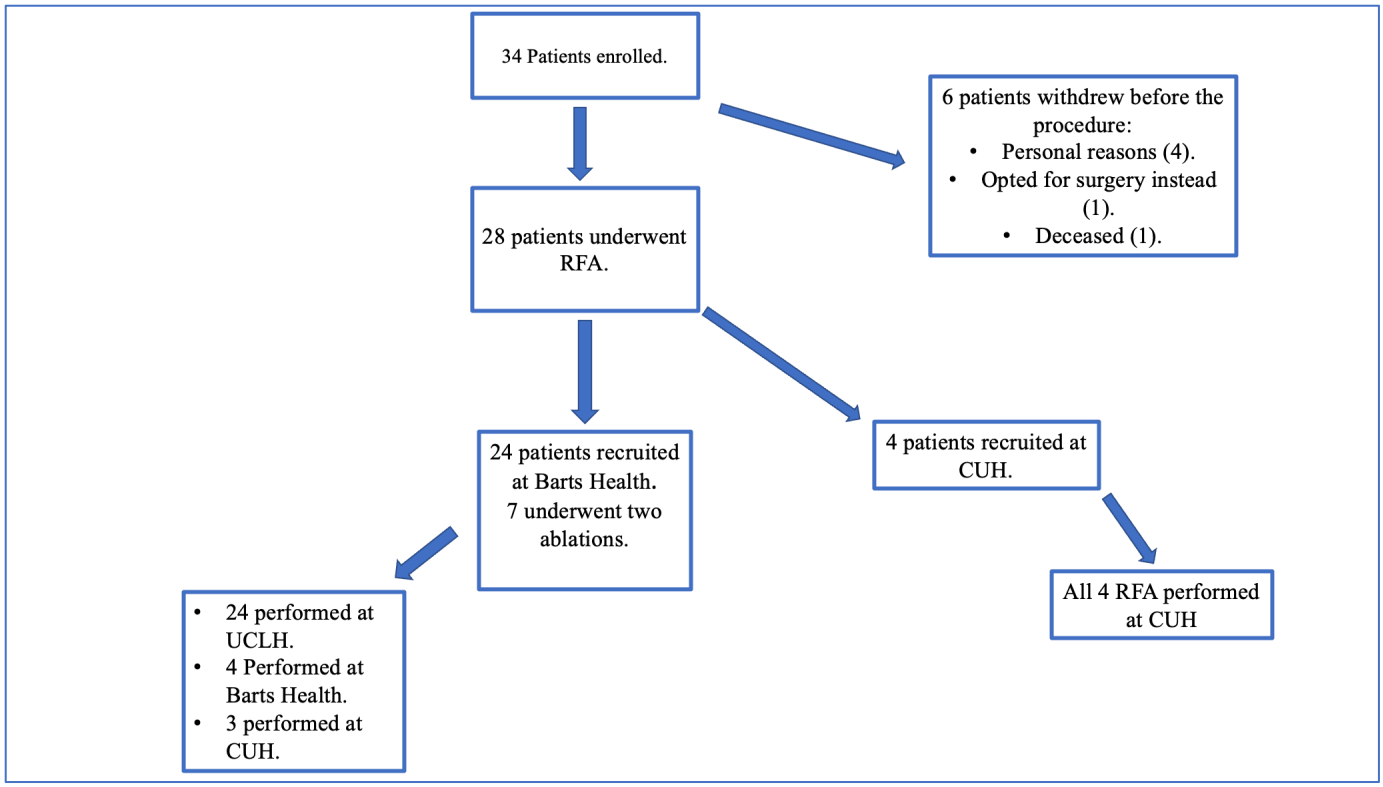

Figure 4 4: A schematic diagram illustrating the enrolment and pathway of patients within the FABULAS study. As mentioned before ablations were performed across three study sites.

Total number(n) of patients: 28

Age (yrs):	
Mean +/- STDev.	57.9 +/- 10.23
Range.	40-77
Sex n. (%):	
Male.	21 (75)
Female.	7 (25)
BMI (kg/m^2):	
Mean +/- STDev.	28.8 +/- 5.8
Ethnicity n. (%):	
Caucasian.	16 (57.1)
Black African.	11 (39.3)
Asian.	1 (3.6)
Study Group n. (%):	
Group 1.	8 (28.6)
Group 2.	12 (42.8)
Group 3.	8 (28.6)
Comorbidities (n):	
Mean.	3.7
Range.	1-12
Baseline medications mean. (range):	
Defined daily dose (DDD).	4.95 (1-14.6)
Number of antihypertensive tablets (n).	3.46 (1-7)
Baseline PA investigations mean. (range):	
Aldosterone (pmol/L).	1301.14 (260-4630)
Plasma Renin activity (nmol/L/hr).	0.79 (0.18-14.8)
Baseline Biochemistry (mean +/- SEM):	
Sodium, Na^+ (mmol/l)	140.6 +/- 2.8
Potassium, K^+ mmol/l).	3.9 +/- 0.5
Bicarbonate (mmol/l).	25.66 +/- 3.4
Urea (mmol/l).	5.66+/- 2.05
Creatinine (umol/l).	89.25+/- 23.2
Baseline Clinic blood pressure mean. (range):	
Systolic (mmHg).	144 (104-184)
Diastolic (mmHg).	84.5 (47-130)
Heart rate (bpm).	63 (47-93)

Table 2: Table illustrating the patient demographics, study groups patients were enrolled in, baseline data for medications, serum investigations, and clinic blood pressure all captured at screening/ baseline. DDD was calculated using the online calculator provided by the WHO.

4.2.2 Procedure data:

The protocol of the procedure is described above in section 4.1 6. 35 ablations occurred over 3 centres. The decision for alpha and beta blockade was determined by protocol and all patients were instructed to take two weeks prior to the ablation. The choice for which anaesthetic was undertaken during the procedure came from the often very experienced anaesthetist present and their comfort. Time was strictly measured from when probe went in and came out.

From the outset of the study, there were different probe options from different suppliers, either Starmed™ or Habib for the EUS probe and Starmed™ or Erbe for the RF generator. The general consensus regarding the tip size of the probe was adenomas >1-1.5cm a 10mm probe was utilised, this was as per endoscopists practice.

	Total number(n) of RFAs: 35
Patients (n): Alpha and beta blockade.	 35 (100%)
Anaesthesia (n). General anaesthesia + arterial line. Deep sedation.	 31 (88.5%) 4 (11.5%)
Average time (minutes): Scope in. Range.	 31.5 15-80
EUS Probe used (n): Starmed. Habib. RFA generator used (n): Starmed. Erbe.	 35 (100%) 0 35 (100%) 0
Size of tip exposure used (n): 5mm. 10mm.	 14 (40%) 21(60%)

Table 3: Data table from 35 RFAs procedures performed. Data such as average time of procedure, equipment utilised, and anaesthetic used was documented.

1. **Number of adenomas:**

Prior to the RFA procedure commencing, the endoscopist would pass the endoscopic ultrasound down and ensure they could fully visualise how many adenomas were present in the adrenal gland. The molecular medicine scan or CT scan reviewed prior to the procedure would often help guide the endoscopist, as to which nodule was the so called “hot” one or “culprit”. In 5 of the 35 RFA procedures, more than one nodule was visualised. In those circumstances, RFA was performed on more than one nodule.

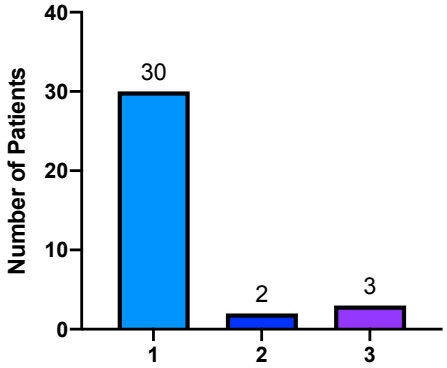

Figure 4 5: Figure illustrating the number of adenomas seen on EUS in all 35 RFA ablations. A total of 43 nodules were visualised, but in the majority (70%) of RFA procedures only one nodule was visualised.

2. **Location of adenomas within the adrenal gland.**

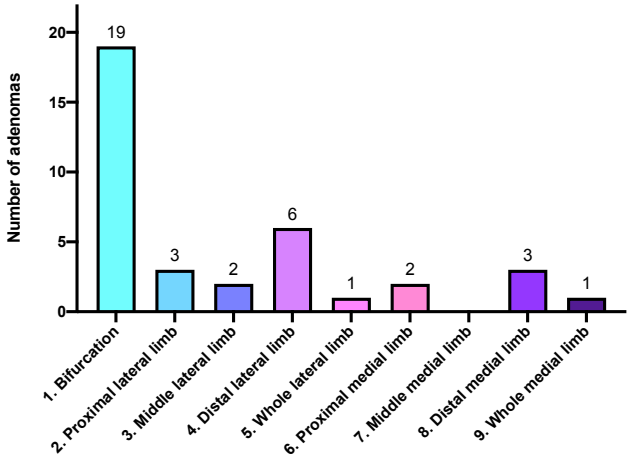

Figure 4 6: Figure illustrating the location of the nodules visualised during the procedure. (N=37) The majority 51% were located within the bifurcation/body of the adrenal gland. 2.7-8 % were located within the proximal to middle lateral and medial limb. 16% were located within the distal lateral limb.

3. **Number of RF bursts/ sequential treatments to the adenomas:**

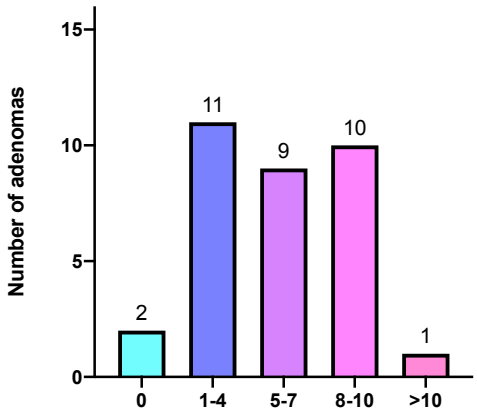

Figure 4 7: Figure illustrating the number of RF sequential treatments given to adenomas during the RFA procedures. 33% of adenomas received 1-4 sequential treatments, 27% received 5-7 and 30% received 8-10 sequential treatments. Some nodules received no treatments, in these particular cases the adenomas were deemed too difficult to treat anatomically. 1 adenoma received 14 bursts. (N=33).

4.2.2 1 Two RFA procedures:

As the primary outcome was safety, it was determined from the outset of the study that where possible two ablations would be offered to patients. The decision to offer a patient a second ablation was determined by the following, a repeat nuclear medicine either ^{11}C metomidate or ^{18}F Ceto scan, performed around 3 months post ablation. This was reviewed in the monthly MDT held with the team from Addenbrookes in CUH. Home and clinic blood pressures were also reviewed, along with medications as well as biochemistry, renin, and aldosterone levels. Patients who had had an excellent response both radiologically, clinically, and biochemically were not offered another procedure, but patients who had had some response either radiologically, clinically, or biochemically and who it was felt would benefit from a second ablation were offered it. In total 9 patients were offered a second ablation, but 7 patients underwent the procedure.

4.2.3 Safety Outcomes:

4.2.3 1 Safety committee and serious adverse events. (SAEs):

The primary outcome of this study was safety of EUS RFA in the treatment of left sided APA. The safety committee met a total of 4 times during the whole study. The safety committee comprised of three highly experienced individuals; a hepatobiliary surgeon, with experience of RFA, a very experienced endocrinologist with good knowledge of PA, and a radiologist specialising in the adrenal gland. No PI was present for any of the safety meetings.

The safety committee first convened after the first two patients and then once again following the following two patients. Where possible recommendations were made, for example, one of the first patients was hypokalaemic on the day of his procedure. This could have contributed to his arrhythmia intraoperatively; therefore, the protocol was amended to include a potassium and magnesium check 24-hour pre-procedure.

There was a total of nine serious adverse events reported and three adverse events. They were all documented on the MACRO database in the serious/adverse event category for full transparency.

At the end of the study, any adverse events uncovered at any time point during the study were discussed at a final safety meeting. These findings included, either an anomaly within a different organ system picked up on the post procedure scan e.g an ovarian cyst, an event such as cerebrovascular event that occurred during the course of the study but a significant time after the intervention, or more serious events that occurred on the day of the procedure.

The following scoring system was applied to each event:

Level of significant event:

0. **No event**
1. **Low:** Asymptomatic or mild symptoms, minimal or no clinical intervention indicated.
2. **Medium:** symptomatic, minimal invasive intervention indicated e.g intravenous fluids.
3. **High:** Severe to life threatening medically significant event. Requiring urgent intervention, hospitalisation, or prolongation of hospitalisation.

Likelihood of significant event being associated with intervention:

0. **No event**
1. **Low:** no association.
2. **Medium:** minimum to moderate association.
3. **High:** as a direct consequence of.

SAE	Event	Severity	Related to Procedure?	SAE reason	Outcome
1	Hospital Acquired pneumonia and Fast atrial fibrillation 2 days post procedure.	3	Yes	Prolonged in-patient hospitalisation	Resolved
2	Hypokalaemia induced atrial fibrillation occurring during the procedure.	3	Yes	Prolonged in-patient hospitalisation	Resolved
3	Post-procedural non-ST elevation myocardial infarct (NSTEMI).	3	Yes	Prolonged in-patient hospitalisation	Resolved
4	Hypertensive episode during the procedure with raised post procedure metanephrines.	2	Yes	Life threatening	Resolved
5	Cerebrovascular event requiring hospital admission.	3	No	Hospital admission	Recovering
6	Pre- procedure admission for optimisation of diabetes control.	1	No	Prolonged in-patient hospitalisation	Resolved
7	Pre- procedure admission for pre-renal hydration.	1	No	Prolonged in-patient hospitalisation.	Resolved
8	Protocolised post RFA CT abdomen found a 15mm right lower renal pole papillary Renal Cell Carcinoma T1a N0M0.	1	No	Cancer	Ongoing
9	Protocolised post RFA CT abdomen showed known renal carcinoma under surveillance following previous treatment to have increased in size.	1	No	Cancer	Ongoing

Table 4: Table describing the nine SAEs within the study. Please note prolonged in-patient hospitalisation referred to any nights stayed in hospital beyond the 1-2 days dictated in the protocol. Often patients remained 1-3 days extra in hospital. This included the two patients who were admitted the night before, one for optimal diabetes management and the second for pre-renal hydration.

AE	Event	Severity	Related to procedure?	Outcome
1.	Protocolised post RFA CT abdomen fluid indicated peri-cholecystic fluid and common bile duct dilatation.	1	No	Resolved.
2.	Protocolised post RFA CT abdomen indicated a right adnexal cystic structure.	1	No	Resolved.
3.	Protocolised post RFA CT abdomen indicated small bilateral pleural effusions.	1	No	Resolved.

Table 5: Table describing the three AEs within the study.

The following SAEs have been discussed below in greater detail as these events were classified as high in severe to life threatening medically significant event. Requiring urgent intervention, hospitalisation, or prolongation of hospitalisation and high as a direct consequence of the intervention.

- Case 1: 78M with a background history of hypertension, PA, and previous episodes of hypokalaemia. Two days post his first RFA procedure, the patient developed fever and tachycardia (heart rate >100 bpm). The routine CT post ablation showed bilateral basal atelectasis/ consolidation in keeping with possible lower respiratory tract infection/ pulmonary oedema. An ECG showed rapidly conducted atrial fibrillation (AF), with rate-related lateral ischaemia. Blood tests showed raised inflammatory markers and hypokalaemia. A diagnosis was made of hospital acquired pneumonia. The patient was treated with fluids and intravenous antibiotics (co-amoxiclav). The hypokalaemia was corrected intravenously, and the patient fully recovered. This event was determined to be medically significant and as a direct consequence of the intervention as the pneumonia developed post procedure within the hospital setting.

- Case 2: 70 M who, during the procedure, developed rapidly conducted AF with haemodynamic instability. DCCV (Direct Current Cardioversion) was deployed three times and sinus rhythm was restored. One further episode of AF with fast ventricular response resolved spontaneously. Hypokalaemia was documented and corrected. The patient subsequently underwent detailed cardiological assessment and continues apixaban, He recovered fully. This was judged to be a medically significant event linked to the procedure.

- Case 3: 77M, whose procedure was uneventful. Shortly after transfer to endoscopy recovery he developed an episode of dull left-sided chest discomfort, initially attributed to positioning on the left side during the procedure. Later the same afternoon he developed further left-sided chest pain. An ECG was performed which indicated: anterolateral ST segment / T-wave changes. Subsequent ECGs (18.18hrs, 18.19hrs) demonstrated resolution of the changes. Troponin was requested at 19.29hrs: 55ng/L (0-58ng/L). The following day a repeat ECG showed no further changes. However, a repeat troponin was significantly elevated at 398ng/L, prompting immediate cardiological assessment and commencement of the ACS (acute coronary syndrome) treatment protocol. In conclusion, this gentleman had a post-procedural non-ST elevation myocardial infarct (NSTEMI). In a patient with longstanding hypertension, most likely background occult coronary atheromatous disease was precipitated by the stress of undergoing a procedure under general anaesthesia. The committee considered this a significant medical event potentially linked to the general anaesthetic administered during the procedure.

Overall, the conclusion of the safety committee was the committee deemed the procedure to be safe and no concerns were raised about the study protocol, the execution of the study, or the procedure within itself.

4.2.3 2 EUS RFA of left adrenal APAs is a safe procedure:

Safety was measured through multiple parameters. Firstly, intra-operative safety measurements were reviewed. One way to review safety was to observe observations such as blood pressure (mmHg) and heart rate (bpm) pre- and intra-procedure. To look for evidence of medulla irritation and catecholamine release, metanephrines were also measured pre-intervention and post-intervention. The decision to measure for metanephrines came from anecdotal reports of hypertensive crises during adrenal RFA [107-110]. One of the theories suggested is that through the production of heat, necrosis can occur to tissue and if the medullary tissue of the adrenal is involved this may lead to a leak of catecholamines, causing raised blood pressure and potentially a serious life-threatening hypertensive crisis.

We measured the following serum by products of catecholamines; normetanephrine and metanephrine these are O-methylated metabolites of the catecholamines norepinephrine (noradrenaline) and epinephrine (adrenaline). Norepinephrine is classically stored within the adrenal medulla but also within the sympathetic nervous system whilst epinephrine is predominantly stored within the adrenal medulla. Careful interpretation of metanephrines was required as multiple external factors could contribute to their rise such as stress, dietary factors but also multiple medications, especially those commonly used within the anaesthetic room, corticosteroids (dexamethasome), sympathomimetics (ephedrine), Beta adrenergic receptor blockers (propranolol) and dopamine D2 receptor antagonist (metoclopramide).

Most safety data for EUS RFA has been obtained from studies where EUS RFA has been performed on pancreatic: cysts, malignancies, metastases, and neuroendocrine tumours. The studies have all pointed to a small risk of haemorrhage (duodenal in their cases), infection, peritonitis, abdominal pain but predominantly pancreatitis. This acute inflammation of the pancreas may arise due to lesions undergoing ablation within the pancreas, leading to cell destruction and irritation or it may be due to heat damaged sustained from the probe in the vicinity of the pancreas [213-217].

A hallmark investigation to ensure safety of the procedure, was a contrast CT scan at 24-48 hours post procedure, which all patients underwent. This was predominantly to check for major haemorrhage, perforation, and organ infarction.

Biochemical markers were also measured, such as Haemoglobin (g/L), a sudden drop in Haemoglobin would raise concern about haemorrhage. The reference values for Haemoglobin are the following, in men: 138 to172 g/L and in females: 121 to 151 g/L. Inflammatory markers for infection such as white cell count (WCC) (reference range 3.6-11.0 x10 ^9/L) and C-reactive protein (CRP) (reference range <3 mg/L) was performed.

Amylase (reference range 40-140 U/L) and Lipase (reference range 10/24- 140/151 U/L) were checked depending on hospital assays to rule out pancreatitis. Liver function tests such as Bilirubin (< 21 umol/L), Alanine transaminase (ALT) (men: 7-40 U/L, females: 7-35 U/L), Alkaline phosphatase (ALP) (30-130 U/L) were performed to ensure no biliary duct injuries and finally, Creatinine Kinase (CK) (Men: 40-320 U/L, females: 25-200 U/L) to rule out tissue breakdown and infarction.

All imaging and biochemical data was complemented with careful observation and examination of the patient. The following data was taking from all 35 EUS RFA in the study.

After the first 10 patients, the safety committee agreed to reduce the post procedure hospital stay from 48 hours to 24 hours.

1. **Pre- and Post-procedure observations:**

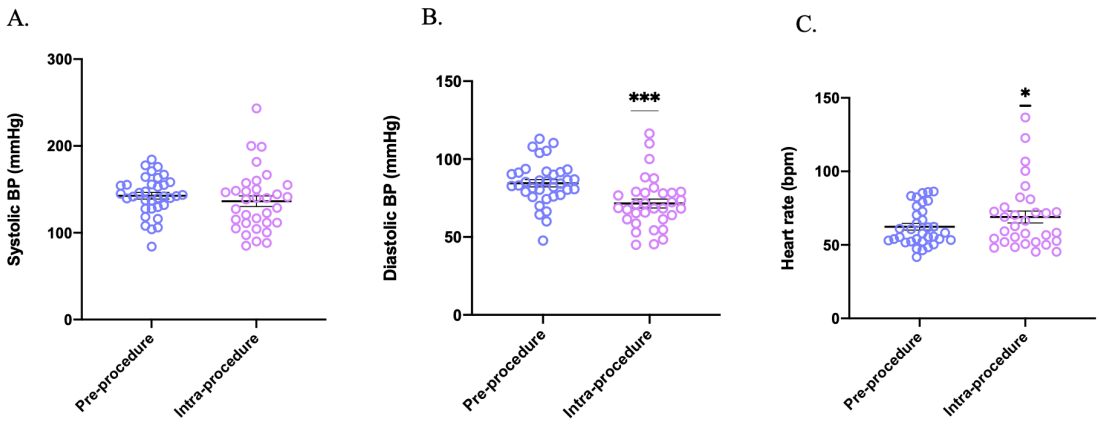

Figure 4 8: A. illustrates systolic blood pressure (mmHg) pre- and intra-procedure, there was no change in systolic BP. **B**. graph indicating diastolic blood pressure (mmHg) pre- and intra-procedure that shows a significant drop intra-procedure (P=<0.0002, paired T-Test). **C.** Heart rate (bpm) pre- and intra-procedure a mild increase in heart rate intra- procedure was observed (P=0.02, Wilcoxon signed rank test). (N=31-34)

Although the systolic blood pressure remained almost on par, the drop in diastolic blood pressure may be indicative of general anaesthetic agents which are known to lower blood pressure, in particular diastolic blood

pressure. Propofol, for example, along with other anaesthetic agents is known to lower not only systolic blood pressure but also diastolic [218, 219].

2. Normetanephrine and Metanephrine levels:

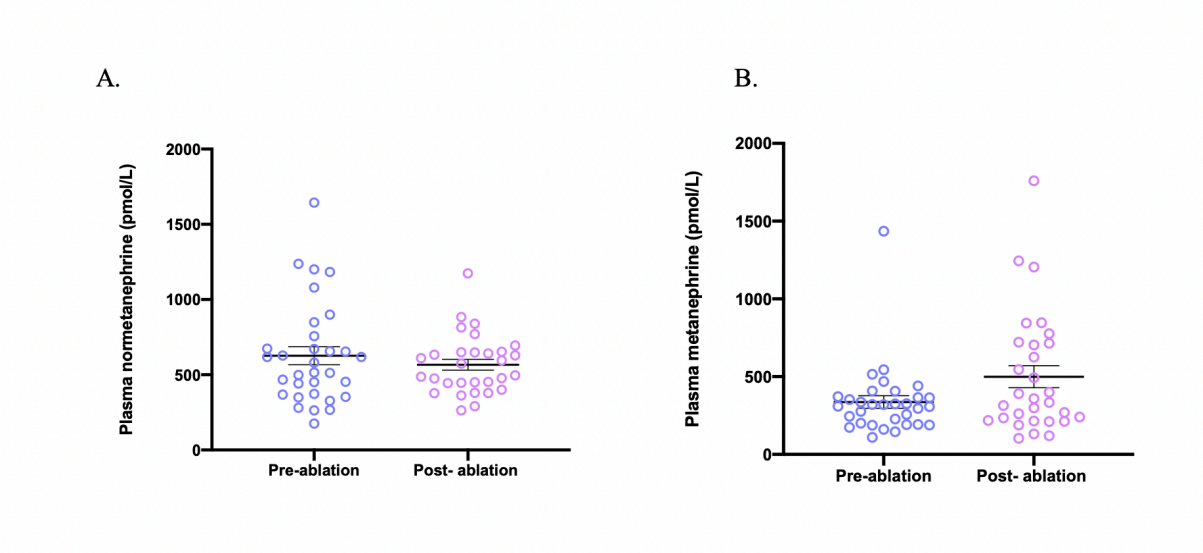

Figure 4 9: A and B: Graph illustrating pre- and post- procedure normetanephrines (pmol/L) and metanephrines. (pmol/L) level. No statistical significance was observed (N=33-32).

Particular note should be made of a strikingly high plasma metanephrine value. This occurred in a 53-year-old 53-year-old male patient with known significant comorbidities of obesity (BMI:43 kg/m^2), type 2 diabetes (on tablet control), atrial fibrillation (previous ablation but currently in AF), cardiac left ventricular impairment, renal impairment (eGFR: 30-40 ml/min/1.73m^2), sleep apnoea and previous thyrotoxicosis (now euthyroid). He was taking 7 antihypertensive medications and this tablet burden was his stated reason for enrolling into FABULAS, the above comorbidities making him an unattractive surgical candidate. The patient underwent two ablations, the first of which in May 2021, was uneventful. On admission for his second ablation in November 2022, his blood pressures pre procedure were satisfactory (140/92 mmHg average,) and he had received the standard alpha and beta blocking regiment described in the protocol (doxazosin 8mg BD and bisoprolol 5mg BD). Shortly after induction and into the procedure his blood pressure dropped to 85/54 mmHg, and he was given ephedrine and metaraminol. His blood pressure then increased to 258/119 mmHg HR:127 bpm, phentolamine and labetalol were administered. Plasma metanephrine was 407 pmol/l pre and 1760 pmol/l post ablation. His blood pressure resolved fully post procedure and he did not require a prolonged hospital stay. The safety committee judged that the hypertensive episode was related to the procedure but that the precise

contribution of adrenal medullary stimulation could not be determined. The overarching safety committee conclusion was alpha and beta blockade was important for pre procedure work up.

3. 24–48-hour post RFA CT scan:

After all, 35 RFA procedures patients underwent a contrast CT scan. No scan indicated any sign of perforation, major haemorrhage, or major organ infarction. In 6 (17%) scans a significant finding was found, as described before this was often in another organ system, such as an ovarian cyst, a renal tumour, pulmonary effusions or in one case common bile duct dilatation. All these findings were referred to and followed up by the appropriate specialities.

4. Haemoglobin, WCC and CRP:

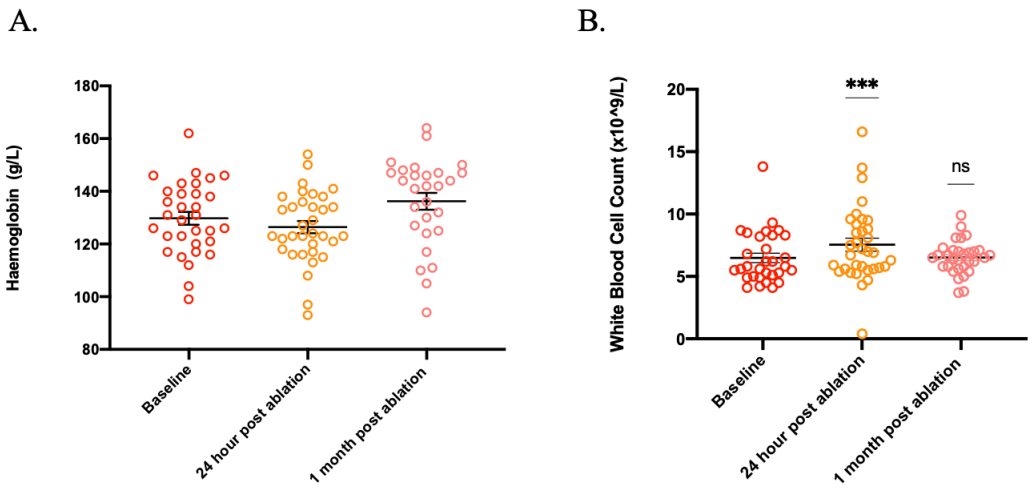

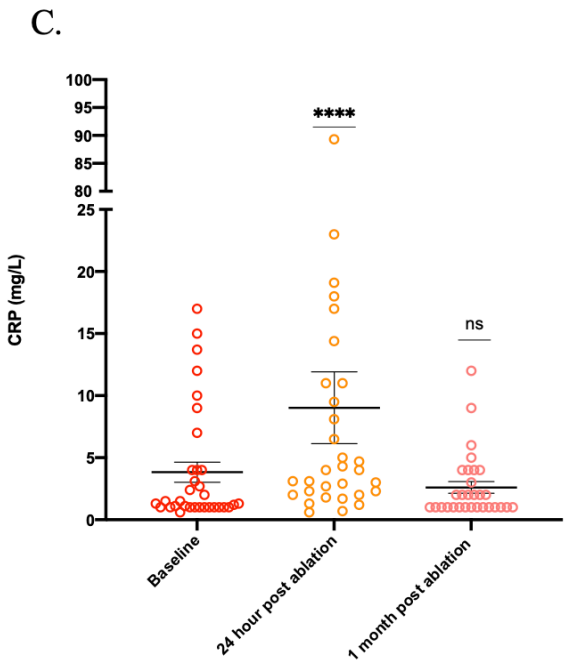

Figure 4 10: Three graphs illustrating Baseline, 24- hour post ablation and 1 month post ablation Haemoglobin (g/L), WCC (x10^9/L) and CRP (mg/L). **A.** Illustrates haemoglobin levels with no change (non-significant) over one month. **B.** indicates a raised WCC (P=0.0006, Wilcoxon signed rank test) at 24 hours, that has normalised by one month later. **C.** Depicts CRP that also increases 24 hours post procedure (P=<0.0001, Wilcoxon signed rank test), that has normalised by one month. (N=31-24)

Any surgical procedure, where foreign objects are introduced into the patient leads to a physiological immune response. The measurement of inflammatory markers post procedures has readily been introduced into routine practice, in order to monitor for post operative infections. The literature around WCC rising or leukocytosis post-surgical procedures is not well described, as it is a common phenomenon post procedures and may be a normal post-surgical response and not associated with infection. [220] CRP (C-reactive protein) is an acute inflammatory response marker, released from hepatocytes. It is thought to be one of the most sensitive markers for the acute phase response. It rises often within 6 hours and peaks by 48-72 hours. [221] It activates the complement pathway; its uprise is in concordance with the immunological response so a higher immune response the higher the upswing.

The significant rise in WCC and CRP is not indicative of increased infection rate post procedure but likely due to a natural immune response to a surgical intervention. Only one case of post procedure infection (hospital acquired pneumonia) was documented within this study.

5. **Amylase (U/L) and Lipase (unit/L).**

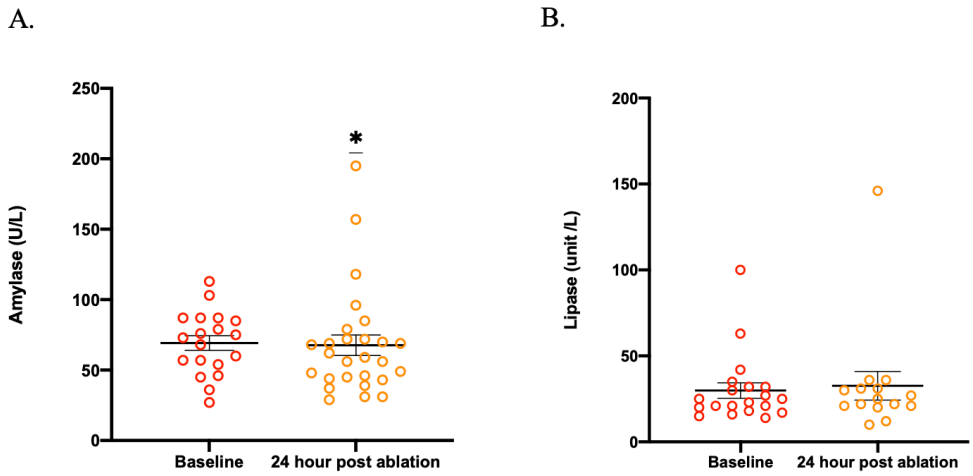

Figure 4 11: Amylase (U/L) and Lipase (unit/L) were measured at Baseline and at 24 hours, in order to rule out any risk of pancreatitis. Graph A. illustrates change in Amylase Baseline vs 24 hours (P=0.04, Wilcoxon signed rank test) and B indicated no change in Lipase from Baseline. (N= 15-27)

No patients within this study were diagnosed with post procedure pancreatitis. A significant rise in the 24-hour amylase as mentioned before may be due to heating of pancreatic tissue, or during the odd procedure if the adenoma was difficult to access the endoscopist had to go through the pancreas to target the adenoma. A rise in amylase within the first 24 hours then settling, with no evolving pancreatitis, has been seen previously in studies looking at EUS RFA of the pancreas [222]. There was no rise in Lipase, however Lipase usually rises quicker than Amylase. It rises 4-8 hours compared to 12-24 hours, therefore suggesting a rise should have been observed in Lipase too. One explanation could be the smaller N number of Lipase samples.

6. **Liver function tests: Bilirubin (umol/L), Alanine transaminase (ALT) (U/L), Alkaline phosphatase (ALP) (U/L):**

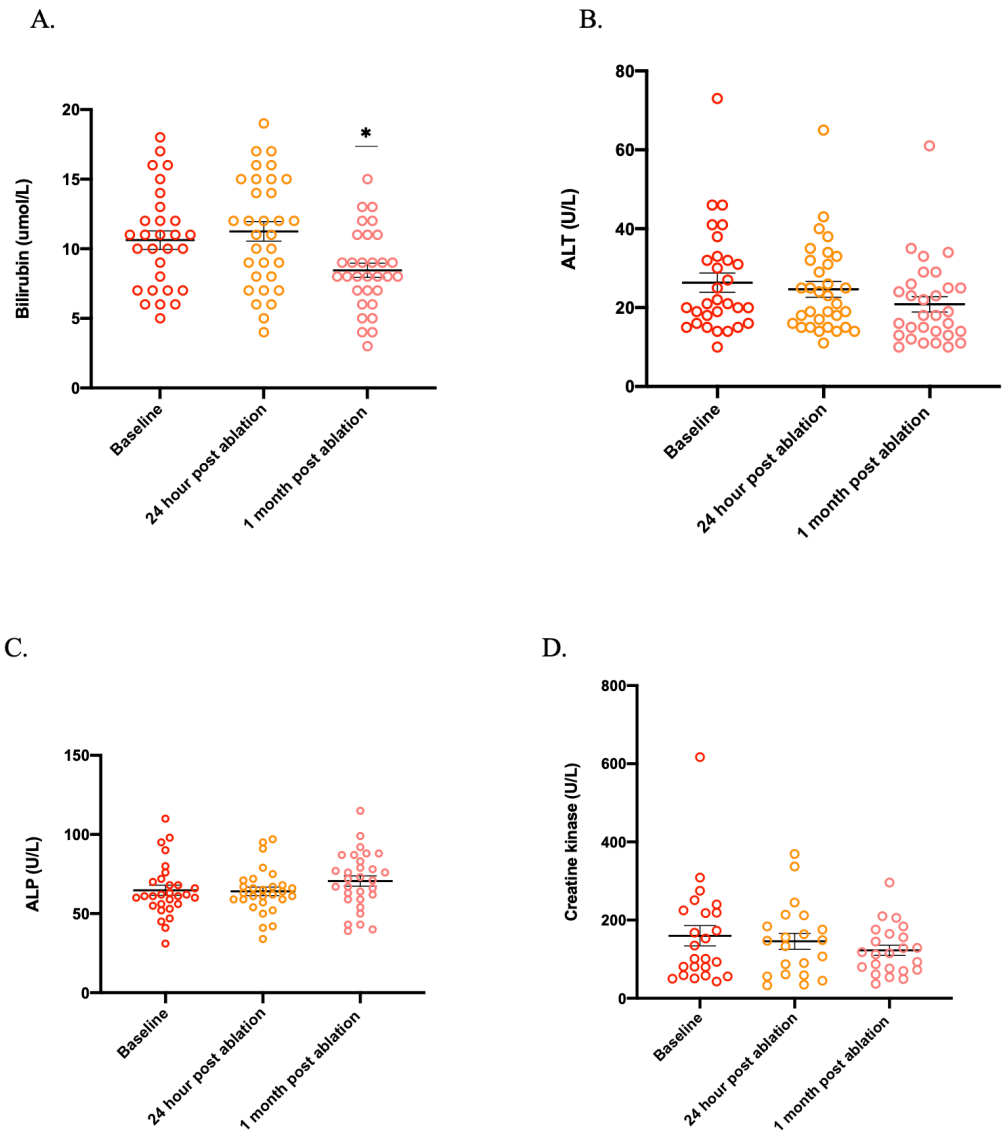

Figure 4 12: A. Bilirubin (umol/L) was measured at Baseline, 24 hours and 1 month post ablation. Baseline vs 1 month post ablation (P=0.01, paired T-TEST) rest non-significant. **B** and **C** graphs indicate ALT (U/L) and ALP (U/L) at Baseline, 24 hours and 1 month with no significant change. **D.** Creatinine Kinase (U/L) measured at Baseline, 24 hours and 1 month post ablation there was no change to any statistical significance.

Bilirubin illustrates a positive P value of P=0.01 one month post ablation, the change in bilirubin levels is likely down to the fact at baseline and at 24 hours in hospital samples were fasted samples whilst at one month in the outpatient setting they were non fasted. RFA-EUS on the APA had likely no impact on bilirubin.

4.3 Efficacy outcomes post 1st ablation:

Efficacy is primarily measured in PA by the international consensus of PASO criteria. The criteria are set out as complete, partial, and absent clinical success and complete, partial, and absent biochemical success.

To meet PASO criteria, data from baseline was compared with data 6 months post procedure. The PASO criteria are the following:

Clinical success:

- **Complete** clinical success is declared when both a. and b. have been met:
    a) Normalisation of BP, SBP <135 mmHg and DPB <85 mmHg of home blood pressures, if home blood pressures not available, then it is defined as clinic blood pressures, SBP <140 mmHg and DBP <90 mmHg.
    b) Cessation of antihypertensive drugs.
- **Partial** clinical success is declared when the criteria for complete clinical success is not met and either a. or b. has occurred:
    a) Reduction in BP, with no increase in antihypertensive drugs. When both i. and ii. has occurred:
        i. BP has normalised or reduced since baseline (either home blood pressure, or clinic blood pressure, if home not available). Reduction has been defined as 1. A reduction of ≥20 mmHg in SBP or 2. A change of <20mmHg in SBP and a reduction of ≥ 10 mmHg in DBP.
        ii. The DDD is <150% of baseline.
    b) Reduction in antihypertensive drugs with no increase in BP:
        i. BP is unchanged from baseline (either home blood pressure, or clinic blood pressure if home not available). Reduction has been defined as 1. No change is defined as <20 mmHg in SBP or 2. < 10 mmHg in DBP.
        ii. The DDD is <50% of baseline.
- **Absent** clinical success is declared when neither completer nor partial clinical success is achieved.

Biochemical success:

- **Complete** biochemical success is declared when both occur:
    - Serum potassium ≥ 3.6 mmol/l and

- Normalisation of ARR (For renin activity: ARR activity =< 750 pmol/l per ng/ml/hr, however if renin mass is used: ARR mass <91 miU/L).

- **Partial** biochemical success will be declared if the criteria for complete are not met and the following occur:
  - Serum potassium ≥ 3.6 mmol/l and
  - ≥50% reduction in serum aldosterone occurs.
- **Absent** biochemical success is declared when neither completer nor partial clinical success is achieved [98].

4.3.1 PASO outcomes:

Data was compiled for 28 patients and their outcomes were declared according to PASO criteria. 4 patients had complete clinical success, 4 patients had partial clinical success and 20 patients had absent clinical success. 14 patients had complete biochemical success whilst 3 had partial biochemical success and 11 had absent biochemical success.

Outcomes were measured with data taken from 6 months post first ablation or 3 months post second ablation. If 6 months data was not available after first ablation, 3 months data was used.

	Clinical			**Biochemical**		
	Complete	Partial	Absent	Complete	Partial	Absent
6 months after 1st ablation	4	4	20	11	4	13
6 months after 1st ablation or 3 months after 2nd ablation *	4	4	20	14	3	11

***7 patients had 2 ablations.**

Table 6: Table indicating the number of clinical and biochemical successes. There was no change in clinical outcomes post second ablation however there were three patients who post second ablation improved to a complete biochemical success. 14.3% of patients had a complete and partial clinical success, whilst 71.4% of

patients were absent of clinical success. 50% of patients at the end of the study achieved complete biochemical success whilst 10.5% achieved partial biochemical success and 39.5% achieved absent biochemical success.

4.3.2 EUS RFA to left sided APAs leads to no change in home blood pressure:

Home blood pressures were recorded three times a day for four days in the run up to the patient's appointment: at baseline, 1 month post ablation, 3 months post ablation, and 6 months post ablation. Blood pressure monitors were allocated to patients at screening, avoiding diversity of blood pressure monitors and therefore potentially readings. Cure would have been deemed a blood pressure <135/85 mmHg. The data includes final outcomes, including those post second ablation.

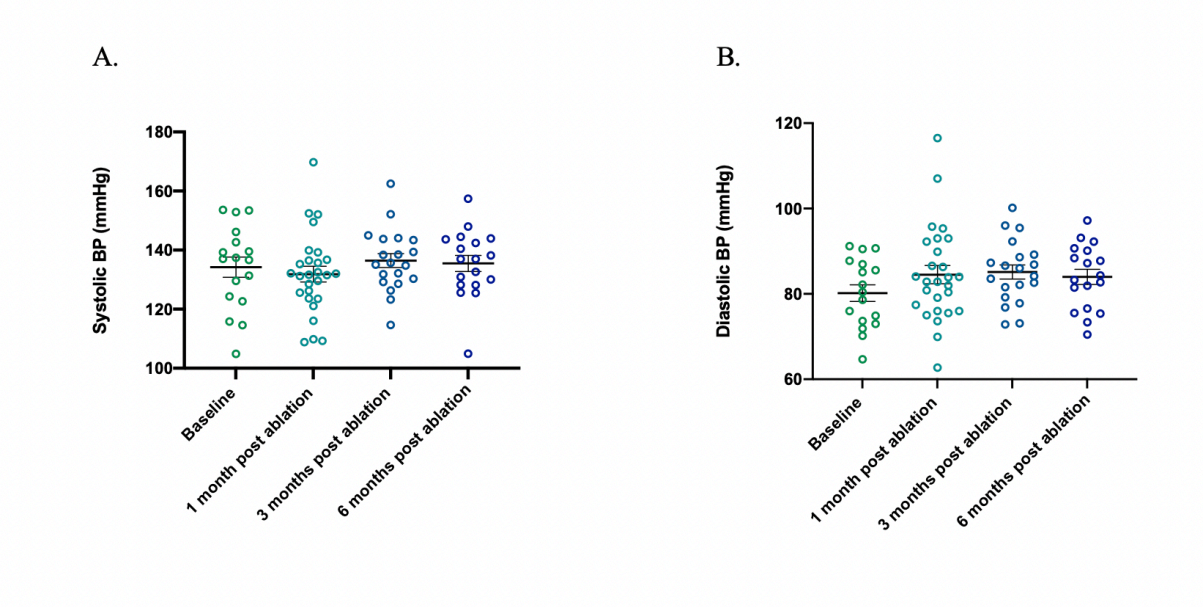

Figure 4 13: A. Systolic home blood pressure (mmHg) readings, indicated no change over the months from baseline to 6 months post ablation. B. Diastolic home blood pressure (mmHg) readings also illustrated no change over the months from baseline to 6 months post ablation.

(N=16)

4.3.3 EUS RFA to left sided APAs led to no change in clinic blood pressures:

At every clinic appointment blood pressure was recorded 3 times and documented. The average of this blood pressure was then taken. Clinical decisions regarding medications were taken with both home and clinic blood

pressure in mind. A cure was considered when the clinic blood pressures averaged <140/90 mmHg. The data includes final outcome including those post second ablation.

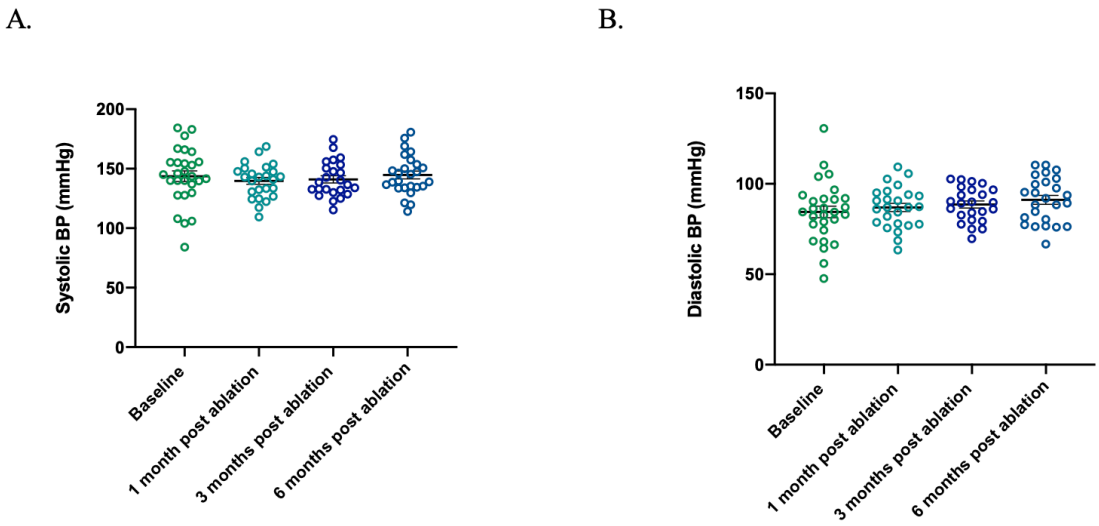

Figure 4 14: A. Systolic clinic blood pressure (mmHg) readings, indicated no change over the months from baseline to 6 months post ablation. B. Diastolic clinic blood pressure (mmHg) readings, there was also no change over the months from baseline to 6 months post ablation. (N=24)

Although there were individual cases of blood pressure improvement reported within the study, within the overall cohort there was no significant change in home or clinic blood pressures.

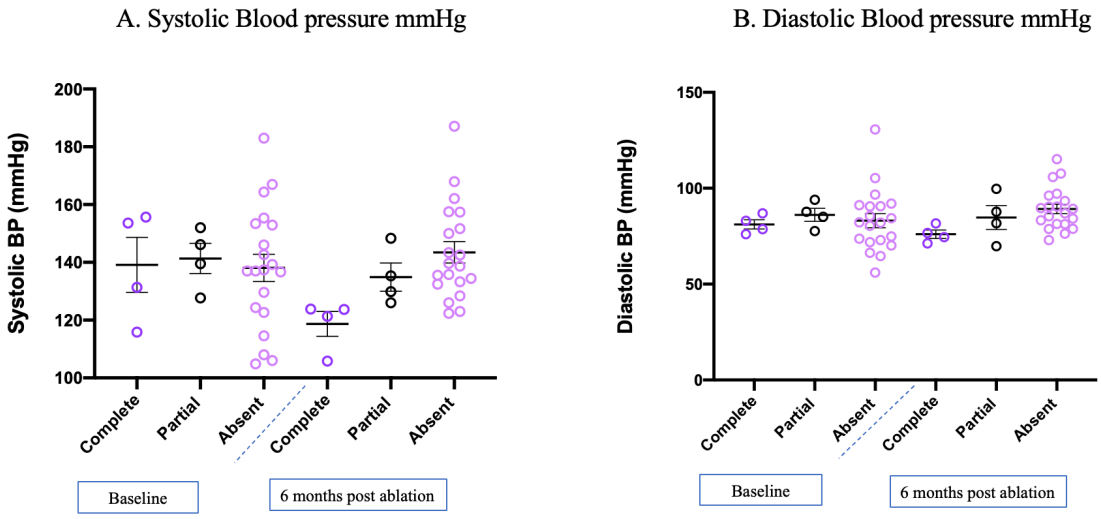

Figure 4 15: Graph A. and B. illustrating systolic and diastolic blood pressure of patients separated by their PASO scoring; complete, partial, and absent at baseline and 6 months. (N=28)

4.3.4 EUS RFA to left sided APAs leads to improvement in electrolytes:

Patients with PA are known to have a mild hypernatremia less than 150 mmol/l. The reference range of sodium is 135-145 mmol/l. The mild hypernatremia is likely due to adjustment of the hypothalamic osmostat, as patients continue to drink normal volumes of fluid [223]. Mild hypernatremia and hypokalaemia are largely due to an increased expression in sodium channels and potassium channel ATPase within the kidney collecting ducts, in the presence of excess aldosterone. This leads to sodium reabsorption, therefore allowing water to passively follow it and potassium to diffuse out of the cells into the lumen of the kidney whenever a sodium ion is reabsorbed [224]. The reference range for potassium: 3.6-5.2 mmol/l.

Serum analysis of sodium and potassium were measured at baseline, 1-, 3- and 6-months post ablation. The data includes final outcomes including post second ablation data.

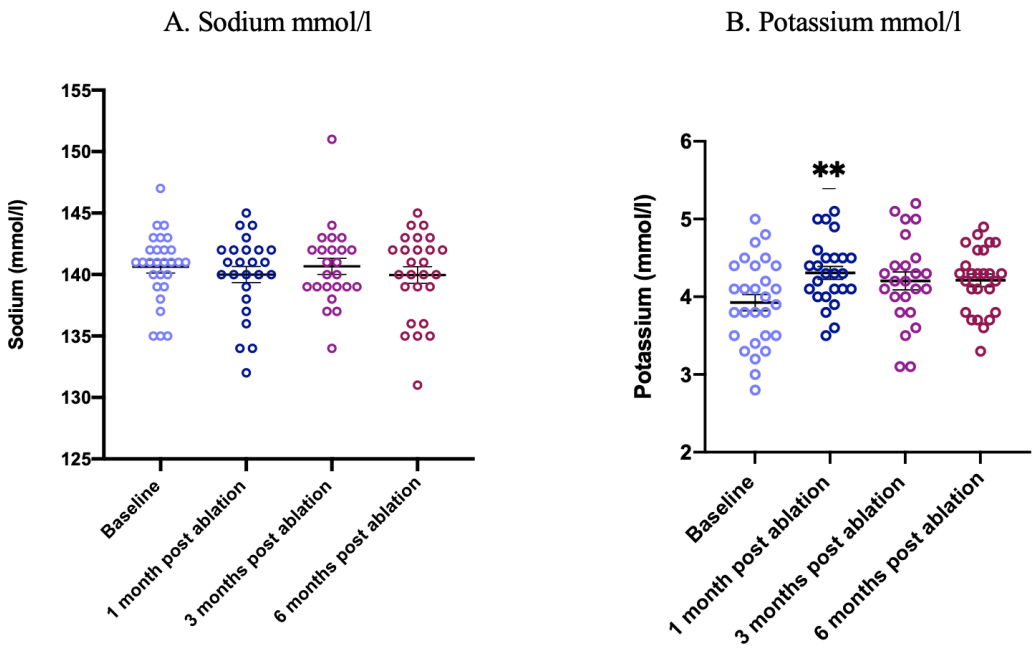

Figure 4 16: A. Graph illustrating the serum sodium mmol/l concentration from baseline to 6 months, no significant change was observed. B. illustrates potassium levels over the course of 6 months. At one month potassium levels were significantly increased (P=0.0045, paired TTEST) from baseline, but no change was observed at 3 or 6 months. (N=24-28)

4.3.5 EUS RFA to left sided APAs leads to an increase in Renin and reduction in aldosterone renin ratio (ARR):

The most important markers for measuring biochemical outcome were renin, aldosterone and therefore the corrected aldosterone renin ratio (ARR). Across the multiple sites renin was often measured with different assays and units. For example, at Barts Hospital renin is measured as activity in nmol/l/hr (PRA), in Cambridge renin mass is measured in mU/L and occasionally renin mass was measured for Barts patients from TDL (The Doctors Laboratory) in London and therefore renin mass was measured in ng/L (pg/ml).

In order to standardise renin, we did the following corrections taken from our much larger study 'MATCH'. [81] We converted all renin's to activity in nmol/l/hr. Firstly renin mass from ng/L was converted to renin mass mU/L by a conversion of 1.67. Then subsequently a conversion factor of 10.989 was used for renin activity (nmol/l/hr) to mass mU/L.

Where there was no 6 months data, 3-month data was used. The data includes final outcomes including 3 months post second ablation data. The normal reference range for PRA is 0.6- 4.3 nmol/l/hr, the normal

reference range for aldosterone: supine: 100 - 450 pmol/L and erect: 100-800 pmol/L. A significant ARR in pmol per nmol/l/hr is a value above 750.

Please note most renin and aldosterone levels were measured on interfering medications at baseline including MRAs, for example diuretics such as amiloride, and patients were even on beta blockers such as bisoprolol. At 6 months two patients remained for medical reasons on MRAs and beta blockers.

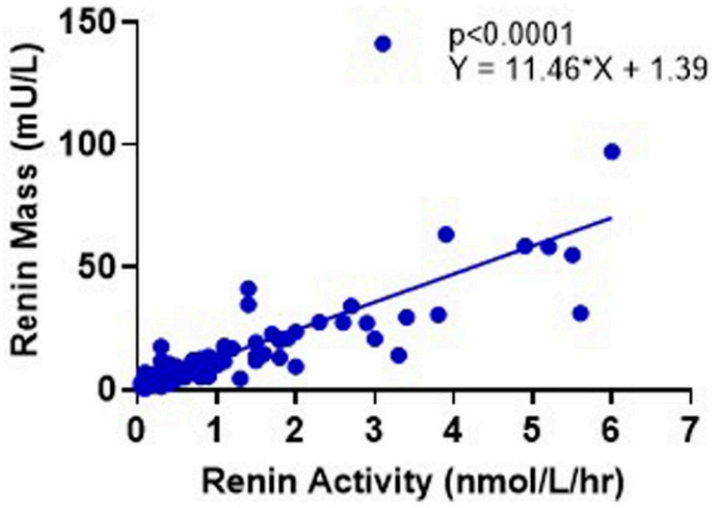

Figure 4 17: Correlation graph between renin mass (mU/L) and renin activity (nmol/l/hr) within Barts patients from the 'MATCH' study. Pearson's correlation r = 0.7851 (95% CI 0.7107 – 0.8422), p < 0.0001 (two-tailed test). ARR thresholds for diagnosing PA: ARRactivity: 1000, ARRmass: 91 (1000/91 = 10.989). n = 136 [81].

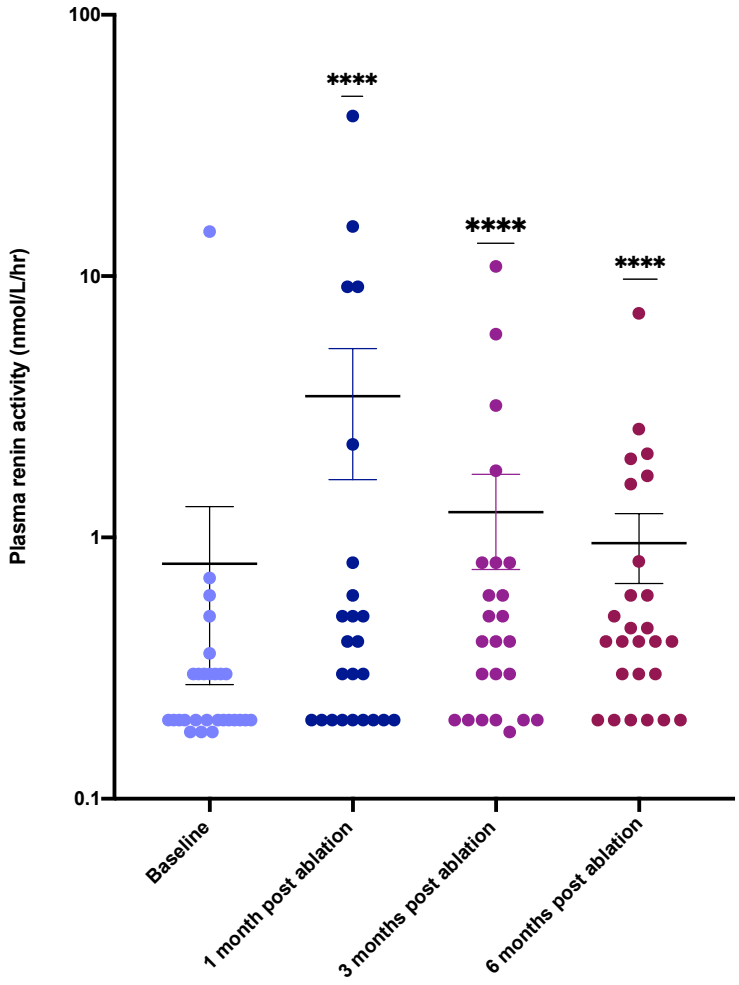

Figure 4 18: Figure illustrating renin activity (nmol/l/hr) at baseline vs ,1, 3, and 6- month post ablation. (P=<0.0001 Wilcoxon signed rank test). This indicates a signficant de-suppresion in renin from baseline. (N=24-28).

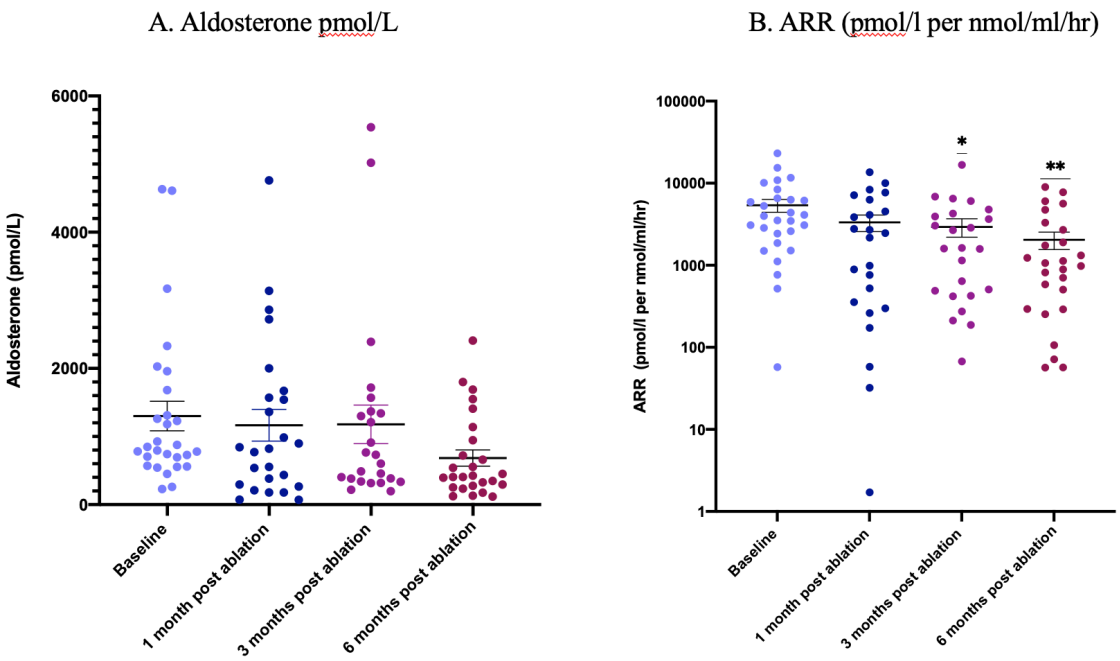

Figure 4 19: A. Graph illustrating Aldosterone (pmol/l) at Baseline vs 1, 3, and 6 months post ablation. B. Scatter dot plot indiciating aldosterone renin ratio calculated with renin activity (pmol/l per nmol/ml/hr) at Baseline vs 1, 3, and 6 months. At 3 months (P=0.027, Wilcoxon signed rank test) and 6 months (P=0.0019, Wilcoxon signed rank test) there is a stastical reduction in ARR. (N=24-28).

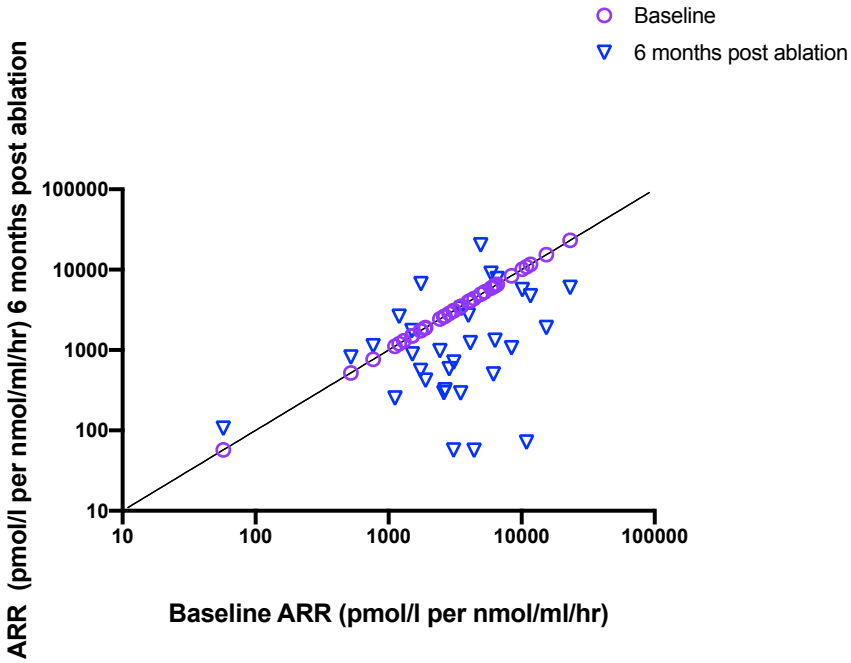

Figure 4 20: A scatter plot diagram illustrating the ARR activity at Baseline vs the 6 months post ablation. (N=24-28). There is a clear reduction in ARR at 6 months. ARR fell from 5379 to 2122.

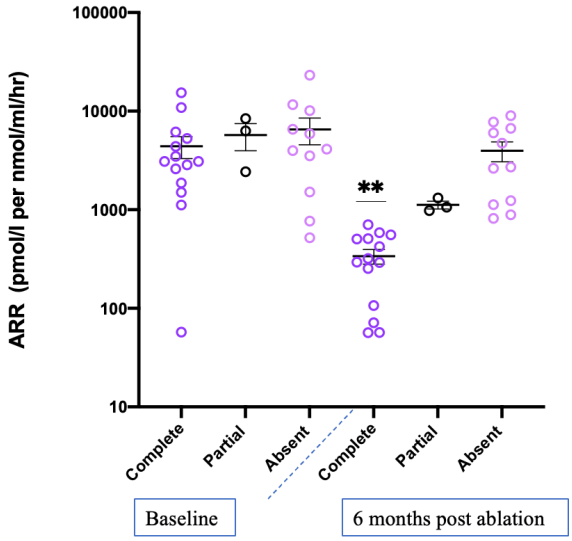

Figure 4 21: Graph illustrating ARR activity separated by those that achieved complete, partial and absent biochemical success comparing baseline vs 6 months post ablation. There was a significant reduction in ARR in the complete group (P=0.0027, paired TTEST) from baseline to 6 months. (N=24-28).

Overall, the renin de-suppressed and the ARR reduced as a consequence, following 35 ablations.

4.3.6: Two EUS RFA to left sided APAs lead to no change in Renin, aldosterone or aldosterone renin ratio (ARR) in this cohort:

As mentioned previously, 7 patients were offered a second ablation during the course of the study. The outcomes of this small cohort were also reviewed separately.

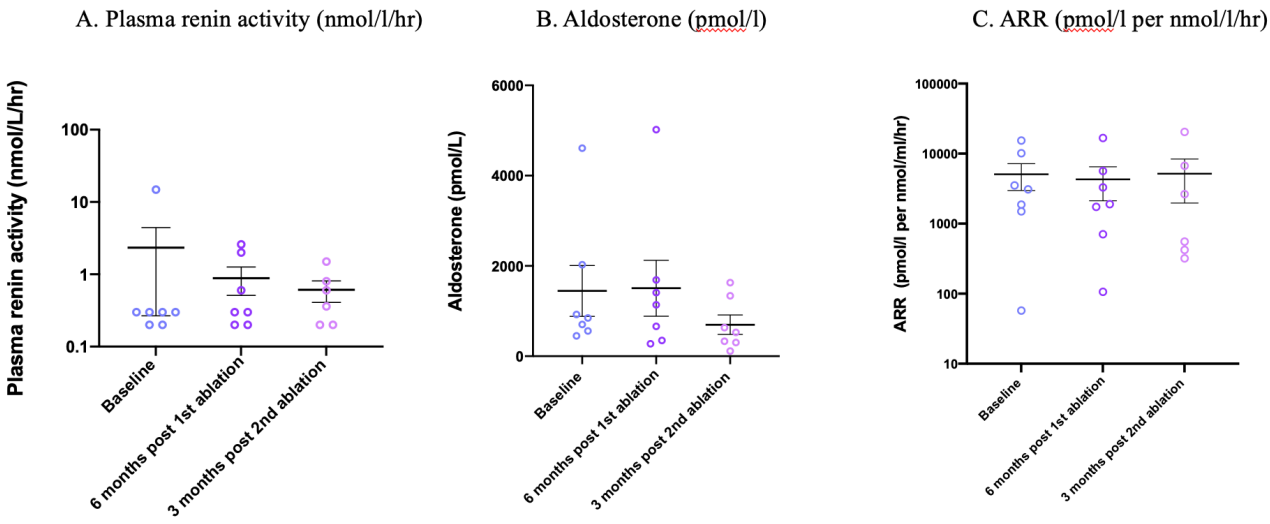

Figure 4 22: A, B and C. indicate graphs of PRA (nmol/l/hr), aldosterone (pmol/l) and ARR activity (pmol per nmol/l/hr) of the 7 patients who underwent two ablations. There was also no change in renin activity, aldosterone or ARR activity. (N=6-7).

4.3.7 Adenoma size and PASO success:

The size of the adenoma was measured at the time of procedure and was compared to clinical and biochemical Success.

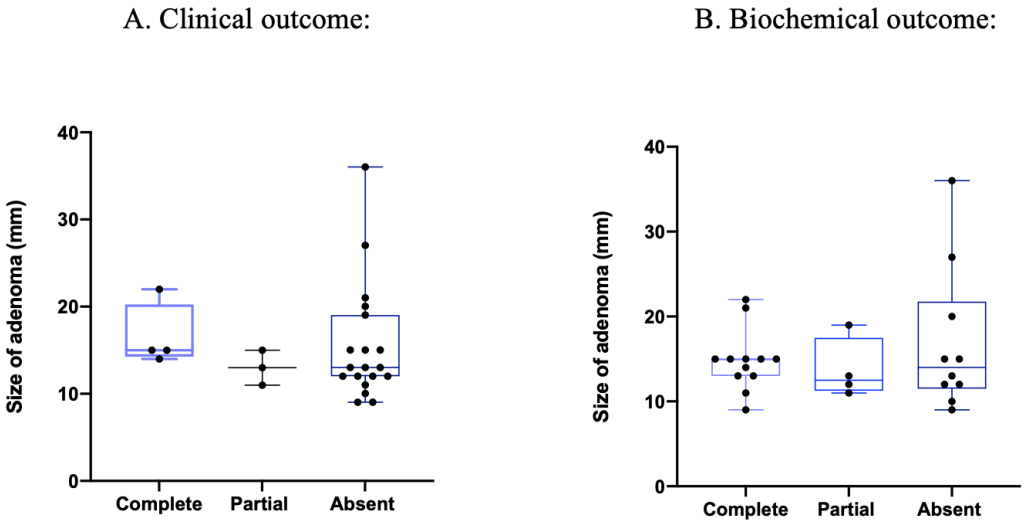

Figure 4 23: A. Size of adenoma compared to clinical success. There was no significance between complete, partial, and absent success, but one could appreciate adenomas that were 1.5- 2cm were more likely to achieve complete clinical success. B. Size of adenoma compared to biochemical success, there was no significant difference, but one could appreciate adenomas between 1.2-1.5 cm were more likely to reach complete biochemical success. The average size of adenoma fell from 13.5 mm pre-ablation to 12mm post ablation.

4.3.8 Number of sequential treatments and PASO success:

The number of sequential treatments administered during the ablation procedures varied. It is clear there was a significant learning curve from the beginning of the study to the end and as more centres and operators became involved.

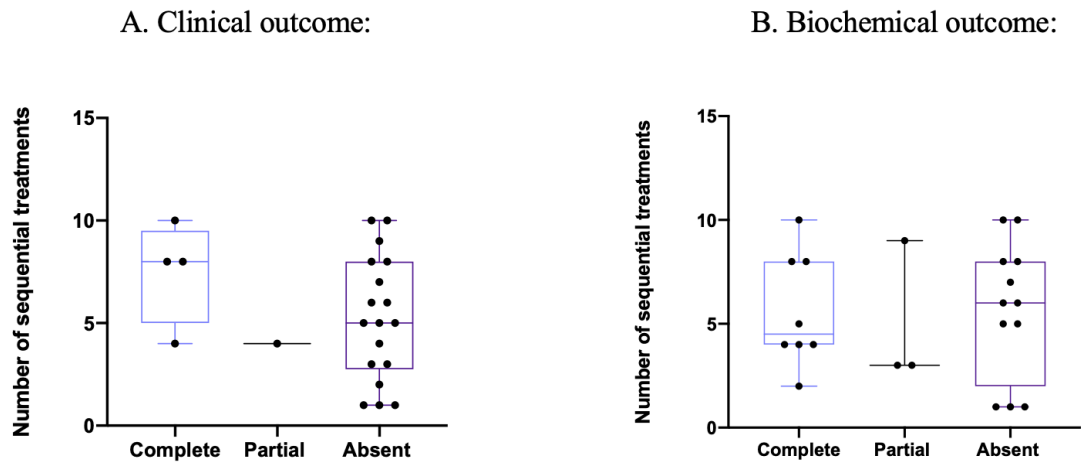

Figure 4 24: A. Clinical success compared to number of sequential treatments, those with > 4 treatments achieved complete clinical success. However, there was no statistical significance. B. Biochemical success compared to number of sequential treatments there seemed to be no difference in complete, partial or absent success.

Patient	Clinical Outcome	Biochemical Outcome	Number of sequential treatments	Clinical Outcome	Biochemical Outcome	Number of sequential treatments
1001	Absent	Absent	1	Absent	Absent	1
1004	Absent	Absent	1	Absent	Complete	1
1005	Absent	Absent	1	Absent	Complete	1
1006	Complete	complete	4			
1008	Absent	Absent	6			
1009	Absent	Absent	7			
1010	Absent	complete	5			
1011	complete	complete	8			
1015	Absent	Absent	10			
1016	Absent	Partial	n/a	Absent	complete	n/a
1017	Partial	Absent	2			
1019	Absent	Complete	4	Absent	Absent	4
1020	Absent	Partial	3			
1021	Absent	Absent	8			
1022	Absent	Absent	8	Absent	Absent	8
1024	Absent	complete	2			
1025	Absent	complete	n/a	n/a	n/a	13
1026	Absent	Absent	6			
1028	Absent	Partial	3			
1029	complete	complete	8			
1031	Absent	Partial	9			
1030	partial	complete	4			
1032	Absent	Absent	10			
1033	complete	complete	10			
2012	Absent	Absent	5			
2013	Absent	Absent	5			
2014	partial	complete	n/a			
2023	partial	complete	n/a			

Table 7: Table illustrating the patients PASO outcomes and the number of sequential treatments they received during the procedure. The first three patients had their first and second ablations before progression to the rest. As the study progressed, patients started to receive more sequential treatments to their adenomas. This could be attributed to operator confidence as the study progressed. n/a= no available data.

4.3.9 EUS RFA to left sided APAs leads to reduction in Defined Daily Dose and number of antihypertensive medications:

Defined daily dose (DDD) and number of antihypertensive medications were reviewed. Medications and doses were documented meticulously at each appointment and where required adjustments were made. Medications were either stopped, titrated down or added in. The DDD was worked out separately by myself and a colleague and then results were compared for maximum accuracy.

4 (14.2%) of patients were on potassium supplementation prior to the procedure and this decreased to 0 (0%) of patients by the end of the study.

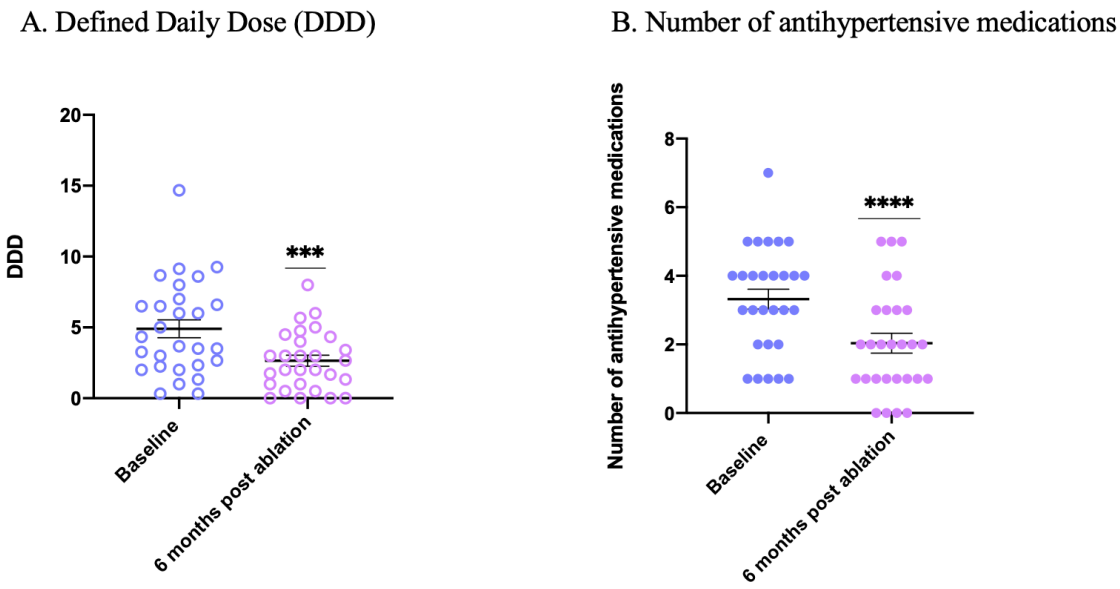

Figure 4 25: A. Graph illustrating DDD at baseline vs 6 months post ablation. There was a significant fall in DDD (P=0.0008, paired TTEST). B. Number of antihypertensive medication from baseline to 6 months post ablation were also reduced significantly (P=<0.0001, Wilcoxon signed rank test). (N=28).

4.3.10 Nuclear medicine scans were instrumental in reviewing outcome post RFA:

27 patients within the study had a pre-procedure molecular medicine scan. 26 performed were ^{11}C metomidate PET scans whilst one patient underwent a pre-procedure ^{18}F CETO scan. The rationale for molecular medicine scans was to aid lateralisation and to provide a road map for the operator at time of ablation. As previously noted, unpublished data strongly points to ^{11}C metomidate and ^{18}F CETO scans being comparable in their efficacy in determining and lateralising APAs. Two patients underwent ^{18}F CETO post first ablation and two following their second ablation. 23 patients underwent ^{11}C metomidate scans post their first ablation and five following their second. One patient opted not to have any scans post ablation.

Scans pre and post ablation were meticulously reviewed at our monthly research MDT by an expert radiologist within the field.

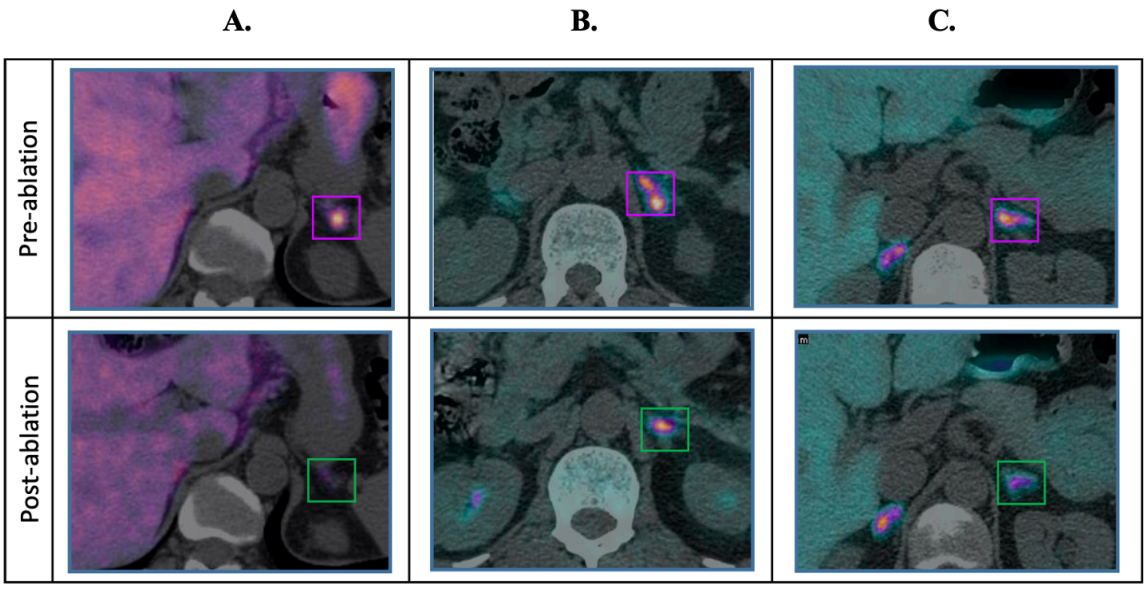

Figure 4 26: Panels indicating ^{11}C metomidate scans pre- and post-ablations. A. illustrates a patient with significant uptake in an APA, with a baseline SUV max ratio left to right of 1.14 and 0.8 3 months, following second ablation. The overall PASO outcome; absent clinical success but complete biochemical success. B. indicates a patient with a baseline SUVmax ratio left to right of 1.62 and 1.04 3 months post ablation. Complete clinical and biochemical success was the outcome. C. illustrates a patient with baseline SUV max ratio left to

right of 1.16 and 1.27 3 months following ablation but now lateralising to the **right**. The outcome was absent clinical and biochemical success. **Images courtesy of Dr Dan Gillet, Cambridge.**

1. SUVmax Ratio Left to Right baseline vs 3 months post ablation:

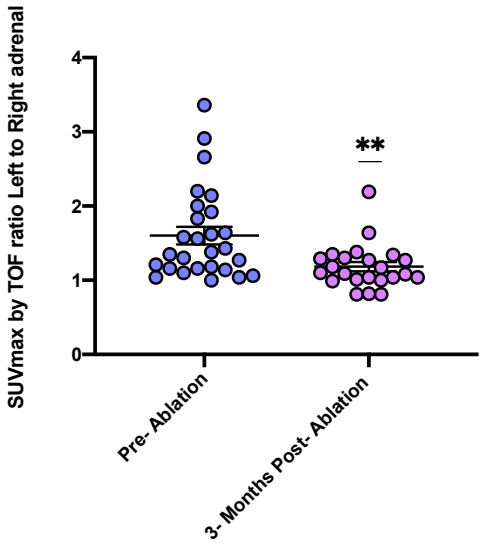

Figure 4 27: Graph indicating a reduction in SUVmax by TOF ratio of Left to right adrenal. It was determined based on previous studies that a ratio cut off of 1.25, signifies lateralisation [80]. 3 months post ablation SUVmax was significantly reduced from baseline (P=0.001, Wilcoxon signed rank test) (N=23-27).

2. SUVmax ratio Left to Right in patients who underwent two ablations:

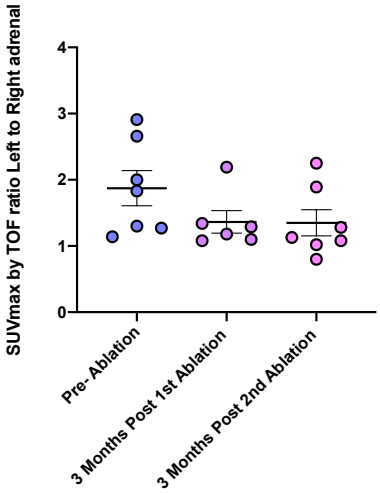

Figure 4 28: Graph illustrating the SUVmax by TOF ratios left to right of the 7 patients who underwent two ablations. A drop in ratio was noted at 3 months post the first ablation, but to no significance.

3. SUVmax by TOF ratio of the active nodule to background adrenal at baseline vs 3-month post ablation:

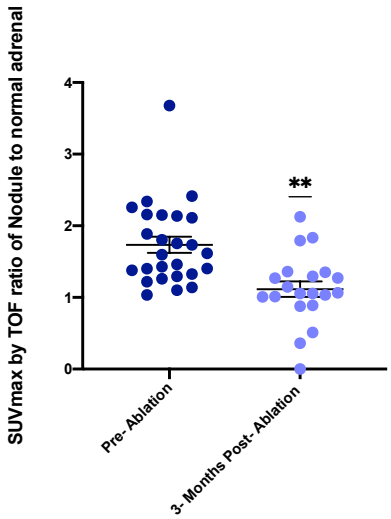

Figure 4 29: Graph looking at SUVmax ratio of the active adenoma to the ipsilateral normal adrenal gland. There was a reduction in ratio in the 3 months post ablation. (P=0.0011, paired TTEST).

4. SUVmax by TOF of left sided APA at baseline vs 3-month post ablation:

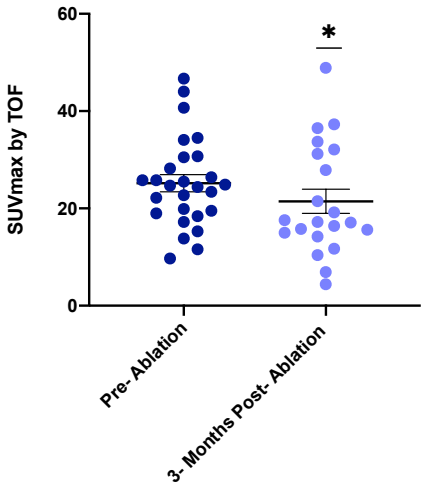

Figure 4 30: Graph illustrating the SUVmax by TOF of left sided APA at baseline vs 3- months post ablation. There was a significant reduction by 3 months of SUVmax by TOF. (P=0.028, paired TTEST).

The molecular imaging outcomes strongly indicate that at the time of intervention, aldosterone producing cells are targeted by the RFA and necrosis of CYP11B2 expressing tissue is likely occurring. The lateralisation ratio has not only decreased significantly compared to the right adrenal gland, but also to the background normal adrenal gland of the left side. The standard uptake value of the isotope also decreased 3 months post ablation. This strengthens the role and value of molecular imaging in RFA.

4.3.11 Urinary electrolytes were unchanged post procedure:

24-hour collections were made of urine at baseline and 6 months post ablation. Volume, 24 -hour urinary sodium, potassium as well as spot urine sodium and potassium were measured.

There have been studies in recent years that have looked at urine sodium and potassium ratios as an alternative to ARR for diagnosis of PA. The physiology of PA leads to a state of increased serum sodium retention, leading to less sodium excreted in urine and more potassium excreted in urine than retained. This is a mild hypernatraemic, hypokalemic state. SUSPUP (serum sodium to urinary sodium to serum potassium to urinary potassium) and SUSPPUP (serum sodium to urinary sodium to (serum potassium)^2 to urinary potassium) are calculations that have been devised as a cheaper and quicker alternative to detect PA. Reference range for SUSPUP is 3.6–22.6 and 0.6–5.3 for SUSPPUP. *Willenberg et al.* found SUSPUP/SUSPPUP results correlated well to ARR [225].

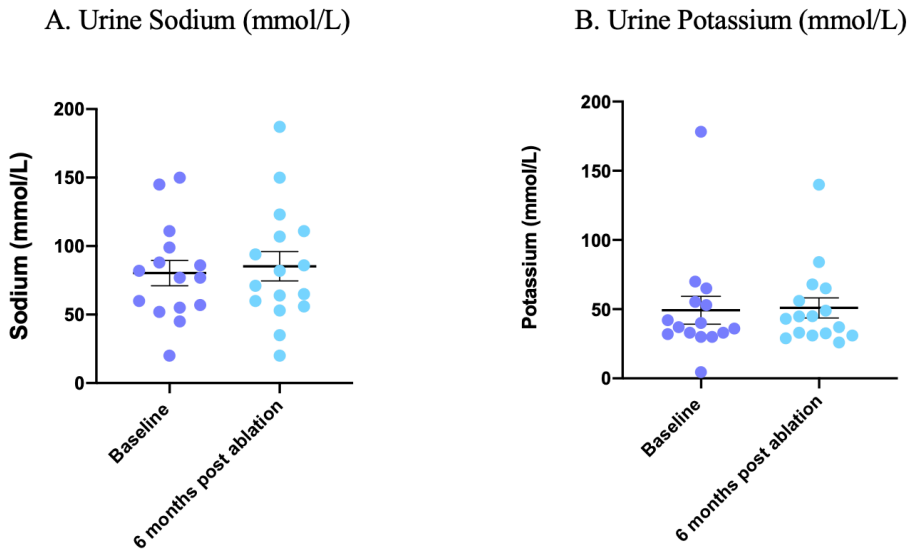

Figure 4 31: A. Graph indicating urine sodium (mmol/l) at baseline vs 6 months post procedure. A slight increase was observed, but was not statistically significant. B. Scatter dot of urine potassium (mmol/l) at baseline vs 6 months post ablation there was no change noted.

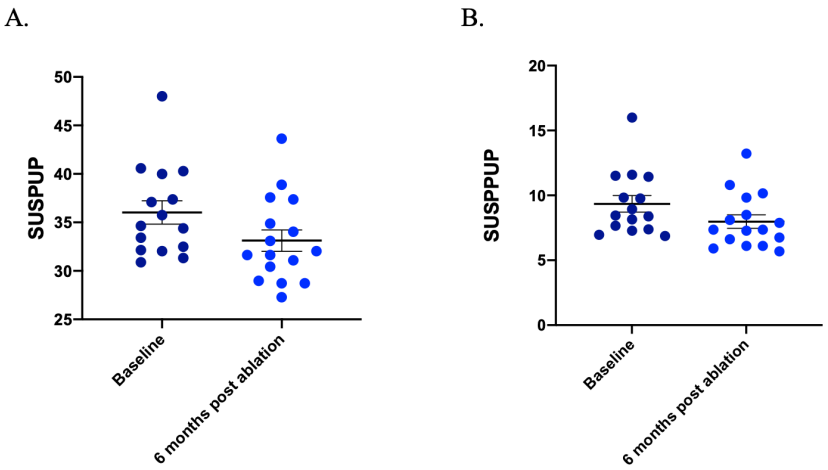

Figure 4 32: A. SUSPUP ratio of patients at baseline vs 6 months post ablation, noted no change. B. SUSPPUP ratio of patients at baseline vs 6 months, noted no change. This did not correlate and was not in keeping with our ARR outcomes within the study.

4.3.12: Histopathology of samples

At the time of procedure an FNA sample was taken and preserved in formalin. These samples underwent staining at CUH in the pathology department. Samples were stained with haematoxylin and Eosin (H and E), CYP11B2, CYP11B1and KCNJ5 antisera.

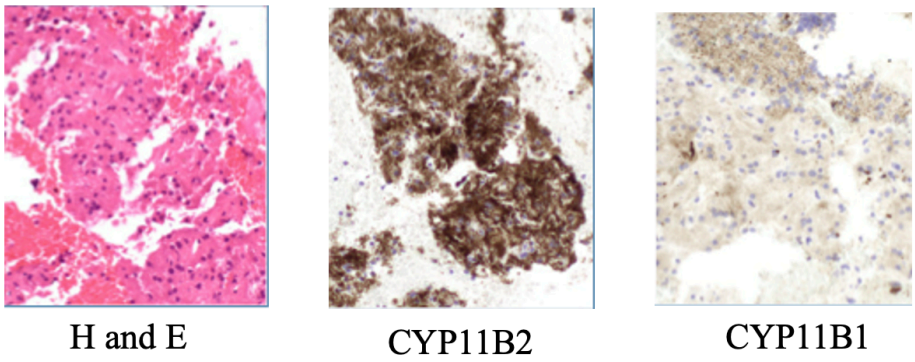

Figure 4 33: Images taking from an FNA biopsy of a study patient at time of RFA. Panel one illustrates H and E staining, in panel 2 dense staining of CYP11B2 is observed and in panel 3 absence of CYP11B1 is appreciated. **Images courtesy of Dr Alison Marker, Cambridge.**

During the course of the study, 13 FNA samples went to CUH to be stained. The degree of staining was reported as strong, medium, and weak by the responsible pathologist and records maintained.

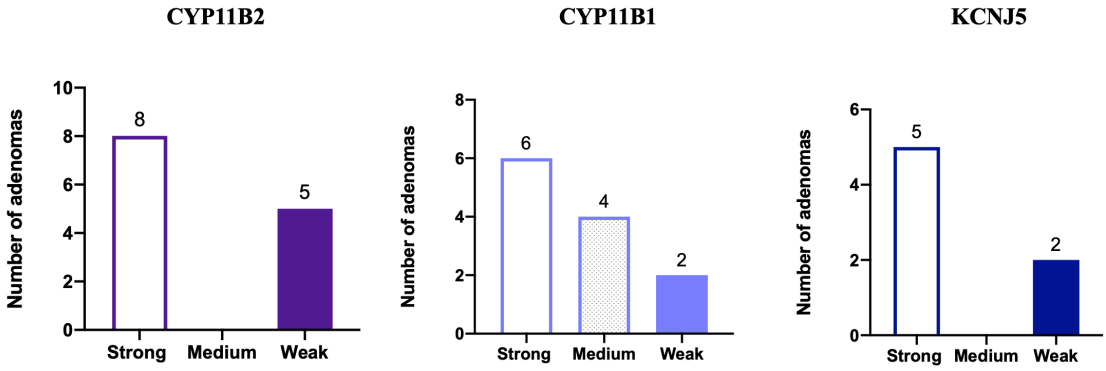

Figure 4 34: Graphs indicating the number of samples who were stained with CYP11B2, CYP11B1 and KCNJ5. The strength of their staining was documented. Some samples stained strongly for CYP11B2 but weakly for CYP11B1 or vice a versa. Some stained strongly for both in keeping with APA histology based on genotype.

4.4 Discussion:

Should the patient consent, the gold standard for a unilateral APA has to date been adrenalectomy. However, in recent years there has been a drive for adrenal cortex sparing thermo-ablation options such as RFA. As this is a benign condition, patients may be reluctant to undergo surgery and the removal of an entire adrenal gland. RFA is appealing to both the patient and healthcare provider, is less invasive, requires less time in hospital and is ultimately less costly.

The complications of laparoscopic adrenalectomy are highlighted in the introduction to this thesis. On the whole, they tend to be rare. Morbidity of laparoscopic adrenalectomy is 6.7-6.8% whilst the mortality rate is <0.5% [92]. Following surgery, patients remain in hospital for up to two to three days. The cost of laparoscopic adrenalectomy to the NHS for each patient is roughly around £3700 [226]. RFA also has a low complication rate and patients are often home one day post procedure. EUS-RFA costs the NHS roughly around £800-1000 pounds per patient (2020/21 National Tariff Payment System).

Surgery, although invasive, does have significant patient benefits. The biochemical success rate is estimated across studies to be 94-100% whilst the clinical success rate varies greatly study to study and has been as low as 22% and as high as 84% [95, 97, 98, 227, 228]. Indicating that some patients benefit from complete clinical and biochemical success post-surgery. Surgery has also proven to be effective with cardiac outcomes. In the 'MATCH' study, N-terminal pro-brain natriuretic peptide (NT-pro BNP) reduced by 31% in patients post adrenalectomy. Natriuretic peptides are readily found within the cardiac wall and are released when there is evidence of heart failure, enabling them to be a well-known cardiac failure marker. This study also indicated a reduction in left ventricular systolic volume (15.8%) and left ventricular end diastolic volume (15.1%) post-surgery. These values seemed to directly correlate with plasma aldosterone levels reduction and illustrate a significant improvement in cardiac function for these patients [81].

All previous RFA studies have been performed percutaneously either to the left or right adrenal gland and were predominantly CT guided. These have been on the whole smaller studies and mostly retrospective. The reports on clinical and biochemical success like adrenalectomy have varied. Complete clinical success has varied from 0-36%, and partial clinical success from 47-71% [101-105, 111], whilst biochemical success in some studies has ranged from 90-100% [101, 102, 229, 230]. It is important to bear in mind that not all these studies strictly used the PASO criteria. These studies however are still promising.

This was the first RFA of APAs study that comprised left sided APA ablation via the endoscopic route under the guidance of an US. This technique of EUS-RFA was previously performed in hepatobiliary pathology such as

liver lesions and most commonly pancreatic conditions both benign and malignant. This procedure offers direct real time visualisation of the adenoma from the end of the endoscope and a clear view of the adenoma and surrounding anatomical structures, giving the operator an advantage over percutaneous methods. However currently it is limited to the left adrenal gland.

In total, 28 patients went through the study. The FABULAS study appealed to many patients. One third of patients were unable to go through the conventional adrenalectomy route due to the perceived risk of their comorbidities or because their unilateral APA diagnosis was ambiguous. Other patients had genuine concerns regarding invasive surgery or had had an unpleasant experience with surgery in the past and opted for it through personal choice.

The primary outcome of this study was safety, and this was achieved. The success of safety was carefully evaluated by an independent safety committee where any adverse or unexpected event was carefully discussed. The predicted adverse events taken from RFA literature such as major haemorrhage, organ infarction and organ perforation did not occur in these 28 patients and 35 RFAs performed. This was scrupulously examined through imaging (non-contrast CT-abdomen), serum analysis of markers, such as haemoglobin and inflammatory markers, and careful examination 24-48 hours post procedure. There were 9 SAEs in total. 3 of these were graded severe in nature and deemed to be procedure related. The grade 3 SAEs ranged from hospital acquired pneumonia, to hypokalaemia induced atrial fibrillation with a fast ventricular rate, to one patient developing a post procedure NSTEMI. These are sadly not unexpected pathologies in a comorbid patient with a long-standing history of PA [9, 10]. All SAEs grade 2-3 and deemed procedure related occurred in patients who were deemed unfit for surgery.

In total, 6 patients required a prolonged in hospital stay. This may initially give the impression that patients remained in hospital for a lengthy stay. However, most cases simply entailed an extra night or two outside of the protocol. The original protocol dictated two nights in hospital for the patient post procedure. Subsequently, after the first 10 patients, with the agreement of the safety committee this requirement was decreased to one night. Two patients required an extra night in hospital outside of protocol, one to be put on a variable rate insulin infusion for pre-procedure diabetes control and the other for pre-renal hydration with intravenous fluids, in order to meet the anaesthetists' requirements. All patients made a full recovery post adverse events that were deemed to be related to the procedure.

We were cautious to mitigate and monitor another significant adverse safety event, namely a hypertensive crisis. There has been a general consensus in recent years within the PA community that alpha and beta blockade prior to RFA of the adrenal gland is good practice [105]. Reports from RFA studies have indicated hypertensive episodes in studies and they ultimately appeared higher (67%) in studies where no alpha and beta blockade was routinely given. In one particular study, however, the adenomas underwent RFA for up to 12 minutes and one can appreciate that the risk of medulla necrosis and catecholamine release would increase significantly over this period of time [111].

Catecholamines have not been previously measured in patients undergoing RFA for APAs or even adrenal lesions but have been carefully monitored in patients undergoing RFA for phaeochromocytomas. This very careful practice involves full beta and alpha blockade, general anaesthetic, nitroprusside drip and catecholamine sampling [231]. In our study, we wanted to assess pre- and post-ablation normetanephrine and metanephrine to see if there was a significant spike following RFA to adenomas, some of which could ultimately be in proximity to the medulla. The results indicated no significant change in metanephrines pre- and intra-operative systolic and diastolic blood pressure. In fact, diastolic blood pressure decreased. There was only one episode of hypertensive crisis during 35 RFAs: the metanephrine level is appreciable on the **Figure 4 9** post ablation as it is significantly elevated. The hypertensive episode was quickly resolved not only by the skill of the experienced anaesthetist but also likely due to the onboard alpha and beta blockade, strengthening the argument for continued use of alpha and beta blockade prior to RFA of the adrenal as a protective measure. 97.2% of cases in this study did not have a hypertensive episode. Future studies may wish to consider, where staffing permits, the same cohort of anaesthetists familiar with the procedure present that are experienced and can readily intervene if necessary.

The secondary outcome of our study was efficacy. In total, we had a complete clinical success rate of 14.3% of patients, and 14.3% of patients with partial clinical success. This percentage is lower than the highest recorded in studies, which was 71%. There was no change in home or clinic blood pressures observed over the six months since baseline. However, four patients came off medications completely and the DDD reduced significantly, as did as the number of antihypertensive medications. All patients on potassium replacement no longer needed supplementation. RFA studies have also pointed to almost halving of either dosing or number of antihypertensive medications following RFA [105, 111, 232]. *Bouhanick et al* in their study however did not

find any change to the DDD over the course of six months [104]. Our patient cohort did not have a significant reduction in blood pressure but there was a significant reduction in their pill burden.

Our patient cohort saw a significant de-suppression of renin, which increased by 50% from baseline by one month post ablation and remained de-suppressed at 6 months post procedure. A reduction in 62% was also seen in ARR by 6 months post ablation, or 3 months post second ablation. This was extremely promising for a novel technique within this field. 50% percent of patients achieved biochemical success within this study, with 10.5 % achieving partial biochemical success.

It must be noted however, renin, aldosterone and ARR samples were all taken on interfering medications, no interfering medications were washed out prior to any samples collected. These results need to be interpreted with caution due to the effect of common antihypertensives on the RAAS. However, it is unclear whether other studies endeavoured to catch a clean ARR post procedure, therefore enabling comparability with previous studies.

This technique had never been performed for APAs before and there was a significant learning curve from the first ablation to the last. During the first three ablations only one treatment was given to the nodule. As the operators became more confident and familiar with the process, more sequential treatments were delivered to adenomas as illustrated in **figure 4 24.** Patients who achieved complete clinical success had >4 sequential treatments. As centres become more proficient and bolder in this procedure, we may see improvement in outcomes.

A crucial guide to ablation success was molecular imaging scans. Previous RFA studies have used scintigraphy and CT scans before and after intervention, but not molecular imaging scans. Patients' scans were meticulously reviewed post ablation. The scans could help us visually to ascertain the reduction in uptake of the isotope by the aldosterone producing cells. Some scans indicated complete reduction whilst others showed reduced or patchy uptake, illustrating the tissue on which the ablation had been performed. In 3 scans, patients lost complete uptake on the left side, but the right side seemed to awaken, leading to lateralisation to the right. The SUVmax ratio left to right significantly reduced in the cohort post ablation (P=0.001). There was also significant reduction in the SUVmax of the adenoma compared to its background adrenal (P=0.0011). These outcomes illustrate the effectiveness of the procedure at targeting aldosterone secreting tissue.

We now know of the presence of adrenal producing micronodules (APMs) within adrenal glands. They are not only found in bilateral disease but may also be present in unilateral disease and may be the most dominant aldosterone auto secreter even if they lie next to an adenoma [233, 234]. Our molecular imaging guided the operator to the most dominant aldosterone secreting nodule to be targeted. However, for good measure if more than one adenoma was visualised all adenomas underwent treatment, where possible. We must also accept that when an adenoma is targeted there may be a micronodule ready to take over the aldosterone secretion either on the same side or contralateral side. This may affect clinical and biochemical success. In a very comorbid patient deemed not fit for surgery, EUS-RFA could have a role in debulking of disease if not cure. A reduction in disease burden would allow patients the possibility of reduced pill burden but not guaranteed cure.

This study did not assess whether EUS RFA led to improved cardiac outcomes either with cardiac MRI or heart failure markers such as NT-Pro BNP. On the results obtained, it is therefore difficult to know whether in this comorbid patient group the cardiac disease burden may have reduced.

During this study we were able to roll out this procedure into three centres with four different operators in a relatively short amount of working time. The study's active time had been delayed significantly due to the pandemic but, when possible, progress was made to set up the procedure in more centres. The skill of endoscopic ultrasound is taught and well within the remit of the training of a gastroenterologist, upper gastro-intestinal surgeon and occasionally radiologist. All often becoming proficient by the end of their training. Endoscopic RFA fellowships often add on a year or two of extra training. Laparoscopic adrenalectomy however, often requires the surgeon to learn advanced laparoscopic surgical techniques, and this can take a lengthy amount of time and involves a steep learning curve [101]. Increasingly, surgical centres are performing fewer adrenalectomies per year, raising concerns of deskilling and the reliance on centres who perform more, therefore, restricting patients' hospital choice. Looking to the future of work force planning and cost savings in an already overstretched understaffed system, the operators of EUS-RFA in the right patient group could offer this service as a viable and cost saving service in multiple centres.

In conclusion this study achieved its ultimate outcome, demonstrating that EUS guided RFA to left adrenal APAs is a safe procedure. It also had a modest effect upon efficacy, indicating that it is a viable alternative to laparoscopic adrenalectomy.

4.5 Future work:

In our FABULAS study FNA samples were also collected, on which to perform RNA sequencing and genotyping. Unfortunately, time towards the end of the study was insufficient to allow me to extract RNA from them, but this would have been an invaluable source of information. PASO outcomes could have been compared to genotype. I could also have determined along with histology, the expression of genes such as *CYP11B2* and *CYP11B1*.

Our study only followed up patients to a maximum of 6 months post ablation. However, these patients are still routinely being seen in clinic. It will be insightful to follow, in particular, those that have been completely or partially cured over a prolonged period of time to see their final outcome.

It would have also been interesting to extend the FABULAS study to enable centres to perform more EUS-RFAs and to gain more experience before future trials. UCLH performed 24 RFAs, CUH 7 RFAs and Barts Health 4. As the next study is already in progress (described in the final discussion) it will likely compare EUS-RFA and percutaneous RFA to some extent. Increasing the patient cohort would also have allowed us to determine which patients do best with RFA and those who do not and may benefit from surgery or long-term medical therapy.

Chapter 5:

Overall Discussion and The Future

The progress achieved within the field of PA over the last half century since its discovery in a Michigan clinic has been commendable. Advocates for this condition have managed to raise awareness and bring it to the forefront of the differential diagnosis. Indeed, PA was once thought to be so rare that, until recent years, <1% was ever diagnosed. PA clinical research groups have endeavoured to better understand its pathophysiology and genetics, the latter through landmark WES studies. The ultimate goal is to streamline investigations and treatment for the increasing PA burden arriving on the physician's doorstep. This so-called 'PA epidemic' has been long debated, but evidence points to increasing diagnoses of the condition. The care and services now required are likely to include early detection of disease, viable biomarkers for genetic type detection, and treatment catered for the individual. In the last few years, efforts have been increased to search for relevant biomarkers for early detection of PA, including biomarkers, such as extracellular vesicles, microRNAs and proteomics. Whilst they could play a role in disease diagnosis, they cannot yet inform us of the subtype [235, 236].

By way of example, we know that *KCNJ5* mutations have high 18OH (18-Hydroxycorticosterone) urinary steroids, which can be easily detected at diagnosis. These patients do extremely well post adrenalectomy. They may also perform well with RFA as they tend to have solitary lesions [81]. Early identification of *KCNJ5* mutants could streamline that patient's pathway straight to surgery with confidence of a good outcome. The same could be said for the non-ion channel mutations, such as our *GNA11Q/CTNNB1* and *CADM-1* mutants. If biomarkers could be found for these mutations, we would know that affected patients would greatly benefit from adrenalectomy.

The first part of my thesis focused on a unique double mutation within PA - *GNA11/Q* and *CTNNB1*. *A*lthough rare, it has shed light on a number of outstanding questions, including: why were these patients so unlike previous *CTNNB1* sole mutants who presented sporadically, not at times of high LH/HCG surge? And why was their clinical and biochemical cure rate 100% compared to sole mutants? Uncovering a larger cohort of these patients, along with clinical data and tissue, has been invaluable. We have illustrated the presence of two co-driving mutations, a rare phenomenon in PA. The double mutation is essential for LHCGR expression in these adenomas, in aldosterone production, and in the rise of unique markers such as TMEM132E. TMEM132E is a protein that clearly has a role to play in PA. I have demonstrated that nAChRs are present within these adenomas and are likely involved in aldosterone production. However, further research will now be required to explain why they are there in adrenal cortical tissue when they have never been described there before. The

‘double mutants’ also expressed high levels of unusual proteins not seen previously in other APAs, for example TMEM132E and SLC35F1. These are typical neuronal markers not usually seen in cortex cells. *CADM-1* mutations also express TMEM132E, but it would be interesting to review the other non-ion channel mutations to see if they also express neuronal tissue markers. Could TMEM132E and SLC35F1 be the much-needed biomarkers in the peripheral bloodstream that could facilitate early detection? And, if nicotinic acetylcholine receptors were also present in other adenomas, could these be explored as a viable therapeutic target?

The majority of the patients in our double mutant cohort presented in pregnancy. There has yet to be a general consensus on the work up of pregnancy in PA. Fewer than 80 cases of PA in pregnancy have ever been reported, suggesting heavily lots of women are going underdiagnosed [129]. This is concerning as in the literature more cases of Cushing’s and phaeochromocytomas have been reported in pregnancy, yet they are rarer in the background population than PA [237] [238]. Most patients in PA are likely being missed. One solitary blood pressure is done in the first trimester and no booking electrolyte bloods are performed. PA will most likely present before 20 weeks, after which gestational causes of hypertension occur, such as gestational hypertension and pre-eclampsia. Presentation of PA varies in pregnancy, from improvement in blood pressure due to physiological changes incurred in pregnancy (progesterone mitigating the aldosterone effect), to the other end of the spectrum with severe hypertension and hypokalaemia. This poses a significant risk to both maternal and foetal well-being. During the course of my thesis, various units across the country contacted me having diagnosed PA in pregnancy, on the basis that our unit had a special interest. One of our team also retrospectively reviewed hypertension antenatal clinics at Barts Health. 158 patients with chronic hypertension were compared to 12 women with post-partum PA. It was discovered that patients with PA had a higher sodium, >140 mmol/l, during their first and third trimester compared to controls. A sodium level of 140 mmol/l and over predicted post- partum PA by 87%. (**Abstract for The International Society of Obstetric Medicine (ISOM) Congress 2022 by Dr Adeela Ashraf, Hypertension and Serum Sodium Concentrations Above 140mmol/L in Pregnancy as a Predictor of Primary Aldosteronism).**

As to future work, I would propose that a prospective study is undertaken involving pregnant women, in order to devise a suitable screening process. This could measure electrolytes or blood pressure so that PA in pregnant women is not missed. This would not only be important for maternal-foetal outcomes, but would also avoid the rebound effect that can occur post-delivery, whereby without the protective progesterone a severe form of PA is unmasked.

If PA were diagnosed in pregnancy, double mutant serum markers such as TMEM132E may be able to provide a genetic diagnosis, and therefore allow safe treatment to be tailored to the patient.

The second part of my thesis focused on a novel thermo-ablative method for left sided APAs, and its safety and efficacy. For many years, a large prospective head-to-head trial of RFA against surgery has been required to compare these two treatment modalities. Excitingly, our research group has already begun recruitment for such a study, called the 'WAVE' study. **WAVE** is a prospective randomised trial comparing radiofrequency ablation **W**ith laparoscopic **A**drenalectomy as an alternati**VE** treatment for unilateral asymmetric primary aldosteronism; ClinicalTrials.gov Identifier: NCT05405101. The aim is to recruit 110 patients over 5 centres. Patients will have to have a diagnosis of unilateral disease and they will be randomised either to surgery or RFA. Left sided RFAs will be performed via the EUS route, and right sided through the CT guided percutaneous route. This study will also answer a critical question: even if we were not to cure the patient of their PA, could their cardiac burden be reduced through RFA? This study will offer a longer follow up period of 1 year.

Within the next couple of years, we expect the diagnosis of PA to rise. If RFA were to match surgery in this study, it would become a more accessible and more cost-effective treatment option. Should the outcome of this study lend superiority to surgery, there would still be a role for EUS-RFA, particularly in patients who may pursue EUS-RFA due to comorbidities dictating surgical caution or those where the diagnosis of unilateral disease is ambiguous. EUS-RFA could also offer a role in the debulking of disease for those that have bilateral disease, but where clear molecular scan avid nodules are seen.

In my thesis, I have sought to illustrate the importance of understanding this condition on a molecular genetic level and the translational value that it holds, as well as the importance of clinical assessment and exploration of novel treatment methods, particularly less invasive adreno-cortex sparing.

References:

1. Funder, J.W., et al., *The Management of Primary Aldosteronism: Case Detection, Diagnosis, and Treatment: An Endocrine Society Clinical Practice Guideline.* J Clin Endocrinol Metab, 2016. **101**(5): p. 1889-916.
2. Collaborators, G.B.D.R.F., *Global, regional, and national comparative risk assessment of 79 behavioural, environmental and occupational, and metabolic risks or clusters of risks, 1990-2015: a systematic analysis for the Global Burden of Disease Study 2015.* Lancet, 2016. **388**(10053): p. 1659-1724.
3. Brown, M.J. and S. Haydock, *Pathoaetiology, epidemiology and diagnosis of hypertension.* Drugs, 2000. **59 Suppl 2**: p. 1-12; discussion 39-40.
4. Mills, K.T., A. Stefanescu, and J. He, *The global epidemiology of hypertension.* Nat Rev Nephrol, 2020. **16**(4): p. 223-237.
5. Oparil, S., et al., *Hypertension.* Nat Rev Dis Primers, 2018. **4**: p. 18014.
6. Klionsky, D.J., et al., *Guidelines for the use and interpretation of assays for monitoring autophagy (3rd edition).* Autophagy, 2016. **12**(1): p. 1-222.
7. Conn, J.W., *Presidential address. I. Painting background. II. Primary aldosteronism, a new clinical syndrome.* J Lab Clin Med, 1955. **45**(1): p. 3-17.
8. Sonino, N., et al., *Psychological assessment of primary aldosteronism: a controlled study.* J Clin Endocrinol Metab, 2011. **96**(6): p. E878-83.
9. Milliez, P., et al., *Evidence for an increased rate of cardiovascular events in patients with primary aldosteronism.* J Am Coll Cardiol, 2005. **45**(8): p. 1243-8.
10. Monticone, S., et al., *Cardiovascular events and target organ damage in primary aldosteronism compared with essential hypertension: a systematic review and meta-analysis.* Lancet Diabetes Endocrinol, 2018. **6**(1): p. 41-50.
11. Stehr, C.B., et al., *Increased levels of oxidative stress, subclinical inflammation, and myocardial fibrosis markers in primary aldosteronism patients.* J Hypertens, 2010. **28**(10): p. 2120-6.
12. Megha, R., et al., *Anatomy, Abdomen and Pelvis, Adrenal Glands (Suprarenal Glands)*, in *StatPearls*. 2022: Treasure Island (FL).
13. Kopf, P.G., et al., *Angiotensin II regulates adrenal vascular tone through zona glomerulosa cell-derived EETs and DHETs.* Hypertension, 2011. **57**(2): p. 323-9.
14. Vinson, G.P., *Functional Zonation of the Adult Mammalian Adrenal Cortex.* Front Neurosci, 2016. **10**: p. 238.
15. Monticone, S., R.J. Auchus, and W.E. Rainey, *Adrenal disorders in pregnancy.* Nat Rev Endocrinol, 2012. **8**(11): p. 668-78.

16. Tait, S.A., J.F. Tait, and J.P. Coghlan, *The discovery, isolation and identification of aldosterone: reflections on emerging regulation and function.* Mol Cell Endocrinol, 2004. **217**(1-2): p. 1-21.
17. Munoz-Durango, N., et al., *Role of the Renin-Angiotensin-Aldosterone System beyond Blood Pressure Regulation: Molecular and Cellular Mechanisms Involved in End-Organ Damage during Arterial Hypertension.* Int J Mol Sci, 2016. **17**(7).
18. Peti-Peterdi, J. and R.C. Harris, *Macula densa sensing and signaling mechanisms of renin release.* J Am Soc Nephrol, 2010. **21**(7): p. 1093-6.
19. Peti-Peterdi, J., *Newly stemming functions of macula densa-derived prostanoids.* Hypertension, 2015. **65**(5): p. 987-8.
20. El Ghorayeb, N., I. Bourdeau, and A. Lacroix, *Role of ACTH and Other Hormones in the Regulation of Aldosterone Production in Primary Aldosteronism.* Front Endocrinol (Lausanne), 2016. **7**: p. 72.
21. Spat, A. and L. Hunyady, *Control of aldosterone secretion: a model for convergence in cellular signaling pathways.* Physiol Rev, 2004. **84**(2): p. 489-539.
22. Hattangady, N.G., et al., *Acute and chronic regulation of aldosterone production.* Mol Cell Endocrinol, 2012. **350**(2): p. 151-62.
23. Craig, M., S.N.S. Yarrarapu, and M. Dimri, *Biochemistry, Cholesterol*, in *StatPearls*. 2022: Treasure Island (FL).
24. Arakane, F., et al., *Steroidogenic acute regulatory protein (StAR) retains activity in the absence of its mitochondrial import sequence: implications for the mechanism of StAR action.* Proc Natl Acad Sci U S A, 1996. **93**(24): p. 13731-6.
25. Ogishima, T., F. Mitani, and Y. Ishimura, *Isolation of aldosterone synthase cytochrome P-450 from zona glomerulosa mitochondria of rat adrenal cortex.* J Biol Chem, 1989. **264**(19): p. 10935-8.
26. Singh, K.D. and S.S. Karnik, *Angiotensin Receptors: Structure, Function, Signaling and Clinical Applications.* J Cell Signal, 2016. **1**(2).
27. Fridmanis, D., A. Roga, and J. Klovins, *ACTH Receptor (MC2R) Specificity: What Do We Know About Underlying Molecular Mechanisms?* Front Endocrinol (Lausanne), 2017. **8**: p. 13.
28. Romero, D.G., et al., *Angiotensin II-mediated protein kinase D activation stimulates aldosterone and cortisol secretion in H295R human adrenocortical cells.* Endocrinology, 2006. **147**(12): p. 6046-55.
29. Gomez-Sanchez, C.E., et al., *Development of monoclonal antibodies against human CYP11B1 and CYP11B2.* Mol Cell Endocrinol, 2014. **383**(1-2): p. 111-7.
30. Muto, S., *Action of aldosterone on renal collecting tubule cells.* Curr Opin Nephrol Hypertens, 1995. **4**(1): p. 31-40.
31. Connell, J.M. and E. Davies, *The new biology of aldosterone.* J Endocrinol, 2005. **186**(1): p. 1-20.
32. Booth, R.E., J.P. Johnson, and J.D. Stockand, *Aldosterone.* Adv Physiol Educ, 2002. **26**(1-4): p. 8-20.
33. Garty, H., et al., *A functional interaction between CHIF and Na-K-ATPase: implication for regulation by FXYD proteins.* Am J Physiol Renal Physiol, 2002. **283**(4): p. F607-15.
34. Funder, J.W., *Aldosterone and Mineralocorticoid Receptors-Physiology and Pathophysiology.* Int J Mol Sci, 2017. **18**(5).

35. Chapman, K., M. Holmes, and J. Seckl, *11beta-hydroxysteroid dehydrogenases: intracellular gate-keepers of tissue glucocorticoid action.* Physiol Rev, 2013. **93**(3): p. 1139-206.
36. Bauersachs, J., F. Jaisser, and R. Toto, *Mineralocorticoid receptor activation and mineralocorticoid receptor antagonist treatment in cardiac and renal diseases.* Hypertension, 2015. **65**(2): p. 257-63.
37. Xing, Y., et al., *Development of adrenal cortex zonation.* Endocrinol Metab Clin North Am, 2015. **44**(2): p. 243-74.
38. Luo, X., Y. Ikeda, and K.L. Parker, *A cell-specific nuclear receptor is essential for adrenal and gonadal development and sexual differentiation.* Cell, 1994. **77**(4): p. 481-90.
39. Achermann, J.C., et al., *A mutation in the gene encoding steroidogenic factor-1 causes XY sex reversal and adrenal failure in humans.* Nat Genet, 1999. **22**(2): p. 125-6.
40. Ishimoto, H. and R.B. Jaffe, *Development and function of the human fetal adrenal cortex: a key component in the feto-placental unit.* Endocr Rev, 2011. **32**(3): p. 317-55.
41. Goto, M., et al., *In humans, early cortisol biosynthesis provides a mechanism to safeguard female sexual development.* J Clin Invest, 2006. **116**(4): p. 953-60.
42. Mesiano, S., *Roles of estrogen and progesterone in human parturition.* Front Horm Res, 2001. **27**: p. 86-104.
43. Scott, H.M., J.I. Mason, and R.M. Sharpe, *Steroidogenesis in the fetal testis and its susceptibility to disruption by exogenous compounds.* Endocr Rev, 2009. **30**(7): p. 883-925.
44. Del Valle, I., et al., *A genomic atlas of human adrenal and gonad development.* Wellcome Open Res, 2017. **2**: p. 25.
45. Unger, N., et al., *Comparison of active renin concentration and plasma renin activity for the diagnosis of primary hyperaldosteronism in patients with an adrenal mass.* Eur J Endocrinol, 2004. **150**(4): p. 517-23.
46. Morganti, A. and L.D.R.A. European study group for the validation of DiaSorin, *A comparative study on inter and intralaboratory reproducibility of renin measurement with a conventional enzymatic method and a new chemiluminescent assay of immunoreactive renin.* J Hypertens, 2010. **28**(6): p. 1307-12.
47. Cinquanta, L., D.E. Fontana, and N. Bizzaro, *Chemiluminescent immunoassay technology: what does it change in autoantibody detection?* Auto Immun Highlights, 2017. **8**(1): p. 9.
48. Burrello, J., et al., *Diagnostic accuracy of aldosterone and renin measurement by chemiluminescent immunoassay and radioimmunoassay in primary aldosteronism.* J Hypertens, 2016. **34**(5): p. 920-7.
49. Young, W.F., Jr., *Minireview: primary aldosteronism--changing concepts in diagnosis and treatment.* Endocrinology, 2003. **144**(6): p. 2208-13.
50. Tiu, S.C., et al., *The use of aldosterone-renin ratio as a diagnostic test for primary hyperaldosteronism and its test characteristics under different conditions of blood sampling.* J Clin Endocrinol Metab, 2005. **90**(1): p. 72-8.
51. Terata, S., et al., *Plasma renin activity and the aldosterone-to-renin ratio are associated with the development of chronic kidney disease: the Ohasama Study.* J Hypertens, 2012. **30**(8): p. 1632-8.

52. Kisaka, T., et al., *Association of elevated plasma aldosterone-to-renin ratio with future cardiovascular events in patients with essential hypertension.* J Hypertens, 2012. **30**(12): p. 2322-30.
53. Mulatero, P., et al., *Diagnosis of primary aldosteronism: from screening to subtype differentiation.* Trends Endocrinol Metab, 2005. **16**(3): p. 114-9.
54. Mulatero, P., et al., *Comparison of confirmatory tests for the diagnosis of primary aldosteronism.* J Clin Endocrinol Metab, 2006. **91**(7): p. 2618-23.
55. Giacchetti, G., et al., *Analysis of screening and confirmatory tests in the diagnosis of primary aldosteronism: need for a standardized protocol.* J Hypertens, 2006. **24**(4): p. 737-45.
56. Mulatero, P., et al., *Captopril test can give misleading results in patients with suspect primary aldosteronism.* Hypertension, 2007. **50**(2): p. e26-7.
57. Kidoguchi, S., et al., *The characteristics of captopril challenge test-positive patients using various criteria.* J Renin Angiotensin Aldosterone Syst, 2019. **20**(3): p. 1470320319870891.
58. Blake, M.A., C.G. Cronin, and G.W. Boland, *Adrenal imaging.* AJR Am J Roentgenol, 2010. **194**(6): p. 1450-60.
59. Young, W.F., et al., *Role for adrenal venous sampling in primary aldosteronism.* Surgery, 2004. **136**(6): p. 1227-35.
60. Kempers, M.J., et al., *Systematic review: diagnostic procedures to differentiate unilateral from bilateral adrenal abnormality in primary aldosteronism.* Ann Intern Med, 2009. **151**(5): p. 329-37.
61. Dekkers, T., et al., *Adrenal vein sampling versus CT scan to determine treatment in primary aldosteronism: an outcome-based randomised diagnostic trial.* Lancet Diabetes Endocrinol, 2016. **4**(9): p. 739-746.
62. Quencer, K.B., *Adrenal vein sampling: technique and protocol, a systematic review.* CVIR Endovasc, 2021. **4**(1): p. 38.
63. Funder, J.W., et al., *Case detection, diagnosis, and treatment of patients with primary aldosteronism: an endocrine society clinical practice guideline.* J Clin Endocrinol Metab, 2008. **93**(9): p. 3266-81.
64. Allolio, B. and M. Fassnacht, *Clinical review: Adrenocortical carcinoma: clinical update.* J Clin Endocrinol Metab, 2006. **91**(6): p. 2027-37.
65. Ota, H., et al., *Dynamic multidetector CT and non-contrast-enhanced MR for right adrenal vein imaging: comparison with catheter venography in adrenal venous sampling.* Eur Radiol, 2016. **26**(3): p. 622-30.
66. Miotto, D., et al., *Impact of accessory hepatic veins on adrenal vein sampling for identification of surgically curable primary aldosteronism.* Hypertension, 2009. **54**(4): p. 885-9.
67. Monticone, S., et al., *Adrenal vein sampling in primary aldosteronism: towards a standardised protocol.* Lancet Diabetes Endocrinol, 2015. **3**(4): p. 296-303.
68. Weinberger, M.H., et al., *Primary aldosteronism: diagnosis, localization, and treatment.* Ann Intern Med, 1979. **90**(3): p. 386-95.
69. Rossitto, G., et al., *Subtyping of Primary Aldosteronism in the AVIS-2 Study: Assessment of Selectivity and Lateralization.* J Clin Endocrinol Metab, 2020. **105**(6).
70. Seccia, T.M., et al., *Adrenocorticotropic hormone stimulation during adrenal vein sampling for identifying surgically curable subtypes of primary aldosteronism: comparison of 3 different protocols.* Hypertension, 2009. **53**(5): p. 761-6.

71. Monticone, S., et al., *Effect of adrenocorticotropic hormone stimulation during adrenal vein sampling in primary aldosteronism.* Hypertension, 2012. **59**(4): p. 840-6.
72. Ye, P., et al., *Regulation of aldosterone synthase gene expression in the rat adrenal gland and central nervous system by sodium and angiotensin II.* Endocrinology, 2003. **144**(8): p. 3321-8.
73. Tang, L., et al., *Clinical Characteristics of Aldosterone- and Cortisol-Coproducing Adrenal Adenoma in Primary Aldosteronism.* Int J Endocrinol, 2018. **2018**: p. 4920841.
74. Piaditis, G.P., et al., *High prevalence of autonomous cortisol and aldosterone secretion from adrenal adenomas.* Clin Endocrinol (Oxf), 2009. **71**(6): p. 772-8.
75. Hiraishi, K., et al., *Clinicopathological features of primary aldosteronism associated with subclinical Cushing's syndrome.* Endocr J, 2011. **58**(7): p. 543-51.
76. Dekkers, T., et al., *Plasma metanephrine for assessing the selectivity of adrenal venous sampling.* Hypertension, 2013. **62**(6): p. 1152-7.
77. Stowasser, M., *Improving the success and reliability of adrenal venous sampling: focus on intraprocedural cortisol measurement.* Clin Chem, 2012. **58**(9): p. 1275-7.
78. Vilela, L.A.P., et al., *KCNJ5 Somatic Mutation Is a Predictor of Hypertension Remission After Adrenalectomy for Unilateral Primary Aldosteronism.* J Clin Endocrinol Metab, 2019. **104**(10): p. 4695-4702.
79. Bergstrom, M., et al., *In vitro and in vivo primate evaluation of carbon-11-etomidate and carbon-11-metomidate as potential tracers for PET imaging of the adrenal cortex and its tumors.* J Nucl Med, 1998. **39**(6): p. 982-9.
80. Burton, T.J., et al., *Evaluation of the sensitivity and specificity of (11)C-metomidate positron emission tomography (PET)-CT for lateralizing aldosterone secretion by Conn's adenomas.* J Clin Endocrinol Metab, 2012. **97**(1): p. 100-9.
81. Wu, X., et al., *[(11)C]metomidate PET-CT versus adrenal vein sampling for diagnosing surgically curable primary aldosteronism: a prospective, within-patient trial.* Nat Med, 2023. **29**(1): p. 190-202.
82. Silins, I., et al., *Para-chloro-2-[(18)F]fluoroethyl-etomidate: A promising new PET radiotracer for adrenocortical imaging.* Int J Med Sci, 2021. **18**(10): p. 2187-2196.
83. Quinkler, M. and P.M. Stewart, *Treatment of primary aldosteronism.* Best Pract Res Clin Endocrinol Metab, 2010. **24**(6): p. 923-32.
84. Kagawa, C.M., J.A. Cella, and C.G. Van Arman, *Action of new steroids in blocking effects of aldosterone and desoxycorticosterone on salt.* Science, 1957. **126**(3281): p. 1015-6.
85. Parthasarathy, H.K., et al., *A double-blind, randomized study comparing the antihypertensive effect of eplerenone and spironolactone in patients with hypertension and evidence of primary aldosteronism.* J Hypertens, 2011. **29**(5): p. 980-90.
86. Pitt, B., et al., *The effect of spironolactone on morbidity and mortality in patients with severe heart failure. Randomized Aldactone Evaluation Study Investigators.* N Engl J Med, 1999. **341**(10): p. 709-17.
87. Amar, L., et al., *Aldosterone synthase inhibition with LCI699: a proof-of-concept study in patients with primary aldosteronism.* Hypertension, 2010. **56**(5): p. 831-8.
88. Schumacher, C.D., R.E. Steele, and H.R. Brunner, *Aldosterone synthase inhibition for the treatment of hypertension and the derived mechanistic requirements for a new therapeutic strategy.* J Hypertens, 2013. **31**(10): p. 2085-93.

89. Freeman, M.W., et al., *Phase 2 Trial of Baxdrostat for Treatment-Resistant Hypertension.* N Engl J Med, 2023. **388**(5): p. 395-405.
90. Gagner, M., A. Lacroix, and E. Bolte, *Laparoscopic adrenalectomy in Cushing's syndrome and pheochromocytoma.* N Engl J Med, 1992. **327**(14): p. 1033.
91. Mellon, M.J., A. Sethi, and C.P. Sundaram, *Laparoscopic adrenalectomy: Surgical techniques.* Indian J Urol, 2008. **24**(4): p. 583-9.
92. Bergamini, C., et al., *Complications in laparoscopic adrenalectomy: the value of experience.* Surg Endosc, 2011. **25**(12): p. 3845-51.
93. Corcione, F., et al., *Vena cava injury. A serious complication during laparoscopic right adrenalectomy.* Surg Endosc, 2001. **15**(2): p. 218.
94. Saunders, B.D., et al., *Who performs endocrine operations in the United States?* Surgery, 2003. **134**(6): p. 924-31; discussion 931.
95. Vorselaars, W., et al., *Clinical Outcomes After Unilateral Adrenalectomy for Primary Aldosteronism.* JAMA Surg, 2019. **154**(4): p. e185842.
96. Sukor, N., et al., *Role of unilateral adrenalectomy in bilateral primary aldosteronism: a 22-year single center experience.* J Clin Endocrinol Metab, 2009. **94**(7): p. 2437-45.
97. Muth, A., et al., *Systematic review of surgery and outcomes in patients with primary aldosteronism.* Br J Surg, 2015. **102**(4): p. 307-17.
98. Williams, T.A., et al., *Outcomes after adrenalectomy for unilateral primary aldosteronism: an international consensus on outcome measures and analysis of remission rates in an international cohort.* Lancet Diabetes Endocrinol, 2017. **5**(9): p. 689-699.
99. Burrello, J., et al., *The Primary Aldosteronism Surgical Outcome Score for the Prediction of Clinical Outcomes After Adrenalectomy for Unilateral Primary Aldosteronism.* Ann Surg, 2020. **272**(6): p. 1125-1132.
100. Ni, Y., et al., *A review of the general aspects of radiofrequency ablation.* Abdom Imaging, 2005. **30**(4): p. 381-400.
101. Liu, S.Y., et al., *Radiofrequency ablation for benign aldosterone-producing adenoma: a scarless technique to an old disease.* Ann Surg, 2010. **252**(6): p. 1058-64.
102. Szejnfeld, D., et al., *Radiofrequency Ablation of Functioning Adrenal Adenomas: Preliminary Clinical and Laboratory Findings.* J Vasc Interv Radiol, 2015. **26**(10): p. 1459-64.
103. Yang, M.H., et al., *Comparison of radiofrequency ablation versus laparoscopic adrenalectomy for benign aldosterone-producing adenoma.* Radiol Med, 2016. **121**(10): p. 811-9.
104. Bouhanick, B., et al., *Radiofrequency ablation for adenoma in patients with primary aldosteronism and hypertension: ADERADHTA, a pilot study.* J Hypertens, 2021. **39**(4): p. 759-765.
105. Cano-Valderrama, O., et al., *Laparoscopic adrenalectomy vs. radiofrequency ablation for the treatment of primary aldosteronism. A single center retrospective cohort analysis adjusted with propensity score.* Surg Endosc, 2022. **36**(3): p. 1970-1978.
106. Costa, N., et al., *Cost Analysis of Radiofrequency Ablation for Adrenal Adenoma in Patients with Primary Aldosteronism and Hypertension: Results from the ADERADHTA Pilot Study and Comparison with Surgical Adrenalectomy.* Cardiovasc Intervent Radiol, 2023. **46**(1): p. 89-97.
107. Keeling, A.N., et al., *Hypertensive crisis during radiofrequency ablation of the adrenal gland.* J Vasc Interv Radiol, 2009. **20**(7): p. 990-1.

108. Chini, E.N., et al., *Hypertensive crisis in a patient undergoing percutaneous radiofrequency ablation of an adrenal mass under general anesthesia.* Anesth Analg, 2004. **99**(6): p. 1867-1869.
109. Carrafiello, G., et al., *Imaging-guided percutaneous radiofrequency ablation of adrenal metastases: preliminary results at a single institution with a single device.* Cardiovasc Intervent Radiol, 2008. **31**(4): p. 762-7.
110. Onik, G., et al., *Life-threatening hypertensive crises in two patients undergoing hepatic radiofrequency ablation.* AJR Am J Roentgenol, 2003. **181**(2): p. 495-7.
111. Sarwar, A., et al., *Clinical Outcomes following Percutaneous Radiofrequency Ablation of Unilateral Aldosterone-Producing Adenoma: Comparison with Adrenalectomy.* J Vasc Interv Radiol, 2016. **27**(7): p. 961-7.
112. Young, W.F., Jr., *Diagnosis and treatment of primary aldosteronism: practical clinical perspectives.* J Intern Med, 2019. **285**(2): p. 126-148.
113. Nishimoto, K., et al., *Case Report: Nodule Development From Subcapsular Aldosterone-Producing Cell Clusters Causes Hyperaldosteronism.* J Clin Endocrinol Metab, 2016. **101**(1): p. 6-9.
114. Nishimoto, K., et al., *Aldosterone-stimulating somatic gene mutations are common in normal adrenal glands.* Proc Natl Acad Sci U S A, 2015. **112**(33): p. E4591-9.
115. Choi, M., et al., *K+ channel mutations in adrenal aldosterone-producing adenomas and hereditary hypertension.* Science, 2011. **331**(6018): p. 768-72.
116. Omata, K., et al., *Aldosterone-Producing Cell Clusters Frequently Harbor Somatic Mutations and Accumulate With Age in Normal Adrenals.* J Endocr Soc, 2017. **1**(7): p. 787-799.
117. Aglony, M., et al., *Frequency of familial hyperaldosteronism type 1 in a hypertensive pediatric population: clinical and biochemical presentation.* Hypertension, 2011. **57**(6): p. 1117-21.
118. Scholl, U.I., et al., *CLCN2 chloride channel mutations in familial hyperaldosteronism type II.* Nat Genet, 2018. **50**(3): p. 349-354.
119. Monticone, S., et al., *Familial hyperaldosteronism type III.* J Hum Hypertens, 2017. **31**(12): p. 776-781.
120. Azizan, E.A., et al., *Somatic mutations in ATP1A1 and CACNA1D underlie a common subtype of adrenal hypertension.* Nat Genet, 2013. **45**(9): p. 1055-60.
121. Teo, A.E., et al., *Pregnancy, Primary Aldosteronism, and Adrenal CTNNB1 Mutations.* N Engl J Med, 2015. **373**(15): p. 1429-36.
122. Beuschlein, F., et al., *Somatic mutations in ATP1A1 and ATP2B3 lead to aldosterone-producing adenomas and secondary hypertension.* Nat Genet, 2013. **45**(4): p. 440-4, 444e1-2.
123. Monticone, S., et al., *Immunohistochemical, genetic and clinical characterization of sporadic aldosterone-producing adenomas.* Mol Cell Endocrinol, 2015. **411**: p. 146-54.
124. Arnesen, T., et al., *Outcome after surgery for primary hyperaldosteronism may depend on KCNJ5 tumor mutation status: a population-based study from Western Norway.* Langenbecks Arch Surg, 2013. **398**(6): p. 869-74.
125. Ip, J.C., et al., *Mutations in KCNJ5 determines presentation and likelihood of cure in primary hyperaldosteronism.* ANZ J Surg, 2015. **85**(4): p. 279-83.
126. Nanba, K., et al., *Genetic Characteristics of Aldosterone-Producing Adenomas in Blacks.* Hypertension, 2019. **73**(4): p. 885-892.

127. Saner-Amigh, K., et al., *Elevated expression of luteinizing hormone receptor in aldosterone-producing adenomas.* J Clin Endocrinol Metab, 2006. **91**(3): p. 1136-42.
128. Wilson, M., et al., *Blood pressure, the renin-aldosterone system and sex steroids throughout normal pregnancy.* Am J Med, 1980. **68**(1): p. 97-104.
129. Forestiero, V., et al., *Primary aldosteronism in pregnancy.* Rev Endocr Metab Disord, 2023. **24**(1): p. 39-48.
130. Riester, A. and M. Reincke, *Progress in primary aldosteronism: mineralocorticoid receptor antagonists and management of primary aldosteronism in pregnancy.* Eur J Endocrinol, 2015. **172**(1): p. R23-30.
131. Ronconi, V., et al., *Progesterone increase counteracts aldosterone action in a pregnant woman with primary aldosteronism.* Clin Endocrinol (Oxf), 2011. **74**(2): p. 278-9.
132. Gant, N.F., et al., *Control of vascular responsiveness during human pregnancy.* Kidney Int, 1980. **18**(2): p. 253-8.
133. Parviainen, H., et al., *GATA transcription factors in adrenal development and tumors.* Mol Cell Endocrinol, 2007. **265-266**: p. 17-22.
134. Zhou, J., et al., *Somatic mutations of GNA11 and GNAQ in CTNNB1-mutant aldosterone-producing adenomas presenting in puberty, pregnancy or menopause.* Nat Genet, 2021. **53**(9): p. 1360-1372.
135. Kim, A.C., et al., *Targeted disruption of beta-catenin in Sf1-expressing cells impairs development and maintenance of the adrenal cortex.* Development, 2008. **135**(15): p. 2593-602.
136. Cadigan, K.M. and M.L. Waterman, *TCF/LEFs and Wnt signaling in the nucleus.* Cold Spring Harb Perspect Biol, 2012. **4**(11).
137. Liu, C., et al., *Control of beta-catenin phosphorylation/degradation by a dual-kinase mechanism.* Cell, 2002. **108**(6): p. 837-47.
138. Akerstrom, T., et al., *Activating mutations in CTNNB1 in aldosterone producing adenomas.* Sci Rep, 2016. **6**: p. 19546.
139. Zheng, S., et al., *Comprehensive Pan-Genomic Characterization of Adrenocortical Carcinoma.* Cancer Cell, 2016. **29**(5): p. 723-736.
140. Assie, G., et al., *Integrated genomic characterization of adrenocortical carcinoma.* Nat Genet, 2014. **46**(6): p. 607-12.
141. Thomas, A.C., et al., *Mosaic Activating Mutations in GNA11 and GNAQ Are Associated with Phakomatosis Pigmentovascularis and Extensive Dermal Melanocytosis.* J Invest Dermatol, 2016. **136**(4): p. 770-778.
142. Polubothu, S., et al., *GNA11 Mutation as a Cause of Sturge-Weber Syndrome: Expansion of the Phenotypic Spectrum of Galpha/11 Mosaicism and the Associated Clinical Diagnoses.* J Invest Dermatol, 2020. **140**(5): p. 1110-1113.
143. Nesbit, M.A., et al., *Mutations affecting G-protein subunit alpha11 in hypercalcemia and hypocalcemia.* N Engl J Med, 2013. **368**(26): p. 2476-2486.
144. Stratton, M.R., P.J. Campbell, and P.A. Futreal, *The cancer genome.* Nature, 2009. **458**(7239): p. 719-24.
145. Azizan, E.A., et al., *Microarray, qPCR, and KCNJ5 sequencing of aldosterone-producing adenomas reveal differences in genotype and phenotype between zona glomerulosa- and zona fasciculata-like tumors.* J Clin Endocrinol Metab, 2012. **97**(5): p. E819-29.

146. Backman, S., et al., *RNA Sequencing Provides Novel Insights into the Transcriptome of Aldosterone Producing Adenomas.* Sci Rep, 2019. **9**(1): p. 6269.
147. Gilchrist, R.L., et al., *The luteinizing hormone/chorionic gonadotropin receptor has distinct transmembrane conductors for cAMP and inositol phosphate signals.* J Biol Chem, 1996. **271**(32): p. 19283-7.
148. Rao, C.V., *Differential properties of human chorionic gonadotrophin and human luteinizing hormone binding to plasma membranes of bovine corpora lutea.* Acta Endocrinol (Copenh), 1979. **90**(4): p. 696-710.
149. Pabon, J.E., et al., *Novel presence of luteinizing hormone/chorionic gonadotropin receptors in human adrenal glands.* J Clin Endocrinol Metab, 1996. **81**(6): p. 2397-400.
150. Millington, D.S., et al., *In vitro synthesis of steroids by a feminising adrenocortical carcinoma: effect of prolactin and other protein hormones.* Acta Endocrinol (Copenh), 1976. **82**(3): p. 561-71.
151. Matsukura, S., et al., *Multiple hormone receptors in the adenylate cyclase of human adrenocortical tumors.* Cancer Res, 1980. **40**(10): p. 3768-71.
152. Bernichtein, S., H. Peltoketo, and I. Huhtaniemi, *Adrenal hyperplasia and tumours in mice in connection with aberrant pituitary-gonadal function.* Mol Cell Endocrinol, 2009. **300**(1-2): p. 164-8.
153. Bernichtein, S., M. Alevizaki, and I. Huhtaniemi, *Is the adrenal cortex a target for gonadotropins?* Trends Endocrinol Metab, 2008. **19**(7): p. 231-8.
154. Schoemaker, N.J., et al., *The role of luteinizing hormone in the pathogenesis of hyperadrenocorticism in neutered ferrets.* Mol Cell Endocrinol, 2002. **197**(1-2): p. 117-25.
155. Bielinska, M., et al., *Gonadectomy-induced adrenocortical neoplasia in the domestic ferret (Mustela putorius furo) and laboratory mouse.* Vet Pathol, 2006. **43**(2): p. 97-117.
156. Desmarchelier, M., et al., *Primary hyperaldosteronism in a domestic ferret with an adrenocortical adenoma.* J Am Vet Med Assoc, 2008. **233**(8): p. 1297-301.
157. Abdallah, M.A., et al., *Human fetal nongonadal tissues contain human chorionic gonadotropin/luteinizing hormone receptors.* J Clin Endocrinol Metab, 2004. **89**(2): p. 952-6.
158. Albiger, N.M., et al., *A case of primary aldosteronism in pregnancy: do LH and GNRH receptors have a potential role in regulating aldosterone secretion?* Eur J Endocrinol, 2011. **164**(3): p. 405-12.
159. Plockinger, U., et al., *Functional Implications of LH/hCG Receptors in Pregnancy-Induced Cushing Syndrome.* J Endocr Soc, 2017. **1**(1): p. 57-71.
160. Carlson, H.E., *Human adrenal cortex hyperfunction due to LH/hCG.* Mol Cell Endocrinol, 2007. **269**(1-2): p. 46-50.
161. Leinonen, P., et al., *Testosterone-secreting virilizing adrenal adenoma with human chorionic gonadotrophin receptors and 21-hydroxylase deficiency.* Clin Endocrinol (Oxf), 1991. **34**(1): p. 31-5.
162. Lopez, A.G., et al., *Expression of LHCGR in Pheochromocytomas Unveils an Endocrine Mechanism Connecting Pregnancy and Epinephrine Overproduction.* Hypertension, 2022. **79**(5): p. 1006-1016.
163. Brieher, W.M. and A.S. Yap, *Cadherin junctions and their cytoskeleton(s).* Curr Opin Cell Biol, 2013. **25**(1): p. 39-46.

164. Sanchez-Pulido, L. and C.P. Ponting, *TMEM132: an ancient architecture of cohesin and immunoglobulin domains define a new family of neural adhesion molecules.* Bioinformatics, 2018. **34**(5): p. 721-724.
165. Liaqat, K., et al., *Further evidence of involvement of TMEM132E in autosomal recessive nonsyndromic hearing impairment.* J Hum Genet, 2020. **65**(2): p. 187-192.
166. Li, J., et al., *Whole-exome sequencing identifies a variant in TMEM132E causing autosomal-recessive nonsyndromic hearing loss DFNB99.* Hum Mutat, 2015. **36**(1): p. 98-105.
167. Liaqat, K., et al., *Identification of CACNA1D variants associated with sinoatrial node dysfunction and deafness in additional Pakistani families reveals a clinical significance.* J Hum Genet, 2019. **64**(2): p. 153-160.
168. Baig, S.M., et al., *Loss of Ca(v)1.3 (CACNA1D) function in a human channelopathy with bradycardia and congenital deafness.* Nat Neurosci, 2011. **14**(1): p. 77-84.
169. Eckrich, S., et al., *Cochlea-Specific Deletion of Ca(v)1.3 Calcium Channels Arrests Inner Hair Cell Differentiation and Unravels Pitfalls of Conditional Mouse Models.* Front Cell Neurosci, 2019. **13**: p. 225.
170. Wu, J. and R.J. Lukas, *Naturally-expressed nicotinic acetylcholine receptor subtypes.* Biochem Pharmacol, 2011. **82**(8): p. 800-7.
171. Gu, S., et al., *Brain alpha7 Nicotinic Acetylcholine Receptor Assembly Requires NACHO.* Neuron, 2016. **89**(5): p. 948-55.
172. Sharara-Chami, R.I., et al., *Glucocorticoid treatment--effect on adrenal medullary catecholamine production.* Shock, 2010. **33**(2): p. 213-7.
173. Bollag, W.B., et al., *Signal transduction mechanisms involved in carbachol-induced aldosterone secretion from bovine adrenal glomerulosa cells.* Mol Cell Endocrinol, 1992. **86**(1-2): p. 93-101.
174. Malaiyandi, L.M., et al., *M3-subtype muscarinic receptor activation stimulates intracellular calcium oscillations and aldosterone production in human adrenocortical HAC15 cells.* Mol Cell Endocrinol, 2018. **478**: p. 1-9.
175. Gu, S., et al., *Hair cell alpha9alpha10 nicotinic acetylcholine receptor functional expression regulated by ligand binding and deafness gene products.* Proc Natl Acad Sci U S A, 2020. **117**(39): p. 24534-24544.
176. Matta, J.A., et al., *Nicotinic acetylcholine receptor redux: Discovery of accessories opens therapeutic vistas.* Science, 2021. **373**(6556).
177. Noviello, C.M., et al., *Structure and gating mechanism of the alpha7 nicotinic acetylcholine receptor.* Cell, 2021. **184**(8): p. 2121-2134 e13.
178. Freedman, R., et al., *Linkage of a neurophysiological deficit in schizophrenia to a chromosome 15 locus.* Proc Natl Acad Sci U S A, 1997. **94**(2): p. 587-92.
179. Wang, S. and Y. Hu, *alpha7 nicotinic acetylcholine receptors in lung cancer.* Oncol Lett, 2018. **16**(2): p. 1375-1382.
180. Hurst, R.S., et al., *A novel positive allosteric modulator of the alpha7 neuronal nicotinic acetylcholine receptor: in vitro and in vivo characterization.* J Neurosci, 2005. **25**(17): p. 4396-405.
181. Tran, P.V., M.K. Georgieff, and W.C. Engeland, *Sodium depletion increases sympathetic neurite outgrowth and expression of a novel TMEM35 gene-derived protein (TUF1) in the rat adrenal zona glomerulosa.* Endocrinology, 2010. **151**(10): p. 4852-60.

182. Kweon, H.J., et al., *NACHO Engages N-Glycosylation ER Chaperone Pathways for alpha7 Nicotinic Receptor Assembly.* Cell Rep, 2020. **32**(6): p. 108025.
183. Magri, C., et al., *New copy number variations in schizophrenia.* PLoS One, 2010. **5**(10): p. e13422.
184. Niehrs, C., *Function and biological roles of the Dickkopf family of Wnt modulators.* Oncogene, 2006. **25**(57): p. 7469-81.
185. Keane, F.M., et al., *Quantitation of fibroblast activation protein (FAP)-specific protease activity in mouse, baboon and human fluids and organs.* FEBS Open Bio, 2013. **4**: p. 43-54.
186. Liu, R., et al., *Fibroblast activation protein: A potential therapeutic target in cancer.* Cancer Biol Ther, 2012. **13**(3): p. 123-9.
187. Bird, I.M., et al., *Human NCI-H295 adrenocortical carcinoma cells: a model for angiotensin-II-responsive aldosterone secretion.* Endocrinology, 1993. **133**(4): p. 1555-61.
188. Samandari, E., et al., *Human adrenal corticocarcinoma NCI-H295R cells produce more androgens than NCI-H295A cells and differ in 3beta-hydroxysteroid dehydrogenase type 2 and 17,20 lyase activities.* J Endocrinol, 2007. **195**(3): p. 459-72.
189. Torre, L.A., et al., *Ovarian cancer statistics, 2018.* CA Cancer J Clin, 2018. **68**(4): p. 284-296.
190. Potter, H. and R. Heller, *Transfection by Electroporation.* Curr Protoc Mol Biol, 2018. **121**: p. 9 3 1-9 3 13.
191. Dana, H., et al., *Molecular Mechanisms and Biological Functions of siRNA.* Int J Biomed Sci, 2017. **13**(2): p. 48-57.
192. Yan, G.M., et al., *Activation of muscarinic cholinergic receptors blocks apoptosis of cultured cerebellar granule neurons.* Mol Pharmacol, 1995. **47**(2): p. 248-57.
193. Yang, Y. and Z. Li, *Roles of heat shock protein gp96 in the ER quality control: redundant or unique function?* Mol Cells, 2005. **20**(2): p. 173-82.
194. Yang, Y., et al., *Heat shock protein gp96 is a master chaperone for toll-like receptors and is important in the innate function of macrophages.* Immunity, 2007. **26**(2): p. 215-26.
195. Liu, B. and Z. Li, *Endoplasmic reticulum HSP90b1 (gp96, grp94) optimizes B-cell function via chaperoning integrin and TLR but not immunoglobulin.* Blood, 2008. **112**(4): p. 1223-30.
196. Wang, Y. and X. Wang, *A Pan-Cancer Analysis of Heat-Shock Protein 90 Beta1(HSP90B1) in Human Tumours.* Biomolecules, 2022. **12**(10).
197. Li, K., et al., *Heat shock protein 90 has roles in intracellular calcium homeostasis, protein tyrosine phosphorylation regulation, and progesterone-responsive sperm function in human sperm.* PLoS One, 2014. **9**(12): p. e115841.
198. Tissier, F., et al., *Mutations of beta-catenin in adrenocortical tumors: activation of the Wnt signaling pathway is a frequent event in both benign and malignant adrenocortical tumors.* Cancer Res, 2005. **65**(17): p. 7622-7.
199. Wu, V.C., et al., *The prevalence of CTNNB1 mutations in primary aldosteronism and consequences for clinical outcomes.* Sci Rep, 2017. **7**: p. 39121.
200. McFarland, C.D., et al., *The Damaging Effect of Passenger Mutations on Cancer Progression.* Cancer Res, 2017. **77**(18): p. 4763-4772.

201. McFarland, C.D., L.A. Mirny, and K.S. Korolev, *Tug-of-war between driver and passenger mutations in cancer and other adaptive processes.* Proc Natl Acad Sci U S A, 2014. **111**(42): p. 15138-43.
202. Bozic, I., et al., *Accumulation of driver and passenger mutations during tumor progression.* Proc Natl Acad Sci U S A, 2010. **107**(43): p. 18545-50.
203. Kato, S., et al., *The Conundrum of Genetic "Drivers" in Benign Conditions.* J Natl Cancer Inst, 2016. **108**(8).
204. Yeh, I., et al., *Combined activation of MAP kinase pathway and beta-catenin signaling cause deep penetrating nevi.* Nat Commun, 2017. **8**(1): p. 644.
205. Piaggio, F., et al., *Secondary Somatic Mutations in G-Protein-Related Pathways and Mutation Signatures in Uveal Melanoma.* Cancers (Basel), 2019. **11**(11).
206. Gazdar, A.F., et al., *Establishment and characterization of a human adrenocortical carcinoma cell line that expresses multiple pathways of steroid biosynthesis.* Cancer Res, 1990. **50**(17): p. 5488-96.
207. Rao Ch, V., X.L. Zhou, and Z.M. Lei, *Functional luteinizing hormone/chorionic gonadotropin receptors in human adrenal cortical H295R cells.* Biol Reprod, 2004. **71**(2): p. 579-87.
208. Kojima, I., et al., *Mechanism of cholinergic stimulation of aldosterone secretion in bovine adrenal glomerulosa cells.* Endocrinology, 1986. **119**(1): p. 284-91.
209. Janossy, A., et al., *Cholinergic regulation of the rat adrenal zona glomerulosa.* J Endocrinol, 1998. **157**(2): p. 305-15.
210. Kuryatov, A., J. Mukherjee, and J. Lindstrom, *Chemical chaperones exceed the chaperone effects of RIC-3 in promoting assembly of functional alpha7 AChRs.* PLoS One, 2013. **8**(4): p. e62246.
211. Kassner, P.D. and D.K. Berg, *Differences in the fate of neuronal acetylcholine receptor protein expressed in neurons and stably transfected cells.* J Neurobiol, 1997. **33**(7): p. 968-82.
212. Koperniak, T.M., et al., *Cell-specific effects on surface alpha7 nicotinic receptor expression revealed by over-expression and knockdown of rat RIC3 protein.* J Neurochem, 2013. **124**(3): p. 300-9.
213. Choi, J.H., et al., *Endoscopic ultrasound-guided radiofrequency ablation for management of benign solid pancreatic tumors.* Endoscopy, 2018. **50**(11): p. 1099-1104.
214. Oleinikov, K., et al., *Endoscopic Ultrasound-Guided Radiofrequency Ablation: A New Therapeutic Approach for Pancreatic Neuroendocrine Tumors.* J Clin Endocrinol Metab, 2019. **104**(7): p. 2637-2647.
215. Girelli, R., et al., *Feasibility and safety of radiofrequency ablation for locally advanced pancreatic cancer.* Br J Surg, 2010. **97**(2): p. 220-5.
216. Arcidiacono, P.G., et al., *Feasibility and safety of EUS-guided cryothermal ablation in patients with locally advanced pancreatic cancer.* Gastrointest Endosc, 2012. **76**(6): p. 1142-51.
217. Scopelliti, F., et al., *Technique, safety, and feasibility of EUS-guided radiofrequency ablation in unresectable pancreatic cancer.* Surg Endosc, 2018. **32**(9): p. 4022-4028.
218. Tsikas, D., J. Jordan, and S. Engeli, *Blood pressure-lowering effects of propofol or sevoflurane anaesthesia are not due to enhanced nitric oxide formation or bioavailability.* Br J Clin Pharmacol, 2015. **79**(6): p. 1030-3.

219. Sweitzer, B.J. and S.J. Howell, *The Goldilocks principle as it applies to perioperative blood pressure: what is too high, too low, or just right?* Br J Anaesth, 2017. **119**(1): p. 7-10.
220. Jung, G.H., et al., *Extremely high white blood cell counts on postoperative day 1 do not predict severe complications following distal pancreatectomy.* Ann Hepatobiliary Pancreat Surg, 2019. **23**(4): p. 377-384.
221. Colley, C.M., et al., *Early time course of the acute phase protein response in man.* J Clin Pathol, 1983. **36**(2): p. 203-7.
222. Rossi, S., et al., *Radiofrequency ablation of pancreatic neuroendocrine tumors: a pilot study of feasibility, efficacy, and safety.* Pancreas, 2014. **43**(6): p. 938-45.
223. Gregoire, J.R., *Adjustment of the osmostat in primary aldosteronism.* Mayo Clin Proc, 1994. **69**(11): p. 1108-10.
224. Valinsky, W.C., R.M. Touyz, and A. Shrier, *Aldosterone and Ion Channels.* Vitam Horm, 2019. **109**: p. 105-131.
225. Willenberg, H.S., et al., *The serum sodium to urinary sodium to (serum potassium)2 to urinary potassium (SUSPPUP) ratio in patients with primary aldosteronism.* Eur J Clin Invest, 2009. **39**(1): p. 43-50.
226. Christakis, I., et al., *Laparoscopic Adrenalectomy for Conn's Syndrome is Beneficial to Patients and is Cost Effective in England.* J Invest Surg, 2018. **31**(4): p. 300-306.
227. Zhou, Y., et al., *Hypertension outcomes of adrenalectomy in patients with primary aldosteronism: a systematic review and meta-analysis.* BMC Endocr Disord, 2017. **17**(1): p. 61.
228. Benham, J.L., et al., *Proportion of Patients With Hypertension Resolution Following Adrenalectomy for Primary Aldosteronism: A Systematic Review and Meta-Analysis.* J Clin Hypertens (Greenwich), 2016. **18**(12): p. 1205-1212.
229. Nunes, T.F., et al., *Percutaneous ablation of functioning adrenal adenoma: a report on 11 cases and a review of the literature.* Abdom Imaging, 2013. **38**(5): p. 1130-5.
230. Mendiratta-Lala, M., et al., *Efficacy of radiofrequency ablation in the treatment of small functional adrenal neoplasms.* Radiology, 2011. **258**(1): p. 308-16.
231. Venkatesan, A.M., et al., *Radiofrequency ablation of metastatic pheochromocytoma.* J Vasc Interv Radiol, 2009. **20**(11): p. 1483-90.
232. Lo, C.H., Y.S. Tyan, and K.C. Ueng, *Immediate Results and Long-Term Outcomes Following Percutaneous Radiofrequency Ablation of Unilateral Aldosterone-Producing Adenoma.* Acta Cardiol Sin, 2020. **36**(2): p. 160-167.
233. Lin, J.H., et al., *Aldosterone-producing nodules and CYP11B1 signaling correlate in primary aldosteronism.* Endocr Relat Cancer, 2022. **29**(2): p. 59-69.
234. Williams, T.A., et al., *International Histopathology Consensus for Unilateral Primary Aldosteronism.* J Clin Endocrinol Metab, 2021. **106**(1): p. 42-54.
235. Carvajal, C.A., et al., *Serum Alpha-1-Acid Glycoprotein-1 and Urinary Extracellular Vesicle miR-21-5p as Potential Biomarkers of Primary Aldosteronism.* Front Immunol, 2021. **12**: p. 768734.
236. Barros, E.R., et al., *Proteomic Profile of Urinary Extracellular Vesicles Identifies AGP1 as a Potential Biomarker of Primary Aldosteronism.* Endocrinology, 2021. **162**(4).
237. Biggar, M.A. and T.W. Lennard, *Systematic review of phaeochromocytoma in pregnancy.* Br J Surg, 2013. **100**(2): p. 182-90.

238. Caimari, F., R. Corcoy, and S.M. Webb, *Cushing's disease: major difficulties in diagnosis and management during pregnancy.* Minerva Endocrinol, 2018. **43**(4): p. 435-445.